

**School of Science and Computing
Department of Imaging and Applied Physics**

The isotopic composition of Zn in natural materials

Osama Yousef Ali Ghidan

**This thesis is presented for the Degree of
Doctor of Philosophy
of
Curtin University of Technology**

August 2008

Declaration

To the best of my knowledge and belief this thesis contains no material previously published by any other person except where due acknowledgment has been made.

This thesis contains no material which has been accepted for the award of any other degree or diploma in any university.

Signature:

Date:

- **Abstract**

This work represents the most recent development of Zn isotopic measurements, and the first identification of Zn isotopic fractionation in natural materials using Thermal Ionisation Mass Spectrometry (TIMS).

The procedures developed in this research systematically evaluates and solves several critical analytical issues involved in TIMS Zn isotopic measurements such as, reducing the size of sample needed to perform an accurate and precise measurement, minimizing the effect of interferences on the Zn fractionation, reducing the blank associated with the analyses, dissolution and purification of different natural samples, and the generally ignored issue of the effect of the ion exchange chemistry (Zn separation) to the fractionation of Zn. These procedures have allowed sub-permil fractionations in the isotopic composition of Zn to be revealed in small Zn sample (1 µg), and the determination of low level (ng) elemental abundance of Zn in samples to be measured accurately by the means of isotope dilution mass spectrometry IDMS.

This thesis uses the rigorous double spike technique to measure fractionation, relative to the internationally proposed absolute Zn isotopic reference material (δ zero), based on a high purity Alfa Aesar 10759, now available to the international isotope community. All the isotopic measurements in natural materials were performed on bulk samples purified by ion exchange chemistry. The isotopic composition of the Zn minerals and igneous rocks agreed with that of the absolute reference material, which makes it possible to consider this reference material as being representative of “bulk Earth” Zn. Significant and consistent fractionation of $\sim +0.3$ ‰ per amu were found in 5 sediments from a range of localities. The consistency of this is attributed to conveyor type oceanic circulations effects.

The results from the two metamorphic samples indicate that the fractionation of Zn in these rocks is the same as found in igneous rocks but are different from the Zn found in sedimentary rocks. This supports the widely held assumption that high temperature and pressure processes do not fractionate the isotopic composition of chalcophile elements, such as has been found for Cd. Clay sample TILL-3 appears to exhibit a consistently slightly positive Zn fractionation of $+0.12 \pm 0.10$ ‰ amu⁻¹, although

inside the uncertainties of both igneous and sedimentary rocks, which is not surprising since Till is thought to be formed from a range of mixed glacial sediments

The isotopic composition of Zn was measured in two plants and one animal sample. The fractionation of $(-0.088 \pm 0.070 \text{ ‰ amu}^{-1})$ of Zn in the Rice (a C3 type plant material) sample suggested that Zn may be used to study Zn systematics in plants. The result obtained for MURST-Iss-A2 (Antarctic Krill) was $+0.21 \pm 0.11 \text{ ‰ amu}^{-1}$ relative to the laboratory standard which is similar to the average Zn fractionation results of $+0.281 \pm 0.083 \text{ ‰ amu}^{-1}$ obtained for marine sediments.

In this work, the isotopic composition of Zn was measured in five stone and two iron meteorites. The range of Zn fractionation in stone meteorites was between -0.287 ± 0.098 and $+0.38 \pm 0.16 \text{ ‰ amu}^{-1}$, and was consistent with previous work, although more measurements would be needed to generalize this to all stone meteorites. In iron meteorites; Canyon Diablo was found to have the greatest fractionation of $+1.11 \pm 0.11 \text{ ‰ amu}^{-1}$ relative to the laboratory standard.

Of all the meteorites studied, Redfields clearly showed an anomalous isotopic composition indicating that this meteorite possesses a significantly different Zn isotopic composition compared to all of the other natural materials measured. Using ^{64}Zn as a reference isotope, significant differences relative to the laboratory standard were found of $+5.6 \pm 0.4\text{‰}$, $+4.4 \pm 3.6 \text{ ‰}$, and $+21.0 \pm 0.9 \text{ ‰}$ and $+27.4 \pm 18.8 \text{ ‰}$ on ^{66}Zn and ^{67}Zn , ^{68}Zn and ^{70}Zn respectively. These significant “Redfields anomalies” can be interpreted in a number of ways in relation to their nucleosynthetic production. Whether Redfields is a primitive type of iron meteorite or not, the Redfields anomaly strongly suggests wide spread isotopic heterogeneity of at least one part of the Solar System and does not support the suggestion that “Zn was derived from an initially single homogeneous reservoir in the early Solar System”.

A pilot study to determine the concentration and the isotopic composition of Zn in River and tap water was performed. The concentration of Zn in River water averaged $6.9 \pm 0.8 \text{ ngg}^{-1}$, while for tap water it ranged from 13.1 ngg^{-1} to 5.2 μgg^{-1} . River water was fractionated by $-1.09 \pm 0.70 \text{ ‰ amu}^{-1}$, while restrained tap water yielded the

maximum fractionation of $-6.39 \pm 0.62 \text{ ‰ amu}^{-1}$ relative to the laboratory standard. The Zn fractionation of tap water is much larger than all other natural samples, although the uncertainty is also significantly greater due to the use of the less precise Daly detector used for these preliminary experimental measurements.

The fractionation of Zn in seven ultra pure Zn standard materials was measured relative to the laboratory standard and found to range from $-5.11 \pm 0.36 \text{ ‰ amu}^{-1}$ for AE 10760 to $+0.12 \pm 0.16 \text{ ‰ amu}^{-1}$ for Zn IRMM 10440. There appears to be some evidence for a relationship between Zn fractionation and its purity. As well as natural materials, the fractionation of Zn was measured in a number of processed materials. None of these results or those obtained for natural materials impact on the currently IUPAC accepted value for the atomic weight of Zn.

Along with fractionation determinations, the concentration of Zn was also measured by Isotope Dilution Mass Spectrometry in all of the samples. The concentration of Zn in five stony meteorites ranged from 26 ± 13 to $302 \pm 14 \text{ } \mu\text{gg}^{-1}$ for Plainview and Orgueil respectively. For ordinary Chondrites, the concentration of Zn in the three samples analysed ranged from 26 ± 13 to $64 \pm 34 \text{ } \mu\text{gg}^{-1}$ for Plainview and Brownfield 1937 respectively. The concentration of Zn was measured in two metamorphic rocks standard materials; the maximum concentration was $101.5 \pm 1.7 \text{ } \mu\text{gg}^{-1}$ in SDC-1. The concentration of Zn present in plant samples studied in this research was 22.15 ± 0.42 , $14.62 \pm 0.27 \text{ } \mu\text{gg}^{-1}$ for Rice IMEP-19 and Sargasso NIES-Number 9 respectively which is within the normal range of Zn concentrations.

Except for meteorites, the final uncertainties consistently cover the ranges of individual concentration measurements and indicate the homogeneity of the samples, including samples from different bottles where available. The final fractional uncertainties obtained for SRMs were all less than 2.8 %, demonstrating the high level of precision possible using IDMS.

I Acknowledgments

This work was carried out under the supervision of Associate Professor Robert D. Loss, whom I would like to acknowledge first. He has supported me with his knowledge, wisdom, and with his valuable time. I have always been privileged to be his student. Also I would like to acknowledge the time and support of my co-supervisor Professor Kevin Rosman. Professor John De Laeter for his financial support, and for his scientific discussions and for reviewing this thesis. During my studies, I have been privileged to use the facilities of the John De Laeter Centre for Mass Spectrometry, and without this support this research would not have been possible. Discussion with Associate Professor Michael Wieser of University of Calgary was always fruitful. I would like to acknowledge Associate Professor Alex Bevan from the Western Australian Museum for donating some samples for this work. All my colleagues in the Isotope Science Group at the Department of Imaging and Applied Physics: Ms. Laurie Burn, Dr. Paul Vallelonga, Ms Lynette Howearth, and Mr. Graeme Burton for his special support in the beginning of my research. Always, I have been lucky to have good friends beside me; Stuart Dunn, Adam Frew; and Ms Lynette Howearth. I would like to acknowledge the warm and kind support by Dr. Brendan McGann, Carmel McManus, Liz Field, Melat Habtemariam, and Ann Smith.

My special thanks and great acknowledgments go to Dr. Fiona Coombes and the Nurse Margaret Smith of Curtin University Health Services, Dr. Fredrick Ng; all for their extra ordinary help and support when I have needed it most. Ms Salam Selina Qtaishat comes first and unprecedented in that category. Also I would like to thank all the friendly staff and students of the Department of Applied Physics for their kindness. I would like to acknowledge Al-Balga Applied University who granted me the scholarship for this PhD.

II	Table of Contents	
□	Abstract	i
I	Acknowledgments	iv
II	Table of Contents	v
III	Table of Figures:	x
IV	List of Tables:	xv
□	Chapter 1: Introduction	1
1.1	Isotope fractionation	1
1.1.1	Natural isotopic variations	1
1.1.2	Extent of natural isotopic fractionation	3
1.2	Zinc: An element from Antiquity	4
1.2.1	Zinc the element	4
1.2.2	Natural abundance of Zn	5
1.2.3	Mass spectrometry of Zn	7
1.3	Aims of the research	9
1.4	Significance and application	10
□	Chapter 2: Literature review	16
2.1	Early isotopic measurements.	16
2.2	Isotopic composition and concentration of Zn in terrestrial materials:	17
2.2.1	Concentration of Zn in natural materials	17
2.2.2	Isotopic composition of Zn in natural materials	22
2.2.3	Causes of isotope fractionation	41
□	Chapter 3: Methods	44
3.1	Mass Spectrometry	44

3.1.1	Principles of Mass spectrometry	44
3.1.2	Thermal Ionisation Mass Spectrometer (TIMS)	45
3.1.2.1	Ion source	46
3.1.2.2	The magnet	47
3.1.2.3	The detection systems	49
3.1.3	Thermal ionisation of Zn	52
3.1.3.1	Thermal ionisation process	52
3.1.3.2	Ionisation efficiency	52
3.2	Contamination	54
3.2.1	Containers	55
3.2.2	Reagent and water purification	55
3.3	Measurement of Blanks.	58
3.4	Sample loading, degassing and heating	60
3.5	Isotopic Analysis methods	64
3.6	Interferences	71
3.7	IDMS and Double spike methods	76
3.7.1	IDMS	76
3.7.2	Double spike technique	80
3.8	Sample purification procedures	88
3.8.1	Overview and types of samples	88
3.9	Sample digestion	92
3.9.1	Terrestrial, biological, and stone meteorites	92
3.9.2	Iron meteorite Dissolution	94
3.10	Ion exchange chemistry	94
3.10.1	Anion exchange procedure	96
3.10.2	Extraction efficiency	96

□	Chapter 4: The elemental abundance of Zn: Results	98
4.1	Introduction	98
4.2	Calibration of the concentration of the double spike	98
4.3	Concentration of geological and environmental reference materials	102
4.3.1	Igneous rocks standard reference materials	104
4.3.2	Sedimentary rocks	106
4.3.3	Metamorphic rocks standard reference materials	108
4.3.4	Clay standard reference materials	109
4.4	Biological standard reference materials	109
4.5	Meteorite	112
4.5.1	Stony meteorites	113
4.5.2	Iron meteorites	114
4.6	Water	115
4.7	Concentration of Zn in other materials	116
□	Chapter 5: Isotopic composition of Zn: Results	117
5.1	Introduction	117
5.2	Laboratory standard	117
5.3	Double spike	124
5.3	Long term reproducibility of measured fractionation	126
5.5	Measurements of fractionation	127
5.5.1	Zn Standard metals	129
5.5.2	Geological materials	133
5.5.2.1	Zn minerals	133
5.5.2.2	Igneous rocks	134
5.5.2.3	Sedimentary rocks	136

5.5.2.4	Metamorphic rocks	139
5.5.2.5	Clay	140
5.5.3	Biological materials	140
5.5.4	Meteorites	142
5.5.4.1	Stone meteorites	143
5.5.4.2	Iron meteorites	144
5.5.4.2.1	Redfields	145
5.5.5	Effect of ion exchange chemistry on Zn fractionation	146
5.5.6	Water	147
5.5.7	Zinc fractionation in other materials	148
□	Chapter 6: The elemental abundance of Zn: Discussion	151
6.1	Introduction	151
6.2	Concentration of Zn in geological materials	154
6.3	Concentration of Zn in biological materials	156
6.4	Concentration of Zn in meteorites	157
6.4.1	Stone meteorites	158
6.4.2	Iron meteorites	161
6.5	Concentration of Zn in water and other materials	164
□	Chapter 7 Isotopic Composition of Zn: Discussion	168
7.1	Analytical considerations	168
7.1.1	Introduction	168
7.1.2	Comparisons considerations	169
7.1.3	Effect of ion exchange chemistry on fractionation.	170
7.1.4	Elemental spiking	171
7.1.5	Fractionation uncertainty budget	172
7.2	Geological Samples	173

7.2.1	Zinc minerals	176
7.2.2	Igneous rocks	177
7.2.3	Sedimentary rocks	180
7.2.4	Metamorphic rocks	183
7.2.5	Clay	183
7.3	Biological materials	184
7.4	Meteorites	188
7.4.1	Stony meteorites	192
7.4.2	Iron meteorites	199
7.4.3	The Redfields anomaly	200
7.5	Water	207
7.5.1	Swan River water	208
7.5.2	Tap water	210
7.6	High purity Zn metals	211
7.7	Other materials	216
7.8	Contribution of Zn isotopic fractionation to the atomic weight of Zn.	219
□	Chapter 8: Conclusions and recommendations	224
8.1	Summary of results	224
8.2	Significant Interpretations	227
8.3	Summary of the recommendations	234
□	References	237
□	Appendix A: Abstract of the Australian Institute of Physics Post Graduate Research Conference. Institute of Human Developmenta	
□	Appendix C: Abbreviations and units	c
□	Appendix D: Detailed isotopic Data	e
□	Appendix E: Detailed data for the concentration determinations	y

III Table of Figures:

- Figure 2. 1: The concentration of Zn in IMEP -19 Rice as measured by different analysts and techniques(IRMM, 2003). 17
- Figure 2. 2: The concentration of Zn in the BIR-1 SRM as measured by different techniques for BIR-1 SRM. Data taken from (Gladney and Roelandts, 1988) 18
- Figure 2. 3: Variation in Zn fractionation of the carbonate fraction of sediments as function of age, (Pichat et al., 2003a) 27
- Figure 2. 4: Three isotope plot relative to ^{64}Zn by (Luck et al., 2005b), data also includes that of other researchers. 34
- Figure 3. 1 The three components of the mass spectrometer: Ion source, Mass analyser and the ion collection system. (Holmes, 2002). 46
- Figure 3. 2: The three components of the mass spectrometer: Ion source, Magnet and the collection system. Figure scanned from (Loss, 1986) 49
- Figure 3. 3: The components of the Daly detector, (De Laeter, 2001) 51
- Figure 3.4: The VG354 TIMS used in this work. 52
- Figure 3. 5: Layout of the IDMS lab, with overall dimensions of 3×3 m 54
- Figure 3. 6: The amount of Zn as a function of amount of MQ water for two separate experiments. The concentration of Zn is represented by the slopes of the lines. The different y intercepts represent different beakers. 56
- Figure 3. 7: The amount of Zn as a function of amount of HCl. The concentration of Zn is represented by the slope of the line $80 \pm 11 \text{ pgg}^{-1}$ 56
- Figure 3. 8: The amount of Zn as a function of amount of HNO_3 . The concentration of Zn represented by the slope of the line, $55 \pm 15 \text{ pgg}^{-1}$. 57
- Figure 3. 9 Procedural blank for the adopted technique. 59
- Figure 3. 10: $^{64}\text{Zn}^+$ current as a function of amount of activator solution used for $1 \mu\text{g}$ Zn sample at temperature $\sim 1550 \text{ C}^\circ$ using the Faraday multicollector. 61
- Figure 3. 11: Faraday multi collector positions and ratios collected. 65

- Figure 3. 12: Mass spectra of Zn isotopes scanned across the Faraday multicollector system as output by the Mass Scanning program. 65
- Figure 3. 13: Tolerated interference of the $^{67}\text{Zn}/^{64}\text{Zn}$ ratio as a function of the $^{66}\text{Zn}/^{64}\text{Zn}$ ratio for 18 laboratory standard analyses. The major range bars represent the maximum tolerable interference possible before affecting any results 68
- Figure 3. 14: Tolerated interference of the $^{68}\text{Zn}/^{64}\text{Zn}$ ratio as a function of the $^{66}\text{Zn}/^{64}\text{Zn}$ ratio. The major range bars represent the maximum tolerable interference possible before affecting any results. 69
- Figure 3. 15: Tolerated interference of the $^{70}\text{Zn}/^{64}\text{Zn}$ ratio as a function of the $^{66}\text{Zn}/^{64}\text{Zn}$ ratio. The major range bars represent the maximum tolerable interference possible before affecting any results 70
- Figure 3. 16: Ni interference as a function of volume of Silica gel using a filament blank. 72
- Figure 3. 17: The apparent fractionation of Zn^+ resulting from permil interferences from CrO^+ . 73
- Figure 3. 18: The apparent fractionation of Zn resulting from various isobaric interferences on each isotope of Zn. 73
- Figure 3. 19: Loading the sample on an ordinary filament (left) and using a modified one (right) showing the filament post closeness to the sample. 74
- .Figure 3. 20: The alternative modified filament 75
- Figure 3. 21: Measured fractionation of 8 mixtures (Lab standard and double spike) at temperature $> 1675\text{ }^\circ\text{C}$. 76
- Figure 3. 22: The isotopic composition of the standard, the tracer “double spike” and a typical mixture (double spike and standard used in this work. 77
- Figure 3. 23: Uncertainty Budget for IDMS measurement of SDC-1 SRM (concentration of $101.5 \pm 1.7\ \mu\text{g g}^{-1}$), measured with the Daly detector 80
- Figure 3. 24: The effect of the sample to spike ratio on the uncertainty of the measured fractionation 81
- Figure 3. 25: The deviation of laboratory standard (normalized relative to the average using the three isotope fractionation laws) relative to the absolute (Ponzevera et al., 2006). Also shown are the fractionation lines using the linear, power and exponential law. 83

- Figure 3. 26: A three isotope ratio space for Zn. So, Mo and To represent the unfractionated isotopic ratios of the sample, mixture and the tracer respectively. 84
- Figure 4. 2: The concentration of Zn spike in 8 different mixtures of spike and standard as used for the calibration of the spike. 102
- Figure 5. 1: The deviation of the isotopic composition of the laboratory standard measured using the Daly detector and using the Faraday multicollector relative to the isotopic composition of proposed absolute standard measured by IRMM 121
- Figure 5. 2: The deviation of the measured $^{66}\text{Zn}/^{64}\text{Zn}$ ratios for 19 analyses as measured on the Faraday multicollector relative to their external average. 122
- Figure 5. 3: Deviation of the $^{67}\text{Zn}/^{64}\text{Zn}$ ratios measured on the Faraday multicollector relative to their external average. 123
- Figure 5. 4: The deviation of $^{68}\text{Zn}/^{64}\text{Zn}$ ratios measured on the Faraday multicollector relative to their external average. 123
- Figure 5. 5: The deviation of $^{70}\text{Zn}/^{64}\text{Zn}$ ratios measured on the Faraday multicollector relative to their external average. 124
- Figure 5. 6: The long term reproducibility of the measured fractionation of the laboratory standard relative to it self. 127
- Figure 5. 7: The deviation of unspiked Zn pure metal AE10760 relative to the laboratory standard. 129
- Figure 5. 8 The deviation of the isotopic composition of a CaCO_3 sample relative to the laboratory standard. 138
- Figure 5. 9: The deviation of the isotopic composition of Zn in Canyon Diablo meteorite relative to the laboratory standard. 144
- Figure 5. 10: The deviation of the isotopic composition of Zn in the Zinc nutrient Tablet relative to the laboratory standard 150
- Figure 6. 1: The concentration of Zn in BCR-1 using IDMS (recommended value is compiled from a wide range of analysts and analytical techniques (USGS, 2006b). 152
- Figure 6. 2: Concentration of Zn in iron meteorites. (The large error bars for Odessa represents the range) 164
- Figure 6. 3: The reproducibility of the concentration of Zn in restrained and unrestrained (fresh) unrestrained (fresh) (fresh) tap water 166

- Figure 7. 1: Zn fractionation as a function of number of passes through an Anion exchange column. 170
- Figure 7. 2: The contributions to the uncertainty of an individual measurement for the fractionation of Canyon Diablo. 172
- Figure 7. 3: Graphical representation of the average measured Zn fractionation ‰ amu⁻¹ in geological materials relative to the absolute isotopic composition of Zn. 175
- Figure 7. 4: Measured Zn fractionation in biological materials relative to the laboratory standard. 185
- Figure 7. 5: Average Zn fractionation in meteorites relative to the laboratory standard. 191
- Figure 7. 6: Concentration and the average fractionation of Zn in measured stony meteorites. The large uncertainties in the concentration are due to the range of values obtained. 198
- Figure 7. 7: Deviation in ‰ of the average of three independent measurements of the isotopic composition of Zn in Redfields iron meteorite, relative to the isotopic composition of Zn in laboratory standard. Ratios are not corrected for machine bias. 202
- Figure 7. 8: The prediction of MZM anomalies for elements by (Hartmann et al., 1985) presented in (Loss and Lugmair, 1990). 205
- Figure 7. 9: Average isotopic fractionation and concentration of Zn in Swan River in two different locations 209
- Figure 7. 10: Isotopic fractionation of Zn ‰ amu⁻¹ in tap water (unrestrained (fresh) tap water and restrained tap water) 210
- Figure 7. 11: Deviation of the isotopic composition of Zn in Alfa Aesar 10760 relative to the laboratory standard (Daly detector, not double spiked) showing a clear fractionation line of -6.34 ± 0.21 ‰ amu⁻¹ uncertainty obtained using the weighted slope) 212
- Figure 7. 12: Zinc isotopic fractionation of pure Zn standard metals relative to Alfa Aesar 10759 “proposed absolute” versus their impurity 215
- Figure 7. 13: Three isotope plot for number of pure Zn standard metals. Uncertainties in graph are 95% confidence level. 216
- Figure 7. 14: The three isotope plot for the Zn fractionation of materials for samples suspected to be affected by, or from an anthropogenic source. 218

- Figure 7. 15: Atomic weight and Zn fractionation ranges in natural materials. The ranges in atomic weights and fractionation in these samples are dominated by the meteorites. 221
- Figure 7. 16: Range of Zn fractionation in processed and natural materials affected by anthropogenic processes. In the case of water samples approximately 50% of the range is due to the associated uncertainties. 222

IV List of Tables:

- Table 1. 1: A summary of the different laboratory standards used as reference, type of materials and methods to measure the isotopic fractionation of Zn. The name of the method is as shown in the relevant reference. 12
- Table 2. 1: Abundance of the isotopes of Zn as measured by different researchers. 23
- Table 2. 2: Isotopic composition of Zn in biological samples compared to a Zn standard (Patterson et al., 1992). The uncertainties shown are the fractional uncertainties in %. 24
- Table 2. 3: Zn fractionation and concentrations in human biological materials. Concentrations are in $\mu\text{g g}^{-1}$ unless specified (Stenberg et al., 2004). 29
- Table 3. 1: Comparison of the contamination of Zn in reagents and MQ water used in this work with that used by Bermin et al.(2006) to measured the isotopic fractionation of Zn in sea water using MC-ICPMS. 57
- Table 3. 2: A comparison between the size of sample used for analysis and the procedure blank in this work compared to that of other analysts using ICP-MS analysis. 60
- Table 3. 3: A comparison for the achievement of this technique for Zn regarding the size of the sample with other modern isotopic TIMS transition elements and Ca is shown. 63
- Table 3. 4: The effect of the difference between the normalization using the linear and exponential law on the measured fractionation. 84
- Table 3. 5: Brief description of high purity Zn metal samples analysed. 89
- Table 3. 6: Type and description of Zn minerals. 89
- Table 3. 7: Description of reference and certified reference materials samples. 90
- Table 3. 8 Description of terrestrial rock sample. 90
- Table 3. 9: Description of stone meteorites. 91
- Table 3. 10: Description of iron meteorites 91

•	Table 3. 11: Description of biological materials	92
•	Table 3. 12: Dissolution steps for all samples except for Iron meteorites	93
•	Table 3. 13: Ion exchange separation procedure of Zn from sample matrix for all samples except iron meteorites.	95
•	Table 4. 1: Concentration of Zn in Basalt BCR-1	104
•	Table 4. 2: Concentration of Zn in BIR-1	104
•	Table 4. 3: Concentration of Zn in Diabase W-2	105
•	Table 4. 4: Concentration of Zn in DNC-1	105
•	Table 4. 5: Concentration of Zn in SGR-1	106
•	Table 4. 6: Concentration of Zn in SCo-1	106
•	Table 4. 7: Concentration of Zn in HISS-1	107
•	Table 4. 8: Concentration of Zn in Murst-Iss-A1	107
•	Table 4. 9: Concentration of Zn in CaCO ₃	108
•	Table 4. 10: Concentration of Zn in SDC-1	108
•	Table 4. 11: Concentration of Zn in QLO-1	109
•	Table 4. 12: Concentration of Zn in TILL-3	109
•	Table 4. 13: Concentration of Zn in biological materials	111
•	Table 4.14: Concentration of Zn in stony meteorite	113
•	Table 4. 15: Concentration of Zn in iron meteorite	114
•	Table 4. 16: Concentration of Zn in water	115
•	Table 4. 17: Concentration of Zn in other materials	116
•	Table 5. 1: The measured isotopic composition of Zn in the laboratory standard measured using the Daly detector not corrected for machine bias.	118
•	Table 5. 2: The measured isotopic composition of 1µg of Zn standard of laboratory standard using the Faraday multicollector not corrected for machine bias.	120

- Table 5. 3: The isotopic composition of the double spike measured using the Daly detector, not corrected for machine bias. 125
- Table 5. 4: The measured isotopic composition of Zn in the double spike solution using the Faraday multicollector system, not corrected for machine bias. 126
- Table 5. 5: Measured isotopic fractionation in high purity metal standards relative to the laboratory standard “the international absolute isotopic composition of Zn”. Two fractionation values are shown reflecting the use of different sets of isotopic ratios. All relative to ^{64}Zn 131
- Table 5. 6: the absolute isotopic composition of Zn in the Zn pure standard metals 132
- Table 5. 7: Measured Zn fractionation, of Zn minerals relative to the laboratory standard (δ zero). Two fractionation values are shown reflecting the use of different sets of isotopic ratios, all relative to ^{64}Zn . 133
- Table 5. 8: Proposed absolute isotopic composition of Zn in Zn minerals 134
- Table 5. 9: Measured Zn fractionation in igneous rocks relative to the laboratory standard (δ zero). Two fractionation values are shown reflecting the use of different sets of isotopic ratios, all relative to ^{64}Zn . 135
- Table 5. 10: Proposed absolute isotopic composition of Zn in igneous rock SRMs 136
- Table 5. 11: Measured Zn fractionation in sedimentary rocks relative to the laboratory standard (δ zero). Two fractionation values are shown reflecting the use of different sets of isotopic ratios, all relative to ^{64}Zn . 137
- Table 5. 12: Proposed absolute isotopic composition of Zn for measured sedimentary rocks. 138
- Table 5. 13: Measured Zn fractionation in Mica Schist SDC-1 relative to the laboratory standard (δ zero). Two fractionation values are shown reflecting the use of different sets of isotopic ratios, all relative to ^{64}Zn . 139
- Table 5. 14: Proposed absolute isotopic composition of Zn for measured metamorphic rocks SRMs 139

- Table 5. 15: Measured Zn fractionation in TILL-3 relative to the laboratory standard (δ zero). Two fractionation values are shown reflecting the use of different sets of isotopic ratios, all relative to ^{64}Zn . 140
- Table 5. 16: Proposed absolute isotopic composition of Zn for measured TILL-3 140
- Table 5. 17: Measured Zn fractionation in biological materials relative to the laboratory standard (δ zero). Two fractionation values are shown reflecting the use of different sets of isotopic ratios, all relative to ^{64}Zn . 141
- Table 5. 18: Proposed absolute isotopic composition of Zn for measured biological materials SRMs. 142
- Table 5. 19: Measured Zn fractionation in stone meteorites relative to the laboratory standard (δ zero). Two fractionation values are shown reflecting the use of different sets of isotopic ratios. All relative to ^{64}Zn . 143
- Table 5. 20: Measured Zn fractionation in Canyon Diablo iron meteorite relative to the laboratory standard (δ zero). Two fractionation values are shown reflecting the use of different sets of isotopic ratios, both relative to ^{64}Zn . 144
- Table 5. 21: The isotopic composition of Zn in the Redfields meteorite (uncorrected for instrument bias). 146
- Table 5. 22: contribution of the anion exchange column chemistry to the measured fractionation relative to the laboratory standard (δ zero). 147
- Table 5. 23: Fractionation of Zn isotopic composition in Swan river water relative to the laboratory standard (δ zero). Two fractionation values are shown reflecting the use of different sets of isotopic ratios, all relative to ^{64}Zn . 148
- Table 5. 24: Fractionation Zn isotopic composition in nutrient Zinc Tablet relative to the laboratory standard (δ zero). Two fractionation values are shown reflecting the use of different sets of isotopic ratios, all relative to ^{64}Zn . 149
- Table 6. 1: A comparison between the new techniques used to measure the concentration of Zn in BCR-1 by IDMS with previous work. 153
- Table 6. 2: Comparison between the Zn isotope dilution measurements obtained in this work for stony meteorites, and those of other researchers. 159

- Table 6. 3: Comparison between the Zn isotope dilution measurements obtained in this work and for iron meteorites and those of other researchers. 162
- Table 7. 1: Compilation of the average isotopic fractionation of Zn in all geological materials measured in this work and compared to the previously measured values using different technique. 174
- Table 7. 2: Compilation of the average isotopic fractionation of Zn in all biological materials measured in this work. 184
- Table 7. 3: Compilation of the average isotopic fractionation of Zn in all meteorites measured in this work, compared to the previously measured values using different techniques. 190
- Table 7. 4: Zn isotope variation (Zn^*) for the Redfields meteorite, reference relative to different isotopes relative to the laboratory standard ‰. 204
- Table 7. 5: Summary of Zn fractionation of water samples measured in this research 208
- Table 7. 6: Summary of the average fractionation of pure Zn metal relative to the laboratory standard (proposed absolute) 213

- **Chapter 1: Introduction**

1.1 Isotope fractionation

1.1.1 Natural isotopic variations

Variations in the isotopic composition of elements due to natural processes was first proposed in 1925, when Briscoe and Robinson from the University of Durham, Armstrong College, in England, redetermined the atomic weight of Boron and concluded that fractionation in the isotopic abundances of Boron is the cause of the change in the atomic weight (Briscoe and Robinson, 1925).

Most polyisotopic elements contain isotopes in fixed proportions, however, these isotopes possess slightly different chemical and physical properties, which produces mass dependent variations in the isotopic abundances when they experience changes in chemical and physical environments.; These small but significant changes in the isotopic abundances enable chemical and physical environments to be explored, and are being used by a wide variety of sciences. The extent of the isotopic variability for selected elements in naturally occurring materials and reagents for selected elements has been compiled by Coplen et al. (2002) and is discussed in the next Section.

This variation in the stable isotopic abundances is known as “isotopic fractionation”. Isotopic fractionation of an element E is usually expressed in terms of relative isotope ratios as “ $\delta^i E$ ” (delta value of isotope i of element E), as presented in Equation 1.1

$$\delta^i E = \left[\frac{n_x(^i E)/n_x(^j E)}{n_{ref} (^i E)/n_{ref} (^j E)} - 1 \right] \quad 1.1$$

Where, “ $\delta^i E$ ” is the delta value of the isotope i of element E in sample X relative to the reference “ ref ”, the terms $\left[\frac{n_x(^i E)}{n_x(^j E)} \right]$, and $\left[\frac{n_{ref} (^i E)}{n_{ref} (^j E)} \right]$ are the ratios of the isotope amounts in material x , and in the reference, “ ref ”.

In this thesis, the values of the measured fractionations are reported in “per mil per atomic mass unit, where per mil “‰” is the difference of the isotopic composition as

part in a 1000 relative to the laboratory standard. This unit is used the differences in the expected in the isotopic composition of Zn are small and expected to be in the per mil scale rather than in the scale of the more conventional %. The fractionation was also calculated using a range of different isotope ratios, not always including ^{66}Zn , hence a notation using $^{66}\delta$ scale, commonly used to express Zn fractionation, such as represented in Equation 1.2. For example, the isotopic fractionation of Zn can be expressed in terms of per mil deviation from a standard value as in the Equation 1.2

$$\delta^x \text{Zn} = \left[\frac{\left({}^x \text{Zn} / {}^{64} \text{Zn} \right)_{\text{Sample}}}{\left({}^x \text{Zn} / {}^{64} \text{Zn} \right)_{\text{Standard}}} - 1 \right] \times 1000 . \quad 1.2$$

Where x is the mass number 66, 67 or 68 of Zn. It is very common to express (δ) in terms of per atomic mass unit (amu).

A positive δ value for the fractionation indicates that the sample is enhanced in the heavier isotopes relative to the reference “laboratory standard”, while a negative δ value indicates that the sample is depleted in the heavier isotopes relative to the reference “laboratory standard” (Coplen et al., 2002)

Isotopic fractionation was observed firstly for O, and H isotope ratios in sea water when Gilfillan (1934) described a method of measuring small differences of the specific gravity of sea water. Large variations in the isotopic composition for the isotopes of C in natural materials was discovered by Murphey and Nier (1941). Theoretical studies and experimental evidence showed that many isotopic variations in terrestrial samples were due to fractionation resulting from geological and biological processes because of differences in the chemical properties of different isotopic molecules (Macnamara and Thode, 1950). The significance of isotopic fractionation became evident following the interpretations of the isotopic composition of oxygen and its use in establishing Paleotemperature scales in 1951, which is heralded as one of the scientific achievements of the last century (Sharp, 2007).

The physicochemical processes responsible for isotopic mass dependent fractionations of an element also occur in both natural and anthropogenic

environments. (Sharp, 2007). Isotopic fractionation can be caused by kinetic and or equilibrium isotope effects during evaporation, diffusion, dissociation reactions and almost all biological reactions. These isotope fractionation effects are rare for high temperature processes, such as high temperature volcanic events in or on Earth. On the other hand, equilibrium isotope effects such as the effect of the atomic mass of the isotope on the atom or molecule bond energy, e.g.; when a light isotope is substituted with a heavier one at low temperatures, will change the internal energies of the different isotopes and produce a mass bias in products and reactants of reactions, (Sharp, 2007). Further discussion on this is provided in Chapter 2.

1.1.2 Extent of natural isotopic fractionation

The extent of isotopic fractionation varies from one element to another, due to many reasons; for example; because of the large relative mass difference between the isotopes of H results in deuterium having a slightly different chemistry; this element displays in the largest isotopic fractionation observed in nature, e.g. from Coplen et al. (2002) the range of $\delta^2\text{H}$ may reach up to +62.4 % in natural materials. Lithium shows a range in $\delta^7\text{Li}$ in natural materials of more than 50 %, while carbon shows a fractionation of greater than 14% in C bearing materials. At the same time, another abundant element, oxygen exhibits a variation in its isotopic fractionation up to 9 % in continental water. Other examples include S, with a fractionation of between -2 to + 6 % in natural materials, and up to $\delta^{65}\text{Cu}$ 9‰ for Cu in natural materials (Coplen et al., 2002). The Coplen et al. (2002) compiled data for Zn is sparse and inconclusive. For many years the isotopic composition of Zn was thought to be invariant, or at least to be less than analytical uncertainty (0.1%) in terrestrial materials. Recent improvements in instrumentation especially those of Multi collector Inductively Coupled Plasma Mass Spectrometry (MC-ICPMS) (reviewed Section 2.2.2) have resulted in many claims to be able to detect very small (sub-permil) fractionations for this element, However, due to analytical considerations (see Chapter 3) and the lack of a suitable absolute standard, the presence of these small Zn fractionations have always been doubtful before this work. This is highlighted by Balistrieri et al. (2008) who stated: “It is likely that both geochemical and biological processes fractionate stable isotopes of important metals, such as Cu and Zn, in these systems. Hence,

careful study of the isotopes of these transition metals may help to identify specific biogeochemical reactions or even finger print sources of metals in many stream systems. Despite this promise, we know very little about the direction and magnitude of isotopic changes for Cu or Zn that might occur as a result of specific chemical processes” (Balistrieri et al., 2008).

This thesis directly addresses these analytical issues with the isotopic fractionation of Zn in natural materials being measured using a high accuracy double spiking method, relative to the δ zero standard (Ponzevera et al., 2006).

1.2 Zinc: An element from Antiquity

1.2.1 Zinc the element

Zinc is an element known from ancient times, being often used in conjunction with copper to make various brass alloys (N.N. Greenwood & Earnshaw 1998a). Two thousand years ago, Zn was known by the Romans as “false Silver” and used to make coins (Cammarota, 1980). The abundance of Zn in the Earth’s crust is about 0.02 %, 76 mg/kg (Greenwood and Earnshaw, 1998a) and it is the twenty third in the order of abundance of the elements (Jackson, 1988). It is more abundant than Copper and about abundant as Rubidium, and plays an important role in a wide range of natural and anthropogenic processes (N.N. Greenwood & Earnshaw 1998a). Zinc along with Cd and Hg belongs to group IIb (12) in the periodic Table, which is characterized as relatively low melting point elements (420 °C for Zn). Zinc has a high ionisation potential (9.39eV) which makes Zn difficult to ionize thermally (Platzner et al., 1997) which has significant implications in this work.

The atomic weight of Zn is 65.38 ± 0.02 , which was based on the mass spectrometric measurements of Ponzevera and his colleagues in 2006 (IUPAC, 2007). Zinc has five stable isotopes, ^{64}Zn , ^{66}Zn , ^{67}Zn , ^{68}Zn and ^{70}Zn , and twenty four radiogenic nuclides (Firestone and Shirley, 1998). In terms of nucleosynthesis, Zn has more in common with the Iron Group elements like Ni. The explosive nucleosynthesis has contributed to the synthesis of ^{64}Zn , whereas the heavier isotopes ^{67}Zn , ^{68}Zn and ^{70}Zn are thought

to be synthesized by “s process”. According to Umeda and Nomoto (2002), the main nucleosynthetic production site and processes for Zn have not been clearly identified. The possibility that Zn is mainly produced by s-processes is not consistent with recent observations for the ratio of Zn to Fe and Zn to He in massive Population III stars (Umeda and Nomoto, 2002)

1.2.2 Natural abundance of Zn

The widespread natural abundance and use of Zn, and its distribution in the environment has significant implications for this project e.g. obtaining sufficient sample, and in sample contamination. Zinc is widely used for the protection of steel by galvanizing, various plating and alloys, paper production, and as a chemical compound in rubber and paints (Wilber et al., 1980). Zinc is the fourth most commonly used metal after Fe, Al and Cu (Nriagu and Pacyna, 1988, Cammarota, 1980). The mining and widespread use of Zn has made it an important source of metal pollution. Most of the anthropogenic emission is due to the production and industrial usage of Zn (Nriagu & Davidson 1980; Nriagu & Pacyna 1988). Twenty percent of the natural emissions come from vegetation, while 5 to 15% of the natural emission of Zn to the atmosphere comes from forests fires or volcanic aerosols. There are many factors that control the level of Zn in the ambient air, wind entrainment of Zn contaminated soil particles, and the aging history and deposition of atmospheric aerosols. Airborne aerosols at remote locations are characterized by high Zn enrichment relative to the crustal rock or to average soil. The lowest Zn concentration measured worldwide in aerosols is $30 \pm 11 \text{ pg/m}^3$, (Nriagu and Davidson, 1980, Zoller et al., 1974), while the maximum concentration of Zn is $78 \mu\text{g/m}^3$, measured above the hot vent of Mount Etna in Sicily in 1978 by Menard and Arnold (Nriagu and Davidson, 1980).

The isotopic composition and abundance of Zn in meteorites has application in cosmochemistry. It has been predicted that 50 % of Zn has been condensed from a gaseous mixture in the solar nebula with solar abundance at 600 K and pressure of 10^{-4} atm (Loss et al., 1990). Since Zn is a relatively volatile element, relative to solar abundance (Solar abundance) it is found in excess in some meteorites and depleted in others. Observed chemical fractionation of moderately volatile elements like Zn that

evaporate or condense at temperature range (650-1350 K) in the early solar nebula could be inherited from the interstellar system (Yin, 2004). The volatility and other characteristics of Zn is very important and could explain a fractionation in the isotopic composition of the element in the processes of forming the planets (Luck et al., 2005a).

Despite the fact that Zn is essential for the physiological processes, it is toxic in elevated concentrations (Shubina and Kolesov, 2002). A number of studies have been carried out to measure the contamination of Zn in the environment (Beyer et al. 2004; Elberling et al. 2002; Madany, Akhter & Al Jowder 1994; Revitt, Hamilton & Warren 1990; Weatherley, Lake & Rogers 1980).

Natural Zn concentrations in the environment range from 2 to 100 pgg^{-1} in sea water, $\sim 300\text{ng}/\text{m}^3$ in air, 100 pgg^{-1} to 50 ngg^{-1} in fresh water, and 100 μgg^{-1} in sediments (WHO, 2004). In river waters, the natural Zn background is between 0.06–0.6 ng/g in relatively undisturbed rivers like those of the Ohio valley (Shiller and Boyle, 1985). The concentration of Zn varies in water such that, under certain circumstances, e.g. tap water can provide up to 10% of the daily intake (WHO, 2004).

- Anthropogenic inputs

The range of Zn as a pollutant is narrow, and depends on many factors, for example, its toxicity, stability, abundance, and its ability to accumulate in the environment. In addition, the range of Zn as a pollutant may be extended depending its compounds (Shubina and Kolesov, 2002). Environmental pollution of Zn has been the focus of many studies, for example; pollution of Zn in soil due to acid rain (Lacatusu et al., 1999), and pollution of Zn in river sediments (Ouyang et al., 2002).

Anthropogenic Zn is a major contributor to the concentration of Zn found in many natural environments. For example, the study of John et al. (2007) measured the isotopic composition of Zn in number of artificial materials in order to investigate the range of Zn fractionation in anthropogenic products with the intention of utilizing the

isotopic composition of Zn as an environmental tracer of anthropogenic contamination (John et al., 2007).

1.2.3 Mass spectrometry of Zn

Recent advances in Mass spectrometry, such as Multiple Collector -Inductively Coupled Plasma -Mass spectrometry (MC-ICP-MS) have opened up the use of intermediate mass elements (mass 20 to 100 amu), which includes Zn, to a wide range of applications. However, the use of MC-ICP-MS is not always the most favourable analytical option for all isotope systems or users (Fantle and Bullen, 2008). Now that Zn isotopic compositions are being measured in wide range of geological and biological materials, the complexities related to the use of MC-ICP MS for precise Zn isotopic ratio measurements are also becoming more apparent (Petit et al., 2008). For example, no mass spectrometric technique is viable in cases where an internal spike is used, and there is an unavoidable interference at one of the spike masses. Since the high energy environment of the plasma source favours the formation of a variety of molecular interferences not seen in TIMS instruments, using a spike with MC-ICP-MS in some cases may prove impossible (Fantle and Bullen, 2008)

Until recently, very little was known about the isotopic composition of Zn in natural materials, most likely due to the fact that it is difficult to produce uncontaminated Zn ion beams of measurable intensity and stability from any reasonable ($\mu\text{g Zn}$) size sample. The pioneering study of Rosman (1972) attempted to measure variation in the isotopic composition of Zn in natural materials, and concluded that thermal ionisation was unsatisfactory for the production of Zn ions for isotopic analysis. Rosman attributed his results to the high ionisation potential of Zn (9.39eV), which led him to investigate the presence of Zn isotopic variation using electron impact ionisation (Rosman, 1972a). No further Zn isotopic fractionation investigations were performed until 1999, when Marechal and her colleague developed a technique to investigate Zn fractionation using magnetic sector MC-ICP-MS and since then all published data has been performed using MC-ICP-MS. As for a number of other

transition metals overcoming these difficulties to produce relatively long-lived and stable ion beams from microgram-sized samples is a non-trivial task (Fantle and Bullen, 2008). The challenge to generate sufficient ions, particularly from small samples, is described in Section 3.1.3.2 in which the ionisation efficiency of Zn measured in this research is presented.

Another challenge for Zn isotopic analyses arises from the fact that Zn is ubiquitous in the environment and present in all natural and anthropogenic systems. Accurate analyses require ultra-clean procedures and techniques to control contamination during sample handling and processing (Martin et al., 1980). Zinc isotopic analyses also require that isobaric elements, like Ni and other possible interfering elements and their oxides, like CrO, FeO, and VO are thoroughly removed from the sample. In addition, elements such as Alkali and Alkaline Earths suppress the ionisation of Zn reducing overall ion beam intensity (Ghidan and Loss, In preparation).

In this dissertation, one of the aims was to focus on the establishment of a reliable technique for Zn isotope analysis by TIMS. These procedures solved problems that arose during Zn analyses that are not published elsewhere because this is the first time an investigation for Zn fractionation has been performed using TIMS and double spike. This should assist future researchers with the isotopic analysis of Zn and possibly other transition elements, and help them to develop new analytical techniques.

The fact that no Zn isotopic fractionation research has been performed using TIMS prior to this work is also related to both perceived and actual difficulties. For example, the requirement for extensive and sometimes complex sample preparation, creating and calibrating a double spike, long analytical times per sample, eliminating low-level interferences, and attaining stable and large ion beams. These aspects are discussed in detail in Sections 4.2, 3.4, 3.5, 3.8, 3.9 and 3.6. These issues are also similar for other transition elements like Fe (Fantle and Bullen, 2008). A comparison of the amount of Zn in the sample used in this work relative to other relatively same ionisation potential transition elements and Ca is shown in Table 3.3 in Section 3.4 (sample loading, degassing and heating). Tackling these difficulties and requirements

are essential in this research as described in the following Sections (the aims of the research).

1.3 Aims of the research

- To develop Zn TIMS measurement techniques and in particular to address critical analytical issues such as, interferences, ionisation efficiency, sample contamination, and the, up to now ignored issue of the contribution of the sample processing to the measured fractionation. This will assist Zn isotope and other transition element analysts to further develop new analytical techniques; this is more explicitly detailed in Chapter three.
- To provide a baseline metrological Zn isotopic compositions to the international scientific community to be exploited for future Zn investigations. This was to be performed by measuring Zn fractionation of standard reference materials (SRMs) relative to the absolute isotopic composition of Zn (δ zero). In addition, the isotopic compositions of a range of pure Zn standard metals were be investigated, so that comparison between researchers can be obtained. The absolute isotopic compositions of Zn in these materials are represented in Chapter five.
- To determine the actual existence and extent of Zn fractionation in nature. Zinc fractionation was investigated in number of geological, biological, extra terrestrial, and processed materials, using a rigorous double spike technique. These results are represented in Chapter five. It was not intended to identify the causes of fractionation or to study fractionation in detail within a specific system.
- To provide general insights into Zn isotopic fractionations found in a wide range of natural materials in an attempt to understand any general systematic Zn fractionation in nature. Discussions regarding, and possible outcomes of the results are presented in Chapter seven.
- Measure the concentration of Zn in natural materials using the accurate and precise Isotope Dilution Mass Spectrometry (IDMS) technique. In particular, the

results obtained for the SRMs will assist the analytical community in developing techniques and for analytical comparative purposes. Zinc abundances in all measured samples are presented in Chapter four and further discussed in Chapter six.

1.4 Significance and application

The significance and the application of this work are summarized as follows:

1.4.1 Analytical technique development

This research is the first to utilize Thermal ionisation mass spectrometry (TIMS) for Zn isotopic fractionation analyses also using a double spike. Previous research by Rosman (1972) concluded that thermal ionisation technique is not capable of producing sufficient ions for Zn isotopic analyses, and could not reveal sub permil Zn fractionation using the electron impact ionisation mass spectrometry. All other, recent analyses are performed using MC-ICP-MS analyses, which according to Petite (2008) has many analytical difficulties including, effects of spectral and non-spectral interferences. Moreover, this research seeks to develop a TIMS Zn isotopic analysis technique which solves critical analytical issues such as the size of the sample, interferences, ionisation efficiency, sample contamination, and the generally underestimated issue of the contribution of sample processing to fractionation.

1.4.2 Systematic study of the existence and extent of Zn fractionation in nature

The first comprehensive investigation of the isotopic composition of Zn was a study by Rosman in 1972 (Rosman, 1972a), but this study was not precise enough to detect sub permil fractionation. Recently Albarède heralded that:“ it must be emphasized that we are at a very early stage of Cu and Zn isotope geochemistry” (Albarède, 2004). Natural Zn fractionations have not been absolutely and or accurately measured prior to this research. This is primarily because of analytical difficulties associated with the use of MC-ICP mass spectrometers, for example, effects of spectral and non-spectral interferences (Petit et al., 2008). Wilkinson et al. (2005) stated that, little is known about the extent of Zn fractionation on the Earth, and extraterrestrial materials, and the processes that control Zn fractionation.

1.4.3 Use of the double spike technique

This work uses the double spike technique to determine Zn isotopic fractionation in all samples. In comparison, other techniques have significant limitations; for example, when it comes to the correction for instrumental mass bias and the contribution of separation Zn using ion exchange chemistry to the fractionation. These limitations have made many claims of Zn fractionation measurements doubtful, both in terms of existence and accuracy. The double spike technique was last used for Zn by Rosman (1972) but the results obtained were not precise enough to detect fractionation of less than 1 ‰ amu⁻¹. Significant advances in instrumentation, combined with the use of double spiking, thermal ionisation and new technique development, should enable an order of magnitude smaller fractionation detection limit to be achieved. Another advantage of the double spike technique is that it enables the concentration of the element to be simultaneously determined. Zinc has five stable isotopes, which makes it possible to apply the double spike calculations using at least two semi independent sets of isotopes so that quality control can be performed.

1.4.5 All measured fractionations are relative to (δ zero) proposed absolute.

The increasing number of measurements, interpretations and applications of the isotopic fractionations of Zn, often involving work done in other laboratories, highlights the need for an internationally accepted “absolute isotopic composition” materials. Without such materials, confident inter-laboratory comparisons cannot be made. At present, an absolute isotopic composition material is not available for Zn. If the fractionation of Zn exists and it is small then the isotopic composition difference between the samples and the reference becomes more important than the actual isotopic composition of the sample (De Laeter, 2004). In addition, to assess the effect of Zn fractionation on the atomic weight of Zn requires the international acceptance of a standard reference material (De Laeter, 2004).

In this work, Zn fractionation for all samples was to be measured relative to a laboratory standard, taken from the same metallic reservoir as the IRMM 3702 (Ponzevera et al., 2006) which is the (δ zero) standard the International Union for

Pure and Applied Chemistry (IUPAC). Measurement relative to this internationally recognised standard will result in internationally accepted absolute isotopic compositions. Accurate results of this type will contribute to development of a systematic explanation for why and how Zn fractionation occurs, and more importantly Zn isotope abundances application in other sciences.

The laboratory standards used as references and the type of materials and methods used in the isotopic fractionation measurements of Zn is shown in Table 1.1.

Table 1. 1: A summary of the different laboratory standards used as reference, type of materials and methods to measure the isotopic fractionation of Zn. The name of the method is as shown in the relevant reference.

Research	Year	Laboratory standard	Material	Method
Rosman	1972	JMC	Natural materials	Electron impact ionisation mass spectrometry
Marechal et al.	1999	JMC 3-0749 L	Natural samples	plasma-source mass spectrometry
Tanimizu et al.	2002	JMC Zn	Pure Zn metals	ICPMS
Pichat et al.	2003	JMC 3-0749L	Oceanic sediments	MC-ICP-MS
Stenberg et al.	2004	Alfa Aesar, Johnson Matthey GmbH, Karlsruhe; (lot NM00558).	Human biological materials	Sector filed MC-ICPMS
Stenberg et al.	2005	Laboratory standard, “lot NM00558; Alfa Aesar, Johnson Matthey	in healthy humans and hemochromatosis [§] sufferer’s whole blood	(MC-ICP-SFMS)
Mason et al.	2005	JMC Zn 3-0749 L	Volcanic ore	MC-ICP-MS

[§] Excessive absorption of dietary iron resulting in a pathologic increase in total body iron stores

Luck et al.	2005	(JMC) 400882B	Meteorites	IC-PMS
Chapman et al.	2006	Johnson Matthey (batch 3-0749L)	SRMs including BCR-1	MC-ICP-MS
Bermin et al.	2006	JMC 3-0749	Oceanic waters	ICPMS
Moynier	2006	JMC 3-0749	Meteorites and Lunar samples	ICP-MS
John et al.	2007	Lyons-JMC Zn	“common anthropogenic Zn products”	MC ICP-MS
Weiss et al.	2007	Johnson Matthey Purontronic Zn metal (Batch NH 27040)	peat bogs	GVi IsoProbe
John et al.	2008	“Lyon JMC”	Seafloor hydrothermal vent fluids and chimneys	ICP-MS
This work	2008	IRMM AE10759	Natural materials	TIMS-Double spike

1.4.6 Analyses of SRMs and common laboratory standards

Of significance to the wider scientific community is that most of the samples analysed in this work were selected from SRMs. The isotopic composition of such standard materials is vital to assess fractionation in similar materials using different analytical techniques. Except for BCR-1, this is the first time where Zn isotopic fractionation will be measured in these samples. The Zn concentrations will also be measured in these SRMs. Accurate analytical results will improve the exploitation of the SRMs and their application.

The absolute Zn isotopic composition for a variety of pure standard Zn materials provided by IRMM (Institute for reference materials and measurements) will also be investigated, and will serve as a valuable resource for analysts in order to measure Zn

fractionation relative to the “ δ zero”. This will assist analysts measuring Zn isotopic fractionation and enable them to compare their results unambiguously with others, hence contributing to greater understanding of Zn isotope fractionation.

1.4.7 Application of Zn fractionation systematics.

Isotopic fractionation measurements undertaken in this research can be applied to study a variety of systems, for example:

- **Geological**

Geological samples analysed in this work were chosen to cover the range of terrestrial rock types and selected Zn minerals to provide analysts with an indication of the fractionation present in these materials. The techniques and methods developed in this work will be applicable to address some important issues in the Earth Sciences and Solar System studies. For example, formation of base metal ore bodies, and oceanic circulation.

- **Biological**

Understanding the pathways of Zn and other transition elements within living systems is of great importance in biological and medical sciences. Variation in the isotopic composition of Zn is thought to occur stepwise along biological pathways (Zhu et al., 2002). Stenberg et al. (2004, 2005) measured Zn fractionation in human whole blood SRMs and used these results as a preliminary application to the study of HFE gene (see Section 2.2.2). These studies demonstrate the possibility for Zn fractionation to be utilized in medical research and to understand human health and disease status. Other biological applications include biological fractionation of Zn isotopes as interpreted by Pichat et al. (2003); as the depletion in the lightest Zn isotope in the surface water of the ocean during the biological blooms (Section 2.2.2). The “Zn hypothesis” by Morel et al. (1993) introduced Zn as a new tool to understand the exchange of CO₂ between the ocean and the atmosphere and to better understand climate change (discussed in Section 2.2.1). These investigations are different from those using enriched stable isotopes as tracers, which are preferred over the use of radioisotopes because of the associated dangers, but have limitations because of the cost associated with the production of enhanced stable isotopes.

- Anthropogenic processes

The wide spread use of Zn in industrial materials and as a by product of many anthropogenic processes results in the possibility of using Zn isotopic fractionation and concentrations to study environmental and other systems. For example, the study of John et al. (2007) used the variation in the isotopic fractionation as an environmental tracer. Measurements of the isotopic composition of Zn in number of artificial materials will be performed in order to investigate the range of Zn fractionation in anthropogenic products (John et al., 2007).

These aims, their significance, and applications are expanded on and placed into the context of the existing literature in the following Chapter.

- **Chapter 2: Literature review**

2.1 Early isotopic measurements.

One of the immediate applications of the discovery of isotopes was to explain the existence of non integer atomic weights. The first atomic weight determination of Zn as recognized by the International Union of Pure and Applied Chemistry (IUPAC) was performed in 1882 and set at “65.05±0.1” “as IUPAC it self represented the significant Figures” was determined by use of chemistry (IUPAC, 1997). The first non chemical determination of the atomic weight of Zn was carried out by Nier in 1936 who used a Mass Spectrograph to investigate the abundances isotopes of Zn (Nier, 1936). The study by Nier clearly showed the presence of the ^{64}Zn , ^{66}Zn , ^{67}Zn , ^{68}Zn and ^{70}Zn , which agreed completely with the earlier research of Bainbridge (1932). In his study, Bainbridge disputed the claim of Aston that the isotopes of ^{65}Zn and ^{69}Zn existed and demonstrated that the observed ions at mass 65 and 69 detected by Aston were not isotopes of Zn, but interferences in the form of hydrides of ^{64}Zn , and hydrides of ^{68}Zn respectively (Bainbridge, 1932). These disagreements were reconciled with Nier’s 1936 study, which clearly showed that there are no stable Zn isotopes at mass 63, 65, and 69 (Nier, 1936). Nier calculated the abundances of Zn isotopes ^{64}Zn , ^{66}Zn , ^{67}Zn , ^{68}Zn and ^{70}Zn , as 50.9%, 27.3%, 3.9%, 17.4%, and 0.5% respectively, yielding an atomic weight of 65.31. However, Nier could not explain the large difference between the chemical value of 65.38, and his mass spectrographic atomic weight value (Nier, 1936).

Hess, and his colleagues (1948), showed that Zn purification processes, by evaporation and its production by electrolytic or chemical reduction of the ore does not change its isotopic abundance (Hess et al., 1948). The isotopic abundance values obtained by Nier and the chemically determined value of the atomic weight were the accepted values for many years.

The link between these early isotopic abundance measurements determinations of atomic weights and this research, is that, the uncertainties in the values of the atomic weights arises entirely from limitations in the accuracy of isotopic abundance

measurements. This was heralded many years ago by the International Commission of Atomic Weights (Cameron and Wichers, 1962).

2.2 Isotopic composition and concentration of Zn in terrestrial materials:

2.2.1 Concentration of Zn in natural materials

Researchers have emphasized that the analyses of SRMs are pivotal, to inter laboratory comparisons, and so that new techniques can be developed (De Laeter, 2004). However, all techniques and or analysts do not produce the same results. An example of is show in Figures 2.1 (Zn SRM, IMEP -19 Rice) and 2.2 (SRM. BIR-1)

Figure 2. 1: The concentration of Zn in IMEP -19 Rice as measured by different analysts and techniques(IRMM, 2003).

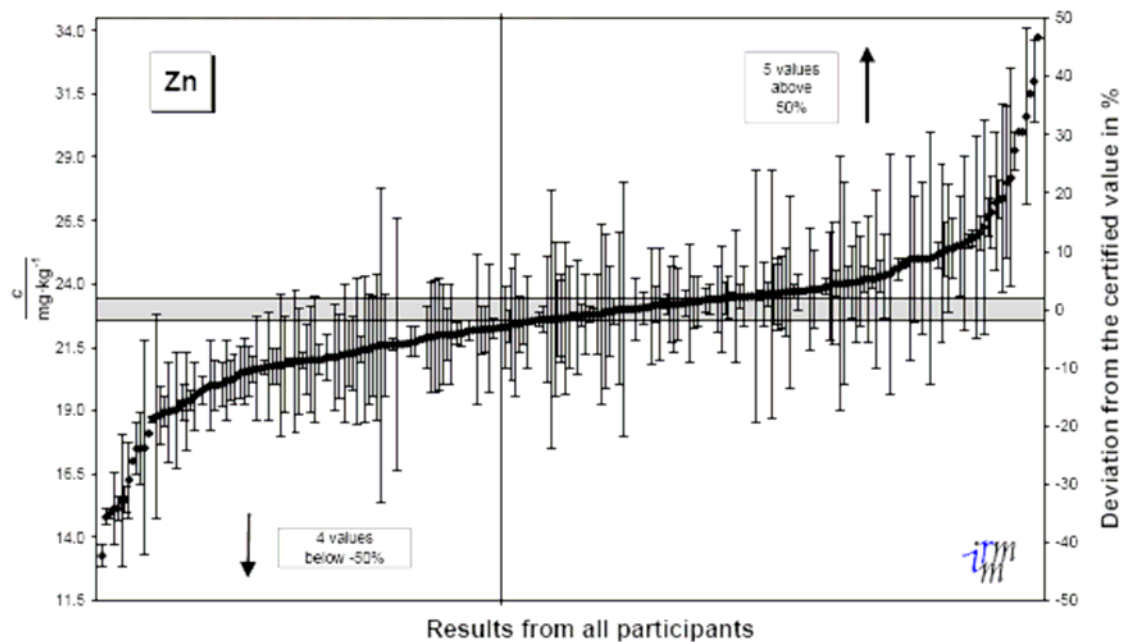
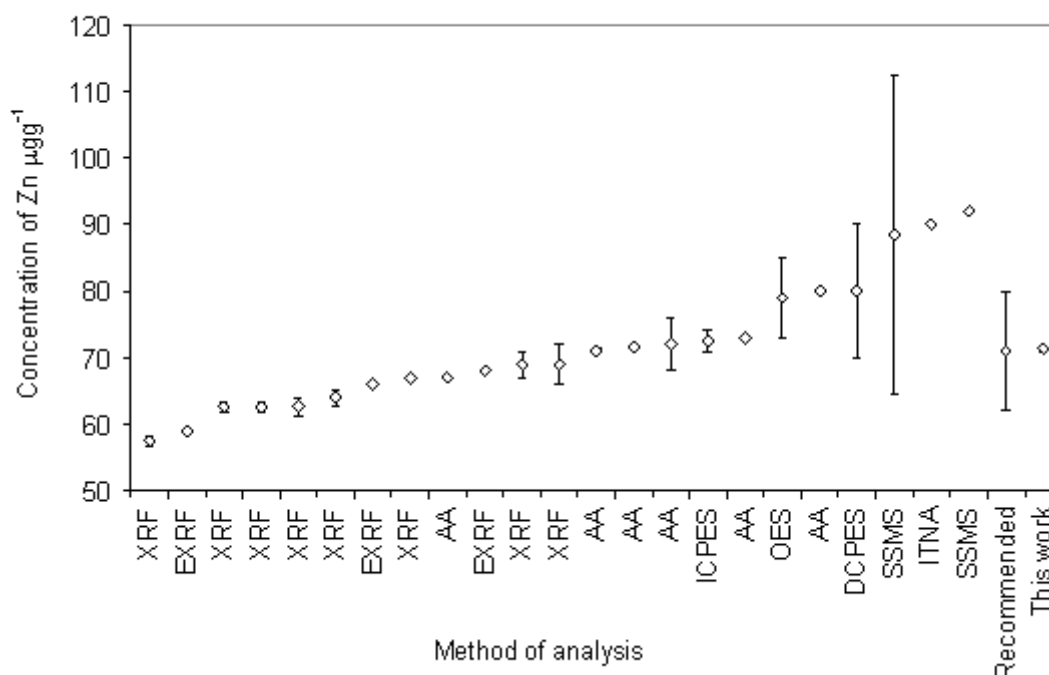


Figure 2. 2: The concentration of Zn in the BIR-1 SRM as measured by different techniques for BIR-1 SRM. Data taken from (Gladney and Roelandts, 1988)



One elemental abundance technique, widely recognised as the “gold standard”, is IDMS. This technique offers many advantages in terms of accuracy, and plays prominent role as a primary method of measurement, which is traceable to the atomic scale. IDMS is also insensitive to loss of element of interest during sample processing after addition of the spike. The disadvantages of IDMS is that, it requires more time, effort and expertise, hence, for these reasons this method is not always suitable for routine use (Mestek et al., 2001). IDMS is discussed detail in Section 3.7.1.

The concentration of Zn in SRMs using IDMS was first performed by (Rosman and Jeffery, 1971). In their study, they measured the concentration of Zn in eighteen SRMs, from five different sources by IDMS, and atomic absorption spectrophotometry, and demonstrated that the isotope dilution technique was more accurate than the atomic absorption method. Rosman and Jeffery (1971) believed that their study could be useful to resolve some of the reported discrepancies between determinations performed in different laboratories.

In two studies by Rosman (1972a, 1972b), which also aimed to measure Zn fractionation in meteorites, the concentration of Zn in number of terrestrial materials using the IDMS was found to range from ($<0.08 \mu\text{gg}^{-1}$ to $90 \mu\text{gg}^{-1}$).

In 1974, Rosman and De Laeter used the IDMS to measure Zn concentration in meteorites and examine the relationship between the abundance of Cd and Zn in their samples. The concentration of Zn in stone meteorites was found to vary from $1.3 \mu\text{gg}^{-1}$ to $535 \mu\text{gg}^{-1}$ for stony and $0.07 \mu\text{gg}^{-1}$ to $76 \mu\text{gg}^{-1}$ for the iron meteorite. As the study of Rosman (1972); Rosman and De Laeter (1974) showed that the abundance pattern of Zn supports the existence of chemical groups in iron meteorites. They emphasized that the inhomogeneity in the concentration of Zn in meteorites could be the main contributor to their ranges, and considered the interpretation of Larimer and Anders, “the abundance of the elements in meteorites depends merely on the physiochemical conditions of the condensing solar nebula” as an interpretation for the inhomogeneity (Rosman and De Laeter, 1974). Recently, the concentration of Zn in lunar soil samples have been measured and found to vary from 6 to $140 \mu\text{gg}^{-1}$, which is similar to terrestrial basalt (Moynier et al., 2006).

The concentrations of Zn in Allende bulk meteorite, and acid residues, were measured using the IDMS technique by Loss and his colleagues in 1990. According to their results, the concentrations of Zn were $112 \mu\text{gg}^{-1}$ in bulk Allende meteorite, CE-1; $230 \pm 15 \mu\text{gg}^{-1}$, CF-1; $148 \pm 2 \mu\text{gg}^{-1}$ and CG-1 with Zn concentration of $480 \pm 10 \mu\text{gg}^{-1}$. The concentration of Zn in Allende measured by Loss and his colleagues in 1990 ($112 \mu\text{gg}^{-1}$) is closely the same as that measured by Rosman and De Laeter in 1974 ($111 \mu\text{gg}^{-1} \pm 3 \%$).

There are many theories and hypotheses concerning the distribution of Zn in seawater. For example, one hypothesis by Slowey and Hood (1971) explains that, the concentration of Zn is greater in the intermediate water because of the sinking of decomposed organisms from the surface, and living organisms in the intermediate

water column, this releases soluble Zn in the intermediate deeper water (Slowey and Hood, 1971).

A new theory regarding the importance of the abundance of Zn in the oceans was introduced by Morel and his colleagues in 1994. A limitation on biological productivity is determined by what is known as the “Zn Hypothesis”, which states that: if the Zn concentration in the ocean is low enough it may limit the oceanic production and influence the carbon cycle (Morel et al., 1994b). This is due to the HCO_3^- uptake by marine phytoplankton, which is important to process the Carbon uptake and is controlled by the concentration of inorganic Zn in the ocean (Morel et al., 1994b).

An excellent example for the application of the study of Zn in the environments is the study of Candelone et al. (1996), the concentration of Zn was studied in 36 Ice samples taken from Greenland covering a continuous period of two years (Spring 1990 to Summer 1992). Despite the fact that this study was performed using Graphite Furnace Atomic Absorption Spectrometry (GFAAS), it is worth mentioning the range of concentration of Zn in this study (from 9-194 $\mu\text{g g}^{-1}$) (Candelone et al., 1996). Another study measured the concentration of Zn in Ice using the (GFAAS) was the study of Hong et al. (1996). Their samples were collected from central Greenland, suggesting that the concentrations of Pb, Cu, Zn and Cd were high during the Saal glacial period 150,000 a ago, and low during the Eemian interglacial period 128,000 ago. From 96,000 to 14,000 a ago; e.g, during the last ice age, the concentrations of all four metals are highly variable, with high concentrations during the stadial (cold) stages, especially during the Last Glacial Maximum, and rather low concentrations during the interstadial (milder) stages. Their results revealed that climate changes have led to large variations in the concentration of Zn in the high latitude troposphere of the northern Hemisphere. (Hong et al., 1996).

The concentration of elements in Fish otolith has revealed important findings in relations to the immigration of fish. In a study by Campana and his colleagues (1995) which measured the concentration of Zn using the ID-ICP-MS in number of Cod otolith (*Gadus morhua*) sampled from six sites in the eastern coast of Canada. The

mean concentration of Zn in the six sites ranged from 0.31 to 1.75 $\mu\text{g g}^{-1}$, and concluded that ID-ICP-MS was an effective discriminator of adjacent populations of the Atlantic Cod. Classification of samples collected from winter cod fishery on the eastern Scotian shelf indicated the annual winter migration out of the gulf of St. Lawrence is more extensive than was previously believed (Campana et al., 1995). An environmental study carried out by Monna and his colleagues in the University of Montpellier II in France 1995, measured the contamination of Zn and the source of its mobilization in a coastal pond in southern France along the Mediterranean Sea, which presents many potential sources of pollution. The isotopic composition of Pb was used to evaluate the effects of pollution and also to trace their origins. Their results yielded a concentration of Zn in water < 35 ppb in the coastal pond. In comparison, the concentration of Zn from other sources was; water treatment plants output (3.43 \pm 0.07 ppb to 23.09 \pm 0.73 ppb), untreated water(8.66 \pm 0.19 ppb to 87.57 \pm 2.25 ppb), water samples taken from highway filtration tanks (0.30 \pm 0.24 ppb to 362 \pm 24 ppb), rain water (21.65 \pm 0.87 ppb to 39.7 \pm 1.1ppb), water taken from Vene River (0.55 \pm 0.02 ppb to 24.19 \pm 0.34 ppb) (Monna et al., 1995).

Another study to measure the concentration of Zn in biological samples using the accurate IDMS technique was carried out by Patterson and his colleagues in 1992 in the department of human nutrition and food system at the University of Maryland, USA. The study investigated the concentration of natural Zn in standard reference materials; bovine liver SRM 1577a, bovine serum SRM 1598 and dried milk powder SRM1549. Their results were: 122 \pm 0.1 $\mu\text{g g}^{-1}$, 0.90 \pm 0.02 $\mu\text{g g}^{-1}$, and 45.7 \pm 2.2 $\mu\text{g g}^{-1}$, respectively. The researchers commented on the results as they were in excellent agreement with certified values (Patterson et al., 1992). Another study on standard materials was done in 1998 by Li and Jiang of the National Sun Yat-Sen University – Taiwan, who measured the concentration of Zn in standard fish samples using electro isotope dilution inductively coupled plasma mass spectrometry technique (ID-ICP-MS) and obtained the following results; for dogfish muscle reference material (DORM-2), dogfish liver reference material (DOLT-1) and oyster tissue (NIST SRM 1633a), of 24.3 \pm 1.4 $\mu\text{g g}^{-1}$, 92.3 \pm 3.0 $\mu\text{g g}^{-1}$, and 783 \pm 36 respectively, which agreed with the certified values of these samples (Li and Jiang, 1998). In another fish otolith study using the IDMS technique; Yoshinaga et al. in 1999, stressed the importance of

the IDMS technique in order to meet the growing demand for the quality control of fish's otolith element analysis, and the SRMs, in developing a routine analytical method and interlaboratory calibrations (Yoshinaga et al., 1999).

In 2001, the concentration of Zn in plants samples were measured using IDMS technique, by Mestek and his colleagues, including a number of certified reference plant samples such as “NIST - SRM1568a” Rice flour. The study was performed using ICP-MS with a quadrupole mass filter and the ion exchange separation. According to Mestek and his colleagues study, all results were found to agree with the certified values (Mestek et al., 2001).

A very important study carried out in University of Oviedo, Spain to measure the concentration of Zn in human biological samples using ID-ICP-MS technique. The aim of their study was to establish a reference value for normal Zn, and other trace elements levels in healthy people of Asturias – Spain. Concentrations were found to be in the range of (0.69-1.01) $\mu\text{g g}^{-1}$ which agreed with the overall reference concentration ranges. Their measured concentration of Zn in standard serum reference material (NIST SRM 1598) was found to be $0.899 \pm 0.006 \mu\text{g g}^{-1}$ which agrees with the certified value of $0.89 \pm 0.06 \mu\text{g g}^{-1}$ (Muniz et al., 1999). There have been many other studies performed to determine the concentration of Zn in human biological samples such as human faeces, urine, and a serum samples (Sturup, 2000).

2.2.2 Isotopic composition of Zn in natural materials

The first survey of the isotopic abundances of Zn in wide range of terrestrial materials, organic materials, Zn ore body, sea water, meteorites and tektites and SRMs was the pioneering work of Rosman (1972). Rosman used the double spike technique (described in detail in Section 3.7.2) to investigate the variation in the isotopic composition of Zn but detected no variations within uncertainties of about 1‰ amu^{-1} (95% confidence) (Rosman, 1972b). The measured Zn isotopic abundance of Zn by Rosman and others is summarized in the Table 2.1.

Table 2. 1: Abundance of the isotopes of Zn as measured by different researchers.

Researcher	Abundance %				
	⁶⁴ Zn	⁶⁶ Zn	⁶⁷ Zn	⁶⁸ Zn	⁷⁰ Zn
(Nier 1936)	50.9	27.3	3.9	17.4	0.5
(Hess et al., 1948)	48.9	27.82	4.17	18.48	0.623
Leland & Neir 1950	48.89	27.81	4.07	18.61	0.62
(Rosman, 1972b)	48.63 ± 0.13	27.9 ± 0.08	4.10 ± 0.03	18.75 ± 0.16	0.62 ± 0.01
(Loss et al., 1990)	49.1843 ± 0.0079	27.769 ± 0.016	4.0321 ± 0.0004	18.415 ± 0.003	0.5996 ± 0.0039
(Chang et al., 2001)	48.268 ± 0.214	27.975 ± 0.051	4.102 ± 0.041	19.024 ± 0.82	0.631 ± 0.006
(Tanimizu et al., 2002)	49.188 ± 0.030	27.792 ± 0.041	4.041 ± 0.009	18.378 ± 0.050	0.600 ± 0.003
(Ponzevera et al., 2006)	49.17040 ± 0.00017	27.730629 ± 0.000096	4.040135 ± 0.000014	18.448241 ± 0.000064	0.610560 ± 0.000003

Since 1972 Zn isotope research has focused mainly on measuring the concentration of Zn in natural materials. In the same study by Loss et al. (1990) which measured the concentration of Zn in bulk and acidic residues of Allende meteorites, they also measured the Zn isotopic composition relative to their laboratory standard. The intension of this work was to search for isotopic anomalies hence their isotope ratios were normalized relative to $^{68}\text{Zn}/^{64}\text{Zn} = 0.37441$ of Rosman (1972), but no significant anomalies were found within their sub epsilon (parts in ten thousands) detection limit. In the same year, the results of another study on the Zn isotopic composition in Allende meteorite inclusions were reported. The aim of their study was to investigate astrophysical models which predicted large excesses of ^{66}Zn to accompany excess in the neutron-rich isotopes of Ca, Ti, Cr, and Ni (Loss and Lugmair, 1990). As will be discussed in Section 7.4.2, they discovered a very small ($<1\epsilon$) but resolvable excess in ^{66}Zn . This result, along with a similar anomaly reported

by Volkenning and Papanastassiou (1990), were the first Zn isotopic anomalies reported in the literature.

As mentioned in Section 2.2.1, and as part of an IDMS Zn concentration measurement, Patterson and his colleagues in 1992 (Patterson et al., 1992) measured the isotopic ratios for human biological materials. One aim of their research was to ascertain whether or not isotopic and other interferences existed. To assess this; they measured the isotopic composition of Zn in the sample following digestion without spike, Zn was extracted and made ready as a solution to be measured on the ICP-MS using a special extraction procedure (Serfass et al., 1986). The least likely of the isotopes to have interference was used as the denominator for the isotopic ratios. Their results are as shown in Table 2.2

Table 2. 2: Isotopic composition of Zn in biological samples compared to a Zn standard (Patterson et al., 1992). The uncertainties here are the fractional uncertainties are calculated from the literature as in Patterson et al. (1992)

Ratio	Expected value	Zn Standard	Breast Milk	Urine	Serum
$^{67}\text{Zn}/^{66}\text{Zn}$	0.147	0.1470 ± 0.53	0.1472 ± 0.78	0.1476 ± 0.82	0.1475 ± 0.73
$^{68}\text{Zn}/^{66}\text{Zn}$	0.672	0.6720 ± 0.55	0.6719 ± 0.56	0.6713 ± 0.72	0.6720 ± 0.43
$^{70}\text{Zn}/^{66}\text{Zn}$	0.0223	0.0222 ± 1.12	0.0224 ± 1.52	0.0222 ± 1.12	0.0221 ± 1.16

It is significant that the researchers considered the isotopic composition of Zn was invariant in nature and were not aware of “variations in the isotopic composition of Zn”, or “Zn isotopic fractionation”. As shown in Table 2.2, the measured isotopic ratios of Patterson and his colleagues “as they thought that time” were close to “theoretical values”. Patterson and his colleagues; thought that they had demonstrated that the isotopic composition if Zn in biological materials was the same as the isotopic composition of Zn in nature. The researchers also concluded that there were no interferences in their measurements. Because the isotopic composition of Zn was thought to be invariant, Patterson and his colleagues stated that, “ if unspiked natural

biological samples do not give the same abundance ratios as the natural Zn standards do, there are interferences present which would cause inaccuracy in the isotope dilution method” (Patterson et al., 1992). Given the large measurement uncertainties, the study of Patterson and his colleagues was clearly unable to detect small sub permil Zn fractionation.

A more significant isotope anomaly for Zn was found during the study of the Vigarano meteorite by Loss et al. (1994) (Loss et al., 1994). Using TIMS, an anomaly was found in a FUN inclusion of $-6.5 \pm 1.5 \text{ ‰}$ (where ‰ is a difference of one part in 10000) on the ^{66}Zn relative to their laboratory standard, which; Loss and his colleagues described as a deviation from the “normal isotopic composition”. The researchers used this result and other cosmochemical data to conclude that large scale inhomogeneity of the condensates existed in the solar nebula (Loss et al., 1994).

This was the case until 1999 when Marechal and her colleagues in “*Laboratoire de sciences de la Terre*” in Lyon -France, developed a procedure to measure the isotopic composition of Zn and Cu in natural samples of Ores, silicates, and biological materials. Using a plasma source mass spectrometer isotopic measurements were performed relative to their laboratory standard with a claimed external precision of 0.04‰ 95% confidence level. In their study, Marechal and her colleagues first applied the “elemental spike” technique to correct for instrumental mass fractionation of Zn. This technique uses an absolute isotopic composition of another element (Cu) which is added to the sample prior to purification by anion-exchange chemistry and analysed in the mass spectrometer to correct for machine bias. As will be discussed in Section 7.1 this technique has significant limitations in terms of accuracy considering they claimed a Zn fractionation of less than 1 permil. The results obtained were, $^{66}\delta \text{Zn} = 0.18 \text{ ‰}$ to $^{66}\delta \text{Zn} = 0.33 \text{ ‰}$ for sedimentary materials, $^{66}\delta \text{Zn} = 0.41 \text{ ‰}$ to $^{66}\delta \text{Zn} = 0.82 \text{ ‰}$ for biological materials, and $^{66}\delta \text{Zn} = -0.19 \text{ ‰}$ to $^{66}\delta \text{Zn} = 0.44 \text{ ‰}$ for Ores (Marechal et al., 1999). These results were the first to claim variability in the isotopic composition of Zn in natural materials Maréchal et al. (1999) did not present any interpretations of their results, although they suggested that the contribution to the fractionation of the purification of Zn by using column chemistry was small when compared to that of Cu. A break through in the field of Zn fractionation was made when they found that the resin appeared to fractionate the isotopic composition of Zn;

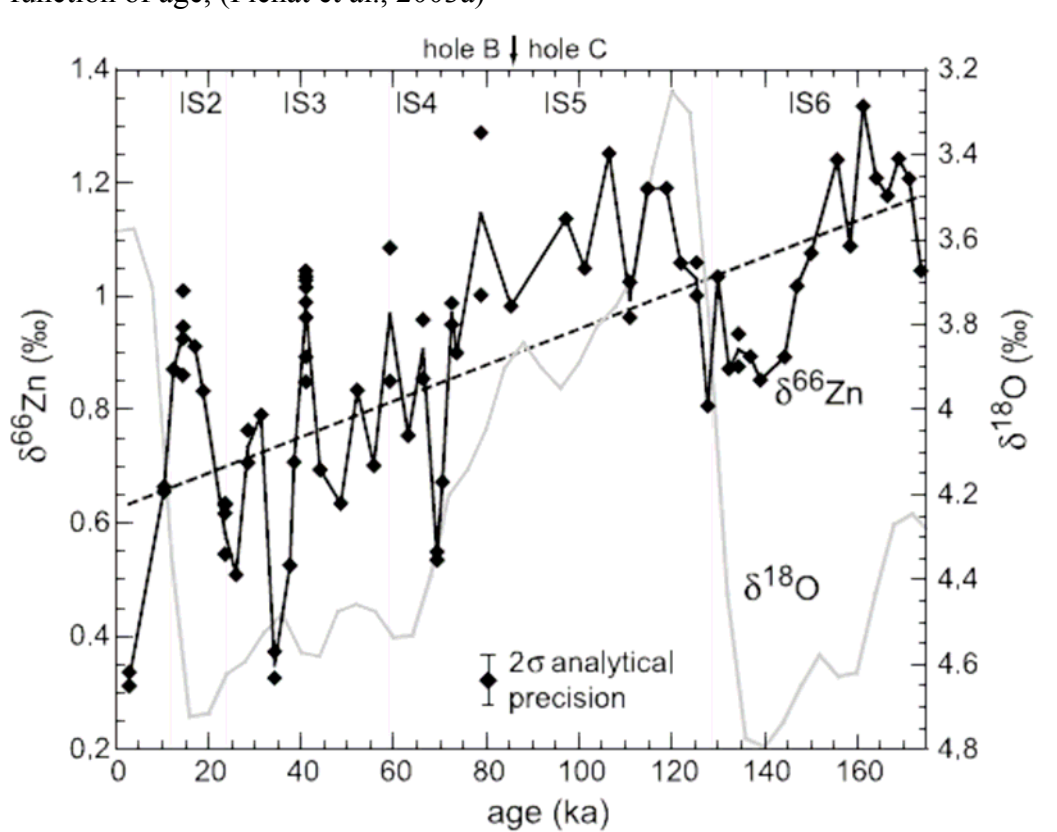
such that the lighter Zn isotopes are preferentially retained by the resin. Maréchal suggested that Zn is isotopically fractionated less than the Cu because Zn only has one oxidation state whereas Cu has three (Marechal et al., 1999), but did not attempt to demonstrate this experimentally. In the following year, Marechal and her colleagues claimed to identify the presence of Zn fractionation in ferromanganese nodules, sediment trap samples, sediments, and organic reference materials. They explained that the sediment trap samples, which were collected from up welling of the coast of Mauritania (Central Atlantic)-showed a seasonal isotopic fluctuation, consistent with biological pumping during the high –productivity period. However, Zn variations in nodules showed an association with the amplitude of seasonal variations rather than with biological productivity (Maréchal et al., 2000).

Because the measured atomic weight and its uncertainty is affected by a possible variation in the isotopic composition, Tanimizu and his colleagues in 2002 investigated possible variations in the isotopic composition of five Zn reagents: JMC Johnson Matthey, NIST-SRM 682, NIST-SRM 683, Nilaco and Cica-Merck. Measuring the deviation from the standard in the samples relative to the JMC Zn, they found that the reagent NIST-SRM 682 was clearly different from other reagents by about 1.2‰ amu⁻¹, with depletion of the heavier isotopes (see Table 2.1). This mass dependent fractionation of NIST –SRM 682 was significant in that they claimed that it reduced the atomic weight of Zn relatively from 65.3756 to 65.3732 (Tanimizu et al., 2002).

In March 2003, a study was carried out by Pichat and his colleagues in “*Laboratoire de Sciences de la Terre*” in France, to investigate if Zn isotopic variations existed in the carbonate fraction of oceanic sediments. If these variations existed; whether they could be used as a paleoceanographic proxy; such that changes in the biological productivity in the equatorial Pacific could be monitored. The rationale was, because the carbonate fraction is composed of shells and fragments, which are the most likely to record biologically, linked changes in the isotopic composition of Zn. In their study using MC-ICP-MS, Pichat and his colleagues measured variations in fractionation of Zn, as ⁶⁶δ, and as a function of the age of the sediments, and obtained a range of ⁶⁶δ of between 0.31‰-1.34‰ relative to their laboratory standard Zn JMC 3-0749L, this is 25 times larger than their overall claimed analytical precision of 0.04‰ (Pichat et al.,

2003a). The measurement is represented in Figure 2.3. It is important to note that this important study was performed using the same elemental spiking technique as that of Marechal et al. 1999, this as discussed in 7.1, which casts considerable concerns regarding their accuracy.

Figure 2. 3: Variation in Zn fractionation of the carbonate fraction of sediments as function of age, (Pichat et al., 2003a)



As represented in Figure 2.3, the older samples have the greatest Zn fractionation ever reported for terrestrial materials. As reported by Pichat and his colleagues, for the Last Glacial Maximum, Holocene transition, temperature is known to have a fractionation effect whose amplitude varies from one element to the other; a 4 C° shift induces a change of 1‰ in $\delta^{18}\text{O}$ for an equilibrium carbonate. Temperature effects on the Zn isotopic composition is unlikely to account for significant Zn fractionation. However, glacial/interglacial variations of the Zn isotopic composition cannot be definitively ruled out. The interpretations introduced by Pichat and his colleagues introduced the concept of “Zn biological fractionation”; or the variation in the isotopic composition due to biological activity (Pichat et al., 2003a). They also suggested that the variability in the $\delta^{66}\text{Zn}$ reflected the thermocline steepness in the eastern

equatorial pacific, where deep water does not fully replenish surface waters. Accordingly, surface waters become depleted in the lighter Zn isotopes due to biological activity. Thus, organisms will build their shells in environments containing heavier Zn isotopes reflecting the composition of seawater at the time of the growth of the organism's shells. When the long lasting thermocline developed, the shells exhibit high $\delta^{66}\text{Zn}$ values which are deposited in the sediments after the death of the organisms. In contrast, low $\delta^{66}\text{Zn}$ values in carbonate sediments correspond to periods of strong trade winds during the upwelling season (Pichat et al., 2003b).

Another significance of Zn is the theory of the exchange of CO_2 between the ocean and the atmosphere being influenced by organic productivity, which is in turn affected by the change in the climate. therefore, the study of biogeochemical cycle of Zn, which is involved in marine biological processes is important to better understand the change in climate (Pichat et al., 2003b). Zinc is depleted from the surface waters by biological pumping and is regenerated by the oxidation of organic matter by bacterial activity and the dissolution of sinking particles. This suggests that variation in the biological fractionation of Zn isotopes could be recorded in deep sea sediments, and thus studying these variations enables changes in biological productivity to be detected (Pichat et al., 2003b). As mentioned earlier in Section 2.2.1, the "Zn hypothesis" suggested that low Zn concentration in sea water limits the growth of phytoplankton "biological productivity" thus, affecting the climate.

The use of Zn isotopes in the study of biological materials has been mostly restricted to the measurement of the concentration of Zn, or to measure the isotopic ratios for metabolic and nutritional studies. The pioneering study by Stenberg and her colleagues at Lulea University of Technology in Sweden, aimed to measure the concentration and the isotopic composition of Zn in human biological materials using sector field MC-ICPMS (Stenberg et al., 2004). Despite the limitations of the techniques, and the accuracy of the elemental spike method adopted, the study is considered unique as it is the first to specifically target human biological samples for future comparability and traceability purposes. The samples analysed included; Whole blood "SERO A/S Batch No OK0336, MR 9067, 404108", Bovine liver "NIST 1577a", bovine Muscle "NIST 8414", human hair powder "Lang fang China – GBW07601", and human hair sampled from subjects between 5 and 42 years old living in Lulea, Sweden. Their results are as shown in Table 2.3, fractionation are

relative to the laboratory standard “Alfa Aesar, Johnson Matthey GmbH, Karlsruhe; lot NM00558).

Table 2. 3: Zn fractionation and concentrations in human biological materials. Concentrations are in μgg^{-1} unless specified (Stenberg et al., 2004).

Sample	Zn concentration “measured” μgg^{-1}	Zn concentration “certified” μgg^{-1}	$^{66}\delta$ ‰
Bovine muscle" SRM- 8414"	140 ± 6	142 ± 14	0.50 ± 0.031
Bovine liver "SRM -1577a"	129 ± 3	123 ± 8	0.04 ± 0.016
Whole blood "lot- 404108"	4.8 ± 0.3 mg L^{-1}		0.30 ± 0.014
Whole blood lot " MR-9067"	$4.7 \pm 0.3 \text{ mg L}^{-1}$	4.78 mg L^{-1}	0.34 ± 0.009
Whole blood lot "OK-0336"	5.0 ± 0.7 mg L^{-1}	4.78 mg L^{-1}	0.31 ± 0.016
Human hair	178 ± 6		-0.46 ± 0.040
Human hair "GB-W07601"	187 ± 10	190 ± 5	0.07 ± 0.027

Despite the limited number of different samples of human hair, Stenberg and her colleagues noticed that $\delta^{66}\text{Zn}$ showed a significant inverse correlation with subject age (Stenberg et al., 2004). The researchers concluded that an average value of $0.32 \pm 0.04\text{‰}$ (2σ) can be assigned as a baseline level for Zn fractionation in human whole blood, relative to the JMC Zn standard, and human hair samples, exhibiting $\delta^{66}\text{Zn}$ values ranging from 0.05 to - 0.60‰, demonstrating that the Zn pool is fractionated between body compartments. Isotope ratio measurements may therefore provide a useful tool for further explorations of the Zn proteome (the entire complement of proteins).

The study by Stenberg and her colleagues is predated by Marechal et al. (1999) from the “*Laboratoire de sciences de la Terre*” in Lyon –France, who measured Zn fractionation in human blood samples and yielded $\delta^{66}\text{Zn}$ $0.41 \pm 0.04\%$ relative to a JMC 3-0749 L solution.

Stenberg and her colleagues continued their research in 2005; using a multicollector Inductively Coupled Plasma Sector Field Mass Spectrometer (MC-ICP-SFMS) and the same techniques as their previous study. They measured Zn fractionation in healthy humans and hemochromatosis sufferer’s whole blood. Their results for $\delta^{66}\text{Zn}$ ranged from $+0.30 \pm 0.06$, to $+0.41 \pm 0.04 \text{ ‰ amu}^{-1}$ relative to their laboratory standard, “lot NM00558; Alfa Aesar, Johnson Matthey”. According to Stenberg and her colleagues, the Fe, as well as the Zn isotopic composition exhibited a tendency toward lower levels of fractionation in the blood of subjects with hereditary Hemochromatosis with homozygous mutation (C282Y/C282Y) of the HFE gene. The results therefore suggest that both Fe and Zn isotopic signatures in whole blood, at least to some extent, reflect polymorphisms in the HFE gene (Stenberg et al., 2005). As stated earlier, the approach adopted by the Stenberg and her colleagues to measure these fractionation has some accuracy limitations, in particular any interlaboratory comparisons. The researchers themselves emphasized their concerns regarding the accuracy of their results, for example, “The first issue to address concerns the accuracy of the Fe and Zn isotope ratio data acquired in the present work” (Stenberg et al., 2005).

In 2005, a study was carried out by scientists from the United Kingdom and France to measure the variation in the isotopic composition of Zn in volcanic ore samples by Mason and his colleagues (Mason et al., 2005). The study analysed samples from three ore facies in the Devonian Alexandrinka volcanic-hosted massive sulphide (VHMS) ore deposit from the Urals in Russia. As in most previous research, the isotopic composition of Zn was measured using MC-ICP-MS. In their study the samples were derived from three different sources: Hydrothermal metasomatic vein stock work, hydrothermal stock chimney, and reworked clastic sulphide. Isotopic Zn fractionation ($\delta^{66}\text{Zn}$) was found to vary from -0.431 to 0.077 ‰ in the stock work samples, -0.027 to 0.231 ‰ in the chimney samples where a systematic increase occurred in $\delta^{66}\text{Zn}$ moving away from the core to rim, and $\delta^{66}\text{Zn}$ from -0.295 to -0.05 ‰ in Clastic zone samples. Mason and other scientists suggested many possible

reasons for their findings such as, equilibrium isotopic partitioning of Zn into chalcopyrite favors isotopically light Zn being accommodated into the chalcopyrite structure; which lead to significant isotopic variability of Zn in the stock work samples. However, the authors suggested two other possible explanations for the variation in the isotopic composition of Zn; a temperature control factor, or, due to local distillation fractionation, exaggerating a small inherent mineralogical fraction. From the authors point of view, the observed variation in the isotopic composition of Zn will allow further constraints to be placed on the controls and extent of transition metal isotope fractionation in ore deposits and ancient seafloor hydrothermal mineralization. The researchers summarized their interpretations of the variation in the isotopic composition of Zn as being linked to the depositional environment and mineralogy (Mason et al., 2005).

In the same year, another study measuring Zn isotopic fractionation in minerals was performed by Wilkinson and his colleagues of Imperial College London (Wilkinson et al., 2005). This study measured Zn fractionation in sphalerite crystals in the Irish Midlands basin ore field formed under well constrained conditions. They used MC-ICPMS, and sample bracketing procedure to correct for machine fractionation. This approach, while an improvement on other methods does not always guarantee the accuracy needed to measure small Zn fractionation. The variations in the Zn fractionation found ranged from -0.17 ± 0.17 to $+1.33 \pm 0.24$ ‰ for $\delta^{66}\text{Zn}$ relative to JMC-30749-L with no systematic geographic pattern. Omitting the highest measured Zn fractionation value, they suggested an average of 0.15 ± 0.19 ‰ for the Irish Sphalerite, They also concluded that neither variation in the source of rock nor the temperature at which rock formation occurred (150 to 200) C° was the primary cause for the observed Zn isotopic fractionation. However, they concluded that their data does not exclude the possibility of temperature-controlled fractionation, but any such effects are too small to be resolved. They found it more plausible that a kinetic fractionation of Zn isotopes could be induced during far-from-equilibrium precipitation of sphalerite, e.g. Zn isotope composition of sphalerite in basement-hosted feeder veins from beneath the ore bodies reflects Zn derived from a large, homogenized, lower Paleozoic basement reservoir by deeply circulating hydrothermal fluids (Wilkinson et al., 2005).

The isotopic composition of Zn in plant biology systems had little attention prior to the study by Weiss et al. (2005) of Imperial College London who studied Zn fractionation in higher plants (Rice, lettuce and tomato) using MC-ICP-MS. Their objectives were to assess if the isotopic fractionation of Zn in higher plants during its uptake, and to explore possible fractionation mechanisms. The researchers emphasized that the extent of isotopic discrimination of transition metals in biological processes is poorly understood, but potentially has important applications in plant and biogeochemical studies. Weiss et al. (2005) measured the isotopic fractionation of Zn during uptake from a nutrient solution for the plant species mentioned above. This study is significant because Zn fractionation in rice is part of this work and will be discussed in Section 7.3. In Weiss et al. (2005) study, the roots exhibited a similar extent of Zn enrichment of heavier isotopes relative to the nutrient solution. This was interpreted by the researchers as a preferential adsorption in the external root surface, which was the opposite to the shoots, where they exhibited a depletion, or an “enhancement in the lighter isotopes”, and was interpreted as an indication that biological membrane transport controls the uptake into the plant’s cells. The extent of Zn fractionation in the shoots depends on Zn speciation in the nutrient (Weiss et al., 2005). According to Weiss et al. study, Zn fractionation for the roots ranged from +0.04 to + 0.09 ‰ amu⁻¹ relative to the nutrient, and ranged from -0.013 to -0.026 ‰ amu⁻¹ from the roots to shoots. These shifts are significant relative to Weiss et al’s analytical reproducibility ($\pm 0.035\text{‰ amu}^{-1}$ (2σ)) and although close to analytical uncertainty, these results may be considered as the first indication of Zn isotopic fractionation in higher plants. Weiss and his colleagues admitted that their explanation for the detected variations are still somewhat speculative and need further investigation (Weiss et al., 2005).

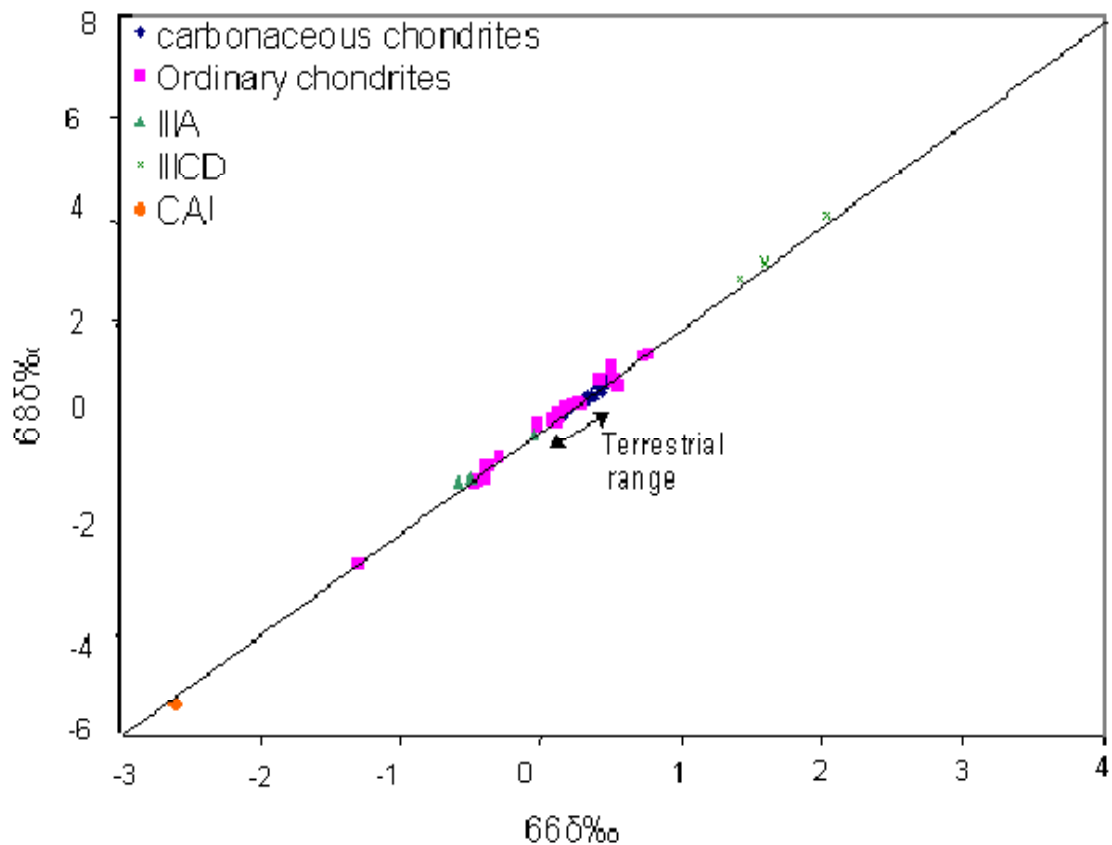
At this point it is worth introducing the concept that plants are considered as a reliable register of C and O fractionation processes formed during photosynthesis (Skrzypek et al., 2007a). Organic matter is never homogeneous in its structure but consists of a variety of subcomponents. The question of whether stable isotopes can be analyzed reliably on whole plants instead of subcomponents has been addressed by many authors, for example; $\delta^{13}\text{C}$ appears to be reliably represented by analysis of bulk plant material instead of a specific subcomponent such as cellulose (Skrzypek et al., 2007a,

Skrzypek et al., 2007b). Zinc is stored in protein-like “Phytate” complexes, the formation of which could contribute to the fractionation of the isotopic composition of Zn. Zinc is also found in plant enzymes and could be fractionated in the remobilization process in the plants culture (Cavagnaro and Jackson, 2007). For example, rice plant is classified as a C3 category of plants; three refers to the number of carbon atoms in the first molecules formed at the end of the initial CO₂ fixation pathway. It is important to mention that in C3 plants like rice, have ability to increase their photosynthetic responses across a range of several μg g⁻¹ of CO₂, this is in contrast to C4 plants which reach saturation quickly as CO₂ concentration increases (Rogers et al., 1994). C3 plants use a Calvin–Benson cycle characterized by the use of ribulose biphosphate carboxylase oxidase (RUBISCO), which has the largest kinetic isotope effect δ¹³C (~26‰) between bulk plant tissue and CO₂ (Chikaraishi and Naraoka, 2003).

Fractionation of Zn in meteorites was measured recently by Luck and his colleagues using IC-PMS in Montpellier- France, (Luck et al., 2005b). Their aim was to measure Zn fractionation in Chondrites and iron meteorites samples, applying the mass spectrometric experimental approach as of Marechal et al. (1999), using a combination of Cu-isotopic correction and standard-bracketing techniques. Luck and his colleagues performed extensive tests on their standards as well as rock samples using duplicate and triplicate analyses to confirm that the chemical procedure did not introduce isotopic fractionation. This claim contradicts previous research on the contribution of the column chemistry to the Zn and Cu fractionation (Marechal and Albarede, 2002). This contradictory conclusion is of serious concern considering their claimed external precision of 0.04-0.05‰ 2σ. The study by Luck et al. (2005b) produced precise Zn isotopic variations for Carbonaceous Chondrites, equilibrated ordinary Chondrites, unequilibrated ordinary Chondrites, iron meteorites, and metal from Brenham pallasite. The δ⁶⁶Zn ranged from -0.05 to +3.68 ‰ for iron meteorites, from -2.65 to +0.44 ‰ for a pieces of bulk Allende, from +0.16 to 0.52 ‰ for carbonaceous chondrites, and from -1.30 to +0.72 for the ordinary chondrites. All were relative to their laboratory standard “Johnson Matthey Company (JMC) 400882B”. As represented in Figure 2.4, Luck and his colleagues reviewed the previously measured Zn fractionation in natural materials, and concluded that; the

isotopic ratios of $^{66}\text{Zn}/^{64}\text{Zn}$, $^{67}\text{Zn}/^{64}\text{Zn}$ and $^{68}\text{Zn}/^{64}\text{Zn}$, varied linearly with the mass difference and forms a common fractionation line with the terrestrial materials (Luck et al., 2005b). From these results they argued or proposed that Solar System Zn was derived from an initially single homogeneous reservoir, as the $\delta^{68}\text{Zn}$ was twice that of the $\delta^{66}\text{Zn}$.

Figure 2. 4: Three isotope plot relative to ^{64}Zn by (Luck et al., 2005b), data also includes that of other researchers.



The study by Luck et al. (2005) yielded a number of possibilities, for example, the isotopic composition of Zn in meteorites is approximately 0.5‰ amu^{-1} larger than the isotopic composition of Zn in natural terrestrial materials. In addition, the variation in the isotopic composition of Zn in Carbonaceous Chondrites is narrower than for other meteorites, ($\sim 0.3\text{‰}$ for $\delta^{66}\text{Zn}$). An interesting suggestion by Luck and his colleagues was that, Zn becomes isotopically lighter in the order of CI, CM, CV-CO. For chondritic meteorites, their study showed no relationship between the date of fall, and $\delta^{66}\text{Zn}$, suggesting that no evidence of weathering effects, or importantly, contamination of the samples. Luck and his colleagues concluded that the results they obtained for these samples represent their formation isotopic composition. They also

went onto suggest that the primordial Zn reservoir was at least at some point in the evolution of the early solar nebula, homogeneous and neither high temperature nor other mass independent processes were identified and no isotope anomaly of nucleosynthetic origin was found (Luck et al., 2005b).

One year later, the isotopic composition of Zn in number of SRMs, including BCR-1 (USGS) was measured using MC-ICP-MS by Chapman et al. (2006) from the Department of Earth Science and Engineering – Imperial College London. The researchers adapted an anion exchange column chemistry protocol that “as they claimed” yielded no contribution to the Zn fractionation. According to their results, the $\delta^{66}\text{Zn}$ for BCR-1 (USGS) was $0.29 \pm 0.12 \text{ ‰}$ (2σ) relative to Zn Johnson Matthey (batch 3-0749L) (Chapman et al., 2006).

Given that water covers a substantial part of the Earth’s surface no isotopic composition measurements of Zn in oceanic waters were performed until 2006 in a study of Bermin and his colleagues (Bermin et al., 2006). The reason for that is the considerable analytical challenge involving the low concentrations of Zn in waters, especially oceanic. A major difficulty of measuring precise and accurate isotopic composition of Zn in seawater is the high concentration of other elements in the same matrix. The significance of Bermin and his colleagues work is that they were the first to implement the double spike technique to check on some of their results of variation in the isotopic composition of Zn in natural samples since the pioneering attempts of Rosman in 1972. And the first to use the double spike technique using ICPMS for Zn, as well as the “standard bracketing” technique, in order to correct for analytical mass discrimination. This study used quantitative co-precipitation to extract small amounts of Zn from up to at least 1 L size samples, achieving a small environmental blank contribution relative to the sample (Bermin et al., 2006). Their blank was low enough to allow use of as little as 100 mL samples of the deep ocean, and ~2 L samples of the most Zn-depleted surface ocean. As expected, their study was hampered by the analytical challenges related to the very low concentration of Zn in seawater, which forced them to utilize procedures like chelating and co-precipitation to pre concentrate large samples of seawater.

To avoid isobaric interferences, Zn was separated from Na, Mg, Ca and other metals present in water in amounts many orders of magnitude larger than the Zn. This concentration procedure was hampered by the need to control the environmental blank. To reduce contamination, Bermin and his colleagues maintained a very low concentration of Zn in the reagents of 25, 29 and 1.7 pgg^{-1} for 15 M HNO_3 , 10M HCl and 18 M Ω H_2O respectively. The contribution of the interference of ^{64}Ni to the ^{64}Zn beam was deemed negligible by comparing with the molecular interference of $^{24}\text{Mg}^{40}\text{Ar}$, which was insignificant. Bermin also concluded that there was no fractionation of Zn isotopes during the column separation. Their study yielded variation in the isotopic composition of Zn relative to JMC 3-0749 of $\delta^{66}\text{Zn} = 0.35 \pm 0.08\text{‰}$ following the Chelex extraction method, and $\delta^{66}\text{Zn} = 0.31 \pm 0.04\text{‰}$ using the co-precipitation method. The latter value was measured using the double spike technique. It was demonstrated that, for the samples taken from the North Pacific, the isotopic fractionation versus depth profiles of the Zn and Cu are more or less mirror images of each other. Bermin and his colleagues openly admitted the difficulties relating to their interpretation as they are the first for seawater, and there might be different factors that may effect the concentration and the isotopic composition of Zn in seawater and oceans, such as, biological usage, and adsorption into particles and redox processes. They recommended that their analytical protocols provides a starting point from which further research can proceed to accurately measure Cu and Zn isotopic compositions in the oceans (Bermin et al., 2006).

In 2006, a new study of the isotopic composition of Zn was conducted using ICP-MS in meteorites and lunar samples by Moynier et al. (2006). This research adopted the same experimental approach of Marechal et al.(1999) to measure Zn fractionation using Cu as an elemental spike. The results obtained were, from $\delta^{66}\text{Zn} -3.83\text{‰}$ in rock samples, to 6.39‰ in the lunar soil, relative to their laboratory standard “JMC 3-0749 L” (Moynier et al., 2006). Their reproducibility was estimated to be ± 0.05 , 95% confidence and the isotopic fractionation $\delta^{68}\text{Zn}$ is also approximately twice the fractionation $\delta^{66}\text{Zn}$ within the experimental uncertainties. The latter results were used to conclude that there are no anomalies in the lunar Zn isotopic composition. In their study Moynier and his colleagues hypothesized that S, Cd, Cu and Zn might behave alike isotopically, and concluded that the absolute fractionation of the isotopic

composition of Zn correspond to nominal evaporative losses of approximately 30 %, but are likely much larger close to lunar grain surfaces (Moynier et al., 2006). As nothing was known regarding Zn fractionation in lunar samples prior to this study, and because the scarcity of the samples, it would appear more efficient to analyse such rare samples using the more absolute double spike technique.

In a study by John et al. (2007) from the Massachusetts Institute of Technology- USA, Zn fractionation was measured in number of “common anthropogenic Zn products”. The intention of such a study was to utilize the isotopic composition of Zn as an environmental tracer of anthropogenic sources. The measurement was performed using the MC-ICP-MS with elemental Cu spike and the standard -sample bracketing technique. The range of $\delta^{66}\text{Zn}$ found was; laboratory standards -9.15‰ to $+0.17\text{‰}$; Zn metal dust purified by thermal distillation $+0.09\text{‰}$ to $+0.19\text{‰}$; Zn metal shot purified by electrochemically $+0.22\text{‰}$; Special High Grade Zn, as represented in US pennies $+0.14\text{‰}$ to $+0.31\text{‰}$; galvanized steel $+0.12\text{‰}$ to $+0.58\text{‰}$; electroplated hardware -0.56‰ to -0.20‰ ; and health products $+0.09\text{‰}$ to $+0.24\text{‰}$ relative to their laboratory standard Lyons-JMC Zn (John et al., 2007).

John and his colleagues concluded that $\delta^{66}\text{Zn}$ in anthropogenic products varies between about $+0.1\text{‰}$ and $+0.3\text{‰}$, and suggested that $\delta^{66}\text{Zn}$ variability within Zn ores may be the primary cause of the observed range. However, if Zn recovery from ores during purification is not complete, isotope fractionation during refining may also impact on the $\delta^{66}\text{Zn}$ of such common anthropogenic Zn. Four of their pure laboratory standard Zn metals were not classified as “common Zn”, and John and his colleagues went on to suggest that the reason for the larger isotopic fractionation seen in laboratory standards may be due to special Zn purification processes. Differences in the purification method used, or use of multiple additional purification steps, may also contribute to the significant variability in $\delta^{66}\text{Zn}$ found in laboratory standards. John and his colleagues went on to conclude that; by constraining the isotopic composition of common anthropogenic Zn, and revealing some of the processes that lead to large deviations from this composition, Zn isotopes may be exploited as an environmental tracer. For example, very negative $\delta^{66}\text{Zn}$ values may indicate Zn that has been electroplated from solutions (John et al., 2007). Once again it is important to note the limitations of the approaches used in John and his colleagues work, in particular the

lack of the reference of their so called “common Zn” relative to (δ zero). This highlights the need for the common use of an absolute reference materials.

Recently, a study to investigate Zn isotopic fractionation was undertaken by Cavagnaro and Jackson (2007) from Monash University -Australia and the University of California Davis-USA. The study used quadrupole IC-PMS to measure the isotopic composition of Zn in mature field grown Tomato, “*Solanum Lycopersicum*”, shoots and fruits, from two genotypes; Mycorrhizal and non Mycorrhizal. In their research, samples were spiked with an elemental spike of standard Ge, and the external calibration was done relative to “Zn Spex Certiprep group Metuchen, NJ”. Their work was limited by the isobaric interference of ^{70}Ge on the ^{70}Zn , and prevented ^{70}Zn being included in any of the concentrations or the isotopic ratios calculations. The isotopic composition of Zn in the shoot was found to be significantly different from that in the fruit for both genotypes with ^{64}Zn , ^{66}Zn abundances significantly less than that in the fruits. Relative to one type of tomato plant, “rmc”, the shoots of another tomato type “76R MYC+” were enhanced in ^{64}Zn , ^{66}Zn and depleted in ^{67}Zn and ^{68}Zn . On the other hand, the fruits were enhanced in ^{66}Zn and depleted in ^{68}Zn relative to “rmc”. The researchers went on to suggest that the differential bonding of Zn isotopes to cellular components was a potential reason for the measured fractionation. They concluded that; a greater understanding of the metabolism is needed before the biological significance of the fractionation differences can be fully appreciated. The variation in the Zn isotopic fractionation between plant parts has the potential to be a useful tool, for example, along with isotopic data from other elements, as a simple screening method. Cavagnaro and Jackson (2007) recommended that more mechanistic studies and research is necessary, because Zn metabolism and its biogeochemical cycling by plants are generally not yet as well understood compared to other nutrients (Cavagnaro and Jackson, 2007). This very interesting study has many wide spread applications. However, it has two significant analytical limitations, the first being the ability of Quadrupole ICP-MS to achieve their claimed uncertainties, and the second related to not using a (δ zero) material as a laboratory reference.

Weiss et al. (2007) utilized a GVi IsoProbe to evaluate the potential of Zn isotopes to identify atmospheric sources and to examine possible post-depositional processes in peat bogs. To separate possible local point sources, and background atmospheric contributions, they analysed the top Sections from three bogs in Finland, situated in the vicinity of a smelter plant, a mining site, and an area isolated from industrial activity. Weiss and her colleagues used elemental spiking with Cu as an internal mass discrimination monitor, and to correct for mass bias effects of the matrix during isotope measurements (Weiss et al., 2007). Zn isotopic fractionation of up to 1.05 ‰ for $\delta^{66}\text{Zn}$, relative to their laboratory standard Johnson Matthey Purotronic Zn metal JMC 3-0749L though the house standard was (Batch NH 27040), found in all three peat bogs, with heavier Zn in the deeper, and lighter Zn in the upper Sections. The researchers implied that multiple Zn fractionation during diagenetic recycling and nutrient recycling alone cannot explain the fractionation pattern. The researchers went on to conclude that; the isotopic composition of Zn is amenable to identify different atmospheric Zn sources, including Zn derived from anthropogenic activities, such as mining and smelting, but biogeochemical processes seriously affect the record and they need to be evaluated and assessed (Weiss et al., 2007).

The isotopic composition of Zn in seafloor hydrothermal vent fluids and chimneys was measured early in 2008 by John and his colleagues from Massachusetts Institute of Technology and other scientific institutes in the USA (John et al., 2008). The samples were selected from several distinct geographic regions along basalt-hosted mid-ocean ridges, and from the sedimented Gulf of California (Guaymas basin) and from the slow spreading mid- Atlantic ridge (TAG Active Mound). The vent fluid chemistry in the area in relation to magmatic events has been well documented and previous studies have reported temporal evolution of the vent systems since 1991. Their data were corrected for instrumental mass (ICP-MS) bias using the Cu internal spike. Their relationship between Cu and Zn instrumental fractionation has been shown to differ from predictions of the exponential mass bias law of Marechal et al. (1999), where, a linear relationship between the natural log of $^{65}\text{Cu}/^{63}\text{Cu}$ and $^{66}\text{Zn}/^{64}\text{Zn}$ in standards was used instead to determine the mass bias relationship. They also used the Zn double spike technique on some samples to check their results obtained using the elemental spiking confirming the Cu elemental spiking technique. Hydrothermal fluid samples were analyzed for elemental concentrations and Zn

isotope composition, revealed $\delta^{66}\text{Zn}$ from 0.00 ± 0.01 ‰ up to 1.04 ‰. Also, Zn isotopic analyses carried out on each of the chimney sulfide samples yielding $\delta^{66}\text{Zn}$ from -0.09 ± 0.02 ‰ up to 1.17 ± 0.01 ‰ relative to Zn Lyon JMC standard (John et al., 2008). The $\delta^{66}\text{Zn}$ uncertainties are for the internal error (2σ s.d.) for triplicate analysis of a single sample. The researchers suggested a significant negative relationship between fluid temperature and $\delta^{66}\text{Zn}$ in hydrothermal fluid system samples. In contrast, they found no significant relationship between $\delta^{66}\text{Zn}$ and concentrations of Zn, $1/\text{Zn}$, Cu, Fe, H_2S , pH, or the Fe/Mn ratio. The researchers proposed several possibilities to explain the variations in fluid $\delta^{66}\text{Zn}$, including, differences in source-rock $\delta^{66}\text{Zn}$, fractionation during phase separation, kinetic or equilibrium fractionation during subsurface precipitation of Zn sulfides, and subsurface redissolution of Zn sulfides. The researchers indicated that the source rocks are not likely the source of isotopic variability. For the fluids studied, phase separation does not appear to be an important factor in fractionating Zn isotopes. The researchers hypothesized that subsurface precipitation of isotopically light Zn sulfides is the main cause of isotopic variation in hydrothermal fluids investigated in their work. The researchers concluded that; with a better understanding of how Zn isotopes are fractionated in hydrothermal systems, Zn isotopic analysis may be a tool to help us understand the plumbing and chemistry of hydrothermal systems (John et al., 2008).

Very recently, Petit et al. (2008) addressed the complexities related to the use of MC-ICP mass spectrometers for precise Cu-Zn isotopic ratio measurements. The researchers indicated that the complexities are also becoming more apparent; for example, the analytical issues such the correction for the machine bias and the effects of spectral and non-spectral interferences (Petit et al., 2008). Their study was introduced as the development of Cu and Zn isotope MC-ICP-MS analyses performed to measure Cu and Zn fractionation of solid materials from the Scheldt estuary (the Scheldt estuary, Belgium-The Netherlands). The Petite et al. study measured the fractionation of the Zn in calibration of the IRMM 3072 Zn certified reference material relative to Lyon JMC Zn (wet plasma) yielded $\delta^{66}\text{Zn} = 0.32 \pm 0.03$ ‰, 0.38 ‰ ± 0.08 and 0.030 ± 0.03 ‰ using three different approaches to correct for machine fractionation as comparison of three correction methods for Cu and Zn

isotope ratio measurements performed in wet or dry plasma. First, SCBC (Sample-Calibrator Bracketing on isotopic ratios Corrected by external normalisation), second approach is SCBM (sample-calibrator bracketing on measured isotopic ratios), and EEN (Empirical External Normalization). Fractionation of Zn in surface sediment taken from the estuaries yielded fractionation from $\delta^{66}\text{Zn}$ 0.21‰ to $1.13 \pm 0.03\%$ relative to JMC Zn. The study of Petite represents a very recent development in ICPMS measurements, with total procedural blanks of 15 ng and 3.5 ng for Zn and Cu respectively representing less than 0.1% of the amount of Cu and Zn loaded on the column, which indicates that there was about 15 μg loaded in the column to perform the measurement. The latest study in the isotopic composition of Zn is the study of Sivry et al. in July 2008, whose aim was to understand and evaluate the impact of metallurgic activity on Zn isotopic fractionation and to assess the potential of Zn isotopes as a tracer of anthropogenic Zn at a river system scale. The researchers measured the Zn isotopic compositions of surface soils, smelting/mining wastes, river and reservoir sediments from a river system were determined for this purpose, using MC-ICP-MS. (Sivry et al., In press).

As reviewed in Sections 2.2.1 and 2.2.2 there have been no previous Zn isotopic fractionation analyses using TIMS, accompanied by use of the double spike technique.

2.2.3 Causes of isotope fractionation

The Extent of natural isotopic fractionation and some of the elements in which it occurs is discussed in Section 1.1.2. Although not the aim of this work, in this Section; the causes of isotope fractionation and how it relates to this work is briefly examined.

Isotopic fractionation for most elements occurs due to equilibrium and non equilibrium (Kinetic) effects. For the non equilibrium effects, isotopic fractionation occurs due to dynamic processes that are incomplete and fast, and some times unidirectional (Criss, 1999). Kinetic fractionation is caused by unidirectional reactions; in which the forward reaction rates usually are mass dependent. More over, in kinetic processes, the lighter isotope of an element is predicted to form the weaker,

and the easier bond to be broken. Since the lighter isotopes is more reactive; they are concentrated in the product of the reactions; leaving the reactants to be enhanced with the heavier isotopes (Coplen et al., 2002).

Examples of fractionation processes due to non equilibrium effects are:

1) Diffusion:

As discussed by Criss (1999); diffusion of gaseous molecules through an orifice which is smaller than the mean of free path of these gaseous molecules, causes non equilibrium effect. According to the kinetic theory of gases; for two isotopic molecules, molecular weights m_1 and m_2 ; the translational velocities v_1 and v_2 can be computed from the relationship 2.1 (Known as Graham's law of diffusion).

$$K.E = \frac{m_1 v_1^2}{2} = \frac{m_2 v_2^2}{2} \Rightarrow \frac{v_1}{v_2} = \sqrt{\frac{m_2}{m_1}} \quad 2.1$$

The bigger “faster” translational velocity will cause the heavier isotopes to be discriminated against (the preferential of the lighter isotopes to escape through the orifice) and causing the residue to be enhanced in the heavier isotopes (Criss, 1999).

2) Evaporation

This is a unidirectional kinetic process; where the higher translational velocities of molecules containing lighter isotopes may allow them to preferentially break through the surface of the liquid into the atmosphere. Accordingly, the residue of the liquid will become more enhanced in the heavy isotopes (Criss, 1999)

3) Kinetic isotope effects

This is due to differences in the dissociation energies of molecules composed of different isotopes. As it is easier to break the bonds of molecules that contain the lighter isotopes, then the lighter isotopes will be preferentially incorporated in the products of incomplete reaction, while the residue of the reaction will be enhanced in the heavier ones (Criss, 1999).

4) Metabolic.

Metabolic effects incorporate the effect of different kinetic fractionation, and some times equilibrium ones. The classic examples are the ^{12}C preferential in the green

plants in processes of photosynthesis, and the utilization of ^{16}O in the respiratory process (Criss, 1999). Kinetic isotope fractionation of biological processes are variable in magnitude and may be in the direction opposite to that of equilibrium isotope fractionation for the same chemical species (Coplen et al., 2002)

Equilibrium fractionation occurs when forward and backward reaction rates for individual isotope exchange reactions are equal (Coplen et al., 2002). Fractionation due to equilibrium processes is large in light elements, such as H, C, and O, as described in Section 1.1.2, because of the low atomic masses of the isotopes of these elements, where the difference in one or more neutrons translates to a significant relative difference in masses of different isotopic forms (Criss, 1999). Another reason for isotopic fractionation is the covalent bond; which exhibit vigorous rotational and vibrational motion, which are affected by the mass of the isotopes, and the resultant mass related differences gives rise to the equilibrium fractionation. In contrast, atoms with metallic or ionic bonds are bonded by electrostatic forces that depend more on the charge of the atom, and little on its mass. Because of this, elements with ionic or metallic bonds relatively do not show substantial fractionation (Criss, 1999).

In general, in equilibrium isotope reactions, the heavy isotope will be enriched in the compound with the higher oxidation state, and commonly in the more condensed state. Thus, for example, ^{13}C is enriched in carbon dioxide relative to graphite, and in graphite relative to methane, and ^2H is enriched in liquid water relative to water vapour (Coplen et al., 2002). Based on the number of Oxidation states, Maréchal et al. (1999) predicted that the extent to which Zn isotopically fractionates would be less than Cu (Marechal et al., 1999). On other hand, Mg was always been expected to show a small fractionation in nature, because the oxidation state of Mg in nature had always been +2 only, although Mg exhibits a fractionation spanning of 4.5 ‰ $\delta^{26}\text{Mg}$ (Coplen et al., 2002).

- **Chapter 3: Methods**

3.1 Mass Spectrometry

3.1.1 Principles of Mass spectrometry

A mass spectrometer is a device used to separate ionic species according to their mass to charge ratio. The basic principle of the mass spectrometer is the deflection of the path of moving ions with mass m , using a magnetic field of known value according to masses of the ions (De Laeter, 2001). To accelerate ions with charge q , the particles are placed in an Electric Field (\mathbf{E}) where they experience a force represented by Equation 3.1.

$$\vec{F} = q \vec{E} \quad 3.1$$

The change in potential energy (ΔU) is given by ($q \Delta V$), and equals the gain in Kinetic Energy ($1/2 mv^2$), where m , represents the mass of the ion, and \vec{v} is the velocity of the ion; thus.

$$\Rightarrow v = \sqrt{\frac{2qV}{m}} \quad 3.2$$

When the ion with velocity \vec{v} enters a uniform magnetic field of strength \mathbf{B} , the ion will experience a sideways force represented as:

$$\vec{F} = q \vec{v} \times \vec{B} \quad 3.3$$

When $\vec{v} \perp \vec{B}$, then this can be written as:

$$|\vec{F}| = qvB \quad 3.4$$

The ion will move in a circular path and equating magnitude of the centripetal force mv^2/R , to the magnetic force in Equation 3.4 enables the path radius R to be determined as:

$$R = \frac{mv}{qB} \quad 3.5$$

Using Equations 3.4 and 3.5 enables R to be expressed as.

$$R = \left(\frac{1}{\left| \vec{B} \right|} \right) \sqrt{\frac{2mV}{q}} \quad 3.6$$

Or

$$R \propto \left(\frac{m}{q} \right) \quad 3.7$$

This means that that radius of curvature of the ion's pathway is proportional to its "mass to charge" ratio.

The resolution of the mass spectrometer is its ability to resolve ions of similar mass and can be represented as:

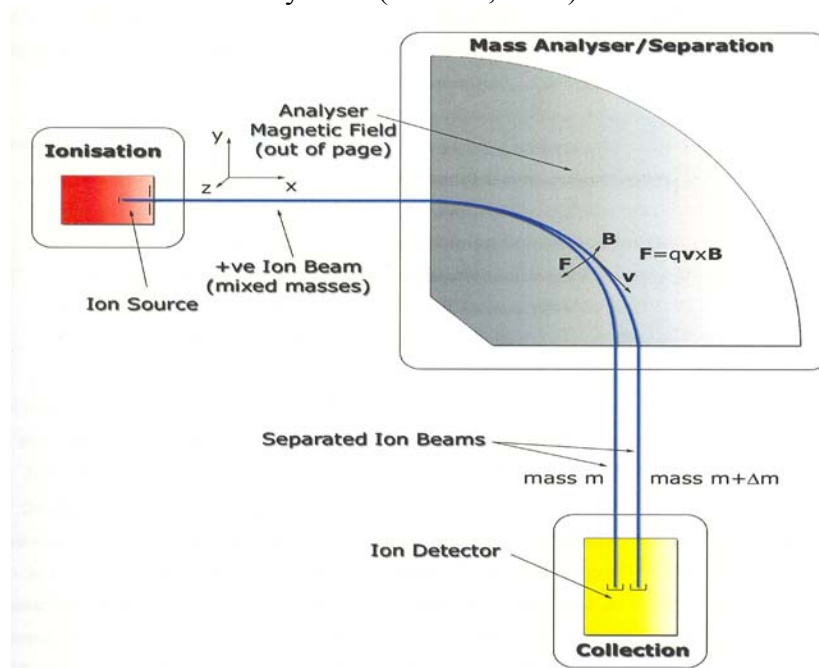
$$\frac{\Delta m}{m} = \frac{\delta}{R} \quad 3.8$$

Where δ is the width of the image slit (De Laeter, 2001). The VG 354 used in this research has a resolution of ~ 500 .

3.1.2 Thermal Ionisation Mass Spectrometer (TIMS)

All the measurements done in this work were performed on a VG 354, Thermal Ionisation Mass Spectrometer "TIMS" located in John De Laeter Centre for Mass Spectrometry at Curtin University of Technology in Western Australia. The machine is a positive thermal ionisation mass spectrometer. All mass spectrometers can be considered as consisting of three closely interacting systems, a source of ions, a mass analyser or magnetic deflector, and an ion detection/collection system as represented in Figure 3.1

Figure 3. 1 The three components of the mass spectrometer: Ion source, Mass analyser and the ion collection system. (Holmes, 2002).



3.1.2.1 Ion source

Ions are generated from samples located in the ion source of the mass spectrometer by placing the sample on high work function rhenium filaments and heating the samples to a temperature of approximately 1400 °C, where effectively simultaneous volatilization and ionisation of the sample occurs over a period of hours (Dickin, 2000).

After the samples are loaded into the ion source and a vacuum established, the samples on the filaments are also degassed. The degassing process enhances ion production, and reduces isobaric interferences that could be present in the sample, or other components of the ion source. This process significantly reduces hydrocarbon interferences and other molecular interferences.

The ionisation process (further described in Section 3.1.3) can produce a significant bias in the final isotope ratios measured by the mass spectrometer. This bias, or instrumental fractionation of the results is generally mass dependent, and occurs because of differential evaporation and ionisation effects, such as lighter isotopes

evaporating preferentially to heavier isotopes early during an analysis leaving the sample containing excess of the heavier isotopes which are released later in the analysis (De Laeter, 2001). Corrections for this effect can be performed by determining the fractionation factor “*f*”, which varies as a function of time and isotopic mass difference. Three approximations are commonly used to determine this factor, linear, exponential, and power law. As described below, this factor as determined by the three approximations are the same within uncertainty for Zn measured on the VG 354 can’t be differentiated. For simplicity, the linear approximation was used, for example, to internally normalize isotope ratio data for some analyses. However, no correction for machine bias was performed and the linear machine bias was assumed for the double spike work as discussed in Section 3.7.2. The Linear law is represented in Equation 3.9.

$$\Rightarrow \frac{R_{tr}}{R_{meas}} = 1 + \Delta m * f_{linear} \quad 3.9$$

Where *R* is the ratio of the heavier isotope *m*₁ to the lighter isotope *m*₂, and $\Delta m = m_1 - m_2$, “*tr*” is the true value and “*meas*” is for measured value.

3.1.2.2 The magnet

The magnetic field separates the ions according to their masses, and focuses the ion beams. The type and shape of the magnet used in mass spectrometers is significant in the formation and focusing of the ion beam into the ion collector. The mass spectrometer used in this work was a 90° sector field magnet. The mass dispersion “*D*” of the mass spectrometer can be defined as the separation of the resolved ions along the focal plane and is proportional to the radius of curvature “the radius of the ion path” (De Laeter, 2001). The other terms are defined in previous Equations.

$$D \propto \left(\frac{\Delta m}{m} \right) R \quad 3.10$$

The applied magnetic field has a focusing effect similar to that of a lens on a light beam, which focuses a diverging beam of ions to a given point. The focusing properties of a homogeneous magnetic sector field for a beam of ions mass *M*. and

velocity v_0 , starting from a point source O, with small angular divergence 2α , where $\alpha \ll 1$. The sector angle φ_m and the ions follow a circular path of radius a_m , hence the beam will be focused at the image point I. This combination is equivalent to a prism and cylindrical lens within an optical system. The focal length of such lens is given by:

$$f_m = \frac{a_m}{\sin \varphi_m} \quad 3.11$$

The object and the image distances l' and l'' can be represented in the following Equations:

$$l' = l'' = 2r$$

$$\varphi = \frac{\pi}{2}, \text{ and } \varepsilon_1 = \varepsilon_2 = 26.5^\circ \Rightarrow$$

$$\Omega = \varphi - \varepsilon_1 - \varepsilon_2$$

$$\Omega = 37^\circ$$

$$D = \left(\frac{r\Delta M}{2M} \right) K$$

$$\text{where, } K = \frac{2 \cos \varepsilon_2 \sin \frac{\varphi}{2} \left(\cos \left[\varepsilon_1 - \frac{\varphi}{2} \right] + q \cos \left[\varepsilon_2 - \frac{\varphi}{2} \right] \right)}{\sin \Omega}$$

$$\text{and, } q = \frac{l'' \sin \Omega}{r \cos^2 \varepsilon_2} - \frac{\cos(\varphi - \varepsilon_2)}{\cos \varepsilon_2}$$

for, ⁶⁸ Zn

$$\Rightarrow D = \frac{r\Delta M}{2 * 68} * 4$$

Equations 3.12

Where, Ω is the angle of magnetic sector, D is the dispersion of the instrument, K is the geometrical factor. The resulting dispersion, D , is the physical separation between the ions at the collector and is a mass dependent.

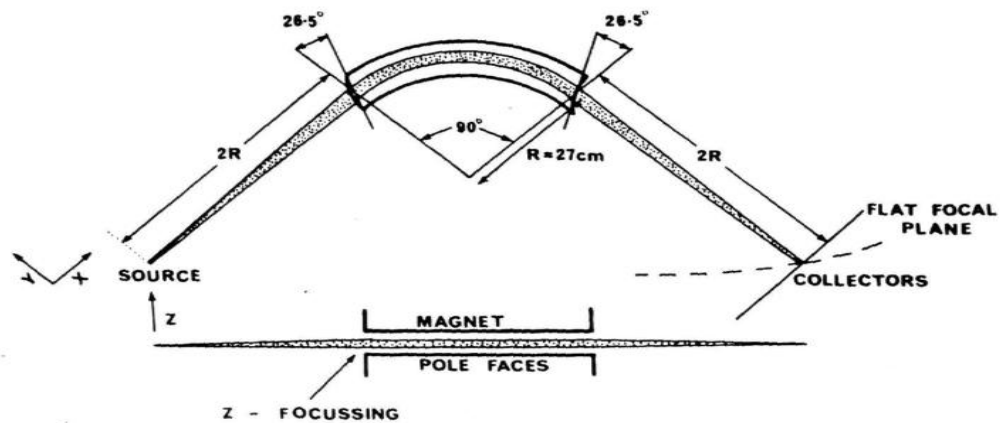
For $\varphi=90$, $\varepsilon_1 = \varepsilon_2 = 0$, and $l' = l'' = r$ yields to $K = 2$ and

$$D = \left(\frac{\Delta m}{m} \right) (270 \times 2)$$

$$\Rightarrow D = 540 \times \left(\frac{\Delta m}{m} \right) \quad 3.13$$

For the VG 354, the radius of the machine is 27 cm. The dispersion D , is a measure of how far apart the masses of Zn are separated and this can be calculated using Equation 3.13. This and the main components of the mass spectrometer are presented in figure 3.2.

Figure 3. 2: The three components of the mass spectrometer: Ion source, Magnet and the collection system. Figure scanned from (Loss, 1986)



3.1.2.3 The detection systems

After the ions have been separated and focused by the magnet they pass into a collector or detector system. Several different detector systems were available on the VG 354 – a Faraday multiple ion collector system, and single Daly collector. The Faraday collectors collect “ N ” ions of charge “ q ” over a given time “ t ”.

$$I = \frac{Nq}{t} \quad 3.14$$

When these charges pass through a resistance R , the resulting current; I , generates a potential $I \cdot R$. In the case of the VG354 the typical ion currents are of the order of 10^{-11} A, which together with a resistance of $10^{11} \Omega$, produces a potential difference of 1 V. This corresponds to about 10^8 singly positively charged ions per second. The minimum uncertainties possible with this system can be calculated using simple counting statistics, with the absolute lower limit of the precision (u) in the current being:

$$u = \frac{1}{\sqrt{N}}$$

3.15

Which; for 10^8 ions is around 1 part in 10,000 but many factors will degrade this Figure. One way of improving the statistics is to collect for several hours and using a larger intensity ion beam. Where isotope ratios are concerned, it is the ratio of the number of ions of each isotope that are measured and it is associated uncertainty estimate. In practical terms, the number of ions of the lesser abundance isotope, intensity and the stability of the ion beam that limits the final uncertainty.

The simplest method of measuring isotope ratios is using a single Faraday collector behind a fixed slit at a focal plane position, and then varying or stepping the magnetic field to sequentially direct the relevant ion beams of the various isotopes into the detector. This “peak hopping” is done repeatedly until a minimum or required uncertainty is achieved (De Laeter, 2001).

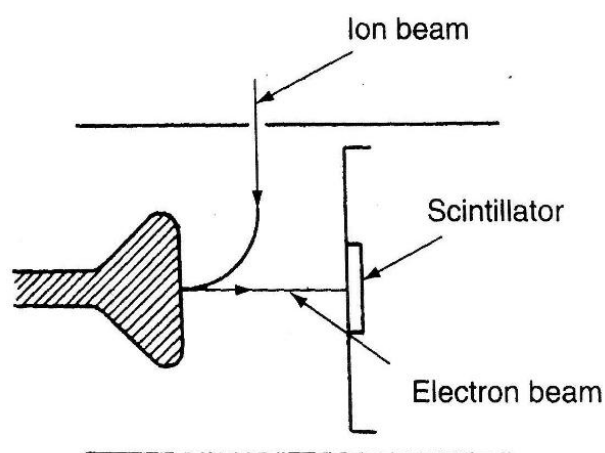
Faraday collectors are deep rectangular shaped buckets coated internally with graphite to reduce charged particle losses. When the positive ion hits the Faraday cup, a secondary electron is produced. Producing more than one secondary electron or the escape of the secondary electron from the cup produces a reading bias and is most likely to occur after long periods of use of and damage to the collection system. The presence of an electrode with small negative electric potential placed at the entrance of the collectors is used to suppress the secondary electrons from escaping from the cup.

A multi Faraday collector is a group set of Faraday collectors, which simultaneously collects all ion beams and significantly reduces problems associated with ion beam instability. The VG354 multicollector consists of a fixed position single “Axial” collector, four variable position high mass collectors (H1, H2, H3, H4) and four variable position lower mass collectors (L1, L2, L3, L4). Two collection approaches are possible, the simplest, Multi Static Collection, where an individual ion beam is directed to a specific collector, requires cross calibration of the collector amplifier gains and linearity and associated electronic systems. In the case of the VG354 this limits the final precision of measurements to around 0.01%. The more complex,

Multiple Dynamic Collection, can obtain precisions of $<0.001\%$ since it does not require amplifier gain calibration but requires a more elaborate setup, takes longer, and requires beam stability. Due to these factors, and several other experimental limitations, in this work it was decided that Multi Static Collection would be more than adequate for this work.

During this work a number of isotopic measurements were performed using the Daly detector. The Daly detector utilizes a highly polished metal electrode or “knob”, held at a high negative potential relative to the exit slit. Positive ions strike the “knob” producing secondary electrons and are accelerated away from the “knob” to hit a grounded scintillator, producing photons which are detected using a photomultiplier (De Laeter, 2001).

Figure 3. 3: The components of the Daly detector, (De Laeter, 2001)



The Daly detector generally has a better signal to noise ratio than Faraday collectors but is limited to operating at $<10^{-12}\text{A}$. Because there was only one Daly detector the overall precision obtainable with this type of detector is generally limited by ion beam stability during the peak jumping data collection sequence (see Section 3.5). In this work the Daly detector was used with a nominal gain of 100, primarily for analysis of ng amounts of Zn such as measuring blanks. A photo of the TIMS located in John De Laeter Centre for Mass Spectrometry is presented as in Figure 3.4.

Figure 3.4: The VG354 TIMS used in this work.



3.1.3 Thermal ionisation of Zn

3.1.3.1 Thermal ionisation process

Thermal ionisation is a generic term used to describe ionisation using thermal energy. The most straight forward method involves placing the sample on a hot surface. The Fermi level of the sample and the surface material are the same, and an exchange of electrons between the surface of the material and the atoms in the sample takes place. When this happens, some of the atoms in the sample are charged and provided they are not tightly bound to the material or non-ionized part of the sample, are ejected with a relatively low energy (De Laeter, 2001).

3.1.3.2 Ionisation efficiency

Thermal ionisation for Zn was investigated by Rosman (1972) but was unsatisfactory for the production of measurable Zn ion currents. Hence Rosman used electron impact ionisation for his study to measure Zn fractionation.

The ionisation efficiency “ E ” is the ratio of the total number of positive ions produced of the element of interest to that of atoms of the same element in the sample; in our case is Zn^+ . This can be represented by the Saha-Langmuir Equation shown in Equation 3.16

$$E = \left(\frac{N^+}{N_0} \right) = A e^{\left(\frac{\phi - I}{KT} \right)} \quad 3.16$$

Where N^+ is the number of positive ions produced from the sample, N_0 is the number of neutral atoms in the sample, A is a constant, and ϕ is the work function of the heating surface, I is the ionisation potential of the sample, in our case the ionisation potential for Zn (9.39 eV), and K is the Boltzmann constant (1.38×10^{-23} J/K), T is the temperature in Kelvin (De Laeter, 2001).

Direct thermal ionisation is extremely effective where the $(\phi - I)$ term is positive. For example in the case of potassium the $(\phi - I)$ term is around 0.7 eV compared to that for Zn of -4.4 eV. Equation 3.16 thus indicates that approximately 12 orders of magnitude fewer Zn^+ ions will be produced by direct thermal heating than for potassium.

To produce sufficient ion beams from high ionisation elements, ionisation enhancing agents or activators, such as silica gel and phosphoric are used. In the case of Pb ($I = 7.4$ eV) ionisation efficiencies using activators of around 10% have been measured for sub-nanogram amounts, but this efficiency has not been possible with Zn. The only determination of the Zn thermal ionisation efficiency using activators found in the literature is that of Loss and Lugmair (1990) of 0.05%.

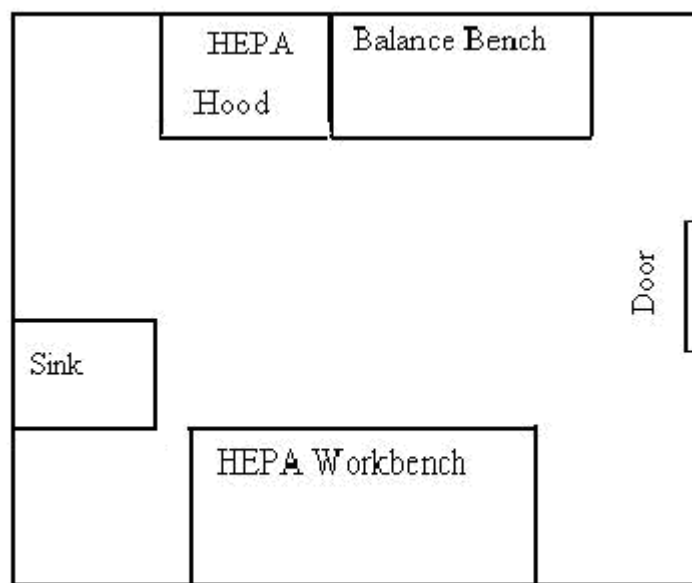
Since Zn has such a high first ionisation potential, it was a challenge to generate sufficient ions, particularly from small samples. An experiment to determine the ionisation efficiency of Zn was performed where 1.80 ± 0.08 μ g of Zn was mixed with a small amount (~ 5.6 μ L per 1 μ g of sample) of silica gel and Phosphoric acid activator. This produced an ion beam $> 10^{-12}$ A for seven continuous hours. This yielded an ionisation efficiency of 0.22 ± 0.07 %, which is more than four times that measured by Loss and Lugmair in 1990. Despite many years of investigation of the chemical physics of silica gel and other ionisation activators, this type of activation is

not well understood (De Laeter, 2001). During this work several other activators such as graphite was trialed but none produced ion beams $> 4 \times 10^{-13} \text{A}$ from $\sim 1 \mu\text{g}$ Zn samples. The Silica gel was thus chosen to be the activator in this work.

3.2 Contamination

All sample preparation was performed in the Curtin University Isotope “IDMS lab”, a laboratory supplied with High Efficiency Particulate Air (HEPA) filtered air (Efficiency 99.995% for particles $> 0.3 \mu\text{m}$) with critical sample evaporations taking place under a clean exhaust hood. A configuration of the IDMS lab is represented in Figure 3.5.

Figure 3. 5: Layout of the IDMS lab, with overall dimensions of $3 \times 3 \text{ m}$



Before commencing any measurement, the exposure blanks were measured in positions in the IDMS lab where work was conducted. The exposure blanks were as follows: 70 pg/day near the sink, 20 pg/day within the exhausting HEPA filter hood, 150 pg/day under the HEPA work bench”, 250 pg/day on the electronic balance bench which is consistent with it being near the entrance. Along with the low exposure blanks in the IDMS lab, a procedural blank accompanied each set of samples. The maximum procedural blank ever measured during the chemical purification was 13

ng, which accompanied the lengthy dissolution of a set of iron meteorites, as mentioned in Section 3.9.2. This is consistent with the fact that the iron meteorite needed more reagents, beakers, and handling than other samples.

3.2.1 Containers

Ultra pure reagents, plastic and Teflon ware that had undergone stringent clean procedures (see Section 3.3) were used to minimize contamination. All Teflon beakers purchased from Salvillex, and polyethylene ion exchange columns were leached in an ultra pure dilute acid baths before use. Teflon ware was soaked in a large HNO₃ bath for two weeks, rinsed with MQ water and transferred to a large HCl bath to be soaked for at least a week. After that, the Teflon ware was taken out of the bath, rinsed with MQ water, filled with 1M HNO₃ and were stored in plastic bags until used.

3.2.2 Reagent and water purification

The MQ water in the IDMS lab was produced by reverse osmosis followed by deionisation. The concentrations of Zn in the Reagents and MQ water was assessed by measuring a range of amounts of Zn using IDMS, as represented in Figures 3.6, 3.7 and 3.8 for MQ water, HCl, and HNO₃ respectively. In all the cases, different amounts of water and reagents were evaporated to dryness after spiking. The experiments were performed using the same beaker for each reagent each time, to assess the contribution of beaker contamination to the measurements i.e. “beaker blank”. As represented in the Figures below, the concentration of Zn in MQ water is 32 to 36 pgg⁻¹, measured from the slopes of the two experiments in Figure 3.6

Figure 3. 6: The amount of Zn as a function of amount of MQ water for two separate experiments. The concentration of Zn is represented by the slopes of the lines. The different y intercepts represent different beakers.

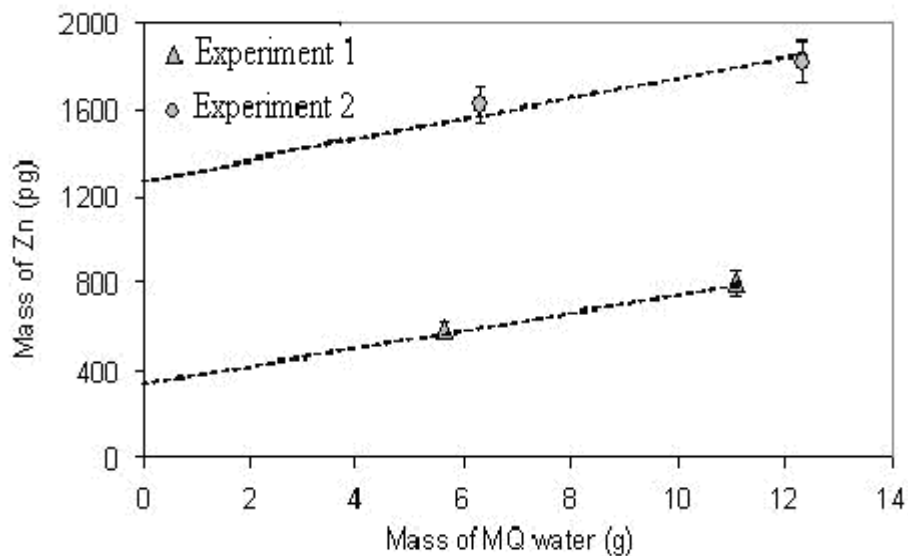


Figure 3. 7: The amount of Zn as a function of amount of HCl. The concentration of Zn is represented by the slope of the line $80 \pm 11 \text{ pgg}^{-1}$

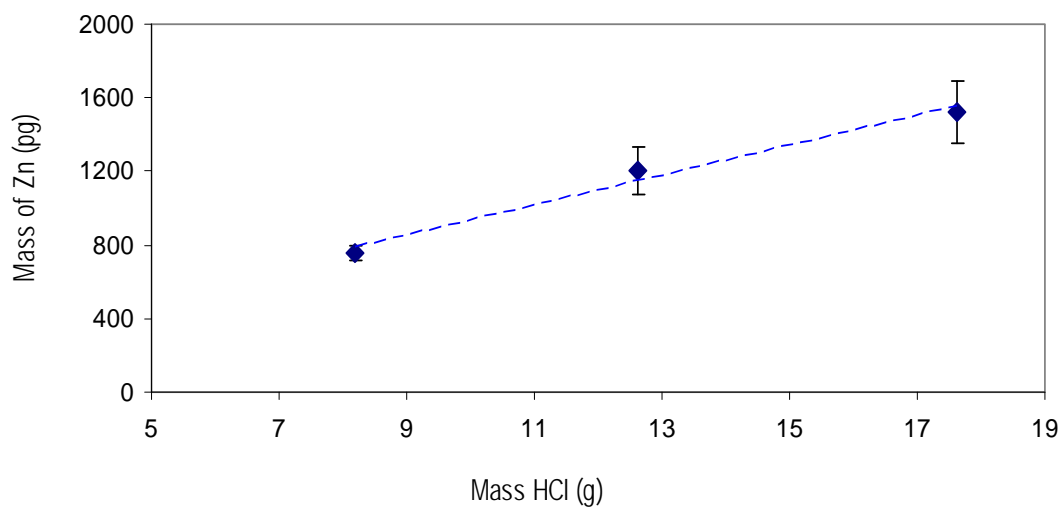


Figure 3. 8: The amount of Zn as a function of amount of HNO₃. The concentration of Zn represented by the slope of the line, $55 \pm 15 \text{ pgg}^{-1}$.

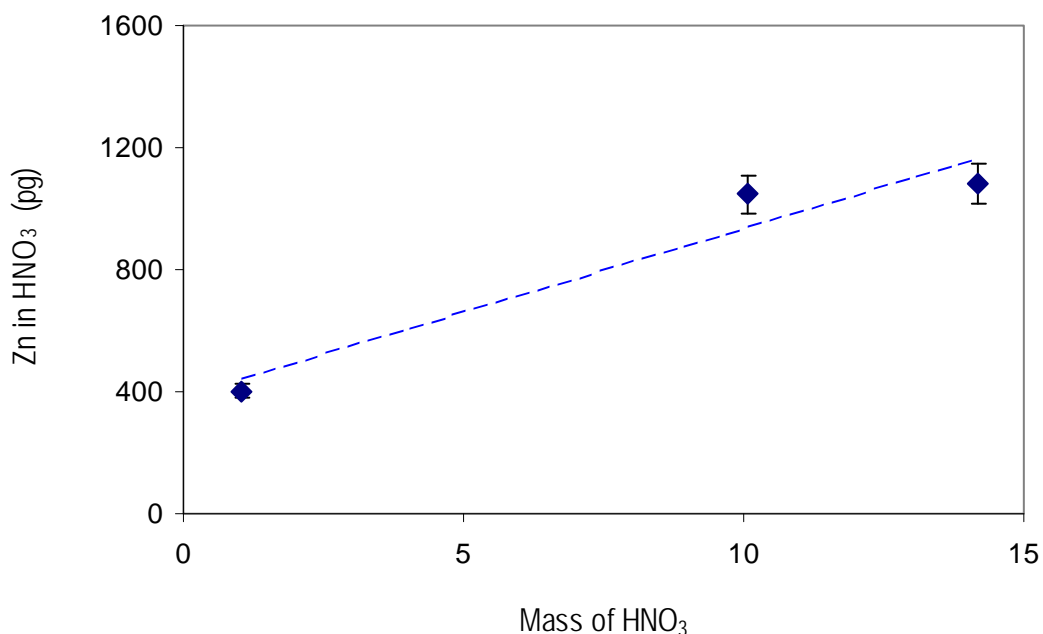


Figure 3.6, shows high beaker blanks, in experiment 1 and 2, $\sim 400 \text{ pg}$, and $\sim 1200 \text{ pg}$ respectively. In Figure 3.7 and 3.8, the beaker blanks are $\sim 400 \text{ pg}$ in both experiments. These difficult experiments also show that even at these levels, the beaker blank does not contribute more than 10% to the largest procedural blanks, nevertheless the beaker blank a long with procedural blank would need to be addressed further for the isotopic and elemental analyses of low level samples e.g. Polar ice.

A comparison of the levels of Zn in the reagents and MQ water used in this work with that of the advanced study of Bermin et al. (2006) measuring water using MC-ICPMS is shown in Table 3.1.

Table 3. 1: Comparison of the contamination of Zn in reagents and MQ water used in this work with that used by Bermin et al.(2006) to measured the isotopic fractionation of Zn in sea water using MC-ICPMS.

Abundance of Zn in Reagent	HCl pgg^{-1}	HNO ₃ pgg^{-1}	MQ water pgg^{-1}
This work	80 ± 11	$55 \pm 15.$	32 to 36
Bermin et al. (2006)	29	25	1.7

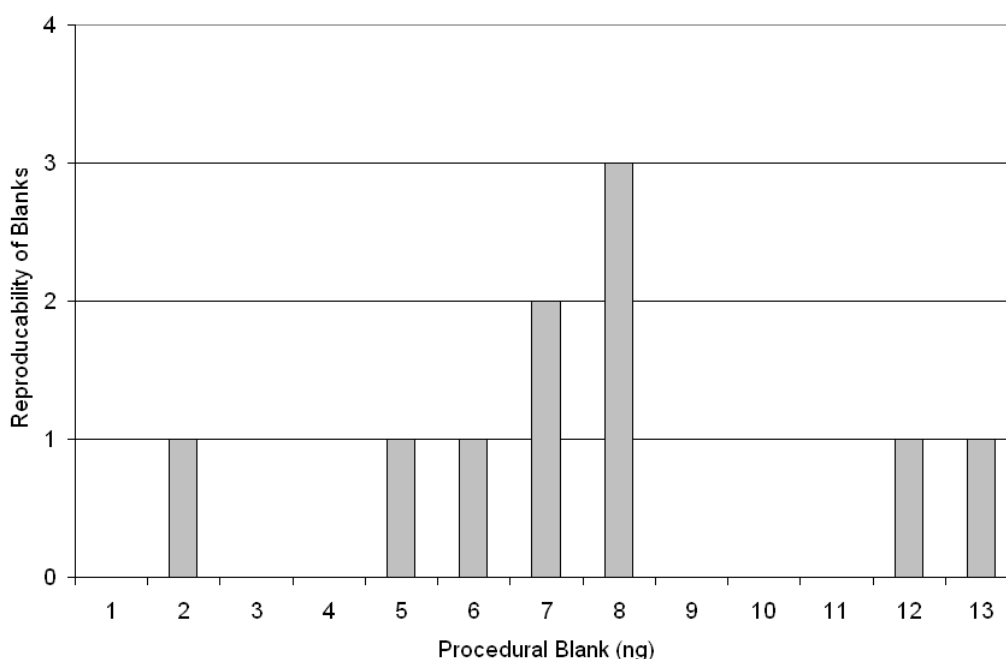
3.3 Measurement of Blanks.

Considerable care was required not to contaminate the samples and where appropriate, a correction for the contamination or blank was applied by measuring the amount of the element added to the procedure by processing a null sample. As the main aim of the research was to bring the TIMS Zn isotopic analyses to an advanced level, it was important to develop a technique for relatively small samples ($1\mu\text{g Zn}$) to be measured for its isotopic composition, and the few ng samples to be measured for their Zn elemental abundance (see Section 3.2). Accordingly, it was important to develop a procedure to reduce the blank associated with each analysis. A rigorous cleaning procedure was developed to minimize the beaker blank. Considerable effort was invested in measuring the concentration of Zn in the MQ, or any of the ultra pure reagents used in this work. It was important to try to plot a consistent line for the amount of Zn in the MQ water as a function of the amount used for the analyses (see Section 3.2.2). This was done after each cleaning sequence for a set of beakers, until negligible blank results were obtained, see Figures (3.7, 3.8 and 3.9). Teflon beakers purchased from Salvillex were handled with great care, and a data base was used to register all the information about each individual beaker by its number. Beakers were classified according to amount of any Zn sample used and whether the beaker contained spike or not. Beakers were filled with 1M HNO_3 solution and left for at least a week on the hot plate with closed lid. After that, beakers were rinsed with MQ water and filled with 1M HNO_3 again and placed on a hot plate with lid on for at least three days. The beakers were then rinsed with MQ water and filled with 1M HNO_3 , closed and soaked in the bath of $\sim 0.2\text{ M HNO}_3$ until use. It is important to mention that, the concentration of Zn in all these baths was closely monitored. There were several baths, for example, a bath only for beakers in which a laboratory standard was used, another bath for beakers used with double spike, bath for beakers used for samples with very low (ng) Zn amounts. As stated earlier beakers were monitored for how much Zn was used in them in each experiment or analyses.

While it may be possible to measure individual blank measurements, in many cases the spread in the distribution of the blank can dominate the final uncertainty of the blank measurement, especially if the procedural blank is relatively large in

comparison to the amount of samples being analysed. In this work, at least one procedural blank was measured with each batch of analyses, the average calculated to be 8 ± 5 ng, which was mostly negligible relative to the measured samples. The largest procedure blank measured during cleaning and sample preparation procedure was 13 ng for iron meteorites. This was expected as dissolving the sample needed more acids. However, a correction for the procedure blank was performed for all the IDMS calculations. The distribution of procedural blanks for the adopted technique is presented in Figure 3.9.

Figure 3. 9 Procedural blank for the adopted technique.



The sample amount to blank ratio obtained in this work is comparable to those most recently obtained for Zn isotopic analysis by MC-ICP-MS analysts. Table 3.2 shows a comparison between the size of sample used for analysis and the procedural blank obtained in this work compared to that of other analysts, all are for using ICP-MS analysis.

Table 3. 2: A comparison between the size of sample used for analysis and the procedure blank in this work compared to that of other analysts using ICP-MS analysis.

	This work	(Pichat et al., 2003b)	(Chapman et al., 2006)	(Luck et al., 2005)	(Petit et al., 2008)
Type of the samples	Natural Materials	Sediments cores	Geological SRMs BCR-1	Meteorites	Suspended Particulate Matter and Sediments
Size of sample used for analysis (μg)	1	0.5 –1	1.5-2.5	0.5-1	Loaded 15 μg Zn on the column chemistry
Procedure Blank (ng)	8 ± 5	<15	28 ± 4	10-20	15

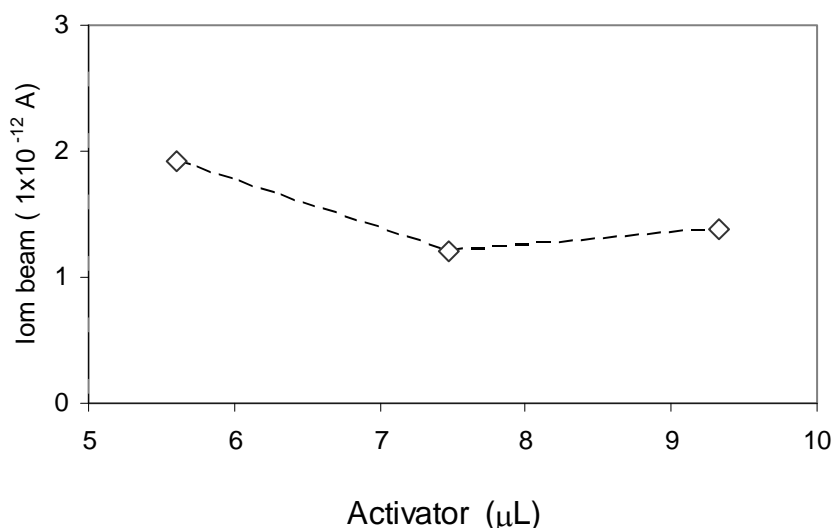
3.4 Sample loading, degassing and heating

Zinc filament loading was investigated as it could contribute to enhancing the ionisation efficiency. A number of trials were performed by loading the same amount of sample (1 μg Zn) on different filament ribbons Re, Pt and Ta materials, to assess the Zn^+ / interference ratio (see Section 3.6). In brief, these experiments yielded no Zn^+ using the Ta ribbon filament while, the Pt filament was no better than the Re in producing Zn^+ , but with increased interferences. This led to the conclusion the Re filaments are the most suitable for this work.

While using more Zn will produce more intense ion beam and will increase the Zn^+ / interference ratio hence reduce the effect of interferences where present, the challenge of this research was to develop a procedure, to produce the optimum ion beam (intensity, stability) within the “permissible temperature” (as discussed in Section 3.6), from the smallest sample possible.

A series of experiments was undertaken to determine the relationship between the silica gel (activator) (8 mgg^{-1}) and the ion beam intensity using the Faraday multi collector at temperature between ~ 1550 to $1600 \text{ }^\circ\text{C}$, the “permissible temperature”, is represented in Figure 3.10.

Figure 3. 10: $^{64}\text{Zn}^+$ current as a function of amount of activator solution used for $1 \mu\text{g}$ Zn sample at temperature $\sim 1550 \text{ C}^\circ$ using the Faraday multicollector.



As represented in Figure 3.10, using $5.6 \mu\text{L}$ of the activator (with a concentration of 8 mgg^{-1}) was sufficient to produce a $^{64}\text{Zn}^+$ ion beam of $\sim 200 \text{ mV}$, at temperature $\sim 1550 \text{ }^\circ\text{C}$, for $1 \mu\text{g}$ Zn sample using the Faraday multicollector. Despite the fact that the majority of nature materials contain Zn on the scale of tens of μgg^{-1} , the aim of this work was to develop the TIMS Zn analyses and make it applicable to smaller sample amount as possible. This was important so that rare and less abundant Zn samples could be analysed. To generate an ion beam suitable for the measurement of isotopic ratios with sufficient precision; such that the predicted sub per mil Zn fractionation could be detected. This size of sample was chosen for three reasons:

- $1 \mu\text{g}$ of Zn is considered to be a small sample in the field of Zn mass spectrometry as used for Zn isotopic fractionation analyses; this is because of the overall difficulty of Zn isotopic analyses
- The $1 \mu\text{g}$ Zn to blank ratio obtained; is equal to or better than the most recent developments in Zn isotope Mass spectrometry (see Table 3.2).

- $\sim 1\mu\text{g}$ Zn sample was relatively readily available for most of the samples except for meteorites.

Despite the fact that the concentration of Zn in most of the samples used in this work is the scale of tens of $\mu\text{g g}^{-1}$, this work never used more than $1\mu\text{g}$ Zn for an isotopic composition measurement. If the problems associated with the variability with the blank could be overcome, the procedures developed are applicable to lesser abundant Zn samples, such as Zn in water and polar ice. When the Faraday multicollector was used, only $1\mu\text{g}$ Zn was used because the double spike technique will allow for the simultaneous determination of fractionation and the concentration using IDMS.

A comparison of the ionisation potential and the amount of Zn required to produce a successful isotope ratio measurement with those of other transition elements and Ca, is shown in Table 3.3. Considering the very high ionisation potential of Zn, the $1\mu\text{g}$ Zn samples used for isotopic analyses represents a useful break through.

Table 3. 3: A comparison for the achievement of this technique for Zn regarding the size of the sample with other modern isotopic TIMS transition elements and Ca is shown.

Element	Zn	Fe	Cr	Ca	Cu	Mo
Ionisation potential	9.39 eV	7.87 eV	6.76 eV	6.1 eV	7.72 eV	7.1 eV
Reference	This work	(Turnlund and Keyes, 1990)	(Ellis et al., 2004)	(Heuser et al., 2002)	(Chapman et al., 2006)	(Wieser et al., 2007)
Size of sample	<1 μ g	5 μ g	250–500 ng)	200–800 ng	1.5-2.5 μ g	1 μ g

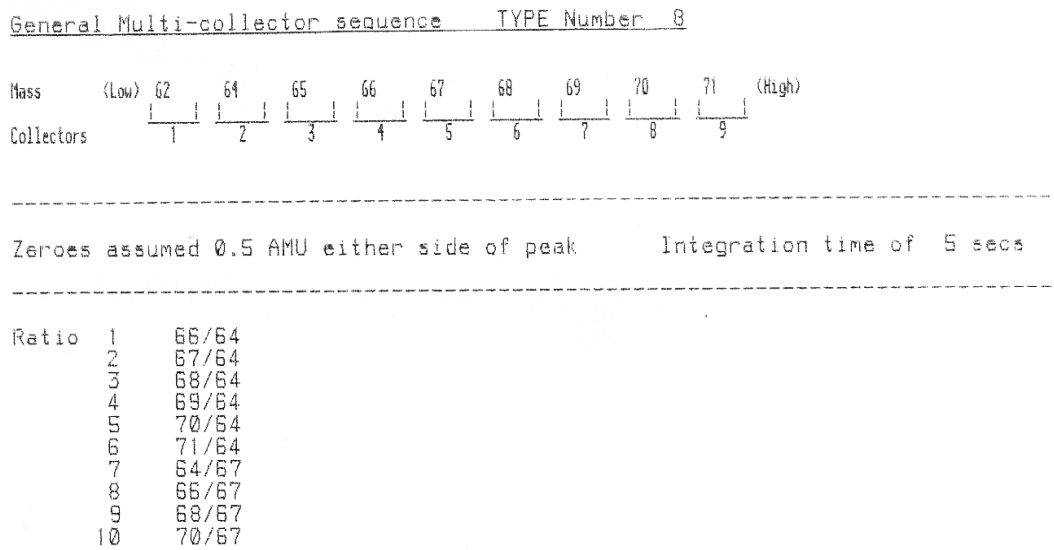
Prior to loading the samples onto the filaments, the filaments were degassed by heating them under vacuum to temperatures of 1850 C° for at least 30 minutes. All Zn samples were loaded using Re filaments, because Re is available in high purity, has a high melting point, and has a relatively high work function which helps to overcome the high ionisation potential, (Dickin, 2000). High purity is also important to minimize isobaric interferences. The zone refined Re filament ribbons dimensions of 0.03 × 0.76 mm were welded onto filament supports embedded in glass beads purchased from Cathodeon. The samples were loaded onto the centre filament of a triple filament assembly after being mixed with the activator; the samples together with the activator were dried by passing an electric current < 2.4 A through the filament. At this point the current was increased 0.2 A / min until the sample/activator mixture bubbled, and fumes were produced, when the current was further increased, until the filament glowed dull red for two to three seconds before turning the current off. Mixing the activator with the samples in their beakers was preferred before loading them onto the filament. The loading technique of Chang and his colleagues (2001) of loading the activator directly onto the filament before loading the sample was used sometimes with no measurable differences in the results between the two loading methods. The idea behind mixing the sample with the activator (which contains H₃PO₄) was to help destroy organic residue on the sample that might left from the ion exchange resin and to help adhere the sample to the filament surface (Dickin, 2000).

The filament beads were loaded into a carousel by first placing them into a filament support holder, which were in turn placed into a 16 sample carousel and placed into the ion source of the mass spectrometer. After establishing a vacuum of 2×10^{-7} mbar, the side filaments were “degassed” by heating them to a temperature of approximately 1600 °C for about 40 minutes, which effectively simultaneously volatilized unwanted components of the samples (Dickin, 2000). The degassing processes also reduced non isobaric interferences that could be present within the sample, the filament bead, the filament holder, and possibly the surrounding environment. Hydrocarbon and molecular interferences could be reduced significantly after this process. Following the sample degassing procedure, each of the samples was analysed. Each sample was heated up to 1350 °C (~3 A) over a period of 15 minutes. At this point the Daly detector was used to find and focus the Zn beam and begin to monitor interferences. Over the next fifteen minutes, the temperature was increased to ~ 1560 °C, producing a $^{64}\text{Zn}^+$ of at least 1×10^{-12} A (100 mV) using standards.

3.5 Isotopic Analysis methods

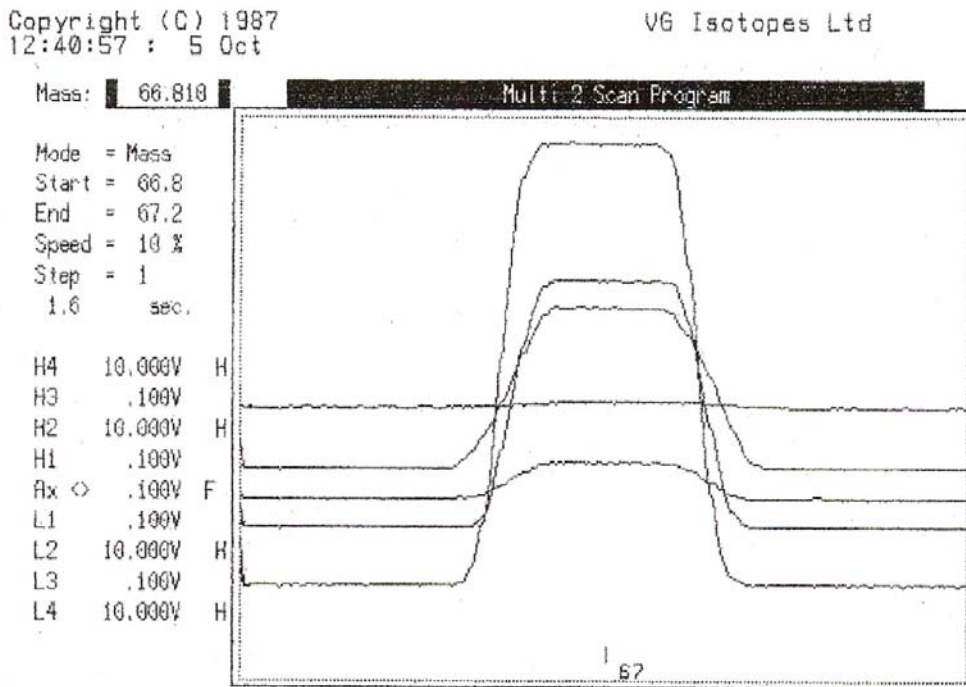
Ion currents were collected by the VG 354 relative to the ^{64}Zn when using the Daly and Faraday detectors. In the case of the Daly, a peak jumping method was used where by the magnetic field was changed sequentially to focus the ion beams for each Zn isotopes (masses 64, 66, 67, 68, 69 and 70 , corresponding to ^{64}Zn , ^{66}Zn , ^{67}Zn , ^{68}Zn , and ^{70}Zn) on to the Daly collector. The time spent on collecting data for each isotope was inversely proportional to its abundance with approximately 5 seconds for lower abundance, and 3 seconds for the higher abundances. Base line data were collected at mass 62.5, and interferences were monitored at a variety of masses as described in the following Section. Data were collected in blocks of ten ratios, with typically 3 blocks being collected for IDMS analysis, and ten blocks for isotope ratio determinations. In between blocks, the ion beam was refocused and if required the intensity was re-established. For Faraday multi collection, masses 64, 65, 66, 67, 68, 69, 70, and 71 corresponding to ^{64}Zn , ^{66}Zn , ^{67}Zn , ^{68}Zn , ^{69}Ga ^{70}Zn and ^{71}Ga , were collected in the L2, L4, Axial, H1, H2, H3 and H4 respectively as represented in Figure 3.11.

Figure 3. 11: Faraday multi collector positions and ratios collected.



The various isotopes of Zn were aligned with the collectors, with 67 in the Axial, using a mass spectrum scanning routine, the output for which is shown in Figure 3.12.

Figure 3. 12: Mass spectra of Zn isotopes scanned across the Faraday multicollector system as output by the Mass Scanning program.



After assuring that a stable ion beam $\geq 1 \times 10^{-12}$ A (100mV) was obtained on the Faraday multi collector, ratios were collected. Ion current baselines were measured 0.5 amu either side of the peaks using integration times of 5 seconds before

measuring a set of isotope ratios. The computer automatically calculated the ratios of masses 66, 67, 68 and 70 relative to 64 and 64, 66, 68, and 70 relative to 67. Isotope ratios were collected in blocks of ten before the ion beam was refocused and if required the intensity was re-established. Using the Faraday multicollector at least 50 ratios of each isotope were collected for the isotopic composition measurements and at least 20 of each were collected for IDMS calculations. For IDMS data the collected ratios were automatically screened for outliers and ratio rejections were limited to no more than 15% of all ratios collected. The calculated uncertainties were expressed using 95% confidence of the mean.

For isotopic composition work a 2.4σ or no more than 85% of the data rejection criteria was used (Loss and Lugmair, 1990). For most samples it was not necessary to reject more than 5% of the collected ratios. An internal normalization was applied to the individual ratios to relatively correct for during the analyses bias, by calculating a fractionation factor using the average of $^{68}\text{Zn}/^{64}\text{Zn}$ ratios as represented in Equation 3.17.

$$f = \frac{\left(^{68}\text{Zn}/^{64}\text{Zn} \right) - \left(^{68}\text{Zn}/^{64}\text{Zn} \right)_{\text{Average}}}{\left(^{68}\text{Zn}/^{64}\text{Zn} \right)_{\text{Average}} * (68 - 64)} \quad 3.17$$

Where f was applied in Equation 3.9 for each ratio. $\left(^{68}\text{Zn}/^{64}\text{Zn} \right)$ is the individual ratio of the ^{68}Zn to ^{64}Zn measured, $\left(^{68}\text{Zn}/^{64}\text{Zn} \right)_{\text{Average}}$ is the average ratio of the ^{68}Zn to ^{64}Zn of the measured ratios.

In order to improve the precision of the measurement, it was important to minimize any possible effects on mass fractionation parameters, such as: the sample size, chemical composition and purity, sample loading procedure on filament, and the length of time of data acquisition, and the rates of sample degassing and heating were held as constant as

Controlling and monitoring the interferences was a major challenge in this research. To assist with detecting any possible interference on all the isotopes measured of the lab standard, three isotope plots were used to show $^{68}\text{Zn}/^{64}\text{Zn}$ as a function of $^{66}\text{Zn}/^{64}\text{Zn}$, $^{67}\text{Zn}/^{64}\text{Zn}$ as a function of $^{66}\text{Zn}/^{64}\text{Zn}$ and $^{70}\text{Zn}/^{64}\text{Zn}$ as a function of

$^{66}\text{Zn}/^{64}\text{Zn}$ along with predicted synthesised linear machine fractionation of the laboratory standard. Examples of these plots are represented in Figure 3.13, 3.14 and 3.15. All the measured ratios were found to be consistent with the predicted linear fractionation line. Also indicated on these plots were the maximum synthesised tolerable interferences on each of the isotopes which would not affect the results of the fractionation represented as range bars. These graphs were vital to demonstrate that the collected ratios of the laboratory standards were fit for the purpose of this research. The possible contribution of these interferences to the fractionation is explicitly discussed in Section 3.6.

Figure 3. 13: Tolerated interference of the $^{67}\text{Zn}/^{64}\text{Zn}$ ratio as a function of the $^{66}\text{Zn}/^{64}\text{Zn}$ ratio for 18 laboratory standard analyses. The major range bars represent the maximum tolerable interference possible before affecting any results

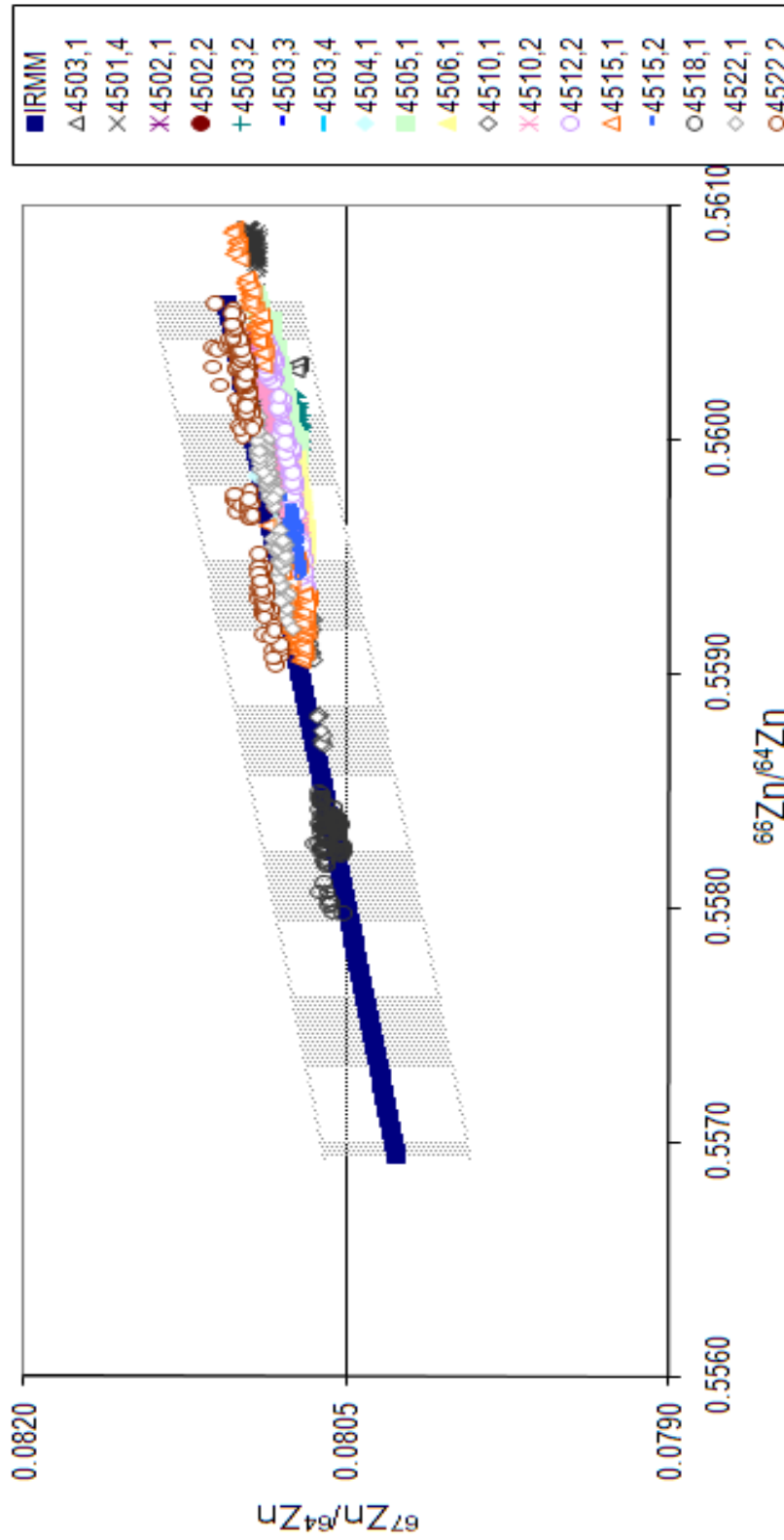


Figure 3. 14: Tolerated interference of the $^{68}\text{Zn}/^{64}\text{Zn}$ ratio as a function of the $^{66}\text{Zn}/^{64}\text{Zn}$ ratio. The major range bars represent the maximum tolerable interference possible before affecting any results.

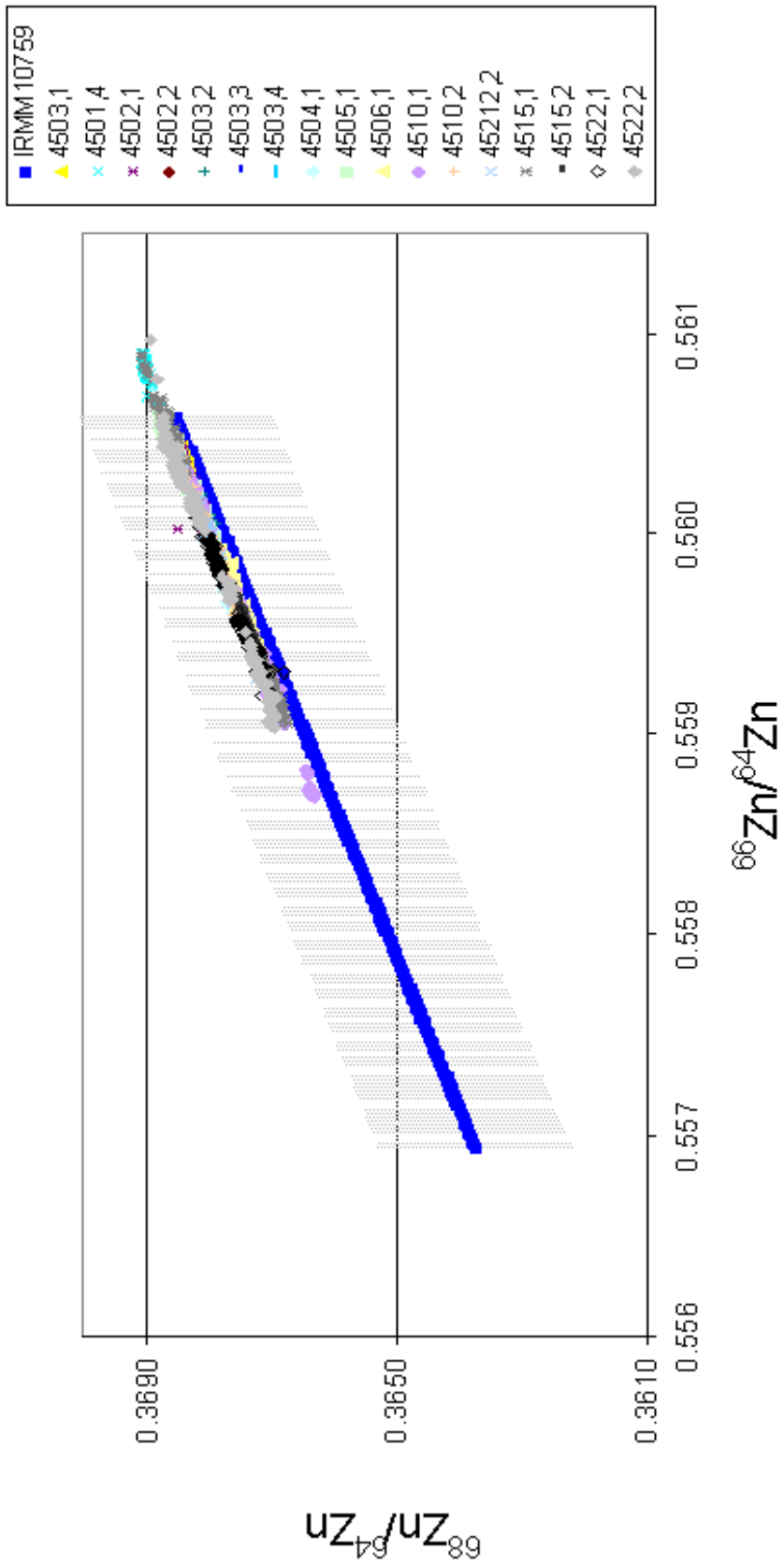
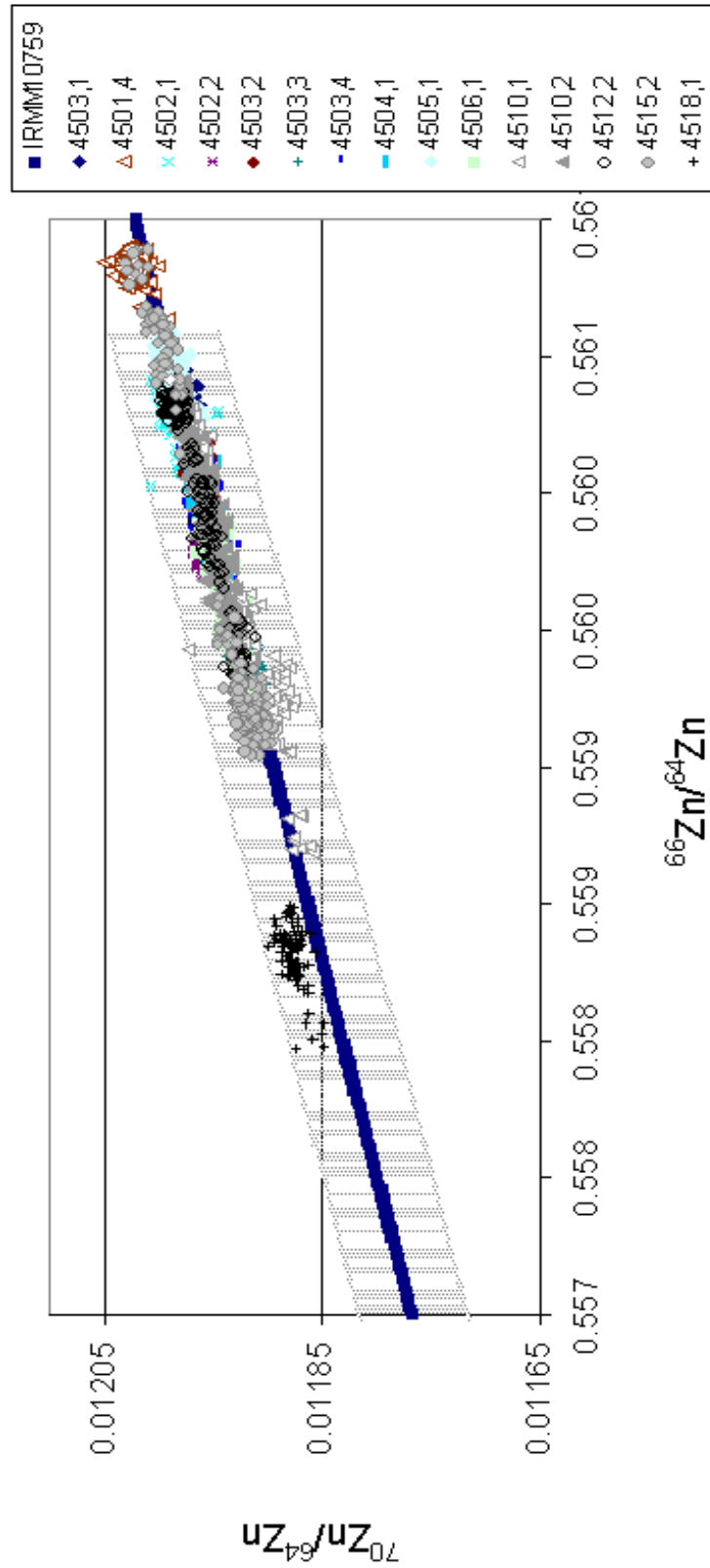


Figure 3. 15: Tolerated interference of the $^{70}\text{Zn}/^{64}\text{Zn}$ ratio as a function of the $^{66}\text{Zn}/^{64}\text{Zn}$ ratio. The major range bars represent the maximum tolerable interference possible before affecting any results



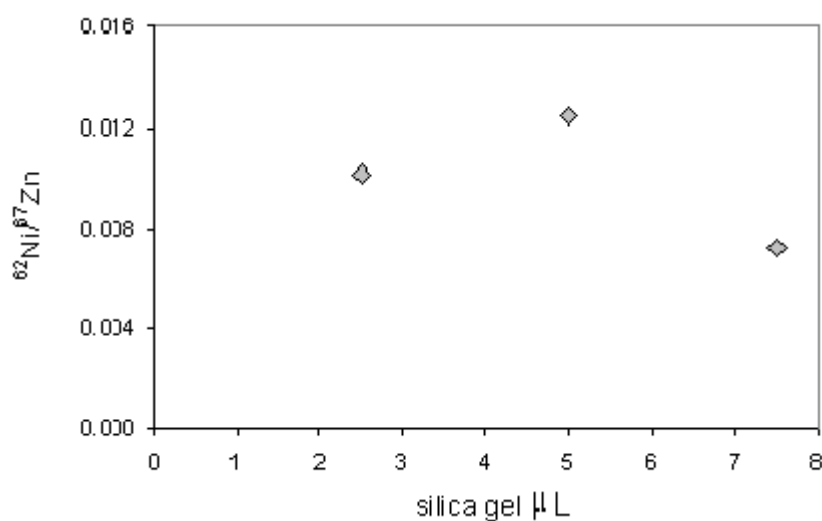
The plots consistently show that the isotopic fractionation is least affected by interferences on the ^{64}Zn , ^{66}Zn and ^{68}Zn . Small interference effects were occasionally observed on mass 70, but provided specific precautions were taken these were never outside the tolerable limit to determine inherent fractionation effects.

3.6 Interferences

To determine the isotopic fractionation of Zn using the double spike technique it was vital to assess and monitor isobaric interferences. This is because; the double spike technique does not correct for any interferences, or for contamination. Because of this, a considerable effort was taken to investigate possible interferences with the aim of eliminating, rather than having to correct for them. Significant possible interferences were, ^{64}Ni on ^{64}Zn , CrO^{16} on ^{66}Zn and ^{68}Zn , and ^{70}Zn , $\text{Fe}^{54}\text{O}^{16}$ on the ^{70}Zn , hence mass scanning of the Zn spectrum and other elements were performed for all isotopic analyses. Evidence of Ni, Cr and Fe was found in the mass spectra of some standards, blanks and samples; the magnitudes of which depended on a range of factors. To investigate the filaments as a potential source of interferences, filament blanks were prepared using different filament ribbon materials Re, Pt and Ta, and the filament blanks were run under the same conditions as those for Re. The measurements yielded no Zn^+ ionisation using the Ta ribbon filament. On the other hand Re ribbon filaments showed a considerable amount of Ni and Fe spectrum as ^{62}Ni , ^{56}Fe , $^{72}(\text{FeO})$ was seen in the scan (there was no Ge spectrum), which indicated interferences on ^{64}Zn and ^{70}Zn from ^{64}Ni and $^{54}\text{Fe}^{16}\text{O}$ respectively. More over, Re ribbon filaments showed a considerable amount of Cr spectrum as ^{52}Cr was obvious in the scan; interferences from CrO on ^{66}Zn , ^{68}Zn , and ^{70}Zn was confirmed as the ratio of the scanned $^{69}\text{Ga}/^{71}\text{Ga}$ was more than 1.50, more than 2 ‰ is the presumed variation in the isotopic composition of Ga by different researchers (IUPAC, 2003). The same approach was used for Pt ribbon filament, which was no better and sometimes worse than the Re ribbon filaments.

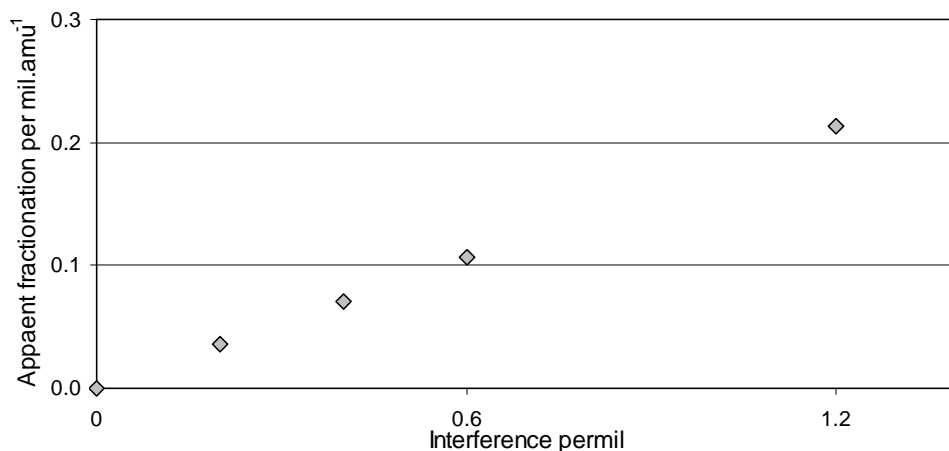
The silica gel was also investigated as a potential source of interferences by collecting ratios of the interfering isotope relative to the ^{67}Zn (the most abundant isotope in the blank sample) using filament blank experiments. Figure 3.16 shows no relationship between the volume of silica gel used and Ni interference. Investigations of ^{69}CrO and ^{72}FeO as a function of amounts of silica gel showed similar uncorrelated results.

Figure 3. 16: Ni interference as a function of volume of Silica gel using a filament blank (Uncertainties for $^{62}\text{Ni}/^{67}\text{Zn}$ are approximately the same size as the symbols used)



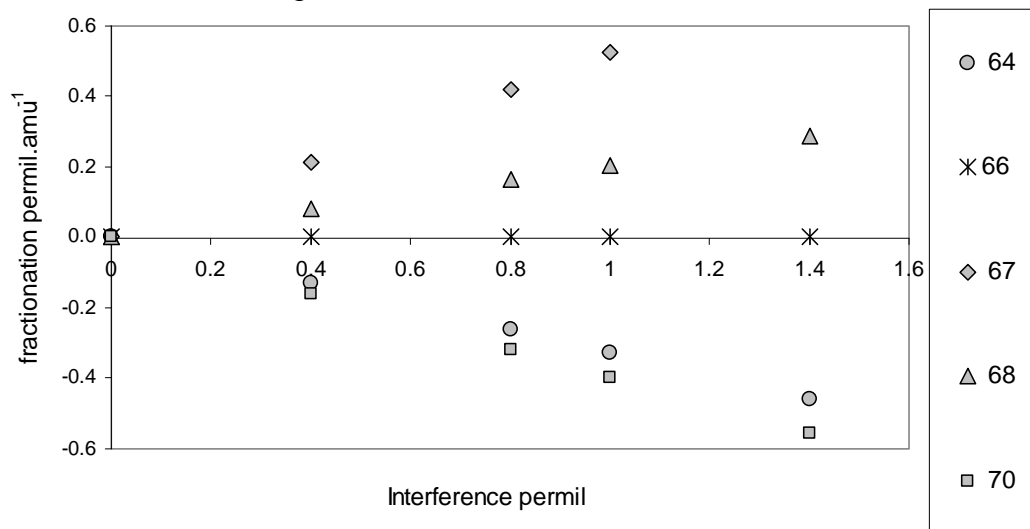
Another suspected source of the interferences was the filament posts. A small piece of the filament post was dissolved and loaded in the TIMS and scanned for Cr, Fe, Ni, Zn, Cu, and Al, but only Fe and Ni clearly observed. Unfortunately, it was not possible to change the post as the alloy used is deliberately designed to minimize thermal expansion against the glass bead by the manufacturer. The effect of interferences on the measured fractionation is theoretically illustrated in Figures 3.17, and 3.18 for Cr and other interferences respectively. These were performed by theoretically imposing interferences relative to the isotopic composition of the mixture (laboratory standard and double spike) and calculating their effect on the fractionation.

Figure 3. 17: The apparent fractionation of Zn^{+} resulting from permil interferences from CrO^{+} .



The effect of the other interferences is as represented in Figure 3.18

Figure 3. 18: The apparent fractionation of Zn resulting from various isobaric interferences on each isotope of Zn.

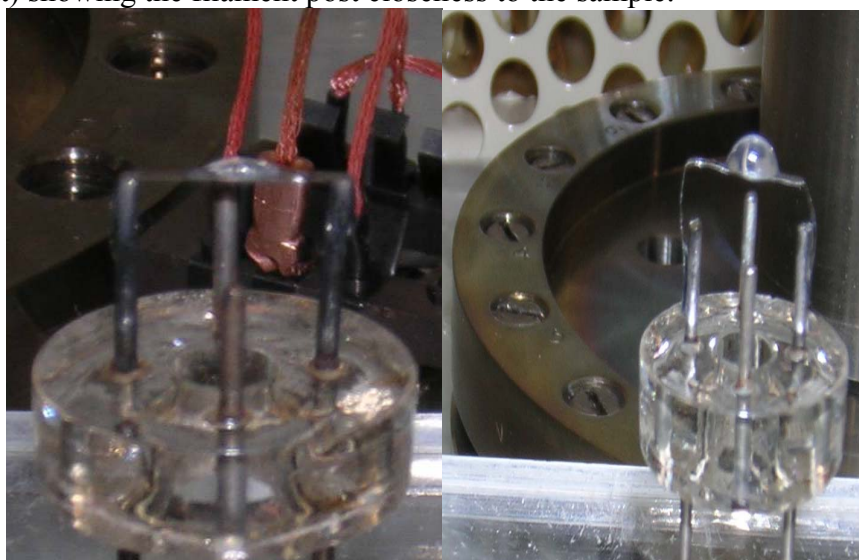


In this research, all fractionation calculations were performed using two sets of isotopes, ($^{64}Zn, ^{67}Zn, ^{68}Zn, ^{70}Zn$) and ($^{64}Zn, ^{66}Zn, ^{67}Zn, ^{70}Zn$). Figure 3.17 and 3.18 uses the first set of isotopes to show the effect of the interferences on these isotopes on the final fractionation values. The reason that ^{66}Zn is not apparently affected is because ^{66}Zn isotope is not used in the model calculations used for this Figure. However, this does not mean that interference on ^{66}Zn does not affect the

fractionation. The same Figure shows that the effect of these interferences will not cancel each other in terms of measured fractionation. As in the results in chapter 5 show that two sets of isotopes were used to calculate the fractionation, which was always consistent within uncertainty. On the other hand, and as represented in Figure 3.18, Zn fractionation is highly sensitive to interferences; such that a 0.4 ‰ interference of the isotopic composition of the standard of any isotope could significantly affect the calculated fractionation, this highlights the difficulty of measuring such fractionation and achieving accurate results.

To minimize the effect of interferences from the filaments posts, a modified filament support structure was investigated whereby the distance between the sample and the filaments posts was increased see Figure 3.19. This was done by cutting away part of the posts in direct contact with the heating surface of the filament, after the filament had been welded onto the posts, and before the sample was loaded onto the filament as represented in Figure 3.19.

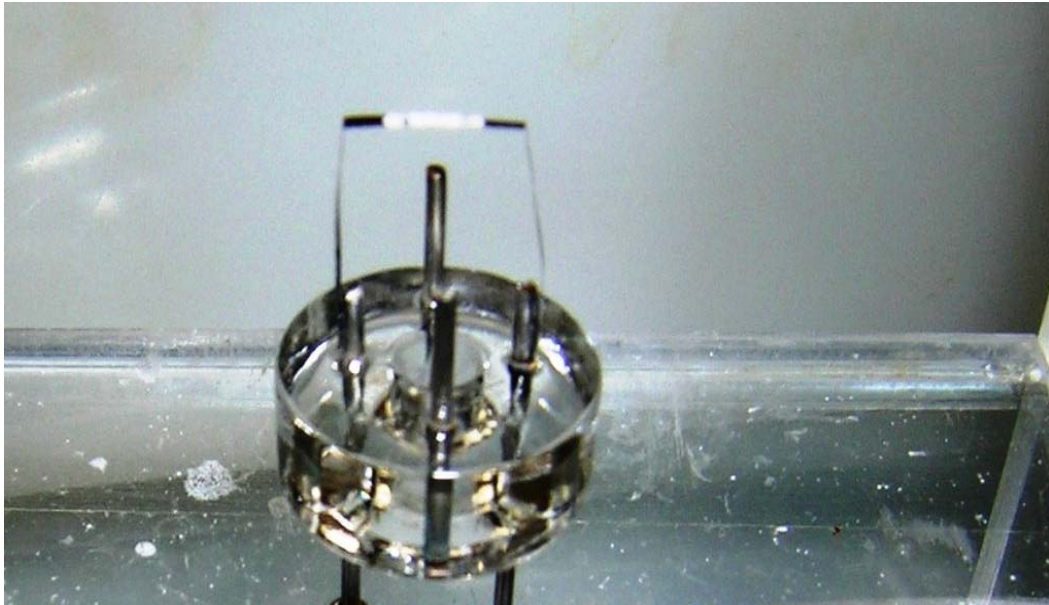
Figure 3. 19: Loading the sample on an ordinary filament (left) and using a modified one (right) showing the filament post closeness to the sample.



Unfortunately the interferences were found to be the same for both types of filaments (normal and modified). The Ni and FeO interferences were reduced at lower temperatures for the modified filament support, but there was no difference between the two filaments at higher temperatures. Other experiments investigating the possible

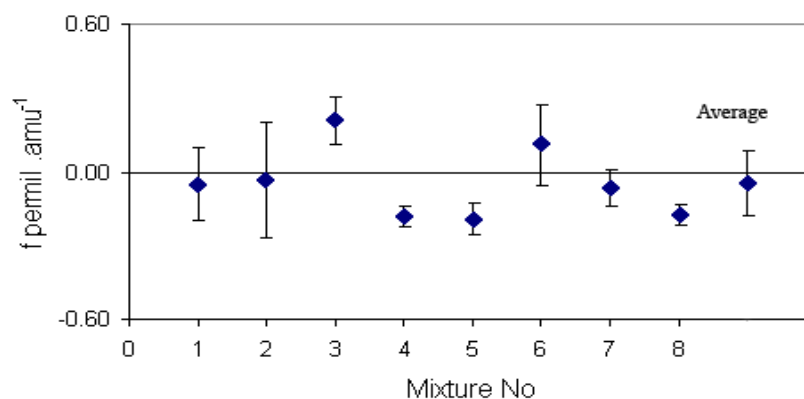
affect of $^{52}\text{CrO}^{16}$ interference ^{68}Zn showed the same pattern as the other interferences. The gap between the filament ribbon and the filament posts was then further increased (see Figure 3.20) using a jig made of stainless steel to bend the filament before being welded, unfortunately, these modifications did not reduce the interferences.

.Figure 3. 20: The alternative modified filament



An indirect preliminary assessment of the effect of interferences in the laboratory standard and double spike was obtained by examining the reproducibility of the Zn fractionation in eight mixtures of the laboratory standard and the double spike. All the measured mixtures should produce the same amount of fractionation within uncertainties (zero). This is because the fractionation of the mixture represents the fractionation of the laboratory standard relative to itself. This demonstrates that the variation in the interferences produced a measured fractionation for all the mixtures within $\pm 0.2 \text{‰ amu}^{-1}$ as represented in Figure 3.21.

Figure 3. 21: Measured fractionation of 8 mixtures (Lab standard and double spike) at temperature > 1675 °C.



Since it is very unlikely that the affect of any of the interferences would be this consistent, Figure 3.21, represents a detection limit or “reproducibility of the fractionation” within $\pm 0.2 \text{ ‰ amu}^{-1}$. Proceeding with our measurements at this point by accepting or ignoring the interferences, would not enable fractionation less than 0.2 ‰ amu^{-1} to be discovered.

In an attempt to reduce the effect of interferences a less concentrated activator was used (8mgg^{-1}), and $5.6\mu\text{L}$ of it was loaded with each sample which enabled the samples to be run consistently at a lower temperatures, around 1560 °C , still producing an ion current $>1 \times 10^{-12} \text{ A}$, compared to $>1675 \text{ °C}$ used for previous measurements. Analysing the sample at the lower temperature minimized the effects of the interferences; such that a final reproducibility of the measured fractionation of $\pm 0.039 \text{ ‰ amu}^{-1}$ was obtained (see Section 5.4 and Figure 5.6).

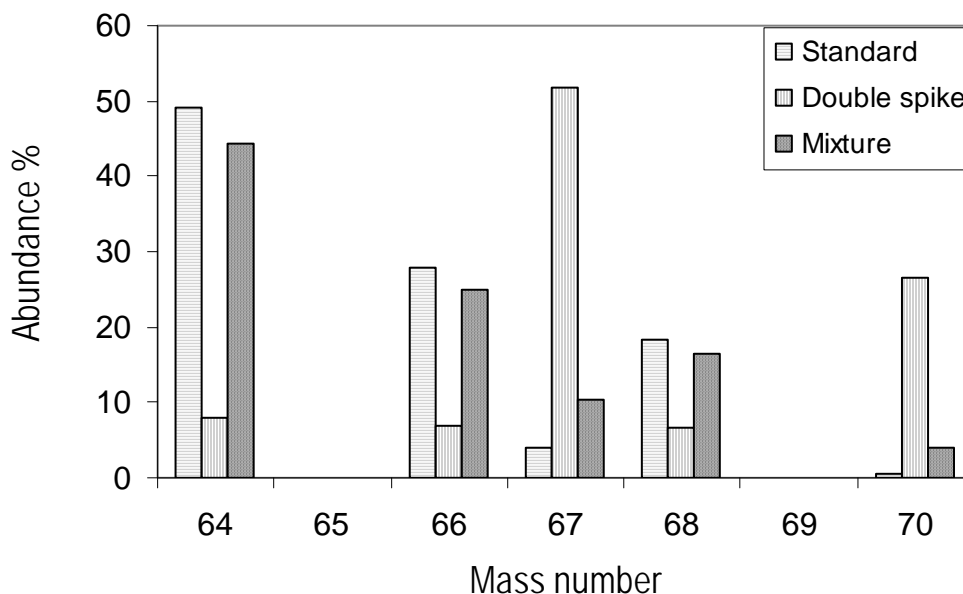
3.7 IDMS and Double spike methods

3.7.1 IDMS

The isotope dilution mass spectrometry technique (IDMS) is well established as one of the most accurate measurements techniques used to determine the amount of virtually any polyisotopic element in a substance (Platzner et al., 1997). A significant advantage of the IDMS technique is that, it measures directly in SI units for amounts

of substance, and can be used over large dynamic range of elemental concentration, because of the large dynamic range of both weighing instruments and the mass spectrometer. Moreover, the technique uses the fact that isotopes are much better representatives of an element than chemical atoms. IDMS analyses uncertainty budget can include any uncertainties introduced in the chemical separation (De Bièvre, 1993), and it is a very sensitive technique enabling nanogram small amounts of Zn to be measured with high external reproducibility (Ghidan and Loss, Submitted). The isotope dilution technique is based on gravimetrically mixing a known amount of an isotopically enriched material (spike) with a known amount of sample. The spike normally consists of a solution containing a known concentration of the element of interest that has been isotopically enriched in one or more of its isotopes. The isotopic composition of Zn for the laboratory standard, the double spike, and the mixture of both are represented in Figure 3.22.

Figure 3. 22: The isotopic composition of the standard, the tracer “double spike” and a typical mixture (double spike and standard used in this work).



Adding a Zn spike to the sample produces a blended isotopic composition or mixture, which varies according to the standard and double spike mixing ratio. Figure 3.22 also represents a typical mixture used in this work and was “the mixture of the double spike and the laboratory standard” used to measure the reproducibility of the measured fractionation.

As shown in Figure 3.22 the isotopic composition of the mixture is in between that of the Zn in a sample and the Zn in the spike. The blended isotopic composition is then measured using the mass spectrometer enabling the original amount of element in sample to be determined algebraically. The isotope dilution Equation can be represented as in Equation 3.17 as represented by (Webster, 1960).

$$x = \left(\frac{\sum_{i=1}^{i=n} A_{ik} M_i}{\sum_{i=1}^{i=n} B_{ik} M_i} \right) \cdot \left(\frac{(B_{ik} - C_{ik})}{(C_{ik} - A_{ik})} \right) \cdot y \quad 3.17$$

Where:

x is the amount of Zn in the sample.

A_{ik} is the Ratio of the abundance of the i^{th} isotope to the k^{th} isotope of the Sample.

B_{ik} is the Ratio of the abundance of the i^{th} isotope to the k^{th} isotope of the spike

C_{ik} is the Ratio of the abundance of the i^{th} to the k^{th} isotope in the mixture.

M_i is the atomic mass of isotope i .

y is the quantity of Zn atoms of Zn in the spike.

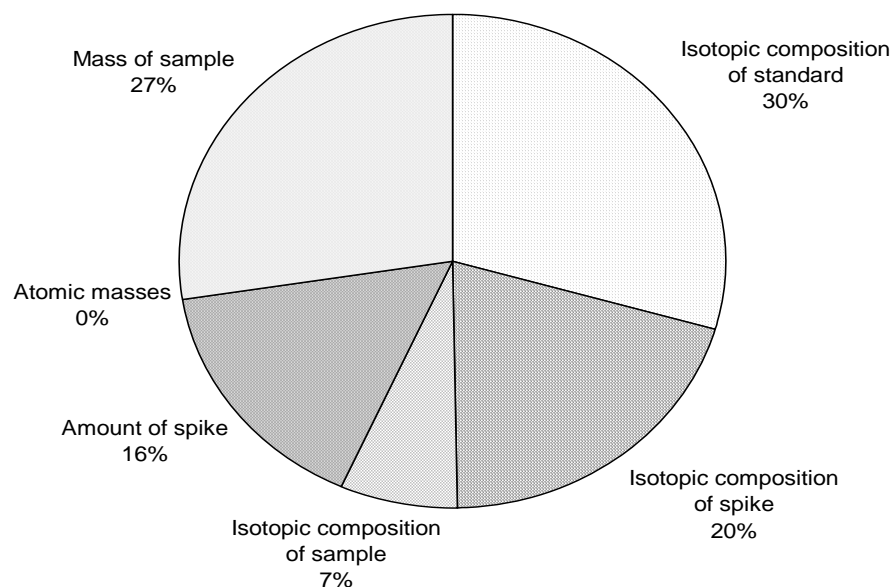
It is essential that the addition of the spike to the sample occurs as early as possible, preferably at the commencement of the sample preparation, and that an adequate equilibration of trace and sample also occurs as soon as possible after this addition. Once this has taken place, loss of sample and 100% recovery of the sample are not critical to the analysis, as the same amount of tracer will be lost from the mixture. However, contamination of (particularly small) samples still remains an issue, which is discussed further in this Section. Some effort is required to optimize the process by using a spike with appropriately enriched stable isotopes, and amount of spike relative to sample used for each sample. IDMS is limited to elements with two or more stable or long lived isotopes, requires destruction of the sample, is relatively expensive, and requires a knowledgeable analyst (Platzner et al., 1997, De Laeter, 2001). A significant advantage of IDMS is that the final result does not depend on high

efficiency chemical extraction procedures, which is a general requirement for other methods (De Laeter, 2001).

Another significant issue is the addition of too much (over spiked) or too little (under spiked) trace. An optimum sample tracer mixture for the spike used in this work is where the $^{68}\text{Zn}/^{67}\text{Zn} \sim 1$. As the availability and cost of the tracer was an important consideration, samples containing large amounts of Zn were spiked with less the optimal amount. On the other hand, measuring contamination levels often involved over spiking, simply so that sufficient Zn would be available for mass spectrometric analysis. As the concentration of Zn in some samples was unknown non optimal spiking sometimes occurred. In these cases it was sometimes necessary to repeat the entire IDMS measurement.

The final uncertainty of IDMS is determined by a number of factors, including all gravimetric measurements, all isotope ratio measurements, and the effect of contamination. As an example, the IDMS budget for SDC-1 sample, measured on the Daly detector is shown in Figure 3.23. Although the relative uncertainty on the procedural blank is large the magnitude of the blank is small in comparison to most sample amounts used hence the final contribution to the overall uncertainty is too small to observe in this budget for this sample. A sensitive component is the mass of the sample since the mass used is minimized to avoid wasting sample and double spike solution. The uncertainty in the isotopic composition of the standard can be reduced by using the Faraday collector but then more spike solution will be required.

Figure 3. 23: Uncertainty Budget for IDMS measurement of SDC-1 SRM (concentration of $101.5 \pm 1.7 \mu\text{g g}^{-1}$), measured with the Daly detector



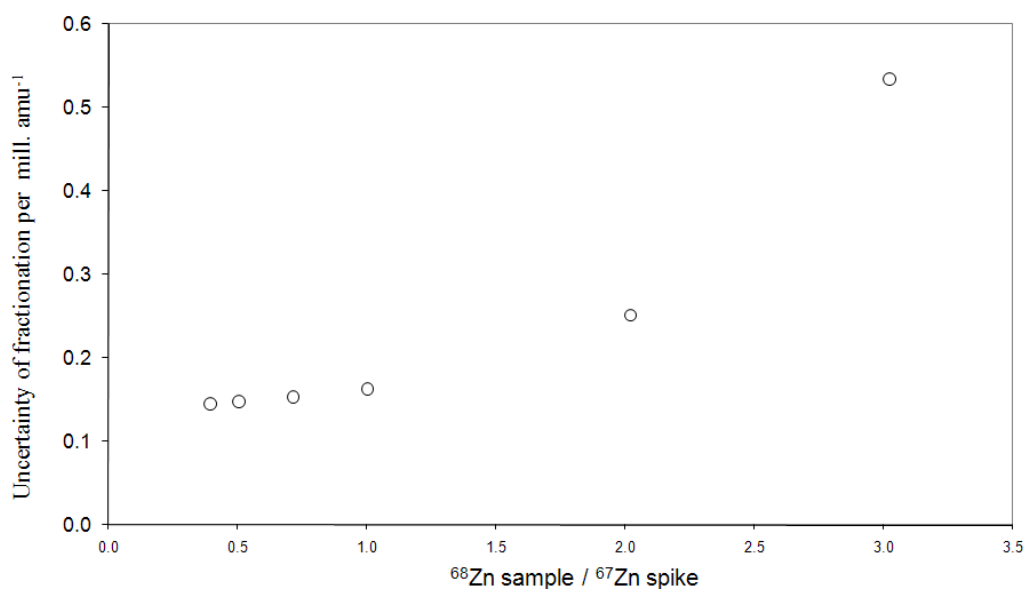
3.7.2 Double spike technique

Apart from the study of Rosman (1972) which could not detect Zn fractionation within uncertainty in natural materials; this is the first time the double spike technique is exploited using TIMS to measure the isotopic fractionation of Zn in natural materials. The previous attempt by Rosman (1972) used the approach of direct solutions of Equations derived in the theory developed by Dodson in 1963 and 1969 (Rosman, 1972a). The Russell (1971) approach of double spiking was used in this work. The isotopic composition of the double spike provides an internal monitor of the instrumental mass fractionation; such that; the isotopic composition of the mixed sample can be corrected (Wieser and De Laeter, 2003), enabling the true isotopic composition of the sample to be measured. The superiority of the double spike technique is that the double spike technique can also correct for any fractionation in the isotopic composition of the sample due to anion exchange chemistry (Rosman, 1972a).

In this work the double spike solution used contained enriched ^{67}Zn and ^{70}Zn , and is the same solution as that prepared by the study of Rosman (1972). This is consistent with an over all increase of the concentration of the double spike ($1.1921 \pm 0.0032 \mu\text{gg}^{-1}$) with the remainder due most likely to evaporation (see Section 5.3). As for IDMS measurements, it is important that all the samples were double spiked directly after weighing. Homogenizing the spike and sample in the early stages of the sample preparation fixes the isotopic ratio of the sample and spike mixture. The sample to double spike ratio contributes to the final uncertainty of the measured fractionation as represented in Figure 3.24.

Because of the high cost of enriched stable isotopes the already available double spike was used and the only major variable that could be optimised was the sample to double spike ratio. To conserve spike, the ratio of sample to spike used in preliminary work was with a ^{68}Zn in the sample to ^{67}Zn in the double spike of approximately 1.6. In the latter part of this work the ratio was reduced to ≤ 1 .

Figure 3. 24: The effect of the sample to spike ratio on the uncertainty of the measured fractionation

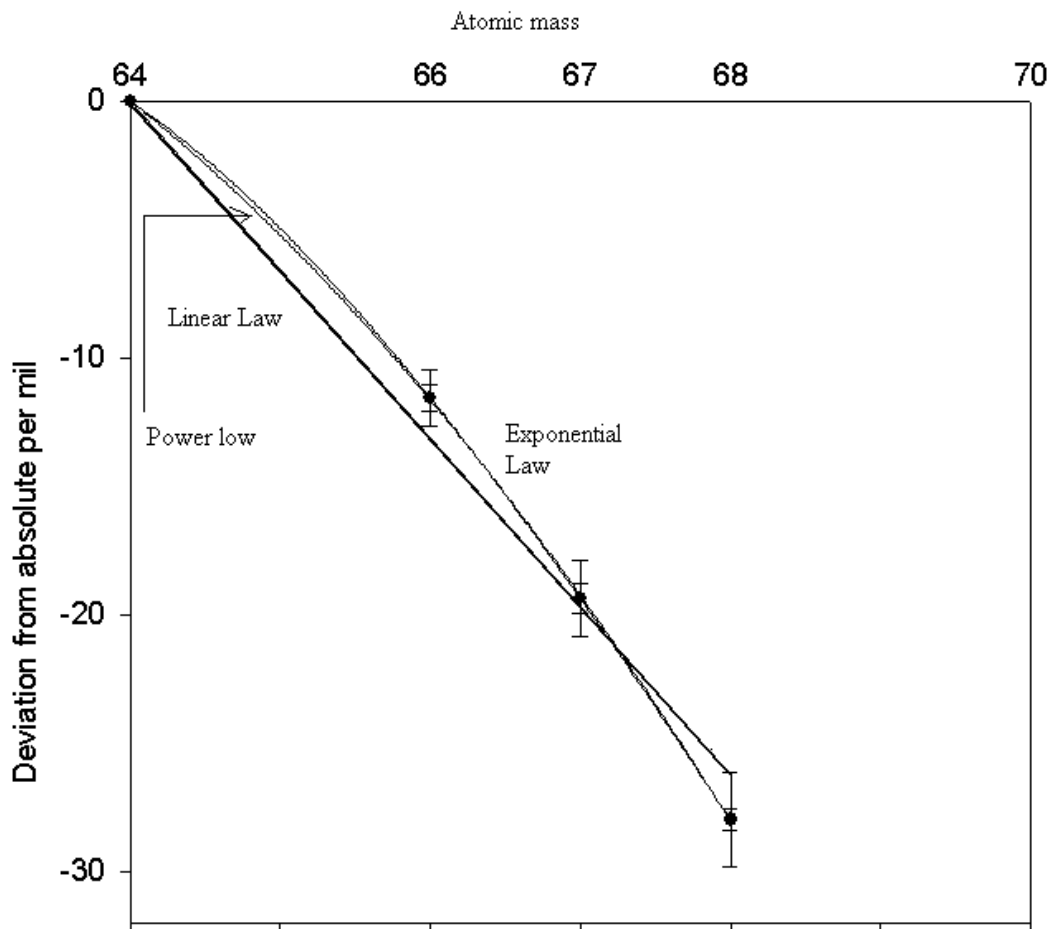


For samples where the concentration of Zn was not known; the Zn abundance in the sample was predicted by comparing the type of the sample being analysed with a

similar type of material from the literature. Complete repeat analyses of these unknown samples were often required to then reach satisfactory final uncertainties.

Russell's approach (1971) requires linearity of both the natural fractionation of the isotopic composition of the element in the sample of interest, and the imposed bias of the machine. The linearity of the natural isotopic composition of Zn in the samples was checked by measuring the isotopic composition of Zn in some samples without double spiking, for example see Figure (5.7, 5.8, 5.9, 5.10). Also this was confirmed by calculating the fractionation of Zn in the samples relative to two sets of isotopes. On the other hand, there is a possibility that Zn analysis using TIMS may not fully exhibit a machine bias that follows a linear law. However, the possible measurement precision for Zn using TIMS is generally greater than the effect of the difference between the linear law and other correction law. Figure 3.25 shows the deviation of laboratory standard (normalized relative to its average, using the linear law, exponential law, and the power law) from δ zero. This shows that the exponential and power fractionation laws fit the observed fractionation closer than the linear law. Though, the linear law does fit within the uncertainty of the observed fractionation. This is similar to Ca, where an 'exponential' law appears to be the best correction of the instrumental mass fractionation (Russell et al., 1978, Hart and Zindler, 1989).

Figure 3. 25: The deviation of laboratory standard (normalized relative to the average using the three isotope fractionation laws) relative to the absolute (Ponzevera et al., 2006). Also shown are the fractionation lines using the linear, power and exponential law.



The effect of the difference between the normalization using the linear and exponential law is small and within the uncertainty of the measured fractionation. To illustrate this the fractionation of the mixture (laboratory standard and double spike) was calculated after the isotopic composition of the mixture was normalized relative to its average using the linear law, and the exponential law. This is shown in Table 3.4, which shows that contribution of the difference between the fractionation laws are well within the uncertainty derived from the double spike deconvolution and support the validity of the approach used.

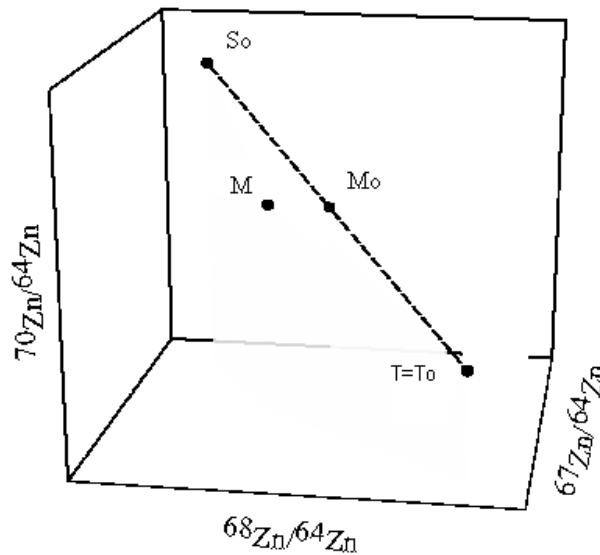
Table 3. 4: The effect of the difference between the normalization using the linear and exponential law on the measured fractionation.

	Normalized using Linear law		Normalized using the exponential law	
	f ‰ amu ⁻¹	± ‰ amu ⁻¹	f ‰ amu ⁻¹	± ‰ amu ⁻¹
Using ⁶⁴ Zn, ⁶⁷ Zn, ⁶⁸ Zn, ⁷⁰ Zn	0.00	0.19	0.01	0.26
Using ⁶⁴ Zn, ⁶⁶ Zn, ⁶⁷ Zn, ⁷⁰ Zn	0.01	0.19	0.02	0.25

In practice determining the fractionation using the double spike where the results obtained using two different sets of isotopes (⁶⁴Zn, ⁶⁶Zn, ⁶⁷Zn, ⁷⁰Zn) and (⁶⁴Zn, ⁶⁷Zn, ⁶⁸Zn, ⁷⁰Zn) produce consistent fractionation values well within uncertainty.

In this approach ⁶⁴Zn as the lightest isotope was chosen to be the reference isotope. Any three unique ratios from any four isotopes of Zn described a vector in a three ratio isotopic compositional diagram (see Figure 3.26).

Figure 3. 26: A three isotope ratio space for Zn. So, Mo and To represent the unfractionated isotopic ratios of the sample, mixture and the tracer respectively.



In this Figure “Measured” represents the measured isotopic composition of the mixture “sample and double spike”. As S_o , M_o and T_o represents the unfractionated compositions of the unspiked sample, mixture and double spike respectively, the

relation between the two compositions S , M , T and S_0 , M_0 , T_0 , is that the later can be represented as points that lie in a straight line. Since S_0 , M_0 , T_0 lie in a straight line, this can be represented by

$$(S_0 - T_0) \otimes (M_0 - T_0) = 0 \quad 3.18$$

With errors represented as:

$$\delta S = S - S_0$$

$$\delta M = M - M_0 \quad 3.19$$

$$\delta T = 0$$

The measured fractionated isotopic composition (labelled “measured” in the diagram) can be corrected using the isotopic composition T , such that $T = T_0$ (Russell 1971). This method uses a three ratio (4 isotope) space, but since Zn has five isotopes, not all isotopes can be represented on the diagram, for example the $^{66}\text{Zn}/^{64}\text{Zn}$ is not represented in this diagram and is not needed in these calculations. This also means that another semi independent isotope space can be generated and double spike calculations performed to cross check that a consistent fractionation value is being obtained.

It is important to note that $T = T_0$, and that, the isotopic compositions S , M and T can be corrected for errors as the errors have regularities. The surface formed by the three isotopic composition vectors of S , M , and T will considered to form a volume V_1 , in the three dimensional isotopic space diagrams, the same applies to isotopic composition vectors of S_0 , M_0 and T_0 Which form volume V_2 . The fractionation per atomic mass unit can be represented as the ratio of the V_1 and V_2 . According to the previous assumptions S , M and T can be represented mathematically as:

$$S = (x, y, z), T_0 = (a, b, c), \text{ and } M = (u, v, w).$$

Equations 3.20, 3.21 and 3.22 is an example represented by Russell (1971) for a Pb using the isotopes ^{204}Pb , ^{206}Pb , ^{207}Pb , and ^{208}Pb , all relative to ^{204}Pb .

$$V_1 = \begin{vmatrix} 2u & 3v & 4w \\ 2x & 3y & 4z \\ u-a & v-b & w-c \end{vmatrix} \quad 3.20$$

$$V_2 = \begin{vmatrix} 2u & 3v & 4w \\ x-a & y-b & z-c \\ u-a & v-b & w-c \end{vmatrix} \quad 3.21$$

In evaluating V_1 and V_2 the linearity is assumed corresponding to the tensor P as represented in 3.22.

$$P = \begin{vmatrix} 2 & 0 & 0 \\ 0 & 3 & 0 \\ 0 & 0 & 4 \end{vmatrix} \quad 3.22$$

The fractionation in permil per atomic mass unit “ f ” can be written mathematically as represented in Equation 3.23.

$$f = \left(\frac{V_2}{V_1} \right) \quad 3.23$$

Where V_1 , V_2 can be determined by calculating the determinant of each matrix “ Δ ” (Russell, 1971).

For Zn, this can be represented without taking into account the fourth ratio which is the $^{66}\text{Zn}/^{64}\text{Zn}$. Then V_1 , V_2 can be represented as represented in Equation 3.20 and 3.21 respectively. Applying this to Zn all ratios relative to ^{64}Zn , this can be presented as in 3.24, 3.25 and 3.26 respectively;

$$P = \begin{vmatrix} 3 & 0 & 0 \\ 0 & 4 & 0 \\ 0 & 0 & 6 \end{vmatrix} \quad 3.24$$

$$V_1 = \begin{vmatrix} 3 * \left(\frac{{}^{67}\text{Zn}}{{}^{64}\text{Zn}} \right)_M & 4 * \left(\frac{{}^{68}\text{Zn}}{{}^{64}\text{Zn}} \right)_M & 6 * \left(\frac{{}^{70}\text{Zn}}{{}^{64}\text{Zn}} \right)_M \\ 3 * \left(\frac{{}^{67}\text{Zn}}{{}^{64}\text{Zn}} \right)_S & 4 * \left(\frac{{}^{68}\text{Zn}}{{}^{64}\text{Zn}} \right)_S & 6 * \left(\frac{{}^{70}\text{Zn}}{{}^{64}\text{Zn}} \right)_S \\ \left(\frac{{}^{67}\text{Zn}}{{}^{64}\text{Zn}} \right)_M - \left(\frac{{}^{67}\text{Zn}}{{}^{64}\text{Zn}} \right)_T & \left(\frac{{}^{68}\text{Zn}}{{}^{64}\text{Zn}} \right)_M - \left(\frac{{}^{68}\text{Zn}}{{}^{64}\text{Zn}} \right)_T & \left(\frac{{}^{70}\text{Zn}}{{}^{64}\text{Zn}} \right)_M - \left(\frac{{}^{70}\text{Zn}}{{}^{64}\text{Zn}} \right)_T \end{vmatrix} \quad 3.25$$

$$V_2 = \begin{vmatrix} 3 * \left(\frac{{}^{67}\text{Zn}}{{}^{64}\text{Zn}} \right)_M & 4 * \left(\frac{{}^{68}\text{Zn}}{{}^{64}\text{Zn}} \right)_M & 6 * \left(\frac{{}^{70}\text{Zn}}{{}^{64}\text{Zn}} \right)_M \\ \left(\frac{{}^{67}\text{Zn}}{{}^{64}\text{Zn}} \right)_S - \left(\frac{{}^{67}\text{Zn}}{{}^{64}\text{Zn}} \right)_T & \left(\frac{{}^{68}\text{Zn}}{{}^{64}\text{Zn}} \right)_S - \left(\frac{{}^{68}\text{Zn}}{{}^{64}\text{Zn}} \right)_T & \left(\frac{{}^{70}\text{Zn}}{{}^{64}\text{Zn}} \right)_S - \left(\frac{{}^{70}\text{Zn}}{{}^{64}\text{Zn}} \right)_T \\ \left(\frac{{}^{67}\text{Zn}}{{}^{64}\text{Zn}} \right)_M - \left(\frac{{}^{67}\text{Zn}}{{}^{64}\text{Zn}} \right)_T & \left(\frac{{}^{68}\text{Zn}}{{}^{64}\text{Zn}} \right)_M - \left(\frac{{}^{68}\text{Zn}}{{}^{64}\text{Zn}} \right)_T & \left(\frac{{}^{70}\text{Zn}}{{}^{64}\text{Zn}} \right)_M - \left(\frac{{}^{70}\text{Zn}}{{}^{64}\text{Zn}} \right)_T \end{vmatrix} \quad 3.26$$

Determinant, Δ of each matrix can then be calculated and fractionation determined using 3.23.

The ratio of sample to spike in the mixture contributes to the uncertainty of the calculated fractionation; such that if θ is the proportion of the sample in the mixture; this can be represented as in Equation 3.24.

$$(M - T_o) = \theta(S - T_o) \quad 3.27$$

The propagated error of the fractionation can be minimized if the mixture contained sufficient sample and double spike (Russell, 1971). A full treatment of the factors involved is discussed by Russell (1971). This Equation can also be utilized to calculate the amount of the sample hence concentration of the element in the sample in the same calculation. For simplicity; the IDMS technique was used in this work to measure the concentration of Zn in all the samples.

A computer program that utilized Monte Carlo to calculate the magnitude of the fractionation together with the 95% confidence associated uncertainty was used (Schediwiy et al., 2006).

To assess the reproducibility of the double spike method, eight separate mixtures of the laboratory standard, Alfa Aesar 10759, and the double spike were analysed and the fractionation of the mixture was calculated relative to the laboratory standard. If everything is working correctly the individual results should produce a zero or nil fractionation (see Section 5.4). The analyses of these standard –double spike mixture was also used as a routine tool to assess that the entire measurement system was working correctly, hence such standard double spike mixture were analysed along with each batch of other samples.

An additional check that the entire procedure is working correctly including checks for interferences was to calculate the fractionation using two different sets of isotopes, which in the case of Zn is possible since it has five stable isotopes.

3.8 Sample purification procedures

3.8.1 Overview and types of samples

The aim of this thesis was to measure the fractionation in a wide range of natural materials. For comparison purposes, a number of other materials were also examined. It is common practice in isotope measurement to use high purity materials as reference laboratory standards hence a selection of these were also analysed (see Table 3.5).

Geological samples analysed in this work were chosen to cover the terrestrial rock cycle, igneous, metamorphic and sedimentary rocks, and selected Zn minerals (Plummer and McGear, 1985), see Tables 3.6, 3.7 and 3.8. The list of biological samples analysed are described in Table 3.11, while the meteorites analysed are described in Tables 3.9 and 3.10. All these samples were available in the Department of Applied physics of Curtin University of Technology.

Table 3. 5: Brief description of high purity Zn metal samples analysed.

Sample	Obtained from / Manufacturer
IRMM 3702 (Absolute)	Proposed to IUPAC as the International absolute standard for the isotopic composition of Zn (Ponzevera et al., 2006)
Alfa Aesar 10759	(Laboratory standard) an aliquot from the absolute IRMM 3702 (Ponzevera et al., 2006)
ac AE 10760	IRMM/ Alfa Aesar
10440	IRMM /Alfa Aesar/JM
ZnO6	IRMM / Devos-Francois
GF6110	IRMM / Goodfellow
GF6120	IRMM / Goodfellow
JMC-2	Johnson Matthey

Table 3. 6: Type and description of Zn minerals.

Sample	Type and description and source
Sphalerite	(ZnFeS) collected from Northampton-WA Australia obtained from Western Australian museum
HydroZincite	(Zn ₅ (CO ₃)OH ₆) collected from Malfidano - Lglesias-Sardinia- Italy. Western Australian museum
Smithsonite	(ZnCO ₃) collected from Bisbee, Arizona- USA. Western Australian museum

Table 3. 7: Description of reference and certified reference materials samples.

Sample	Type and description
BCR-1	Basalt, Columbia River. BCR-1 is the same as the newly produced BCR-2 (USGS, 2006b)
BIR-1	Icelandic Basalt Rock" (USGS, 2008)
W-2	Diabase Rock" (USGS, 2008)
SGR-1	Green River Shale "Sedimentary rocks from the green river". Collected from Mahogany zone of the Green River Formation. It is a petroleum and carbonate-rich shale. (USGS, 2008)
SCo-1	Cody Shale "Sedimentary Rock" collected in Natrona County, Wyoming, USA. It is typical of the upper Cretaceous silty marine shales (USGS, 2008)
DNC-1	Dolerite (USGS, 2008)
QLO-1	Quartz Latite (USGS, 2008)
SDC-1	Mica Schist (USGS, 2008)
HISS-1	Marine sediments collected from Hibernia. The coast of Newfoundland (National Research Council Canada, 2007)
Till-3	Clay. Collected 8 Km east of Cobalt, Ontario. Characterized for major element oxides. Zn values still provisional (National Resources Canada, 2007)
Murst-Iss-A1	Antarctic Sediments, Production of the Instituto Superiore di Sanita Rome- Italy

Table 3. 8 Description of terrestrial rock sample.

	Sample	Type and description
Terrestrial Rock CaCO ₃	Rock	Calcite (calcium carbonate) mixed with layers of malachite (copper carbonate hydroxide) (Bevan, 2007)

Table 3. 9: Description of stone meteorites.

Sample	Class	Description/origin
Allende	CV3	Carbonaceous Chondrite 1969 (Arizona State University, 2006) /WA Museum
Orgueil	CI1	Tarn-et-Garonne, France stone; carbonaceous Chondrite 1864 (Arizona State University, 2006)
Brown field 1964	H5	Terry Co., Texas, USA ordinary Chondrite 1964 (Arizona State University, 2006)
Brown field 1937	H3	stone; ordinary Chondrite fall in Terry Co., Texas, USA 1937 (Arizona State University, 2006)
Plain View	H5	Hale Co., Texas, USA stone; ordinary Chondrite (Arizona State University, 2006)

Table 3. 10: Description of iron meteorites

Sample	Class	Descriptions/origin
Canyon Diablo	IAB	Coconino Co., Arizona, USA Find, 1891, iron; coarse Octahedrite (Arizona State University, 2006)
Redfields	No classificati	Redfields is close to group Iib, but out side its limits. Find 1969-WA –Australia (De Laeter et al., 1973)
Kumerina	IIC	Western Australia, Australia iron; plessitic Octahedrite (Arizona State University, 2006)
Mundrabilla	IIICD	Nullabor Plain, Western Australia, Iron; medium Octahedrite (Arizona State University, 2006)
Odessa	IAB	Ector Co., Texas, USA iron; coarse Octahedrite. Find 1922 (Arizona State University, 2006)
Warburton	IVB	Western Australia, Australia iron; a taxite. Find 1963 (Arizona State University, 2006)
Youanmi	IIIAB	Western Australia, Australia Iron; medium octahedrite. Find 1917 (Arizona State University, 2006)

Table3. 11: Description of biological materials

Sample	Description/origin
NIES 9	Sargasso "Sea weed" (<i>Sargassum fulvellum</i>). Collected from Shimoda Bay-Japan (National Institute for Environmental Studies, 2007)
IMEP -19	Rice. Provided by NMIJ-Japan. Originates from rice grown in water contaminated with Cadmium. The Cadmium amount content in this rice material was envisaged to be close to the upper limit as stated in Japanese regulations. The rice was reprocessed and prepared at IRMM (IRMM, 2007).
Murst-Iss-A2	Antarctic Krill. Krill, fished between 1993-1995 from the Southern Ocean produced in the frame of PNRA-Italy (Caroli et al., 2001)

3.9 Sample digestion

3.9.1 Terrestrial, biological, and stone meteorites

The same sample digestion and purification procedure was used for both the isotope dilution and the isotopic composition measurements. All sample preparation was performed in the Curtin University Isotope IDMS laboratory, a laboratory supplied with HEPA filtered air (Efficiency 99.995% for particles >0.3µm) with critical sample evaporations taking place under a HEPA clean hood.

A known amount of each sample material was weighed into a clean screw-capped 15 mL PFA (Salvillex) beaker, together with a known amount of Zn spike.

Approximately 2 g of HF acid and 2 g of HNO₃ were added and left overnight, the lid was screwed on, and the beaker was heated in a microwave oven for about 30 seconds at 800 Watt, and then left for 10 minutes to cool. The samples were then placed on a hot plate and taken to dryness, followed by the addition of 2 g of concentrated HNO₃ to the residue, placed in a microwave oven for 30 seconds, allowed to cool, and then taken to dryness on a hotplate (see also Table 3.11). A 2 g aliquot of concentrated HCl was added and the sample was heated in a microwave oven for 20-30 seconds for

three to four times, with the sample allowed to cool to room temperature in between each heating. At this stage a clear solution was present and the sample beaker was taken to dryness on a hot plate. If any leakage of the solution from the beaker while microwaving the sample was observed, then the microwave heating was reduced to 20 seconds to avoid losing sample. This was because each sample material interacts differently with the reagents and some may have relatively vigorous chemical reactions than others. All standard reference materials were dissolved using the same technique, except HISS-1 where step 7 was replaced by adding ~3 g of Aqua Regia, and the sample was left on hot plate with lid on for more than 10 hours before proceeding to step 9 (see Table 3.11). At this point it appeared that the majority of the solids had dissolved and it was now necessary to remove any nitrates before proceeding with the ion exchange separation. The remaining salts were then dissolved with 0.3 g of $>0.6 \text{ Mol L}^{-1}$ HCl, covered with the beaker lid and heated on the hot plate for several hours. At this stage the sample was ready for chemical purification. Some samples dissolved completely and quickly compared to others following the same procedure. For example, biological standard reference materials like IMEP-19 and NIES No 9 rapidly dissolved in the early stages of the digestion procedure and hence there was no need for repeated sample dissolution steps. On the other hand it was necessary to follow all steps to completely dissolve standard reference materials like HISS-1, Murst-ISS-A1, and TILL-3.

Table 3. 12: Dissolution steps for all samples except for Iron meteorites

Step No	Description (Lid refers to the beaker lid)
1	Weigh out sample
2	Add known amount of Spike, ~2 g HF, ~2 g HNO ₃ , Leave over night "with lid off" under the HEPA clean hood.
3	Place Lid on & Microwave 30 s (3 to 4 times)
4	Lid off and dry sample on hot plate.
5	Add ~2g HNO ₃ . Lid on & Microwave
6	Lid off and dry sample on hot plate
7	Add ~2g HCl, Lid on & Microwave for 30s (3 to 4 times)
8	Lid off and dry sample on hot plate
9	Add ~2g HCl $\geq 4 \text{ Mol L}^{-1}$. Leave on hot plate with lid on, prior to loading onto the column chemistry for Zn separation

An approximate knowledge of the concentration of Zn in the sample was useful to minimize the amount of sample and double spike used, and to optimize the double spike to sample ratio. Unfortunately this was not the case for meteorites, for which limited amounts of rare and valuable samples were available. In some samples the amounts of Zn were found to be different than the reported in the literature.

3.9.2 Iron meteorite Dissolution

The dissolution of iron meteorites was undertaken using a technique developed by Wieser and De Laeter (2008), where a small piece (0.6 to 2.5 g) of iron meteorite was sawn from its parent using an alcohol cleaned iron metal cutting saw. The samples were decontaminated by dissolving the outer surface of the sample by soaking with HCl ($\sim 8 \text{ mol L}^{-1}$) for approximately twenty minutes. The remaining sample was rinsed and placed in clean beaker under HEPA clean hood to dry. It was generally found that the sample has lost $\sim 0.2 \text{ g}$ of its size after this decontamination. Following the weighing of the sample into the clean beaker, 8 mol L^{-1} HCl was added and left with lid on the hot plate for more than six hours, and then checked to see if any of the solid samples was left in the beaker. The dissolved sample was transferred to another clean beaker, while the remaining undissolved sample was removed, rinsed with high purity water (MQ water, $>18.2 \text{ M}\Omega$ resistivity), dried and weighed, and brought back to be used for another analysis if required. The difference between the original sample used and the undissolved sample was considered to be the mass of the sample (Wieser and De Laeter, 2008).

3.10 Ion exchange chemistry

To analyse samples by thermal ionisation mass spectrometry, it was necessary to remove materials that produce isobaric interferences such as ^{64}Ni , and other molecular interferences. An additional requirement for TIMS analysis is to remove elements such as; Fe, Cu, Ga, K, Na from the sample, which suppress the ionisation of Zn, or produce unstable ion beams (Albarède and Beard, 2004). The samples were separated

using an ion exchange procedure as described in Table 3.13 using Dowex AG1-X8 anion exchange resin, either (100-200), or (200-400) mesh size.

Table 3. 13: Ion exchange separation procedure of Zn from sample matrix for all samples except iron meteorites.

Stage	Reagent & volume used	No of repeat
Cleaning steps	MQ water 5 mL	6
	HNO ₃ 1Mol l ⁻¹	1
	MQ water 5 mL	1
	HCl 5mL >2Mol L ⁻¹	1
	MQ water 5 mL	1
	HCl 5mL >2Mol L ⁻¹	1
Loading the sample	The sample was loaded on the column as ZnCl ₂ in 0.6 Mol L ⁻¹	
Elution of unwanted species	HCl 5mL 0.6 Mol L ⁻¹	3 to 4 times
Extracting Zn	HNO ₃ 1Mol L ⁻¹	2 to 3 times

Ion exchange columns made from polyethylene pipettes and supporting frits were leached in low concentration nitric acid for weeks to remove any residual Zn. The size of the resin column volume (CV) used was 0.7 ml of Dowex AG1-X8 anion exchange resin, either (100-200), or (200-400) mesh size. The measured column extraction efficiencies showed no significant difference between the two resin mesh sizes. The resin was then washed with 6 full columns (FC) of MQ water followed by 1 FC of 1 mol L⁻¹ HNO₃, 1 FC MQ water, and few column volumes of HCl of concentration >2 mol L⁻¹. The sample was loaded in HCl of concentration ~0.6 mol L⁻¹, followed by 3 FC of 0.6 Mol L⁻¹ HCl to remove the Fe, Cu, Ga, Ge and Ni, and the Zn was then extracted using 1 FC 1 mol L⁻¹ HNO₃ and taken to dryness.

At least one procedural blank was processed with every batch of samples and was found in all cases, apart from some meteorites to be negligible relative to the amount of the samples being measured, although a correction was always applied. Although the blank for each batch could be measured to better than ±0.02 ng, as discussed above, the variability in the blank (8 ± 5) ng was the key factor that determined its final uncertainty (see Figure 3.9). Although the possible sources of the blank were

investigated, there was no clearly identifiable cause of the variability. The amounts of Zn contamination that could be attributed were; beaker blank < 0.3 ng, digestion reagents ~ 1.3 ng, ion exchange column, 1.0 ± 0.2 ng, and a filament blank of 0.06 ng. Thus the total calculated identifiable blank of <2.5 ng is less than half of any of the measured blanks. The variability of the blank remains a key factor in the analysis of low concentration samples.

3.10.1 Anion exchange procedure

Zinc in samples was separated from other elements using an ion exchange procedure as represented in Table 3.12. The only variation used for the anion exchange separation procedure was for iron meteorites where the sample was loaded into the column with ~ 5 mol L⁻¹ HCl, other wise all samples were loaded into the column with 0.6 mol L⁻¹ HCl. It was necessary to load the iron meteorites samples with a higher concentration of HCl, so that the iron will stay in the Fe⁺² state. In this case, the Fe⁺² state was easily identified from its green color, a lower concentration of HCl would transform Fe⁺² to Fe⁺³, which can only be removed by using a very dilute HCl, which also removes Zn. Thus, it was preferred to load the sample solution with ~ 5 mol L⁻¹ HCl (Wieser and De Laeter, 2008).

The fractionation of Zn due to the separation of Zn from other substances using Anion exchange column procedures is represented in Section 5.5.5, and further discussed in Section 7.1.

3.10.2 Extraction efficiency

The extraction efficiency was determined several times by loading a known amount of Zn onto an ion exchange column, and measuring the amount eluted using IDMS. The column efficiency for the separation of Zn from the reference materials procedure was measured to be 93 ± 4 %, while for the iron meteorite procedure the column efficiency was measured to be 91 ± 4 %. It should be noted that high extraction efficiency is not required for an accurate IDMS analysis or isotopic composition measurement using the double spike technique. Appreciable, achieving high

extraction efficiency was important so as not to lose any appreciable amounts of rare and valuable samples.

- **Chapter 4: The elemental abundance of Zn: Results**

4.1 Introduction

Elemental abundance measurements of all the samples analysed in this work are presented in this Chapter. Also included are the results for the concentration determination of the double spike and an associated discussion thereof. Discussions are limited to analytically related matters with a full discussion presented in Chapter 6.

4.2 Calibration of the concentration of the double spike

An essential requirement of isotope spiking techniques is the accurate determination of the concentration of the double spike (Anbar, 2004). Accurate calibrations of isotopic spikes require considerable skill and effort, and is a time consuming process.

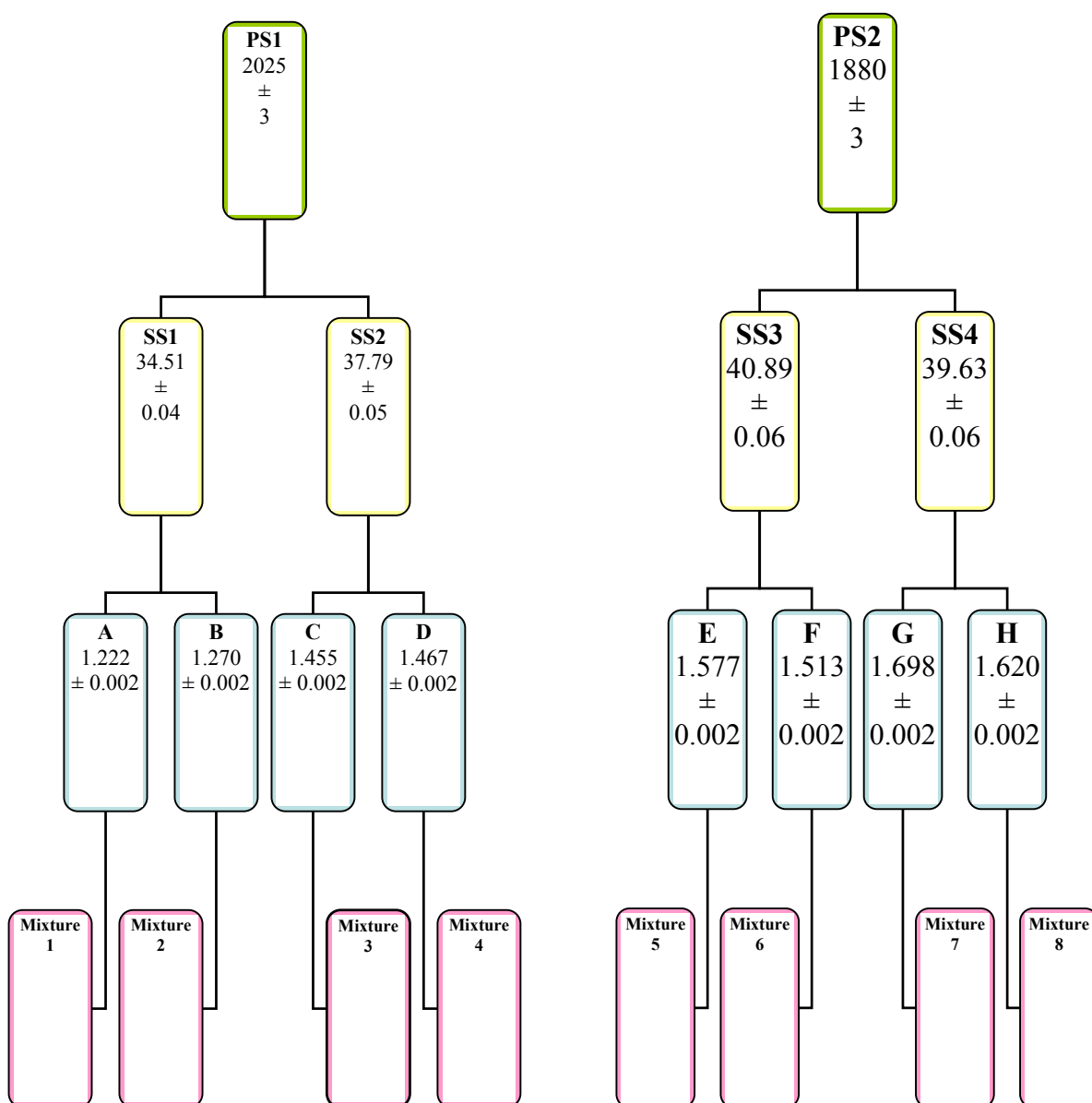
The double spike solution used during all this research was prepared by Rosman in 1972, and a solution with concentration $\sim 1 \mu\text{g g}^{-1}$ was available for this study. Because the solution had been prepared some decades before, and stored in glass flask, the isotopic composition and concentration were remeasured.

The weights of solutions used during the double spike calibration were measured using an electronic balance with reading uncertainty of ± 0.1 mg. A set of new polyethylene bottles of various sizes, and 15 mL Teflon PFA beakers, were cleaned for the calibration process purpose. The solutions were prepared in the IDMS laboratory, clean room laboratory (see Section 3.2).

The calibration procedure followed was similar to that used in the mass spectrometry Section at the National Bureau of Standards (NBS) in the 1970s (Rosman, 2008). Two approximately equal masses of known weight of high purity Zn (99.9999%), Alfa 10760 obtained from IRMM was dissolved into dilute HNO_3 , producing two Primary solutions PS1 & PS2. Two secondary solutions from PS1 (SS1 and SS2) and two

secondary solutions from PS2 (SS3 and SS4) were prepared resulting in four solutions with approximately the same concentration. A further two dilute solutions were prepared from each of the SS solutions, resulting in eight different solutions (A, B, C, D, E, F, G and H with approximately the same concentration). Solution A and B from SS1, C and D from SS2, E and F from SS3, G and H from SS4. Known aliquots of each solution; A, B, C, D, E, F, G and H, were mixed with known amount of the spike producing eight different mixtures. These eight mixtures were evaporated to dryness and their isotopic composition measured using (TIMS). A diagrammatic representation of the solution preparation sequence, and the final concentrations are shown in Figure 4.1

Figure 4. 1: Solution preparation sequence for the f concentration of the double spike. Values shown are the concentrations in $\mu\text{g}\text{g}^{-1}$.



Approximately 400 to 600 ng of Zn from each of the mixtures was loaded in to the TIMS; producing $^{64}\text{Zn}^+$ ion beam up to 800 to 900 mV using the Daly detector. The isotopic composition of each mixture was used to calculate the amount of Zn in each aliquot of the double spike using the isotope dilution Equation in reverse as represented in Equation 4.1.

$$N_x = \left[\frac{S}{\left(\frac{\sum X_i A_i}{\sum Y_i A_i} \right) * \left(\frac{(R_y - R_b)}{(R_b - R_x)} \right)} \right] \quad 4.1$$

Where;

N_x is the amount of Zn in the double spike sample.

S is the accurately known amount of Zn from the standard in the mixture.

$\sum X_i A_i$ is the sum of the isotopic ratio of isotope i of Zn relative to ^{67}Zn in the measured standard multiplied by the atomic mass of isotope i "A" of Zn.

$\sum Y_i A_i$ is the sum of the isotopic ratio of isotope i relative to ^{67}Zn in the measured double spike multiplied by the atomic mass of isotope i .

R_y is the ratio of any isotope to the mass unit ^{67}Zn in the double spike.

R_b is the ratio of the same isotope used in R_y relative to ^{67}Zn in the mixture.

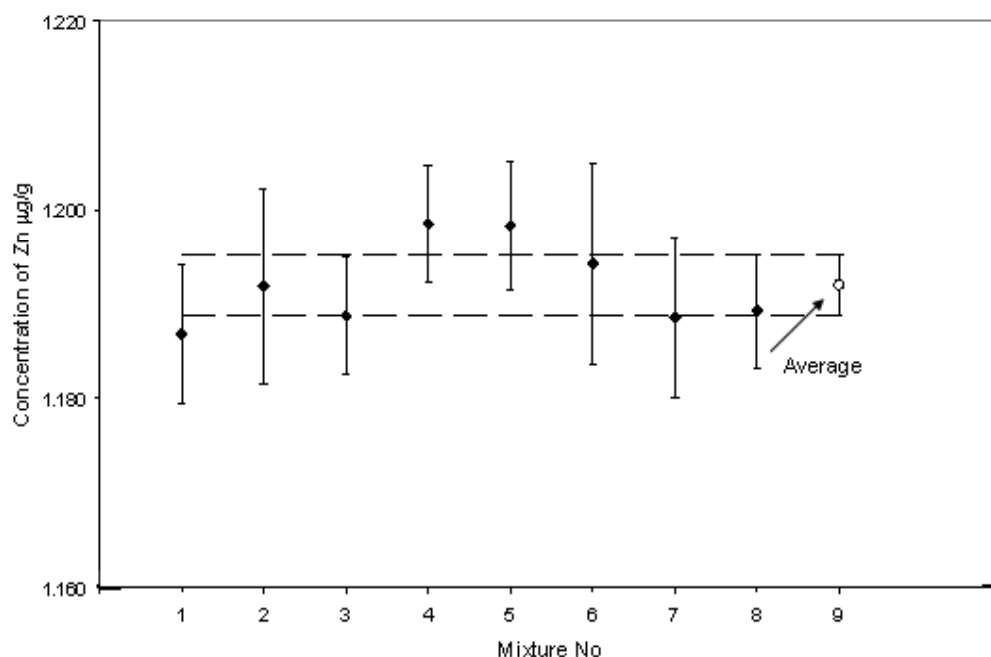
R_x is the same isotopic ratio in the standard.

To assess the possible effect of contamination during the calibration, a procedural blank was prepared along the same lines as a mixture, and measured in the TIMS. The maximum contribution of Zn from the blank to any mixture was less than 0.09% of the amount of Zn in the mixture, and was subtracted from the final amount.

Accordingly, the concentration of Zn in the double spike was $(1.1921 \pm 0.0032) \mu\text{g g}^{-1}$; the external uncertainty is the 95% confidence interval, with fractional uncertainty 0.27% as represented in Figure 4.2.

During the calibration of the double spike using IDMS it is assumed that the double spike, mixture and standard all fractionate in the mass spectrometer to the same amount. Provided suitable tracer standard mixing ratios are used the uncertainty introduced in the fractionation differences between these is a second order effect and does not contribute significantly in the final uncertainty.

Figure 4. 2: The concentration of Zn spike in 8 different mixtures of spike and standard as used for the calibration of the spike.



The above figure clearly shows that all the uncertainties for each of the concentrations are within the 95 % confidence interval of the average. The uncertainties in the individual concentrations measurements include the uncertainties associated with the weighing and isotopic ratios measurements.

4.3 Concentration of geological and environmental reference materials

All geological samples were dissolved, purified, and isotopically analysed according to the procedures described in Sections 3.9.1, 3.10, and 3.5 respectively. Isotopic ratios for the geological samples were measured using the Daly or the Faraday multicollector, and their results are discussed in Section 6.2. The measured concentrations of Zn in the standard reference materials (SRMs) analyzed are represented grouped according to rock type e.g. Tables in Sections 4.3.1, 4.3.2, 4.3.3, and 4.3.4 show the values obtained for igneous, sedimentary, metamorphic rocks, and clay respectively. It is important to note that, all the results in the Tables, for example analysis X. y; refers to the analysis of aliquot y from reservoir X, if not; then the analysis was performed using different reservoir.

The uncertainty for each individual measurement is shown at the 95% confidence level, determined using the uncertainty calculation software ISO GUM Workbench software (Metrodata GmbH, 1996). The results obtained all agree with each other within individual measurement uncertainties, with final fractional uncertainties all being less than 2.8%, demonstrating the high levels of precision possible using IDMS comparing to other methods. All repeat analyses agree with each other within experimental uncertainties demonstrating homogeneity in the concentration of Zn in all these SRMs, including samples taken from different bottles.

To ensure accuracy, all of the component inputs of each measurement were examined. For example, the double spike concentration is traceable against the balances which were in turn calibrated using reference weights. In cases where variability in concentration was more significant than individual measurement, a statistical method (GUM) was used to arrive at final uncertainties, or the uncertainty was expanded to cover the range of values. For example, the final procedural blank of 8 ± 5 ng was based on the overall range of the individual blank values obtained. Different ion detection systems (Daly, Faraday) produced different relative uncertainties for isotope ratio measurements. An example of the contribution of the each individual value in the IDMS Equation was performed in the measurements of SDC-1 as represented in Figure 3.23 in Section (3.7.1).

4.3.1 Igneous rocks standard reference materials

The concentration of Zn in igneous rocks samples were measured and are shown in Tables 4.1 - 4.4

Table 4. 1: Concentration of Zn in Basalt BCR-1

Mass of Sample (g) ^r	Analyses No	Concentration ($\mu\text{g g}^{-1}$)	\pm 95%
0.0965	1	128.0	1.0
0.0870	2	130.8	1.0
0.0841	3	130.5	1.0
0.0623	4	130.9	1.3
0.1738	5	131.9	3.4
	5.1	131.3	3.4
	5.2	131.4	3.4
	Average	130.7	1.8
	Recommended value by (USGS, 2006a)	127	9

^r Uncertainty $\leq 0.8\%$ of the size of the sample

Table 4. 2: Concentration of Zn in BIR-1

Mass of Sample (g) ^r	Analysis No	Concentration ($\mu\text{g g}^{-1}$)	\pm 95%
0.0949	1	71.3	0.5
0.0835	2	71.3	0.5
0.0790	3	71.3	1.6
0.0890	4	72.1	2.0
	4.1	72.1	2.0
	Average	71.6	1.3
	Recommended value by (USGS, 1998a)	71	9

^r Uncertainty $\leq 0.8\%$ of the size of the sample

Table 4. 3: Concentration of Zn in Diabase W-2

Mass of Sample(g) ^Y	Analysis No	Concentration ($\mu\text{g g}^{-1}$)	\pm 95%
0.0620	1	77.4	0.6
0.0737	2	77.0	0.5
0.1381	3	77.3	2.2
	3.1	77.3	2.0
	3.2	77.3	2.0
	3.3	77.4	2.0
	3.4	77.3	2.0
0.0429	4	78.6	2.4
	4.1	79.1	2.5
	4.2	78.6	2.4
0.0605	5	77.8	2.3
	5.1	77.4	2.3
	5.2	77.5	2.3
	Average	77.7	1.1
	Recommended value by (USGS, 1995b)	80	2

^Y Uncertainty $\leq 0.8\%$ of the size of the sample

Table 4. 4: Concentration of Zn in DNC-1

Mass of Sample (g) ^Y	Analysis No	Concentration ($\mu\text{g g}^{-1}$)	\pm 95%
0.0556	1	67.3	0.5
0.0587	2	66.8	0.5
0.0628	3	67.1	0.5
0.0905	4	67.1	2.0
	4.1	67.2	2.0
	4.2	67.3	2.0
0.0456	6	67.6	2.1
	6.1	67.5	2.1
	6.2	67.6	2.1
	Average	67.3	1.1
	Recommended value by (USGS, 1995c)	70.0	2.4

^Y Uncertainty $\leq 0.8\%$ of the size of the sample

4.3.2 Sedimentary rocks

The concentration of Zn in Marine sediments rock samples was measured using the IDMS is represented in Tables 4.5 - 4.9. All samples are SRMs except CaCO₃.

Table 4. 5: Concentration of Zn in SGR-1

Mass of Sample (g) ^Y	Analysis No	Concentration ($\mu\text{g g}^{-1}$)	\pm 95%
0.0528	1	74.4	0.6
0.0442	2	74.9	0.7
0.0367	3	74.4	0.7
0.1173	4	72.7	1.9
	4.1	72.7	1.9
	4.2	73.4	2.0
	4.3	73.2	2.0
	Average	73.7	1.2
	Recommended value by (USGS, 2001)	74	9

^Y Uncertainty $\leq 0.8\%$ of the size of the sample

Table 4. 6: Concentration of Zn in SCo-1

Mass of Sample (g) ^Y	Analysis No	Concentration ($\mu\text{g g}^{-1}$)	\pm 95%
0.1213	1	101.0	0.7
0.0904	2	103.2	0.8
0.0810	3	102.2	0.7
0.1051	4	100.6	3.3
	4.1	100.7	3.3
	4.2	100.6	3.3
	Average	101.4	2.0
	Recommended value by (USGS, 1995a)	100	8

^Y Uncertainty $\leq 0.8\%$ of the size of the sample

Table 4. 7: Concentration of Zn in HISS-1

Mass of Sample (g) ^r	Analysis No	Concentration ($\mu\text{g g}^{-1}$)	\pm 95%
2.2131	1	3.9	0.1
	1.1	3.9	0.1
	1.2	3.9	0.1
	1.3	3.9	0.1
	1.4	3.9	0.1
	1.5	3.9	0.1
0.4496	2	3.8	0.1
0.2787	3	3.8	0.1
0.8557	4	3.7	0.1
	4.1	3.7	0.1
2.5908	5	4.0	0.1
	5.1	4.0	0.1
	Average	3.87	0.06
	Recommended value by (National Research Council Canada, 2007)	4.94	0.79

^r Uncertainty $\leq 0.8\%$ of the size of the sample

Table 4. 8: Concentration of Zn in Murst-Iss-A1

Mass of ample (g) ^r	Analysis No	Concentration ($\mu\text{g g}^{-1}$)	\pm 95%
0.3732	1	54.1	1.4
	1.1	54.0	1.4
	1.2	54.1	1.4
0.3883	2	53.5	1.4
	Average	53.9	1.4
	Recommended value by (Italian National Programme for Research in Antarctica, 1996)	51.9	3.2

^r Uncertainty $\leq 0.8\%$ of the size of the sample

Table 4. 9: Concentration of Zn in CaCO₃

Mass Sample (g) ^Y	Analysis No	± 95%	concentration (µgg ⁻¹)	± 95%
0.9060	1	0.0003	4.42	0.14
	1.1	0.0003	4.41	0.14
Average			4.42	0.20

^Y Uncertainty ≤ 0.8% of the size of the sample

4.3.3 Metamorphic rocks standard reference materials

The concentration of Zn in two metamorphic rocks was measured using the IDMS and is represented in Tables 4.10 - 4.11.

Table 4. 10: Concentration of Zn in SDC-1

Mass of sample (g) ^Y	Analysis No	Concentration (µgg ⁻¹)	± 95%
0.0709	1	102.1	0.4
0.0767	2	100.1	0.7
0.0585	3	101.1	0.8
0.0701	4	101.6	3.2
	4.1	101.5	3.2
	4.2	101.4	3.2
	4.3	102.1	3.2
	4.4	102.0	3.2
	Average	101.5	1.7
	Recommended value by (USGS, 1998b)	103	8

^Y Uncertainty ≤ 0.8% of the size of the sample

Table 4. 11: Concentration of Zn in QLO-1

Mass of Sample (g) ^r	Analysis No	Concentration ($\mu\text{g g}^{-1}$)	\pm 95%
0.0461	1	59.5	0.5
0.0426	2	60.1	0.5
0.0384	3	58.9	0.6
0.0946	4	61.0	1.8
	4.1	61.3	1.8
	4.2	61.1	1.8
	Average	60.3	1.1
	Recommended value by (USGS, 1998c)	61	3

^r Uncertainty $\leq 0.8\%$ of the size of the sample

4.3.4 Clay standard reference materials

The concentration of Zn in TILL-3 clay sample was measured using the IDMS technique and was as represented in Table 4.12

Table 4. 12: Concentration of Zn in TILL-3

Mass of sample (g) ^r	Analysis No	Concentration ($\mu\text{g g}^{-1}$)	\pm 95%
0.2325	1	48.5	1.2
	1.1	48.4	1.2
0.4113	2	48.4	1.2
	2.1	48.4	1.2
	2.2	48.4	1.2
0.3269	3	48.2	1.3
	Average	48.4	1.0
	Recommended value	Not provided	Not provided

^r Uncertainty $\leq 0.8\%$ of the size of the sample

4.4 Biological standard reference materials

All three biological samples were dissolved, purified, and isotopically analysed according to the procedures described in Sections 3.9.1, 3.10, and 3.5 respectively. Isotopic ratios for all the biological samples were measured using the Faraday

multicollector, and their results are discussed in Section 6.3. The measured concentrations of Zn in the biological standard reference materials (SRMs) analyzed are represented in Table 4.13; the values obtained for Rice, Sargasso “Sea weed” and Antarctic Krill. It is important to note that, all the results in the Tables, for example analysis **X. y**; refers to the analysis of aliquot **y** from reservoir **X**, if not; then the analysis was performed using different reservoir.

Table 4. 13: Concentration of Zn in biological materials

	Mass of Sample (g) ^r	Analysis No	Concentration ($\mu\text{g g}^{-1}$)	\pm 95%
Rice IMEP-19	0.4373	1	22.2	0.6
		1.1	22.2	0.6
		1.2	22.2	0.6
		1.3	22.1	0.6
		1.4	22.2	0.6
		1.5	22.1	0.6
	0.4612	2	22.1	0.6
		2.1	22.1	0.6
		Average	22.15	0.42
		Recommended value by (IRMM, 2007, IRMM, 2003)	22.99	0.44
Sargasso NIES Number 9	0.5213	1	14.69	0.38
		1.1	14.70	0.38
		1.2	14.68	0.37
		1.3	14.68	0.39
		1.4	14.67	0.38
		1.5	14.67	0.38
	0.3777	2	14.41	0.37
		2.1	14.44	0.37
		Average	14.62	0.27
		Recommended value (National Institute for Environmental Studies, 2007)	15.6	1.2
Krill Murst-Iss- A2	0.1052	1	64.3	1.6
	0.1073	2	63.0	1.6
		2.1	63.1	1.6
			Average	63.5
		Recommended value By (Caroli et al., 2001)	66.0	2.0

^r Uncertainty $\leq 0.8\%$ of the size of the sample

4.5 Meteorites

All meteorite samples were dissolved, purified, and isotopically analysed according to the procedures described in Sections 3.9, 3.10, and 3.5 respectively. All isotope ratios for the meteorites samples were measured using the Faraday multicollector. The meteorites samples were classified according to their type; stone meteorites and iron meteorites, and their results are discussed in Section 6.4. In the case of Brownfield 1964, Brownfield 1937, and Plainview, no final uncertainties are provided because measurements were performed using different sub-mass sample; which shows of the apparent inhomogeneity in these meteorites.

4.5.1 Stony meteorites

Table 4.14: Concentration of Zn in stony meteorite

Meteorite	Mass of sample (g) ^r	Analysis No	Concentration ($\mu\text{g g}^{-1}$)	\pm 95%
Allende	0.3830	1	75.8	2.0
		1.1	75.7	2.0
		1.2	75.7	2.0
		Average	75.7	2.3
Orgueil	0.0142	1	302	10
		1.1	302	10
		Average	302	14
Brownfield 1964	0.1142	1	35.9	0.9
		1.1	35.9	0.9
		1.2	35.7	0.9
	0.4222	2	33.6	0.9
		2.1	33.6	0.9
		2.2	33.6	0.9
	Range	33.6-35.9		
Brownfield 1937	0.1589	1	80	2
		1.1	80	2
		1.2	80	2
	0.3638	2	46	1
		2.1	46	1
		2.2	46	1
	Range	46-80		
Plainview	0.2035	1	21.5	0.6
		1.1	20.1	0.6
	0.2176	2	28.2	0.7
		2.1	27.5	0.7
	0.2851	2.2	27.5	0.7
		3	32.7	0.9
		3.1	32.7	0.9
		3.2	32.6	0.8
	0.8058	3.3	32.7	0.8
		4	25.7	0.7
		4.1	25.7	0.7
	4.2	25.7	0.7	
	Range	20.1- 32.7		

^r Uncertainty $\leq 0.8\%$ of the size of the sample

4.5.2 Iron meteorites

For iron meteorites, all concentrations are in μgg^{-1} microgram per gram unless indicated. The concentration of Mundrabilla, Warburton, and Kumerina are in ngg^{-1} .

Table 4. 15: Concentration of Zn in iron meteorite

Meteorite	Mass of sample (g)	Analysis No	Concentration μgg^{-1}	\pm 95%
Canyon Diablo ^r	0.0932	1	24.0	0.6
		1.1	24.0	0.6
		1.2	23.8	0.6
		1.3	23.8	0.6
		1.4	23.8	0.6
		Average	23.88	0.54
Mundrabilla ^{r,Π}	0.3665	1	72	14
		1.2	83	14
		1.3	74	14
		Average	76	17
Redfields [‡]	0.4599	1	7.2	0.3
		1.1	7.2	0.3
		1.2	7.2	0.3
		Average	7.20	0.35
Warburton ^{‡, Π, A}	1.0966	1	19.0	5.3
		1.1	19.3	5.3
		Average	19.2	7.5
Kumerina ^{r,Π}	2.0897	1	387	10
		1.1	372	10
		Average	380	14
Odessa ^r	0.4100	1	26.0	0.7
		1.1	26.1	0.7
		1.2	26.1	0.7
	1.5214	2	13.3	0.3
		2.1	13.5	0.3
		2.2	13.5	0.3
		Range	13-26	
Youanmi ^r	1.6084	1	0.95	0.03
		1.2	0.95	0.03
		Average	0.950	0.042

^Π Concentrations are in ngg^{-1} . [‡] Uncertainty $\sim 3.1\%$ of the size of the sample.

^rUncertainty $\leq 0.8\%$ of the size of the sample. ^A The external uncertainty in the measurement is over estimated, and the measurement represents the IDMS detection limit of this research.

4.6 Water

All water samples were purified and isotopically analysed according to the procedures described in Sections, 3.10, and 3.5 respectively. All isotope ratios for the water samples were measured using the Daly detector where the measurement uncertainty were scarified because the aim of the experiments was initially only to measure the concentration of Zn in the samples. The water samples were classified according to their source; river water, restrained tapwater, and unrestrained (fresh) tapwater, and their results are discussed in Section 6.5. Water samples were collected in containers of 500 mL from a water tap in the Department of Applied Physics at Curtin University of Technology in Western Australia. The samples were collected directly from the tap after shutting the tap for more than a week to restrain the water. For unrestrained (fresh) tap water; the samples were collected after leaving the same water tap open for more than 20 minutes, this was to make sure that there was no restrained water remaining in the pipes of all the building. The results are as represented in Table 4.16, where it should be noted that the concentrations vary from ngg^{-1} for river and unrestrained (fresh) tap water, to μgg^{-1} for restrained tap water.

Table 4. 16: Concentration of Zn in water

Source	Mass of sample (g)	Analysis No	Concentration	\pm 95%
Swan river Victoria Park ^{‡, Π}	15	1	6.5	0.4
Swan river Bayswater ^{‡, Π}	16	1	7.2	0.5
Restrained tap water ^π	0.5128	1	5.2	0.3
		1.1	5.1	0.2
Unrestrained (fresh) tap water ^{‡, Π}	14.972	1	13.01	0.49
	15.010	2	13.08	0.50

[‡] Uncertainty \sim 0.01% of the size of the sample. ^Π Concentration is ngg^{-1} .

^π Uncertainty ~ 0.14% of the size of the sample

4.7 Concentration of Zn in other materials

Although not natural materials, the concentrations of Zn in these materials were measured for comparative purposes with same like materials or with their Zn expected concentration by their producers. All samples were dissolved, purified, and isotopically analysed according to the procedures described in Sections 3.9, 3.10, and 3.5 respectively. All isotope ratios were measured using the Daly detector, where the aim of the experiment was only initially to measure the concentration of Zn in these samples. The results are as presented in Table 4.17, where it should be noted that the concentration of Zn in Zinc tablet is measured as mg/ Tablet (mass of tablet 0.5203 ± 0.0002 g), while it is in g/ kg for the steel sample. A full discussion of these results is shown in Section 6.5.

Table 4. 17: Concentration of Zn in other materials

Sample	Mass Sample(g)	± (g)	Analysis No	Concentration	± 95%
Zinc Tablet _α	0.0967	0.0005	1	21.00	0.60
Zinc plated steel _β	0.0153	0.0003	1	5.32	0.10
			1.1	5.11	0.09
			1.2	5.18	0.09
			1.3	5.22	0.10
			Average	5.21	0.10

^α Concentration is in mg per Tablet. ^β Concentration is in g per kg.

- **Chapter 5: Isotopic composition of Zn: Results**

5.1 Introduction

In this Chapter the isotopic composition of laboratory standards, enriched stable isotopes mixtures (double spike) and samples are presented. Fractionation calculated from the double spiking procedure and proposed absolute isotopic compositions are also shown. Discussions are limited to analytically related matters, with a full discussion presented in Chapter 7.

5.2 Laboratory standard

A number of different measurements for the laboratory standard Zn Alfa Aesar 10759 were performed taking into account the two different detector systems (Daly and Faraday) used. This laboratory standard is taken from the same reservoir as the IRMM 3702 proposed (δ zero) standard (Ponzevera et al., 2006). It is important to note that the laboratory standard used in this work is the same as the international proposed absolute isotopic composition of Zn by IUPAC. The use of a consistent standard by all isotope analyses is essential for the comparison of Zn isotope fractionation. Laboratory standards were measured using the Daly detector used in the determination of the concentration of Zn in some SRMs. These standards are shown in Table 5.1. The isotope analysis procedures used for both collectors are as described in Section 3.5.

Table 5. 1: The measured isotopic composition of Zn in the laboratory standard measured using the Daly detector not corrected for machine bias.

No	Date	Zn(ng)	$^{66}\text{Zn}/^{64}\text{Zn}$	$^{67}\text{Zn}/^{64}\text{Zn}$	$^{68}\text{Zn}/^{64}\text{Zn}$	$^{70}\text{Zn}/^{64}\text{Zn}$
1	19-Jul-04	47	0.5530(3)	0.07973(7)	0.3585(3)	0.01159(3)
2	30-Aug-04	47	0.5529(2)	0.07990(7)	0.3586(2)	0.01165(3)
3	30-Sep-04	47	0.5523(3)	0.07938(8)	0.3584(2)	0.01150(1)
4	04-Oct-04	47	0.5520(2)	0.07954(8)	0.3574(4)	0.01150(2)
5	07-Oct-04	47	0.5524(2)	0.07958(6)	0.3579(2)	0.01149(1)
6	11-Oct-04	47	0.5525(2)	0.07947(7)	0.3583(4)	0.01151(2)
7	27-Oct-04	14	0.5536(2)	0.07978(6)	0.3590(3)	0.01161(3)
8	08-Nov-04	47	0.5526(2)	0.07961(7)	0.3583(2)	0.01156(2)
9	12-Nov-04	14	0.5528(2)	0.07986(8)	0.3584(2)	0.0139(2)
10	21-Jan-05	14	0.5538(4)	0.07996(9)	0.3593(3)	0.01161(4)
11	18-Feb-05	14	0.5532(1)	0.07969(3)	0.3586(1)	0.01172(2)
12	16-Mar-05	14	0.5528(2)	0.07960(5)	0.3583(2)	0.01151(2)
13	03-Apr-05	14	0.5535(2)	0.07977(6)	0.3592(2)	0.01161(3)
14	17-Jan-06	14	0.5525(3)	0.07946(7)	0.3576(3)	0.01143(3)
15	16-Feb-06	14	0.5537(4)	0.0800(1)	0.3595(7)	0.0115(1)
16	29-Mar-06	14	0.5533(2)	0.07966(5)	0.3595(2)	0.01163(2)
17	29-Mar-06	15	0.5513(2)	0.07938(7)	0.3564(2)	0.01149(3)
18	05-Apr-06	14	0.5526(2)	0.07955(9)	0.3588(2)	0.01158(4)
19	29-Mar-06	14	0.5535(2)	0.07963(5)	0.3596(2)	0.01158(2)
20	29-Mar-06	14	0.5513(2)	0.07938(7)	0.3564(2)	0.01149(3)
21	05-Apr-06	14	0.5526(2)	0.07955(9)	0.3588(2)	0.01158(4)
22	07-Apr-06	14	0.5519(2)	0.07946(9)	0.3571(3)	0.01148(3)
23	27-Apr-06	14	0.5518(2)	0.07960(5)	0.3575(1)	0.01155(3)
24	29-Jul-06	14	0.5521(2)	0.07953(6)	0.3576(1)	0.01158(4)
25	07-Sep-06	14	0.5512(2)	0.07929(5)	0.3565(1)	0.01142(2)
26	08-Sep-06	14	0.5511(3)	0.07931(7)	0.3569(2)	0.01133(2)
27	10-Sep-06	14	0.5515(3)	0.07938(8)	0.3564(3)	0.01134(3)
28	10-Sep-06	14	0.5513(4)	0.0797(1)	0.3572(5)	0.01149(3)
29	10-Sep-06	14	0.5514(2)	0.07976(6)	0.3573(2)	0.01147(3)
30	10-Sep-06	14	0.5515(2)	0.07970(8)	0.3564(2)	0.01143(3)
31	11-Sep-06	14	0.5526(3)	0.0797(1)	0.3585(3)	0.0115(1)
32	11-Sep-06	14	0.5534(3)	0.07968(7)	0.3593(2)	0.01154(4)
33	16-Nov-06	40	0.5519(3)	0.0796(1)	0.3579(3)	0.0115(1)
34	20-Nov-06	40	0.5520(3)	0.07962(1)	0.3578(3)	0.01159(4)
Average			0.55240	0.079610	0.35803	0.01160
σ			0.00082	0.00018	0.00100	0.00042
$\pm 95\%$			0.00028	0.000060	0.00034	0.00014

The ratios presented in Table 5.1 were normalized relative to their average $^{68}\text{Zn}/^{64}\text{Zn}$ ratio and yielded isotopic ratios as $^{66}\text{Zn}/^{64}\text{Zn} = 0.55240 \pm 0.00010$, $^{67}\text{Zn}/^{64}\text{Zn} = 0.079610 \pm 0.000051$, $^{68}\text{Zn}/^{64}\text{Zn} = 0.35803$, and $^{70}\text{Zn}/^{64}\text{Zn} = 0.01160 \pm 0.00014$. The isotopic compositions obtained using the Daly were used to calculate the

concentrations of Zn in samples using IDMS, where smaller samples of ~300 ng were used. The Daly enables small amounts of sample and double spike solution to be used. The more precise Faraday multi collector was used to measure the isotopic composition of critical samples and standards, the laboratory standard, double spike, the mixture of the laboratory standard and the double spike, and the isotopic composition of the double spiked samples. The measured isotopic composition of Zn laboratory standard measured using the Faraday multi collector is as shown in Table 5.2. The fractionation of final isotopic composition normalized to $^{68}\text{Zn}/^{64}\text{Zn}$ of the absolute standard is -0.019‰ amu^{-1} , compared to the external reproducibility of the measured fractionation of $\pm 0.039\text{‰ amu}^{-1}$. The reproducibility of measured fractionation is further discussed in Section 5.4, and represented in Figure 5.6. As shown in Table 5.2, all samples were 1 μg except a few samples, which are indicated.

Table 5. 2: The measured isotopic composition of 1µg of Zn standard of laboratory standard using the Faraday multicollector not corrected for machine bias.

No	Date	⁶⁶ Zn/ ⁶⁴ Zn	⁶⁷ Zn/ ⁶⁴ Zn	⁶⁸ Zn/ ⁶⁴ Zn	⁷⁰ Zn/ ⁶⁴ Zn
1	19-May-07	0.55889(9)	0.08081(3)	0.3665(1)	0.01185(2)
2	19-May-07	0.5579(1)	0.08068(4)	0.3652(2)	0.01182(3)
3	23-May-07	0.5582(1)	0.08063(3)	0.3656(1)	0.01185(2)
4	03-Jun-07	0.5591(2)	0.08099(9)	0.3667(3)	0.01185(5)
5	09-Jun-07	0.5570(1)	0.08054(5)	0.3643(1)	0.01177(6)
6	23-Jun-07	0.55724(5)	0.08053(2)	0.36432(6)	0.01179(2)
7	14-Jul-07	0.55707(6)	0.08046(4)	0.36420(7)	0.01176(2)
8	21-Jul-07	0.55666(6)	0.08043(2)	0.36368(6)	0.01176(2)
9	04-Aug-07	0.55680(7)	0.08050(8)	0.36404(9)	0.01169(5)
10	11-Aug-07	0.5578(1)	0.08052(8)	0.3651(1)	0.01163(7)
11	18-Aug-07	0.5573(1)	0.08048(5)	0.3645(1)	0.01176(5)
12	25-Aug-07	0.55700(7)	0.08049(2)	0.36404(9)	0.01173(2)
13	09-Sep-07	0.5573(1)	0.08055(4)	0.3645(2)	0.01178(3)
14	17-Sep-07	0.5567(3)	0.0803(2)	0.3637(2)	0.0116(2)
15	17-Sep-07	0.55691(7)	0.08045(5)	0.36415(7)	0.01177(4)
16	17-Sep-07	0.5577(1)	0.08072(3)	0.3649(1)	0.01187(4)
17 ^Ψ	17-Sep-07	0.55725(7)	0.08057(3)	0.36441(7)	0.01178(3)
18 ^Ψ	17-Sep-07	0.5579(1)	0.08061(9)	0.3651(1)	0.0118(1)
19 ^Ψ	17-Sep-07	0.55710(7)	0.08065(6)	0.36431(8)	0.01174(5)
Average		0.55746	0.080577	0.36469	0.011768
σ		0.00069	0.000143	0.00074	0.000070
± 95%		0.00031	0.000065	0.00034	0.000032

^Ψ Sample size is 500 ng.

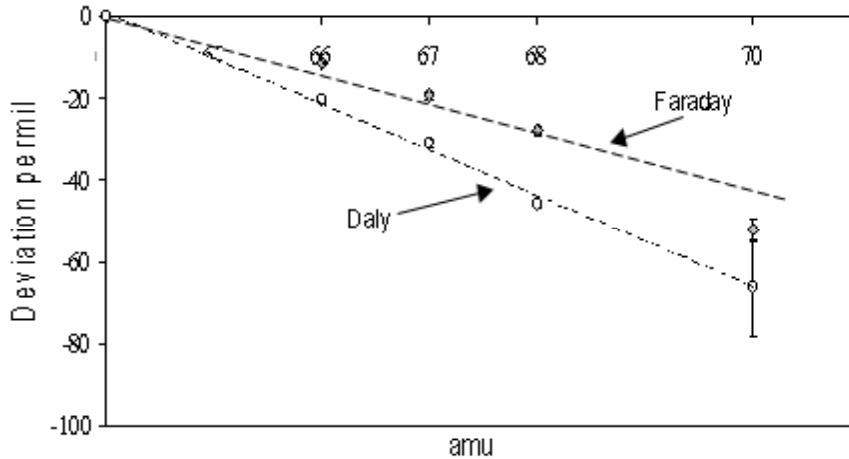
The ratios presented in Table 5.2 were normalized relative to their average ⁶⁸Zn/⁶⁴Zn ratio and yielded an isotopic ratios as ⁶⁶Zn/⁶⁴Zn = 0.557491 ± 0.000036, ⁶⁷Zn/⁶⁴Zn = 0.080583 ± 0.000031, ⁶⁸Zn/⁶⁴Zn = 0.364734, and ⁷⁰Zn/⁶⁴Zn = 0.011770 ± 0.000026.

The uncertainties for the isotopic composition of Zn in the laboratory standard using the Faraday detector appears larger than those measured by the Daly. This due to the fact that these uncertainties are for the average isotopic composition of Zn in the standard before normalizing to their average. More over, the Faraday uncertainties are the external uncertainties affected by “n” number of measurements (Fraday n=19) While Daly (n=34) hence the small “n” has a naturally higher uncertainty.

The deviation of the isotopic measurements of the laboratory standard measured using the Daly detector and using the Faraday multicollector relative to the isotopic

composition of proposed absolute standard measured by IRMM (Ponzevera et al., 2006) is represented in Figure 5.1

Figure 5. 1: The deviation of the isotopic composition of the laboratory standard measured using the Daly detector and using the Faraday multicollector relative to the isotopic composition of proposed absolute standard measured by IRMM



The extent of the deviation of the laboratory standard measured in the Faraday multi collector and that on the Daly can be presumed to define the bias of the machine used in this research. As represented in Figure 5.1, the extent of the deviation from the measured proposed absolute by IRMM of the standard measured on the Daly detector is approximately, twice the deviation of that measured using the Faraday multi collector; -6.9 ‰ amu^{-1} for the Faraday, and -11.2 ‰ amu^{-1} for the Daly. This is to be expected, because of the nature of detectors and the collection processes. Also and according to the square root ratio of masses; the measurement using the Faraday multi collector is to introduce a “bias” of $|7.3| \text{ ‰ amu}^{-1}$, and according to the ratio of the masses; the Daly is to introduce a “bias” of $|15.6| \text{ ‰ amu}^{-1}$ and is generally consistent with that found. As represented in Figure 5.1, the “bias” for both collectors appears to be linear relative to the absolute. However, the Faraday collector data may be more exponential than linearly biased relative to the absolute as represented in Figure 3.24. However, if a correction is to be introduced; the linear law is still a valid approach to correct for this machine bias. The linear law as represented in Equation 3.9 in Section 3.1.2.1 and exponential law as represented in Equations 5.1.

$$R_c = R_o \left(\frac{m_1}{m_2} \right)^\beta \quad 5.1$$

Where R_c , R_o are the corrected and uncorrected isotopic ratios.
 β is the correction factor.

The uncertainty of the deviation of the laboratory standard measured using both detectors is too small to be shown in Figure 5.1.

The deviation of $^{66}\text{Zn}/^{64}\text{Zn}$ ratio, $^{67}\text{Zn}/^{64}\text{Zn}$ ratio, $^{68}\text{Zn}/^{64}\text{Zn}$, and $^{70}\text{Zn}/^{64}\text{Zn}$ ratio, all measured using the Faraday multicollector from the average of all the runs is shown in Figures 5.2; 5.3, 5.4 and 5.5 respectively. In general the reproducibility increases as analytical experience was gained, but it proved very difficult to obtain all measured results within individual measurement uncertainties, limiting any assessment of fractionation by direct sample standard comparison to ± 0.5 per mil per atomic mass unit. This clearly demonstrates the need for double spiking to discriminate between instrument bias and sample fractionation.

Figure 5. 2: The deviation of the measured $^{66}\text{Zn}/^{64}\text{Zn}$ ratios for 19 analyses as measured on the Faraday multicollector relative to their external average.

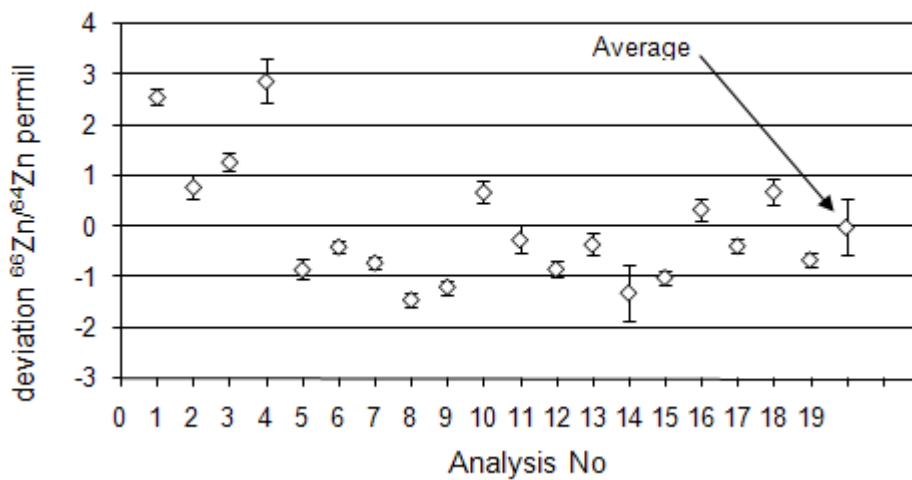


Figure 5. 3: Deviation of the $^{67}\text{Zn}/^{64}\text{Zn}$ ratios measured on the Faraday multicollector relative to their external average.

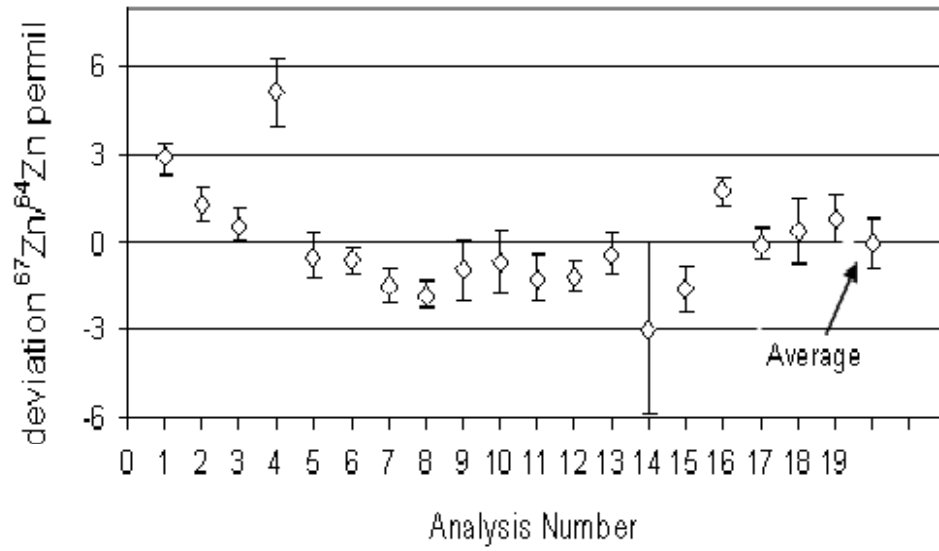


Figure 5. 4: The deviation of $^{68}\text{Zn}/^{64}\text{Zn}$ ratios measured on the Faraday multicollector relative to their external average.

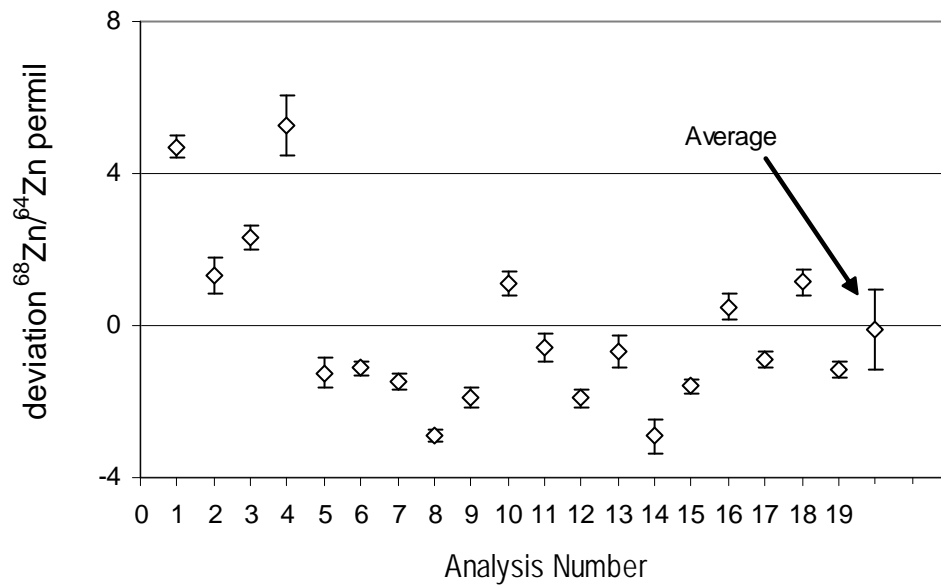
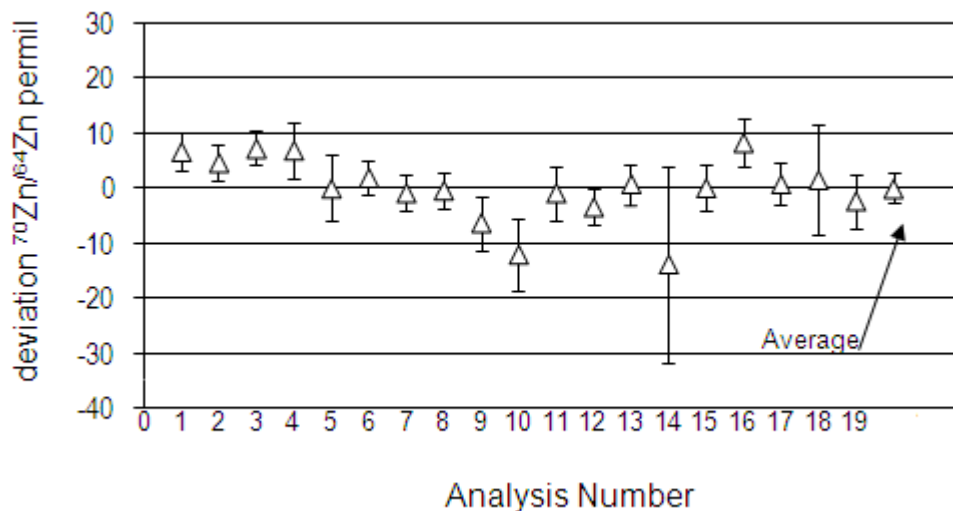


Figure 5. 5: The deviation of $^{70}\text{Zn}/^{64}\text{Zn}$ ratios measured on the Faraday multicollector relative to their external average.



5.3 Double spike

The isotopic composition of the double spike solution was measured using the Daly detector for IDMS measurements and the Faraday multicollector for fractionation and IDMS. The measurements were performed in the same manner as described in Section 3.5, which is the same as that described for the laboratory standard in Section 5.1. The measured isotopic compositions of the double spike are shown in Tables 5.3, and 5.4 for the Daly and Faraday respectively.

Table 5. 3: The isotopic composition of the double spike measured using the Daly detector, not corrected for machine bias.

No	Date	$^{64}\text{Zn}/^{67}\text{Zn}$	$^{66}\text{Zn}/^{67}\text{Zn}$	$^{68}\text{Zn}/^{67}\text{Zn}$	$^{70}\text{Zn}/^{67}\text{Zn}$
1	22-Jan-05	0.1509(3)	0.1307(2)	0.1270(2)	0.5145(6)
2	25-Jan-05	0.1534(4)	0.1310(2)	0.1269(2)	0.5134(7)
3	27-Jan-05	0.1551(2)	0.1330(1)	0.1283(1)	0.5126(4)
4	18-Feb-05	0.1549(8)	0.1311(3)	0.1284(3)	0.519(2)
5	18-Feb-05	0.1523(5)	0.1310(3)	0.1279(2)	0.514(2)
6	17-Mar-05	0.15(2)	0.133(7)	0.128(7)	0.52(2)
7	05-Apr-05	0.155(1)	0.1328(8)	0.1286(6)	0.515(2)
8	10-Apr-05	0.1533(4)	0.1320(2)	0.1277(2)	0.512(1)
9	23-Apr-05	0.1576(2)	0.1333(2)	0.1284(2)	0.5110(5)
Average		0.1540	0.13193	0.12794	0.5142
σ		0.0020	0.00101	0.00061	0.0023
$\pm 95\%$		0.0016	0.00081	0.00049	0.0018

The ratios presented in Table 5.3 were normalized relative to their average $^{70}\text{Zn}/^{67}\text{Zn}$ ratio and yielded an isotopic ratios as $^{64}\text{Zn}/^{67}\text{Zn} = 0.1540 \pm 0.0018$, $^{66}\text{Zn}/^{67}\text{Zn} = 0.13193 \pm 0.00089$, $^{68}\text{Zn}/^{67}\text{Zn} = 0.12794 \pm 0.00049$, and $^{70}\text{Zn}/^{67}\text{Zn} = 0.51416$.

The Daly measured isotopic composition of the double spike was used to calculate concentrations of Zn in small samples. The isotopic composition of the double spike measured using the Faraday multicollector was used to determine sample fractionation. In Table 5.4, the internal uncertainty especially for the minor isotopes of each individual measurements is relatively large, this is also because; none of the individual ratios were normalized relative to their average.

Table 5. 4: The measured isotopic composition of Zn in the double spike solution using the Faraday multicollector system, not corrected for machine bias.

Number	$^{66}\text{Zn}/^{64}\text{Zn}$	$^{67}\text{Zn}/^{64}\text{Zn}$	$^{68}\text{Zn}/^{64}\text{Zn}$	$^{70}\text{Zn}/^{64}\text{Zn}$
1	0.8780(3)	6.780(2)	0.8673(2)	3.5402(9)
2	0.8755(5)	6.750(4)	0.8638(5)	3.525(2)
3	0.878(2)	6.86(2)	0.870(2)	3.582(8)
4	0.885(1)	6.91(1)	0.877(1)	3.609(5)
5	0.874(1)	6.797(8)	0.864(1)	3.549(4)
6	0.8899(4)	6.952(4)	0.8823(4)	3.630(1)
7	0.874(3)	6.83(2)	0.866(3)	3.57(1)
8	0.8788(3)	6.703(2)	0.8634(4)	3.500(1)
9	0.8821(3)	6.734(2)	0.8679(5)	3.516(2)
10	0.876(6)	6.82(7)	0.865(7)	3.56(3)
11	0.8887(3)	6.963(2)	0.8801(3)	3.636(1)
Average	0.8800	6.828	0.8698	3.565
σ	0.0057	0.087	0.0068	0.045
\pm (95% confidence)	0.0034	0.052	0.0041	0.027

The ratios presented in Table 5.3 were normalized relative to their $^{68}\text{Zn}/^{64}\text{Zn}$ average and yielded an isotopic ratios as $^{66}\text{Zn}/^{64}\text{Zn} = 0.8800 \pm 0.0017$, $^{67}\text{Zn}/^{64}\text{Zn} = 6.828 \pm 0.033$, $^{68}\text{Zn}/^{64}\text{Zn} = 0.86978$, and $^{70}\text{Zn}/^{64}\text{Zn} = 3.565 \pm 0.012$.

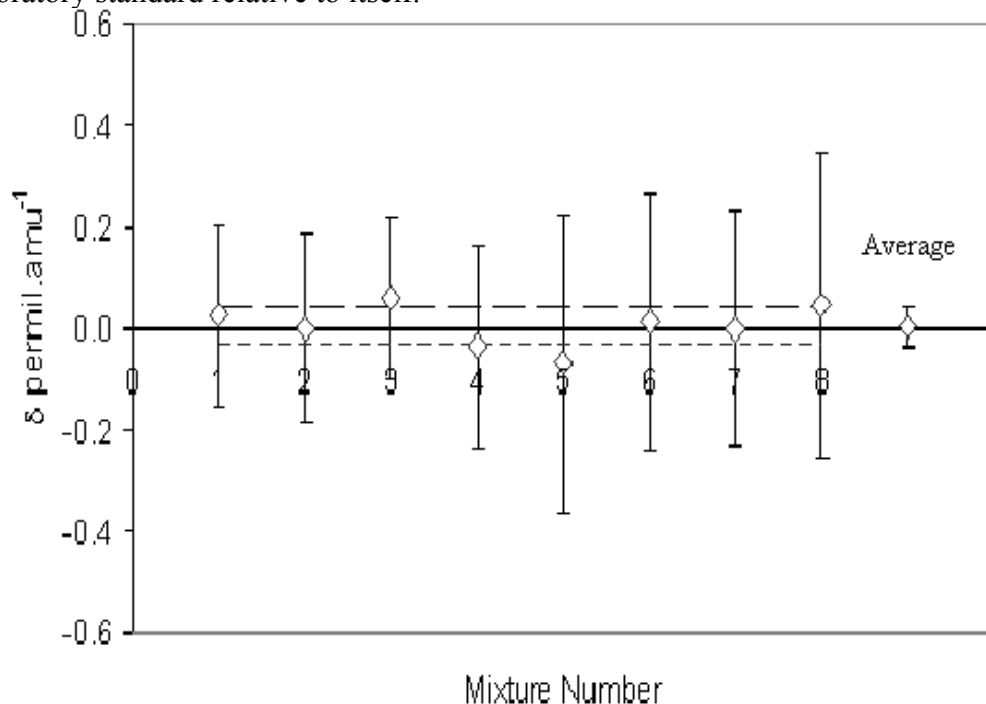
As mentioned earlier, the uncertainty accompanied with the isotopic composition of the double spike was set to zero when performing the calculations for the fractionation.

5.4 Long term reproducibility of measured fractionation

A mixture of the laboratory standard and the double spike was prepared to assess the long term reproducibility (two years) of fractionation measurements. Theoretically such a mixture must yield zero fractionation because it is measuring sample

fractionation relative to itself (laboratory standard). The mixture isotopic composition was measured using the Faraday multicollector ($n = 8$) and was found to be: $^{66}\text{Zn}/^{64}\text{Zn} = 0.563812 \pm 0.000026$, $^{67}\text{Zn}/^{64}\text{Zn} = 0.231813 \pm 0.000050$, $^{68}\text{Zn}/^{64}\text{Zn} = 0.374732$, and $^{70}\text{Zn}/^{64}\text{Zn} = 0.090991 \pm 0.000027$. The long term reproducibility is represented in Figure 5.6

Figure 5. 6: The long term reproducibility of the measured fractionation of the laboratory standard relative to itself.



Although the internal fractionation uncertainties are approximately 0.15 per mil per amu are the average of the measured fractionation of this mixture over two years was $+0.006 \pm 0.039 \text{ } \text{‰} \text{ amu}^{-1}$ (95% confidence limit). These highly reproducible results can represent a form of fractionation detection limit of $0.039 \text{ } \text{‰} \text{ amu}^{-1}$, and would be the minimum possible fractionation that could be detected by the entire measuring system.

5.5 Measurements of fractionation

A survey of the isotopic composition of Zn in wide range of more than 35 different natural materials was conducted representing the first survey of Zn fractionation in

natural materials using the double spike technique since that of Rosman (1972a). Geological samples measured were chosen to cover the rock cycle of the Earth as discussed in Section 3.8.1. Samples were chosen with the intention of covering a range of materials with significant potential for fractionation; pure Zn standard metal materials, geological materials, biological materials, and meteorites. Of significance to the wider scientific community, most of the samples were SRMs, where knowing the isotopic composition of such standard materials is vital to assess fractionation in similar materials using different analytical techniques e.g ICP-MS.

Both measured fractionation relative to the laboratory standard and the absolute isotopic compositions of the samples are represented. The uncertainty for each individual fractionation determination is provided at the 95% confidence level, whereas the final uncertainty for each sample was calculated using the normal distribution using GUM (Metrodata GmbH, 1996). The fractionation obtained all results agree with each other within individual measurement uncertainties. For all of the samples, the fractionation was calculated using two sets of isotopes. Ongoing quality control was also confirmed by measuring the zero fractionation mixture (laboratory standard and double spike) in a number of batches of samples. Calculating the fractionation using different set of isotopes also helped to determine whether there were any anomalies or interferences on any of the Zn isotopes. The fractionation for each individual sample was determined using two different sets of isotopes and were found to agree with each other within the uncertainty, except for those obtained for the Redfields meteorite (see Section 5.4.4.2.1 and Section 7.4.2). As presented in most of the results the uncertainty of the fractionation calculated using the two set of isotopes is relatively the same, this could be because most of the ratios were normalized relative to the average $^{68}\text{Zn}/^{64}\text{Zn}$ ratio of each analysis, which makes the uncertainty of $^{68}\text{Zn}/^{64}\text{Zn}$ zero for the mixture of the sample and double spike. The isotopic composition of some samples was measured without double spiking, to determine if the fractionation could be detected outside uncertainty e.g. Canyon Diablo (see Section 5.4.4.2). It was important to demonstrate that there were no nonlinear effects or isotopic anomalies in any of the Zn isotopes which is a requirement of the double spike technique. All the results in the Tables (5.9- 5.20),

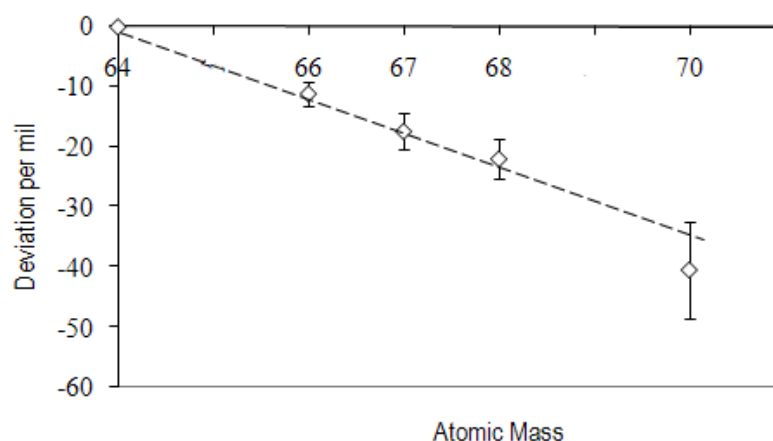
use the following notation; analysis **X.y**, refers to the analysis of aliquot **y** from reservoir **X**. If not shown; then the analysis was performed using different reservoir.

The absolute isotopic composition of Zn in most of the samples was calculated by applying the measured fractionation factor to the absolute isotopic composition of Zn.

5.5.1 Zn Standard metals

The isotopic composition of some samples was measured without double spiking to determine if the Zn fractionation could be observed directly and to determine if there were any nonlinear effects. While plotting the deviation of the isotopic composition of any sample relative to the laboratory standard is a traditional technique for assessing fractionation, it is not able to detect small sub-permil effects as found for Zn in many samples. In addition this method does not correct accurately for machine induced fractionation, the isotopic composition of unspiked Zn in the laboratory standard AE-10760, is shown in Figure 5.7.

Figure 5. 7: The deviation of unspiked Zn pure metal AE10760 relative to the laboratory standard.



The deviations show a clear linear dependence and indicate no sign of any isotopic anomaly or interference at any of the Zn isotopes.

Pure standard Zn materials provided by IRMM were measured for fractionation relative to the laboratory standard and their proposed absolute isotopic composition are as shown in Table, 5.5, and 5.6 respectively. The isotopic composition of these

samples was performed using the more precise Faraday multicollector unless stated, e.g Zn metal Alfa Aesar10760. The results are discussed in Section 7.6.

Table 5. 5: Measured isotopic fractionation in high purity metal standards relative to the laboratory standard “the international absolute isotopic composition of Zn”. Two fractionation values are shown reflecting the use of different sets of isotopic ratios. All relative to ^{64}Zn

Standard Zn metal	Experiment No	f ‰ amu ⁻¹ Using $^{67}\text{Zn}, ^{68}\text{Zn}, ^{70}\text{Zn}$	± ‰ amu ⁻¹	f ‰ amu ⁻¹ Using $^{66}\text{Zn}, ^{67}\text{Zn}, ^{70}\text{Zn}$	± ‰ amu ⁻¹
Ac AE 10760	1*	-5.0	0.7	-4.7	0.5
	2*	-5.3	0.8	-4.8	0.7
	3*	-5.4	0.6	-5.4	0.5
	4*	-4.7	0.7	-4.3	0.7
	5*	-5.4	0.7	-5.1	0.6
	6*	-3.1	4.0	-2.6	4.1
	7*	-4.9	1.4	-5.0	1.3
	8*	-5.7	0.9	-6.2	0.7
	9*	-5.2	0.4	-5.3	0.3
	10*	-5.4	0.6	-5.2	0.5
	11*	-5.4	0.6	-5.6	0.6
	12	-5.3	0.3	-5.2	0.3
	13	-5.6	0.4	-5.6	0.4
	Average	-5.11	0.36	-5.00	0.36
10440	1	0.13	0.18	0.12	0.18
	2	0.11	0.26	0.13	0.27
	Average	0.12	0.16	0.12	0.16
ZnO6	1	-4.38	0.19	-4.47	0.19
	2	-4.55	0.22	-4.63	0.23
	3	-4.63	0.24	-4.67	0.25
	Average	-4.52	0.13	-4.59	0.13
GF6110	1	-0.19	0.26	-0.20	0.26
	2	-0.23	0.24	-0.26	0.24
	Average	-0.21	0.18	-0.23	0.18
GF6120		-0.23	0.28	-0.20	0.28
		-0.10	0.25	-0.16	0.25
		0.06	0.21	0.05	0.22
	Average	-0.09	0.14	-0.10	0.15
IRMM -3702	1	0.15	0.20	0.13	0.18
	2	0.03	0.29	-0.07	0.27
	Average	0.09	0.18	0.03	0.16
JMC-2	1	-0.01	0.20	0.06	0.20
	2	0.08	0.19	0.06	0.21
	3			0.05	0.18
	Average	0.04	0.14	0.06	0.14

*Measured using Daly detector

Using these measured fractionation the absolute isotopic composition of these samples can be determined. The uncertainties of the final ratios combined with that obtained for the fractionation are propagated to produce 95% confidence level uncertainty as shown in Table 5.6.

Table 5. 6: the absolute isotopic composition of Zn in the Zn pure standard metals

Standard Zn metal		Ratio	±
IRMM- Ac AE 10760	$^{66}\text{Zn}/^{64}\text{Zn}$	0.55821	0.00051
	$^{67}\text{Zn}/^{64}\text{Zn}$	0.080907	0.000097
	$^{68}\text{Zn}/^{64}\text{Zn}$	0.36753	0.00057
	$^{70}\text{Zn}/^{64}\text{Zn}$	0.012037	0.000035
10440	$^{66}\text{Zn}/^{64}\text{Zn}$	0.56411	0.00035
	$^{67}\text{Zn}/^{64}\text{Zn}$	0.082196	0.000052
	$^{68}\text{Zn}/^{64}\text{Zn}$	0.37537	0.00029
	$^{70}\text{Zn}/^{64}\text{Zn}$	0.012427	0.000026
ZnO6	$^{66}\text{Zn}/^{64}\text{Zn}$	0.55887	0.00033
	$^{67}\text{Zn}/^{64}\text{Zn}$	0.081052	0.000047
	$^{68}\text{Zn}/^{64}\text{Zn}$	0.36841	0.00025
	$^{70}\text{Zn}/^{64}\text{Zn}$	0.012081	0.000024
GF6110	$^{66}\text{Zn}/^{64}\text{Zn}$	0.56373	0.00036
	$^{67}\text{Zn}/^{64}\text{Zn}$	0.082114	0.000057
	$^{68}\text{Zn}/^{64}\text{Zn}$	0.37487	0.00032
	$^{70}\text{Zn}/^{64}\text{Zn}$	0.012402	0.000027
GF6120	$^{66}\text{Zn}/^{64}\text{Zn}$	0.56387	0.00034
	$^{67}\text{Zn}/^{64}\text{Zn}$	0.082144	0.000049
	$^{68}\text{Zn}/^{64}\text{Zn}$	0.37506	0.00026
	$^{70}\text{Zn}/^{64}\text{Zn}$	0.012411	0.000025
IRMM3702	$^{66}\text{Zn}/^{64}\text{Zn}$	0.56407	0.00036
	$^{67}\text{Zn}/^{64}\text{Zn}$	0.082188	0.000056
	$^{68}\text{Zn}/^{64}\text{Zn}$	0.37533	0.00032
	$^{70}\text{Zn}/^{64}\text{Zn}$	0.012425	0.000026
JMC-2	$^{66}\text{Zn}/^{64}\text{Zn}$	0.56401	0.00034
	$^{67}\text{Zn}/^{64}\text{Zn}$	0.082175	0.000048
	$^{68}\text{Zn}/^{64}\text{Zn}$	0.37524	0.00026
	$^{70}\text{Zn}/^{64}\text{Zn}$	0.012421	0.000025
IRMM Alfa Aesar 10759	$^{66}\text{Zn}/^{64}\text{Zn}$	0.56398	0.00030
	$^{67}\text{Zn}/^{64}\text{Zn}$	0.08217	0.00004
	$^{68}\text{Zn}/^{64}\text{Zn}$	0.37520	0.00017
	$^{70}\text{Zn}/^{64}\text{Zn}$	0.01242	0.00002

5.5.2 Geological materials

The measured fractionation and the absolute isotopic compositions relative to the laboratory standard, were measured in number of geological materials. The geological materials are mainly SRMs and are grouped according to their rock type, igneous, sedimentary, metamorphic rocks and clay. The uncertainty for each individual measurement was treated the same as those for the high purity Zn metal calculations. Despite the fact that, large amount of Zn in these samples is available for measurements, Zn isotopes were measured using no more that 1 μg Zn to be loaded using the more precise Faraday multi collector.

5.5.2.1 Zn minerals

Zinc fractionation was measured in number of Zn minerals as shown in Table 5.7. In addition, the absolute isotopic compositions of Zn in these minerals were determined, and are represented in Table 5.7. All isotopic ratios for these samples were measured using the Faraday multi collector using no more than 1 μg Zn. All these minerals were donated from the Museum of Western Australia. The results are discussed in Section (7.2.1)

Table 5. 7: Measured Zn fractionation, of Zn minerals relative to the laboratory standard (δ zero). Two fractionation values are shown reflecting the use of different sets of isotopic ratios, all relative to ^{64}Zn .

Mineral	Experiment No	f ‰ amu ⁻¹ Using ^{67}Zn , ^{68}Zn , ^{70}Zn	± ‰ amu ⁻¹	f ‰ amu ⁻¹ Using ^{66}Zn , ^{67}Zn , ^{70}Zn	± ‰ amu ⁻¹
Sphalerite	1	-0.09	0.30	-0.12	0.30
	2	0.08	0.21	0.07	0.21
	Average	-0.01	0.18	-0.02	0.18
HydroZincite	1	0.07	0.18	0.12	0.19
	2	-0.16	0.29	-0.03	0.30
	Average	-0.04	0.17	0.04	0.18
Smithsonite	1	0.17	0.18	0.17	0.18
	2	-0.13	0.21	-0.16	0.21
	Average	0.02	0.14	0.0	0.14

Table 5. 8: Proposed absolute isotopic composition of Zn in Zn minerals

Mineral		Ratio	±
Sphalerite	$^{66}\text{Zn}/^{64}\text{Zn}$	0.56397	0.00036
	$^{67}\text{Zn}/^{64}\text{Zn}$	0.082166	0.000057
	$^{68}\text{Zn}/^{64}\text{Zn}$	0.37519	0.00032
	$^{70}\text{Zn}/^{64}\text{Zn}$	0.012418	0.000026
HydroZincite	$^{66}\text{Zn}/^{64}\text{Zn}$	0.56392	0.00036
	$^{67}\text{Zn}/^{64}\text{Zn}$	0.082156	0.000055
	$^{68}\text{Zn}/^{64}\text{Zn}$	0.37513	0.00030
	$^{70}\text{Zn}/^{64}\text{Zn}$	0.012415	0.000026
Smithsonite	$^{66}\text{Zn}/^{64}\text{Zn}$	0.56399	0.00034
	$^{67}\text{Zn}/^{64}\text{Zn}$	0.082171	0.000050
	$^{68}\text{Zn}/^{64}\text{Zn}$	0.37522	0.00027
	$^{70}\text{Zn}/^{64}\text{Zn}$	0.012419	0.000025

5.5.2.2 Igneous rocks

Fractionation was measured in number of SRMs igneous rocks relative to the laboratory standard; Basalt BCR-1, Icelandic Basalt BIR-1, Diabase W-2, and Dolerite DNC-1. The measured fractionation and the absolute isotopic compositions of the samples are represented in the Table 5.9, and 5.10 respectively. All isotopic ratios for these samples were measured using the Faraday multi collector using no more than 1 µg Zn. The results of the isotopic fractionation of igneous rocks are discussed in Section (7.2.2). The ratios were obtained from digesting a sample of <0.3 g.

Table 5. 9: Measured Zn fractionation in igneous rocks relative to the laboratory standard (δ zero). Two fractionation values are shown reflecting the use of different sets of isotopic ratios, all relative to ^{64}Zn .

Sample	Analysis No	f ‰ amu ⁻¹ Using $^{67}\text{Zn}, ^{68}\text{Zn}, ^{70}\text{Zn}$	± ‰ amu ⁻¹	f ‰ amu ⁻¹ Using $^{66}\text{Zn}, ^{67}\text{Zn}, ^{70}\text{Zn}$	± ‰ amu ⁻¹
Basalt BCR-1	1	0.06	0.15	0.13	0.16
	2	-0.03	0.20	-0.11	0.20
	Average	0.02	0.12	0.01	0.13
Icelandic Basalt BIR-1	1	0.04	0.21	0.07	0.21
	2	-0.05	0.22	-0.02	0.22
	Average	-0.01	0.15	0.02	0.15
Diabase W-2	1	0.27	0.19	0.31	0.20
	1.1	0.21	0.32	0.34	0.33
	2	0.26	0.29	0.23	0.32
	3	0.07	0.20	0.00	0.21
	3.1	0.07	0.19	0.01	0.20
	4	0.12	0.23	0.04	0.24
	Average	0.17	0.10	0.16	0.10
Dolerite DNC-1	1	-0.14	0.15	-0.25	0.15
	1.1	-0.17	0.30	-0.22	0.30
	2	0.15	0.34	0.11	0.34
	2.1	-0.19	0.37	-0.17	0.38
	Average	-0.09	0.15	-0.13	0.15

Table 5. 10: Proposed absolute isotopic composition of Zn in igneous rock SRMs

SRM		Ratio	±
Basalt BCR-1	$^{66}\text{Zn}/^{64}\text{Zn}$	0.56399	0.00033
	$^{67}\text{Zn}/^{64}\text{Zn}$	0.082171	0.000046
	$^{68}\text{Zn}/^{64}\text{Zn}$	0.37522	0.00024
	$^{70}\text{Zn}/^{64}\text{Zn}$	0.012419	0.000025
Icelandic Basalt BIR-1	$^{66}\text{Zn}/^{64}\text{Zn}$	0.56397	0.00034
	$^{67}\text{Zn}/^{64}\text{Zn}$	0.082166	0.000051
	$^{68}\text{Zn}/^{64}\text{Zn}$	0.37519	0.00028
	$^{70}\text{Zn}/^{64}\text{Zn}$	0.012418	0.000025
Diabase W-2	$^{66}\text{Zn}/^{64}\text{Zn}$	0.56416	0.00032
	$^{67}\text{Zn}/^{64}\text{Zn}$	0.082207	0.000043
	$^{68}\text{Zn}/^{64}\text{Zn}$	0.37544	0.00022
	$^{70}\text{Zn}/^{64}\text{Zn}$	0.012430	0.000024
Dolerite DNC-1	$^{66}\text{Zn}/^{64}\text{Zn}$	0.56387	0.00035
	$^{67}\text{Zn}/^{64}\text{Zn}$	0.082144	0.000051
	$^{68}\text{Zn}/^{64}\text{Zn}$	0.37505	0.00028
	$^{70}\text{Zn}/^{64}\text{Zn}$	0.012411	0.000025

5.5.2.3 Sedimentary rocks

A number of SRMs sedimentary rocks were also investigated for Zn fractionation relative to the laboratory standard; Green River Shale, SGR-1, Cody Shale SCO-1, Marine sediment Hiss-1, and Murst-Iss-A1. The measured fractionation and the absolute isotopic compositions of the samples are shown in the Table 5.11, 5.12 respectively. The results for sedimentary rocks are discussed in Section (7.2.3). All isotopic ratios for these samples were measured using the Faraday multi collector using no more than 1µg Zn. The source of these samples is as represented in Section (3.8.1), all the isotopic composition of the double spiked samples was obtained from the digestion of small samples of <0.3 g.

Table 5. 11: Measured Zn fractionation in sedimentary rocks relative to the laboratory standard (δ zero). Two fractionation values are shown reflecting the use of different sets of isotopic ratios, all relative to ^{64}Zn .

SRM	Analysis No	f ‰ amu ⁻¹ Using ^{67}Zn , ^{68}Zn , ^{70}Zn	± ‰ amu ⁻¹	f ‰ amu ⁻¹ Using ^{66}Zn , ^{67}Zn , ^{70}Zn	± ‰ amu ⁻¹
Green River Shale, SGR-1	1	0.24	0.37	0.28	0.39
	2	0.35	0.23	0.43	0.24
	Average	0.30	0.22	0.36	0.23
Cody Shale SCo-1	1	0.05	0.26	-0.05	0.26
	2	0.05	0.34	-0.03	0.33
	2.1	0.09	0.3	-0.04	0.29
	Average	0.06	0.17	-0.04	0.17
Marine sediment HISS-1	1	0.37	0.23	0.37	0.25
	1.1	0.24	0.2	0.24	0.22
	1.2	0.34	0.18	0.32	0.18
	2	0.3	0.19	0.27	0.19
	Average	0.31	0.10	0.30	0.11
Murst-Iss- A1	1	0.29	0.16	0.31	0.17
	1.1	0.35	0.19	0.27	0.2
	1.2	0.29	0.16	0.34	0.17
	2	0.29	0.20	0.33	0.20
	Average	0.305	0.089	0.312	0.093
CaCO ₃	1	0.51	0.28	0.39	0.27
	1.1	0.35	0.23	0.27	0.24
	Average	0.43	0.18	0.33	0.18

In a separate analysis, the isotopic composition of Zn in CaCO₃ was measured without double spiking the samples, as represented in Figure 5.8. The isotopic fractionation of Zn in the sample represents no sign of any anomaly or interference at any of the Zn isotopes. More over, the graph shows a deviation (slope) of +1.4 ‰ amu⁻¹ relative to the laboratory standard, this is 3 times greater than what was measured (+0.43 ± 0.18) for this material by double spiking the sample. This may come from the machine bias and other factors, and illustrates the fact that this approach for measuring the isotopic composition is not able to detect small Zn isotopic fractionation. A discussion regarding the isotopic fractionation of sedimentary rocks is detailed in Section 7.2.3.

Figure 5. 8 The deviation of the isotopic composition of a CaCO₃ sample relative to the laboratory standard.

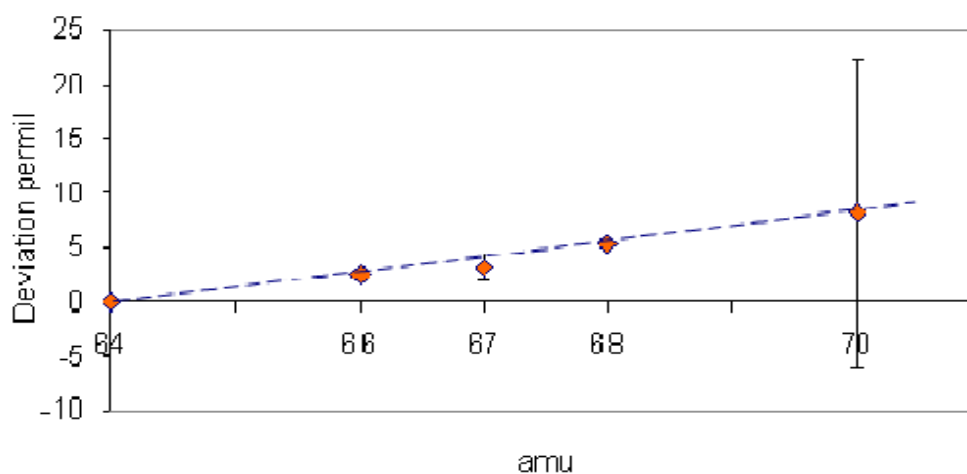


Table 5. 12: Proposed absolute isotopic composition of Zn for measured sedimentary rocks.

SRM		Ratio	±
Green River Shale, SGR-1	⁶⁶ Zn/ ⁶⁴ Zn	0.56431	0.00039
	⁶⁷ Zn/ ⁶⁴ Zn	0.082240	0.000064
	⁶⁸ Zn/ ⁶⁴ Zn	0.37564	0.00036
	⁷⁰ Zn/ ⁶⁴ Zn	0.012440	0.000028
Cody Shale SCo-1	⁶⁶ Zn/ ⁶⁴ Zn	0.56404	0.00036
	⁶⁷ Zn/ ⁶⁴ Zn	0.082181	0.000055
	⁶⁸ Zn/ ⁶⁴ Zn	0.37528	0.00030
	⁷⁰ Zn/ ⁶⁴ Zn	0.012422	0.000026
Marine sediment HISS-1	⁶⁶ Zn/ ⁶⁴ Zn	0.56432	0.00032
	⁶⁷ Zn/ ⁶⁴ Zn	0.082242	0.000043
	⁶⁸ Zn/ ⁶⁴ Zn	0.37566	0.00022
	⁷⁰ Zn/ ⁶⁴ Zn	0.012441	0.000024
Murst-Iss-A1	⁶⁶ Zn/ ⁶⁴ Zn	0.56431	0.00032
	⁶⁷ Zn/ ⁶⁴ Zn	0.082241	0.000041
	⁶⁸ Zn/ ⁶⁴ Zn	0.37565	0.00021
	⁷⁰ Zn/ ⁶⁴ Zn	0.012441	0.000024
CaCO ₃	⁶⁶ Zn/ ⁶⁴ Zn	0.56446	0.00037
	⁶⁷ Zn/ ⁶⁴ Zn	0.082272	0.000057
	⁶⁸ Zn/ ⁶⁴ Zn	0.37584	0.00032
	⁷⁰ Zn/ ⁶⁴ Zn	0.012450	0.000027

5.5.2.4 Metamorphic rocks

Mica Schist SDC-1, and Quartz Latite QLO-1 metamorphic rocks; were measured for fractionation relative to the laboratory standard. These results and the absolute isotopic compositions of the samples are shown in the Table 5.13 and 5.14 respectively. The size of the sample for all the measurements was no more than 1 µg Zn from <0.5 g of dissolved sample. All the isotopic ratios were measured using the Faraday multi collector. Zinc isotopic fractionation in metamorphic is discussed in Section (7.2.4)

Table 5. 13: Measured Zn fractionation in Mica Schist SDC-1 relative to the laboratory standard (δ zero). Two fractionation values are shown reflecting the use of different sets of isotopic ratios, all relative to ^{64}Zn .

SRM	Analysis No	f ‰ amu ⁻¹ Using $^{67}\text{Zn}, ^{68}\text{Zn}, ^{70}\text{Zn}$	± ‰ amu ⁻¹	f ‰ amu ⁻¹ Using $^{66}\text{Zn}, ^{67}\text{Zn}, ^{70}\text{Zn}$	± ‰ amu ⁻¹
Mica Schist SDC-1	1	0.18	0.38	0.19	0.38
	1.1	0.11	0.24	0.17	0.25
	1.2	0.2	0.25	0.18	0.25
	2	0.04	0.27	-0.01	0.27
	2.1	0.03	0.28	-0.06	0.28
	Average	0.10	0.13	0.09	0.13
Quartz Latite QLO-1	1	0.06	0.20	0.07	0.20
	2	-0.09	0.22	-0.11	0.23
	Average	-0.02	0.15	-0.02	0.15

Table 5. 14: Proposed absolute isotopic composition of Zn for measured metamorphic rocks SRMs

Sample	Ratio	±	
Mica Schist SDC-1	$^{66}\text{Zn}/^{64}\text{Zn}$	0.56408	0.00033
	$^{67}\text{Zn}/^{64}\text{Zn}$	0.082191	0.000048
	$^{68}\text{Zn}/^{64}\text{Zn}$	0.37534	0.00025
	$^{70}\text{Zn}/^{64}\text{Zn}$	0.012425	0.000025
Quartz Latite QLO-1	$^{66}\text{Zn}/^{64}\text{Zn}$	0.56395	0.00035
	$^{67}\text{Zn}/^{64}\text{Zn}$	0.082161	0.000051
	$^{68}\text{Zn}/^{64}\text{Zn}$	0.37516	0.00028
	$^{70}\text{Zn}/^{64}\text{Zn}$	0.012417	0.000025

5.5.2.5 Clay

The only Clay sample measured for fractionation was the SRM TILL-3 as represented in Table 5.15. The results calculated using two set of isotopes are consistent and within the uncertainty of each other. The absolute isotopic composition of the sample is as represented in Table 5.16. The result of this material is discussed in Section 7.2.5. The size of the sample used in these measurements were always < 1 µg, and all the isotopic ratios were measured using the more precise Faraday multi collector.

Table 5. 15: Measured Zn fractionation in TILL-3 relative to the laboratory standard (δ zero). Two fractionation values are shown reflecting the use of different sets of isotopic ratios, all relative to ^{64}Zn .

SRM	Analysis No	f ‰ amu ⁻¹ Using $^{67}\text{Zn}, ^{68}\text{Zn}, ^{70}\text{Zn}$	± ‰ amu ⁻¹	f ‰ amu ⁻¹ Using $^{66}\text{Zn}, ^{67}\text{Zn}, ^{70}\text{Zn}$	± ‰ amu ⁻¹
TILL-3	1	0.14	0.16	0.17	0.17
	1.1	0.09	0.18	0.03	0.18
	2	0.12	0.20	0.12	0.20
	Average	0.12	0.10	0.11	0.11

Table 5. 16: Proposed absolute isotopic composition of Zn for measured TILL-3

Mineral		Ratio	±
TILL-3	$^{66}\text{Zn}/^{64}\text{Zn}$	0.56411	0.00032
	$^{67}\text{Zn}/^{64}\text{Zn}$	0.082196	0.000043
	$^{68}\text{Zn}/^{64}\text{Zn}$	0.37537	0.00022
	$^{70}\text{Zn}/^{64}\text{Zn}$	0.012427	0.000024

5.5.3 Biological materials

SRMs biological materials; IMEP-19 (Rice); Sargasso (NIES-9) and Antarctic krill (MURST ISS-A2), were measured for fractionation relative to the laboratory standard. The isotopic ratios of all the samples were measured using the Faraday multi collector. The measured, fractionation and the absolute isotopic compositions of the samples are shown in Tables 5.17, 5.18 respectively. All biological materials isotopic ratios were measured using the Faraday multi collector. using no more than 1 µg Zn. The results are discussed in Section 7.3.

Table 5. 17: Measured Zn fractionation in biological materials relative to the laboratory standard (δ zero). Two fractionation values are shown reflecting the use of different sets of isotopic ratios, all relative to ^{64}Zn .

SRM	Analysis No	f ‰ amu ⁻¹ using $^{67}\text{Zn}, ^{68}\text{Zn}, ^{70}\text{Zn}$	± ‰ amu ⁻¹	f ‰ amu ⁻¹ using $^{66}\text{Zn}, ^{67}\text{Zn}, ^{70}\text{Zn}$	± ‰ amu ⁻¹
IMEP-19 (Rice)	1	-0.09	0.18	-0.04	0.17
	1.1	-0.16	0.21	-0.20	0.22
	1.2	-0.09	0.16	-0.09	0.16
	1.3	-0.09	0.16	-0.04	0.18
	1.4	-0.08	0.16	-0.07	0.16
	2	-0.02	0.15	-0.02	0.15
	Average	-0.088	0.070	-0.077	0.071
NIES-9 (Sargasso)	1	0.01	0.22	0.07	0.23
	1.1	0.16	0.18	0.18	0.19
	1.2	0.10	0.20	0.24	0.20
	1.3	0.08	0.16	0.08	0.16
	1.4	0.10	0.20	-0.04	0.20
	2	0.10	0.17	0.07	0.18
	2.1	0.17	0.18	0.14	0.19
	3	0.00	0.21	0.00	0.22
Average	0.090	0.068	0.092	0.070	
Murst-ISS -A2 (Antarctic Krill)	1	0.25	0.20	0.18	0.21
	2	0.15	0.18	0.19	0.19
	2.1	0.22	0.21	0.09	0.23
	Average	0.21	0.11	0.15	0.12

Table 5. 18: Proposed absolute isotopic composition of Zn for measured biological materials SRMs.

SRM		Ratio	±
IMEP-19 (Rice)	$^{66}\text{Zn}/^{64}\text{Zn}$	0.56387	0.00031
	$^{67}\text{Zn}/^{64}\text{Zn}$	0.082144	0.000039
	$^{68}\text{Zn}/^{64}\text{Zn}$	0.37506	0.00019
	$^{70}\text{Zn}/^{64}\text{Zn}$	0.012411	0.000024
NIES-9 (Sargasso)	$^{66}\text{Zn}/^{64}\text{Zn}$	0.56407	0.00031
	$^{67}\text{Zn}/^{64}\text{Zn}$	0.082188	0.000039
	$^{68}\text{Zn}/^{64}\text{Zn}$	0.37533	0.00019
	$^{70}\text{Zn}/^{64}\text{Zn}$	0.012425	0.000023
Murst-ISS-A2 (Antarctic Krill)	$^{66}\text{Zn}/^{64}\text{Zn}$	0.56420	0.00032
	$^{67}\text{Zn}/^{64}\text{Zn}$	0.082217	0.000045
	$^{68}\text{Zn}/^{64}\text{Zn}$	0.37550	0.00023
	$^{70}\text{Zn}/^{64}\text{Zn}$	0.012433	0.000025

5.5.4 Meteorites

A major limitation of meteorite isotopic analyses was the low concentrations of Zn, and the availability of sufficient amounts. The samples were grouped according to their type, stone and iron meteorites; as shown in Tables 5.19 and 5.20. As most of the meteorites measured in this work are rare, this emphasized the significance of the developed procedure (see Section 3.4) with all analyses having performed using no more than 1 µg Zn, and the level of contamination and blank was tightly controlled (see Section 3.2, 3.3). All isotopic ratios were measured using the more precise Faraday multi collectors. The absolute isotopic compositions of Zn in the measured meteorites were not determined because further investigations are required in terms of the homogeneity of Zn in the meteorites and if the isotopic composition of Zn in the meteorite is due to the contribution of the inclusions or the bulk sample, (see Section 7.4).

5.5.4.1 Stone meteorites

Table 5. 19: Measured Zn fractionation in stone meteorites relative to the laboratory standard (δ zero). Two fractionation values are shown reflecting the use of different sets of isotopic ratios. All relative to ^{64}Zn .

Meteorite	Analysis No	f ‰ amu ⁻¹ using ^{67}Zn , ^{68}Zn , ^{70}Zn	± ‰ amu ⁻¹	f ‰ amu ⁻¹ using ^{66}Zn , ^{67}Zn , ^{70}Zn	± ‰ amu ⁻¹
Allende	1	0.33	0.23	0.21	0.25
	1.1	0.44	0.22	0.28	0.23
	Average	0.38	0.16	0.24	0.17
Orgueil	1	0.25	0.23	0.19	0.24
	1.1	0.35	0.20	0.35	0.20
	Average	0.30	0.15	0.27	0.16
Brown field _1937	1	-0.11	0.16	-0.05	0.17
	1.1	-0.13	0.17	-0.13	0.18
	1.2	-0.23	0.16	-0.17	0.18
	Average	-0.157	0.094	-0.12	0.10
Brown field _1964	1	-0.22	0.17	-0.19	0.17
	1.1	-0.32	0.17	-0.37	0.18
	1.2	-0.32	0.17	-0.27	0.18
	Average	-0.287	0.098	-0.28	0.10
Plainview	1	0.37	0.18	0.36	0.18
	1.1	0.21	0.18	0.30	0.18
	1.2	0.35	0.17	0.35	0.18
	Average	0.31	0.10	0.34	0.10

5.5.4.2 Iron meteorites

Table 5. 20: Measured Zn fractionation in Canyon Diablo iron meteorite relative to the laboratory standard (δ zero). Two fractionation values are shown reflecting the use of different sets of isotopic ratios, both relative to ^{64}Zn .

Meteorite	Analysis No	f ‰ amu ⁻¹ using $^{67}\text{Zn}, ^{68}\text{Zn}, ^{70}\text{Zn}$	± ‰ amu ⁻¹	f ‰ amu ⁻¹ using $^{66}\text{Zn}, ^{67}\text{Zn}, ^{70}\text{Zn}$	± ‰ amu ⁻¹
Canyon Diablo	1	1.08	0.20	1.19	0.20
	2	1.13	0.19	1.17	0.20
	2.1	1.13	0.16	1.18	0.17
	Average	1.11	0.11	1.18	0.11

In another independent experiment, the isotopic composition of Zn in Canyon Diablo meteorite was measured without double spiking the samples. This is represented in Figure 5.9, which shows the isotopic fractionation of Zn in the sample is linear hence represents no sign of any anomaly or interference at any of the Zn isotopes.

Figure 5. 9: The deviation of the isotopic composition of Zn in Canyon Diablo meteorite relative to the laboratory standard.

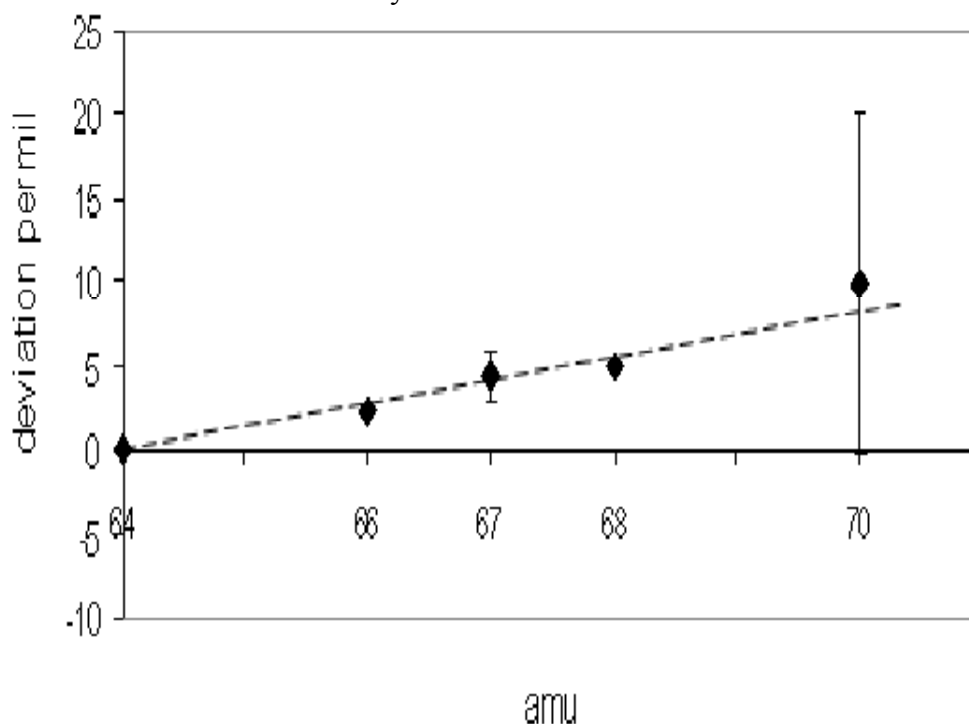


Figure 5.9 also shows a deviation (slope) of $+1.6 \pm 0.2 \text{ ‰ amu}^{-1}$ relative to the laboratory standard, this is greater than what was measured ($+ 1.11 \pm 0.11$) for this meteorite by double spiking the sample. The higher first value ($+1.6 \text{ ‰ amu}^{-1}$) most likely from the machine bias and other factors, and illustrates the necessity of the double spike technique. On the other hand, this significant deviation relative to the laboratory standard is an indication for the presence of a virtual natural isotopic fractionation of Zn in this meteorite. A discussion regarding the isotopic fractionation of Zn in this meteorite is detailed in Section 7.4.2

5.5.4.2.1 Redfields

During the double spike analysis of the Redfield meteorite, it was evident that using two set of isotopic ratios, the fractionation values obtained did not agree. Upon further investigation; it was clear that Redfields contain isotopically anomalous Zn. Thus, the double spike fractionation determination could not be used, and further investigation was required, Table 5.21 thus contains the raw isotopic ratios uncorrected for instrument bias.

Table 5. 21: The isotopic composition of Zn in the Redfields meteorite (uncorrected for instrument bias).

		Ratio	± 95%
Experiment 1	66/64	0.561012	0.000068
	67/64	0.081125	0.000037
	68/64	0.37319	0.00016
	70/64	0.012059	0.000029
Experiment 2	66/64	0.55975	0.00010
	67/64	0.080851	0.000058
	68/64	0.37223	0.00018
	70/64	0.012074	0.000062
Experiment 3	66/64	0.56094	0.00067
	67/64	0.08081	0.00087
	68/64	0.37166	0.00092
	70/64	0.01212	0.00067
Average ^Δ	66/64	0.56057	0.00023
	67/64	0.08093	0.00029
	68/64	0.37236	0.00032
	70/64	0.01209	0.00022

5.5.5 Effect of ion exchange chemistry on Zn fractionation

To assess the effect of ion exchange chemistry on fractionation, laboratory standard was loaded on to (0.7 ml of AG1-X8 anion exchange resin 200-400 mesh size) anion exchange column before being double spiked (see Section 3.10.1). The standard was eluted from the column and double spiked, and analysed in the mass spectrometer. Similar aliquots were taken to, two, or three, or four times through anion exchange chemistry before being double spiked, and measured for Zn fractionation. The results of these experiments are shown in Table 5.22. Although the effect is small there appears to be strong evidence that the anion exchange chemistry fractionates Zn. This important finding is further discussed in Section 7.1.

^Δ The uncertainty in the average was estimated as the 95% confidence using Monte Carlo approach.

Table 5. 22: contribution of the anion exchange column chemistry to the measured fractionation relative to the laboratory standard (δ zero).

Number of anion exchange columns	f ‰ amu ⁻¹	± ‰ amu ⁻¹
0 ^u	0.006	0.039
1	0.19	0.21
2	0.25	0.18
3	0.28	0.19
4	0.29	0.19

5.5.6 Water

The fractionation of Zn in a range of water samples was determined. River water samples were collected from two locations in the Swan River in Western Australia, and water samples collected from the domestic water supply. The initial aim of these collections was to measure the concentration of Zn in these water samples using IDMS. However, as the samples were double spiked, the fractionation could also be determined. Unfortunately, the isotopic ratio measurements in these samples were performed using the Daly, which has a poorer measurement precision relative to Faraday multi collector, and resulted in a final significantly larger measured fractionation uncertainty compared to other results. Never the less, the results suggest further investigation is warranted.

The fractionation of Zn was measured in domestic water, taken from a tap in the Department of Applied Physics at Curtin University of Technology in Western Australia. Up to 17 g of river water was required for the measurements; because of the low abundance $\sim 7 \text{ ngg}^{-1}$ of Zn in the samples of river water, and unrestrained (fresh) tap water (see Section 4.6). The isotopic composition of the double spiked sample was measured using the less precise Daly detector and are as shown in Table 5.23 and discussed in Section 7.5.

^u The result of the measured fractionation of the mixture (laboratory standard and double spike) relative to the laboratory standard obtained as long term reproducibility of the fractionation (see Section 5.4).

Table 5. 23: Fractionation of Zn isotopic composition in Swan river water relative to the laboratory standard (δ zero). Two fractionation values are shown reflecting the use of different sets of isotopic ratios, all relative to ^{64}Zn .

Source	Experiment No	f ‰ amu ⁻¹ Using ^{67}Zn , ^{68}Zn , ^{70}Zn	± ‰ amu ⁻¹	f ‰ amu ⁻¹ Using ^{66}Zn , ^{67}Zn , ^{70}Zn	± ‰ amu ⁻¹
Swan river - Victoria Park	1	-1.37	0.87	-1.8	0.82
Swan river- Bayswater	1	-0.81	1.09	-0.74	1.09
	Average	-1.09	0.7	-1.27	0.68
Restrained tap water	1	-6.39	0.62	-7.22	0.64
Unrestrained (fresh) tap water	1	0.87	4.86	-1.19	5.49
	3	0.24	1.47	-0.28	1.84
	Average	0.56	2.60	-0.7	2.904

The large fractionation uncertainties obtained reflects the very low concentration of Zn, and hence, use of the Daly detector. To use the Faraday multicollector, at least ten times more sample is needed, which requires the development of special sample handling facilities, which unfortunately could not be developed due to the lack of time.

5.5.7 Zinc fractionation in other materials

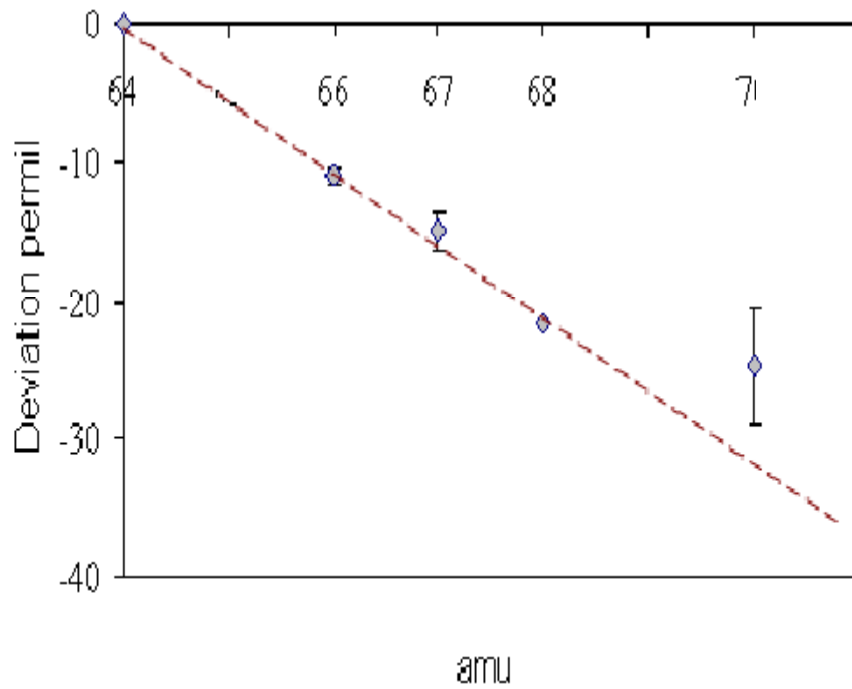
Although not natural materials, the fractionation of Zn in Nutrient Zinc Tablet, and Zinc plated steel sheet sample was measured as preliminary investigations. All isotope ratios were measured using the Daly detector, since familiarity with this detector was being explored. The concentration results are provided in Section 4.7. Table 5.24 shows the measured Zn fractionation in these materials which are further discussed in Section 7.7.

Table 5. 24: Fractionation Zn isotopic composition in nutrient Zinc Tablet relative to the laboratory standard (δ zero). Two fractionation values are shown reflecting the use of different sets of isotopic ratios, all relative to ^{64}Zn .

Material	Experiment No	f ‰ amu ⁻¹ Using ^{67}Zn , ^{68}Zn , ^{70}Zn	± ‰ amu ⁻¹	f ‰ amu ⁻¹ Using ^{66}Zn , ^{67}Zn , ^{70}Zn	± ‰ amu ⁻¹
Nutrient Zinc Tablet	1	-2.14	0.48	-2.99	0.54
Zinc plated steel sheet	1	-1.28	1.60	-1.30	1.68
	2	-1.88	1.21	-1.88	1.21
	Average	-1.6	1.0	-1.6	1.0

In a totally different experiment, the isotopic composition of Zn in the Zinc nutritional Tablet was measured without double spiking. This is represented in Figure 5.10 which shows the isotopic fractionation of Zn in the sample is linear and represents no sign of any anomaly or interference at any of the Zn isotopes. Moreover, the graph shows a deviation (slope) of -4.24 ‰ amu⁻¹ relative to the laboratory standard, this is twice what was measured (-2.1 ± 0.5) for this material by double spiking the sample. The disagreement between these values ($+1.6$ ‰ amu⁻¹) may come from the machine bias and other factors and demonstrates that unspiked samples should not be used for measuring Zn isotopic fractionation.

Figure 5. 10: The deviation of the isotopic composition of Zn in the Zinc nutrient Tablet relative to the laboratory standard



On the other hand, this significant deviation relative to the laboratory standard is an indication for the presence of some isotopic fractionation of Zn in this material.

- **Chapter 6: The elemental abundance of Zn: Discussion**

6.1 Introduction

In this Chapter the elemental abundances of Zn in a range of natural materials is discussed and comparisons made with previous measurements. As discussed previously, most of the samples analysed in this project were standard reference materials “SRMs”.

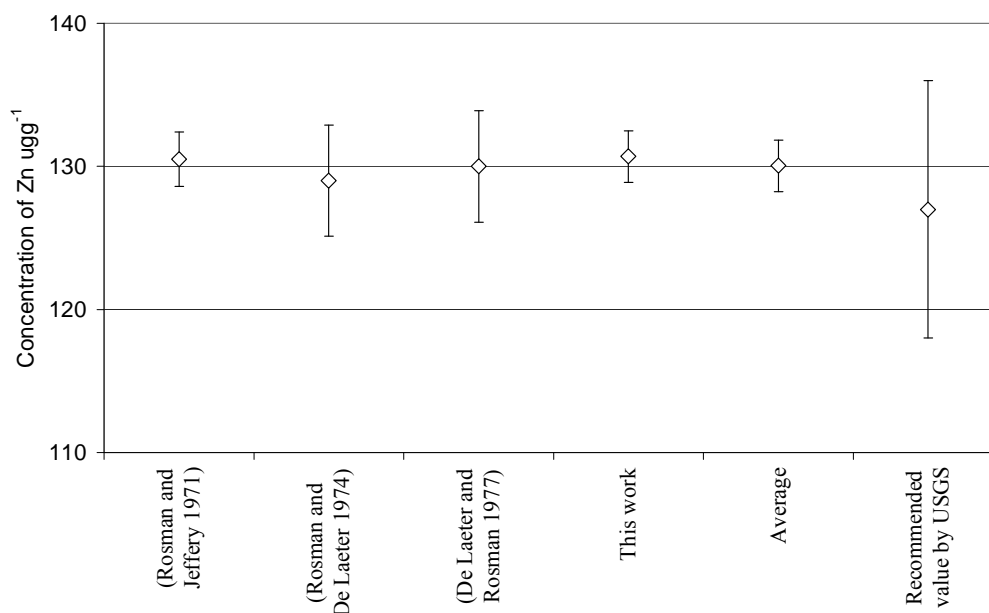
The abundance measurements were performed using IDMS (see Section 3.7.1), with the individual results detailed in Chapter 4. The final uncertainty on the average value for the concentration of each SRMs was determined using ISO GUM using the t-distribution to estimate the 95% confidence interval, and utilizing the appropriate degree of freedom for each sample. Except for meteorites, the final uncertainties consistently cover the ranges of individual concentration measurements and indicate that samples are homogeneous, including those samples from different bottles. The final fractional uncertainties obtained for the SRMs were all less than 2.8%, demonstrating the high level of precision possible using IDMS. Since the recommended values for SRMs are generally statistically compiled from a wide range of analysts and analytical techniques over many years, they have a limited physical meaning, it is not unexpected that these will have a wider range of uncertainties compared to any single analyst/analytical technique, limiting the value of these types of recommended values of SRMs to verify high accuracy analytical results. The uncertainties obtained in this work are all considerably smaller than those for certified SRMs or recommended values based on compiled results. Unfortunately a detailed comparison of the results obtained in this work with reported values is not possible since a number of reported values do not provide uncertainties and full details regarding the type of uncertainties accompanying each individually reported result are not always available.

Because BCR-1, NIES No 9 and IMEP-19 are the only samples to have been measured previously by IDMS, a direct comparison is possible for these samples with previous measurements. All measurements in this work agree with the previous IDMS

measurements but with smaller relative uncertainties. For the remaining SRMs, (Diabase W-2, Basalt BIR-1, Quartz Latite QLO-1, Mica Schist SDC-1, Shale SGR-1, Shale-Cody SCo-1, Dolerite DNC-1, Marine sediments Hiss-1, Clay Till-3, Antarctic sediments Murst-ISS-A1, Antarctic Krill Murst-ISS-A2), this work is the first reported Zn concentration measurements for these samples using IDMS, except for HISS-1 for which IDMS was performed using ICP-MS. Only an approximate value for the concentration of Zn in TILL-3 was provided by the National Resources Canada as a certified value for the element is not yet available (National Resources Canada, 2007).

A comparison with previously measured Zn abundances in BCR-1 using the IDMS technique is represented in Figure 6.1. All previously reported IDMS measurements show agreement with each other with an average of $129 \pm 1 \mu\text{g g}^{-1}$, where the uncertainty covers all reported IDMS values.

Figure 6. 1: The concentration of Zn in BCR-1 using IDMS (recommended value is compiled from a wide range of analysts and analytical techniques (USGS, 2006b). Uncertainties shown are at the 95% confidence interval.



The techniques developed in this work have enabled a major improvement over previous IDMS measurements with a reduction of between two and three times of the final concentration uncertainty, while also using ~10 times less sample than previously reported.

A comparison of the different IDMS techniques and results obtained for Zn concentration in BCR-1 is shown in Table 6.1.

Table 6. 1: A comparison between the new techniques used to measure the concentration of Zn in BCR-1 by IDMS with previous work. Uncertainties shown are at the 95% confidence interval.

	This work	Rosman & Jeffrey (1971)	Rosman & De Laeter(1974)	De Laeter and Rosman (1977)
Results $\mu\text{g g}^{-1}$	130.7 ± 1.8	130.5 ± 1.9	$129 \pm 3\%$ 128.3 ± 3.5	130 ± 3.9
Mass of samples (g)	<0.03g	3	3	0.51
Blank	$8 \pm 5\text{ng}$	1.2-1.7 μg	1.2-1.7 μg	3% of mass of Zn in sample

The size of sample analysed will become increasingly important as sub-components of systems will need to be analysed when assessing Zn isotope fractionation. Hence analysts will increasingly need to perform accurate and precise measurements of smaller samples. For example Zn analysis on Polar Ice and the application of mass spectrometry for studying the Human Immunodeficiency Virus Protein Complexes (Zn finger) (Chan et al., 2007, Joseph A. Loo, 1998), add to that the investigation of molecular interaction within biological macromolecular complexes by Mass Spectrometry (Satoko, 2006).

To improve the precision of the measured concentration of Zn requires that the sample –spike amount ratio be optimised. Despite not doing so in a systematic manner, these results represent the most accurate and precise concentrations measured for Zn in these samples, and are a major outcome of this work. At the same time it might be worth mentioning that these concentrations relate only to the individual SRMs, and may not represent the concentration of Zn in the similar materials.

6.2 Concentration of Zn in geological materials

The concentration of Zn in geological materials measured in this research is shown in Tables 4.1 to 4.12. Zinc in Basaltic materials depends on factors such as the composition of the source materials, the degree and mechanism of melting and melt extraction, the subsequent degree of magmatic fractionation by crystallization, and finally the possible contamination of the magma during this fractionation processes by a process called AFC (Assimilation with Fractional Crystallization) (Hofmann, 2003). The range of Zn concentration found in igneous rocks in this work (67.3 ± 1.1 to $130.7 \pm 1.8 \mu\text{g g}^{-1}$), is most likely explained by different mantle sources (Allegre et al., 1995). It is interesting to compare this range with the range of the concentration of Zn in lunar soil samples measured recently by Moynier et al. (2006) and found to vary from 6 to $140 \mu\text{g g}^{-1}$ (Moynier et al., 2006). Icelandic Basalt BIR-1, Diabase W-2, and Dolerite DNC-1 represent igneous rock SRMs that have not been measured previously using IDMS. The only previous IDMS measurements on geological materials were those of BCR-1 discussed in the previous Section.

A typical error budget for IDMS is represented in Figure 3.23 in Section 3.7.1. The main contribution (30%) to an individual concentration uncertainty for samples measured using the Daly detector; is from the uncertainty in the isotopic composition of the laboratory standard, followed by the uncertainty in the mass of the sample (27%). Most of the IDMS analyses were measured using a less than optimum spiking to sample ratio, $^{68}\text{Zn sample}/^{67}\text{Zn spike} < 1$, because of the need to conserve the double spike solution. Generally this was not a significant problem, apart from those

samples with high abundances being analysed using the Faraday multi collector, which required more sample and therefore more spike. This clearly demonstrated by the larger uncertainties obtained for analyses 5.0 to 5.2 in Table 4.1 (Section 4.3.1), which have twice the uncertainty of the other results. The uncertainty obtained for BCR-1 is similar to that obtained by Rosman and Jeffery (1971) primarily due to this effect. A significant improvement in this research is the reduced amount of sample required for IDMS, for example Rosman and Jeffery (1971) used 0.51 g of BCR-1 sample for their IDMS analysis. In contrast only 1/8 (0.06g) of this amount was required to perform a reliable measurement (see Table 6.1).

In contrast to igneous rocks, the concentration of Zn in sedimentary rocks varies widely, from $3.867 \pm 0.058 \mu\text{g g}^{-1}$ to $101.4 \pm 2.0 \mu\text{g g}^{-1}$, for HISS-1 and SCo-1 respectively (see Section 4.3.2) which is consistent with the reported average abundance of Zn in such rock types, (Heinrichs et al., 1980). No other IDMS measurements are available for any of the measured sedimentary SRMs measured in this work. In the same manner as igneous rocks, the main contributor to the uncertainty is due to the sample spiking ratio although the estimated final uncertainty is still less than 2.6 % for the Murst-Iss-A1. Of the two remaining rocks analysed (metamorphic), as represented in Section 4.3.3, the concentration of Zn was $61 \pm 3 \mu\text{g g}^{-1}$ for QLO-1, and $101.5 \pm 1.7 \mu\text{g g}^{-1}$ for SDC-1. In terms of the uncertainty accompanying these measurements, the sample spiking ratio is once again the greatest contributor to the uncertainty of the measurements, although the maximum uncertainty obtained is that for CaCO_3 (not a SRM) represents less than 5% of the measured concentration. All these uncertainties can be improved by optimizing the sample spike ratio.

6.3 Concentration of Zn in biological materials

As represented in Section 4.4, the concentration of Zn in three biological materials was measured using IDMS. From the plant kingdom, the concentration of Zn in Rice and Sargasso Seaweed was found to be 22.15 ± 0.42 , $14.62 \pm 0.27 \mu\text{gg}^{-1}$ respectively. The maximum uncertainty of the average of these values is less than 2.8% of the average value, calculated using the “t” distribution using GUM. The abundance of Zn available in these type of materials is classified by the World Health Organisation (WHO) as being in the “moderate Zn nutrient” category (WHO, 2004). According to a study by Mestek et al. (2001) these plants can be considered of normal Zn concentration (Mestek et al., 2001). The concentration of Zn in Rice “IMEP-19” was found to be $22.15 \pm 0.42 \mu\text{gg}^{-1}$, the recommended value by the IRMM for the IMEP-19 is $22.99 \pm 0.44 \mu\text{gg}^{-1}$, also measured using the IDMS as a Primary method measurement (IRMM, 2007). Both results agree well within uncertainty of each other. The closest other comparison available is Zn in Rice “NIST-SRM 1568a”, as measured by at $19.4 \pm 1.3 \mu\text{gg}^{-1}$ and $19.6 \pm 1.6 \mu\text{gg}^{-1}$ (Mestek et al., 2001).

The normal levels of Zn in most crops and pastures is in the range $10\text{--}100 \mu\text{gg}^{-1}$ (WHO, 2004). According to (WHO, 2004), some plants are Zn accumulators, but the extent of the accumulation in plant tissues varies with soil and plant properties. This raises the issue of undertaking systematic and detailed trace metal studies of elements such as Zn in plants as a function of many factors and is one of the recommendations of this research.

Krill is important species in the oceanic bio cycle; for example, Antarctic krill “*Euphausia Superba* Dana” has a heterogeneous circumpolar distribution in the Southern Ocean and has a close association with sea ice. Where the circumpolar oceanic circulation and interaction with sea ice is important in determining the large-scale distribution of krill and its associated variability (Thorpe et al., 2007).

The concentration of Zn in MURST-Iss-A2 “Krill” SRM is $63.5 \pm 1.8 \mu\text{gg}^{-1}$. This SRM has also been analyzed using inductively coupled plasma atomic emission

spectrometry (ICP-AES), and graphite furnace atomic absorption spectrometry (GF-AAS) methods by Gasparics et al. (2000) yielding a concentration of $69.5 \pm 2.3 \mu\text{g g}^{-1}$ (Gasparics et al., 2000). The 8% difference can be attributed to a number of factors; neither ICP-AES nor GF-AAS are primary methods, inadequate correction for Zn contamination, or genuine variability between aliquots of this SRM. MURST-Iss-A2 “Krill” standard material has also not been measured previously using the IDMS, so a direct comparison can’t be made.

According to WHO (2001), concentrations of Zn in plants and animals are higher near anthropogenic point sources of Zn contamination. This suggests Zn abundance studies in animals are worthy of consideration. Moreover, interspecies variations in Zn abundances are considerable; and vary for instance, with life stage, sex, season, diet and age (WHO, 2001).

6.4 Concentration of Zn in meteorites

Most of the meteorites measured in this work are rare and scientifically valuable. This highlighted the significance of the approach developed to perform measurements using small sample (size of sample loaded on the filament). A sample as small as 19 ng Zn was measured in this work (see Table 4.15 in Section 4.5.2), and $1 \mu\text{g}$ was the maximum size of sample used to measure the fractionation using the double spike technique. The double spike technique also allows the elemental abundance to be measured using IDMS during the same analyses. It is important to emphasize that, although the procedure blank has been reduced compared to previous work, the variability in the blank (see Section 3.3) remains the limiting factor in analysing these samples. Despite the fact that the inhomogeneity of Zn in meteorites is well documented, it could be possible that previous measurements have been affected by contamination. A comparison between this work and that of other researchers obtains for stone and iron meteorites are shown in Tables 6.2, and 6.3, respectively.

The abundance of Zn in meteorites and its relationship with the abundances of other elements is important in understanding the formation of the solar nebula. (Larimer and Anders, 1967, Larimer, 1967, Larimer and Anders, 1970, Larimer, 1973). In these

references it is argued that the abundance of elements in meteorites depend mainly on the physiochemical conditions of the condensing solar nebula.

The elemental abundance of Zn was measured in seven iron and five stony meteorites samples, described in Section 3.8.1. The abundance results for stony meteorites presented in Section 4.5.1 (Table 4.14). For the iron meteorites, the results are represented in Section 4.5.2 in Table from 4.15. All the uncertainties are 95% confidence interval uncertainties as determined using the “t” distribution in GUM ISO statistical methods.

6.4.1 Stone meteorites

The concentration of Zn in five Stone meteorites ranged from 26 ± 13 to 302 ± 14 $\mu\text{g g}^{-1}$ for Plainview and Orgueil respectively. For ordinary Chondrites; the maximum and minimum value for the concentration of Zn in the three samples are, (range of) 20.1 to 32.7 $\mu\text{g g}^{-1}$, and (range of) 46 to 80 $\mu\text{g g}^{-1}$ for Plainview and Brownfield 1937 respectively. In the case of Carbonaceous Chondrites, Zn was found to be present at 76 ± 2.3 , and 302 ± 14 $\mu\text{g g}^{-1}$ for Allende (CV3) and Orgueil (CI1), respectively.

Due to the rarity of samples, Zn concentrations in the Allende and Orgueil meteorites was measured three and two times respectively from one digestion of each meteorite. On the other hand, the other stone meteorites were measured from replicate sample digestions, which is why the values are shown as a range. The most likely explanation for this range values is the inhomogeneity of Zn in these meteorites, which is also consistent with the inhomogeneous structure of these meteorite types.

Table 6. 2: Comparison between the Zn isotope dilution measurements obtained in this work for stony meteorites, and those of other researchers.

Meteorite	Meteorite Type	Zn concentration μgg^{-1} (this work)	Zn concentration μgg^{-1} (previous work)	Size of sample used by the previous researcher	Size of blank in the previous work
Allende	CV3	75.7 ± 2.3	111^{Γ} (99, 144) $^{\delta}$	Dissolved 0.20g^{Γ} $0.5 - 1\mu\text{g}$ $^{\delta}$ (ICPMS)	$0.2 \pm 0.1\mu\text{g}^{\Gamma}$ $10-20 \text{ng}^{\delta}$
Orgueil	CI1	302 ± 14	(261, 340) $^{\delta}$	$0.5 - 1\mu\text{g}$ (ICPMS) $^{\delta}$	$10-20 \text{ng}^{\delta}$
Brownfield 1964	H5	33.6 to 35.9			
Brownfield 1937	H3	46 to 60	45^{Γ} $42.2 \pm 0.6^{\nabla}$ 47.7^{δ}	Dissolved 0.57g^{Γ} $<10 \mu\text{g}^{\nabla}$ $0.5 - 1\mu\text{g}$ $^{\delta}$ (ICPMS)	$0.2 \pm 0.1\mu\text{g}^{\Gamma}$ $10-20 \text{ng}^{\delta}$
Plainview	H5	20.1 to 32.7	32^{Γ} 38^{∇} 32.1 to 45.2	Dissolved 0.63g^{Γ} $<10 \mu\text{g}^{\nabla}$	$0.2 \pm 0.1\mu\text{g}^{\Gamma}$

*Uncertainty shown in Table 6.1 is the 95% confidence for the measured concentrations. $^{\Gamma}$ (Rosman and De Laeter (1974)). $^{\delta}$ in (Luck et al., 2005b). $^{\nabla}$ (Rosman 1972).

For the two Brownfield meteorites and Plainview, the uncertainty in the Zn concentration was estimated from the range. As shown in Table 6.2, The Orgueil meteorite has the highest Zn abundance of all the measured samples. The concentration of Zn in Orgueil CI Chondrite measured in this work ($302 \pm 14 \mu\text{gg}^{-1}$) agrees with the recommended concentration of Zn in Orgueil and the average Zn concentration in CI Chondrites by Anders and Grevesse (1989) ($311 \mu\text{gg}^{-1}$), (312

μgg^{-1}) respectively, and with the recommended Zn concentration in Orgueil compiled by Lodders (2003) ($318 \pm 26 \mu\text{gg}^{-1}$). These recommended values are based on elemental abundances in CI Chondrites surveyed from the literature and the mean concentration (by mass) for each meteorite were computed from all reliable analytical data. The importance of the Zn abundance in Orgueil comes from the fact that CI Chondrites are the most primitive Chondrites in the sense that they are not chemically fractionated when relative abundances are compared to the photosphere (Lodders, 2003). The Zn elemental abundance in CI Chondrites is the representative of the abundance of Zn in the Solar System. Hence the concentration of Zn for Orgueil meteorite used by Anders and Grevesse (1989), Lodders (2003) of 311 and $318 \pm 26 \mu\text{gg}^{-1}$ respectively, was used to calculate the atomic abundance of Zn in the Solar System yielded a recommended Zn atomic abundance of $N(\text{Zn}) = 1226$ relative to 10^6 Si . As shown in Table 6.1, the concentration of Zn in Orgueil measured in this work is $302 \pm 14 \mu\text{gg}^{-1}$ agrees with that recommended by Lodders (2003) to calculate the Atomic abundance of Zn in the Solar System.

Zinc concentrations in Brownfield 1964 do not appear to have been measured previously and the value obtained in this work appears is outside the range obtained for Brownfield 1937 also measured in this work. The ratio of Zn abundance in Orgueil to that in Brownfield 1937 as measured in this research is ~ 5.7 , on the other hand, such a ratio was measured by Rosman and De Laeter (1974) for Cd and found ~ 5.1 (Rosman and De Laeter, 1974), presuming that, the Brownfield meteorite measured by Rosman and De Laeter (1974) is the Brownfield 1937.

The lower concentration of Zn in Brownfield 1964 (ordinary Chondrite) compared to Carbonaceous Chondrites is consistent with that found for Cd by Rosman and De Laeter (1974). Despite the inhomogeneity in the concentration of Zn in these meteorites is tangible, it is worth mentioning that the average concentration of Zn in three ordinary H Chondrites measured in this research is $51 \mu\text{gg}^{-1}$ is more than the $36 \mu\text{gg}^{-1}$ determined by Rosman and De Laeter (1974). It is interesting to note that, according to the results of this work, stony meteorites show wider range of Zn

abundance, ranging from 26.4 to 302 μgg^{-1} , compared to 0.0192 to 23.88 μgg^{-1} for iron meteorites. It has been suggested by Wombacher et al. (2003) that the depletion of Zn, “moderately volatile element”, is uniform in ordinary Chondrites (Wombacher et al., 2003). Although supported by the results of this work such a conclusion can't be confirmed given the limited number of samples analysed.

6.4.2 Iron meteorites

The concentration of Zn in a number of iron meteorites compared to previous work is shown in Table 6.3, (summary and comparative Table with that of previous researchers).

The range of concentration of Zn in iron meteorites was found to be in the range of 0.0192 ± 0.0075 to (13 to 26) μgg^{-1} for Warburton and Odessa respectively, and are within the range found by Rosman for iron meteorites (Rosman, 1972b). As shown in Table 6.3, there is poor agreement with previous results, for example a significant difference in the concentration of Zn exists for Mundrabilla, while the results for Odessa represents the best agreement. This supports the conclusion of previous researchers that the concentration of Zn in iron meteorites is inhomogeneous (Rosman and De Laeter, 1974). The significance of the blank and the size of the samples in regard to these measurements were discussed previously.

Table 6. 3: Comparison between the Zn isotope dilution measurements obtained in this work and for iron meteorites and those of other researchers. (The uncertainty shown for this work is the external precision, 95% confidence, for the number of analyses obtained from one samples digestion, except for Odessa which was analyzed a number of times from different dissolutions.)

Meteorite	Zn concentration $\mu\text{g g}^{-1}$ (this research)	Zn concentration $\mu\text{g g}^{-1}$ (Previous work)	Size of dissolved sample used by the previous researcher	Size of blank in the previous work
Canyon Diablo	24 ± 0.5	49^{∇} 76.1^{Γ}	3.2g^{Γ}	$0.2 \pm 0.1\mu\text{g}^{\Gamma}$
Mundrabilla	0.076 ± 0.017	17.5^{Γ} $15.5^{\nabla}, 19.5^{\nabla}$	3.8g^{Γ} $<1.5\text{g}^{\nabla}$	$0.2 \pm 0.1\mu\text{g}^{\Gamma}$
Redfields	7.2 ± 0.4	$0.94 \pm 0.02^{\nabla}$ 9.89^{Γ}	$<12\text{g}$ 3.06g^{Γ}	$0.2 \pm 0.1\mu\text{g}^{\Gamma}$
Warburton	0.019 ± 0.008	$0.026 \text{ to } 0.90^{\nabla}3$ 0.35^{Γ}	$<24\text{g}^{\nabla}$ 10.07^{Γ}g	$0.2 \pm 0.1\mu\text{g}^{\Gamma}$
Kumerina	0.380 ± 0.014	0.22^{Γ} $0.036 \pm 0.005^{\nabla}$	10.36g^{Γ} $<37\text{g}^{\nabla}$	$0.2 \pm 0.1\mu\text{g}^{\Gamma}$
Odessa	13-26	29^{Γ} 30.9^{∇}	4.87g^{Γ} $<1.4, 1.9, 2.4$ g^{∇}	$0.2 \pm 0.1\mu\text{g}^{\Gamma}$
Youanmi	0.95 ± 0.04			

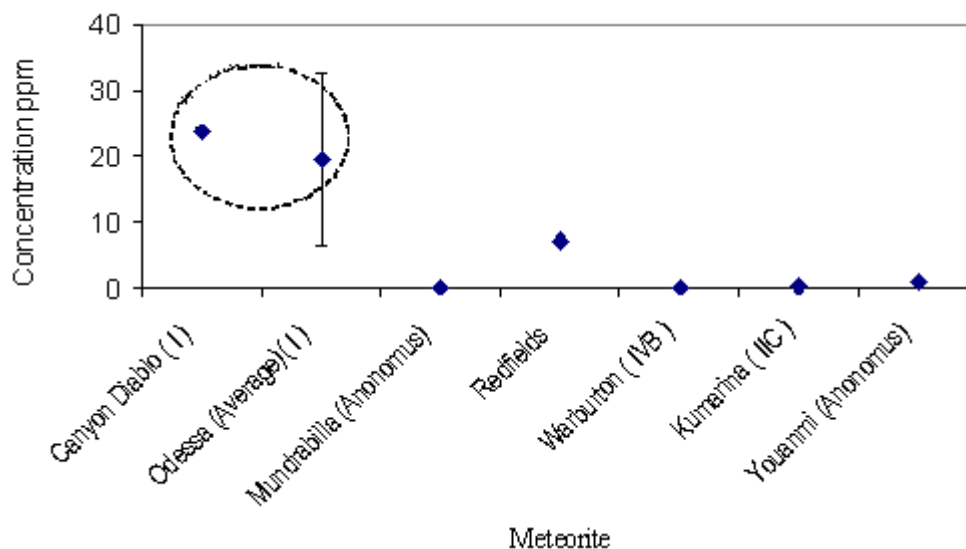
Γ (Rosman and De Laeter (1974)). ∇ (Rosman 1972).

The relationship between Zn and Cd in stone meteorites was not the aim of this research, but the narrow range of Zn concentrations found supports the conclusion of Rosman and De Laeter (1974) (Rosman and De Laeter, 1974) that the H Chondrites

possess a relatively small range of Zn values compared to the corresponding Cd values. The strikingly different abundance pattern between these two elements in iron meteorites is in contrast to their abundance range in ordinary Chondrites (Rosman and De Laeter, 1974)

A significant difference between this and previous work on Zn in meteorites is the smaller sample size used for the analysis (0.09 to 2.09 g). Given that the smaller the sample used, the more likelihood of striking or missing small Zn rich components or inclusions, which can produce a wider range of abundances than previously observed. For example, Rosman and De Laeter (1974) measured Warburton and Canyon Diablo using sample sizes of 10.07 and 3.2 g respectively and obtained results of between 0.02 and $1.9\mu\text{gg}^{-1}$ for Warburton using different sample sizes (Rosman, 1972b, Rosman and De Laeter, 1974). Whereas, this work obtained a result of $19.2 \pm 7.5\text{ ngg}^{-1}$ for the same meteorite, but from only one dissolution. This may also explain the significant differences between the results obtained for Mundrabilla and Odessa compared to previous work. This is a significant development of this work, where smaller samples can now be analysed. The smallest sample dissolution in this work is that of Orgueil 14.2 mg, while the smallest amount used to perform a measurement in this research is Warburton where 1.097 g was digested representing $\sim 19\text{ng}$ of Zn. At this level, the correction for the procedural blank is critical, which is reflected in the large uncertainty for the concentration of this sample. To measure any samples with such low Zn concentrations will require a significant reduction in the procedural blank or sample sizes will need to be increased. However, increasing the sample size is not always appropriate. Hence, concentrations of Zn similar to that in Warburton can be considered as the concentration detection limit for these types of analyses. All iron meteorites measured in this research are from different chemical groups, except for Canyon Diablo and Odessa, which are both from chemical group I. Although the number of sample analysed is small, the concentration of Zn for these meteorites as a function of chemical grouping, see Figure 6.2, supports the conclusion of Rosman and De Laeter (1974) that the abundance pattern of Zn in iron meteorites is different between the chemical groups (Rosman and De Laeter, 1974).

Figure 6. 2: Concentration of Zn in iron meteorites. (The large error bars for Odessa represents the range)



Apart from Canyon Diablo and Redfields, the low concentration of Zn in these meteorites limited the number of fractionation measurements that could be made. Since Canyon Diablo clearly shows Zn fractionation (see Section 5.4.2), and Redfields appears isotopically anomalous, the study of Zn isotopes in iron meteorites clearly needs a further investigation. To achieve this, further work is required to reduce the blank relative to amount of sample. This could open up a number of possibilities with respect to understanding the formation of iron meteorites, and the relationship between stone and iron meteorites in the same manner as previous investigations using oxygen, by Clayton and Mayeda in 1978 (Clayton and Mayeda, 1978).

6.5 Concentration of Zn in water and other materials

The abundance of Zn in water samples was measured using IDMS, demonstrating that this research is applicable to ngg^{-1} Zn concentration materials. The results for which are shown in Section 4.6, and shown in Table 4.16. The accompanying external uncertainty shown is the 95% confidence interval. The average concentration of Zn in two different locations of Swan River waters was found in to $6.9 \pm 0.8 \text{ ngg}^{-1}$. In contrast to these, the natural Zn back ground is nominally $\sim 3 \text{ nmol kg}^{-1}$ ($\sim 0.2 \text{ ngg}^{-1}$), for example, the concentration of dissolved Zn in relatively undisturbed rivers of the

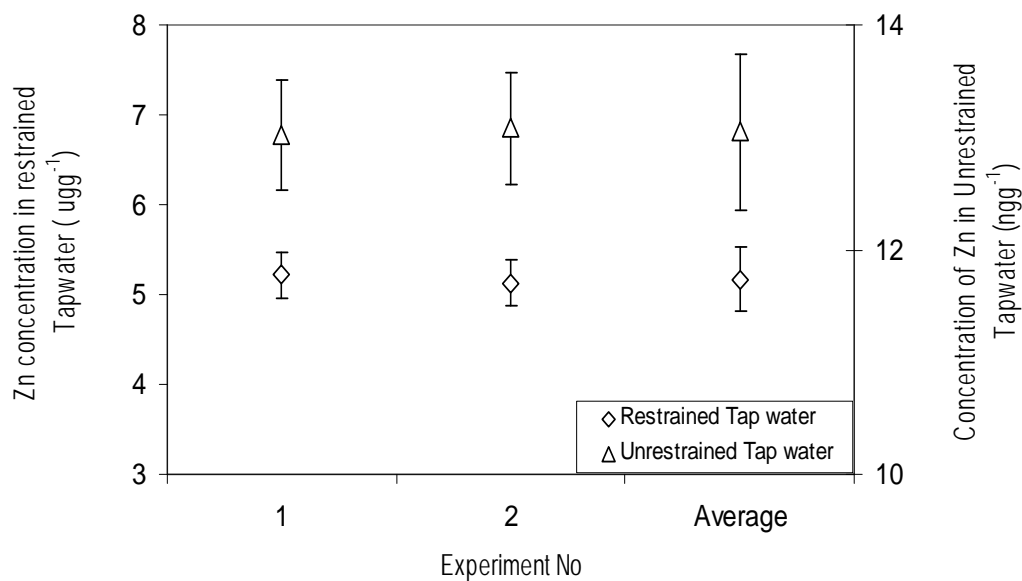
Ohio valley was around $0.06\text{--}0.6\text{ ngg}^{-1}$ (Shiller & Boyle, 1985). This 12 times greater amount might be due to the fact that the Swan River takes its water from intensive farming catchment, and passes through the middle of a major city, and this predicts the increase of Zn concentration in the river. Despite this, the measured concentration of Zn was far less than the normal maximum permissible level for drinking water (3mg/L) according to the “Australian drinking water guide lines 2004” (National Health and Medical Research Council, 2004).

As represented in Figure 7.9, the significance of the results obtained suggests that, generally, the concentration of Zn in Swan River water did not change between the two different sampling locations along the river, which is perhaps to be expected given that Swan River waters along the Section sampled are mixed by a relatively strong current. There is also a strong possibility that fertilizers used in nearby agricultural areas, or other anthropogenic inputs are the sources of this Zn.

The concentration of Zn in tap water is presented in Section 4.6 and Figure 6.3, which also show a high level of external reproducibility. As represented in Figure 6.3, the accompanied uncertainties are 95% confidence, the uncertainty of the average was estimated as the square sum of the uncertainties of measurements one and two.

It is interesting to note that the concentration of Zn in fresh flowing (unrestrained (fresh)) tap water is ~ 400 times less than the concentration of Zn in the restrained tap water, with average concentrations of; $13.1 \pm 0.8\text{ ngg}^{-1}$ and $5.2 \pm 0.4\text{ }\mu\text{gg}^{-1}$ respectively. The simplest predicted explanation for this is that the restrained tap water was held in the water pipes for a week before being released, and during that time Zn may leach out of the pipes and joints as they slowly corrode. As mentioned in Section 2.2.1, according to the Australian drinking water guide lines 2004 (National Health and Medical Research Council, 2004), maximum Zn levels in drinking water has been based on the taste threshold of 3 mg/L .

Figure 6. 3: The reproducibility of the concentration of Zn in restrained and unrestrained (fresh) tap water



Higher Zn concentrations can impart an undesirable taste and a cloudy appearance, and Zn concentrations over 0.5 mg/L may indicate corrosion problems (National Health and Medical Research Council, 2004). These results indicate that concentration of Zn in restrained tap water is above the permissible Zn abundance in water and that the 40 year old Department of Applied Physics building plumbing system may have a corrosion problem. It should also be noted that most water authorities recommend flushing taps for several minutes that have been closed for some time to minimize these taste effects. At the same time, it is important to mention that the intake of 5, 7, and 9.5 mg of Zn is recommended daily for children, women and men respectively (Sturup, 2000). Also the World Health Organization “WHO” indicates that 10% of daily Zn intake can be provided from drinking tap water (WHO, 2003), which represent ~ 1.2 mg/day of Zn (National Health and Medical Research Council, 2004). Although the Zn concentration measured in restrained tap water is not hazardous to human health. The difference in the Zn concentration between restrained and unrestrained (fresh) tap water also indicates additional localized source of Zn input to the restrained water and this may be different, and may be can be traced by the isotopic composition of Zn of that source, but a detailed study would be required

The concentration of Zn was also measured by IDMS in a Zn vitamin Tablet and Zn plated steel fragment. The results of these samples are shown in Section 4.7 (Table 4.17). As expected the concentration of Zn was high in both samples; being 21.0 ± 0.6 mg per Tablet and $5.21 \pm 0.1 \text{ g}\cdot\text{kg}^{-1}$ for the Zn plated steel sample. Interestingly, the concentration of Zn in the nutritional Tablet was 16% less than was advertised by the manufacturer, although it was not clear if the stated Zn concentration in the Tablets was for the elemental or a compound form. Also the Zn was measured from a small fraction of a Tablet, and the homogeneity in the Zn concentration in the Tablet is not known.

Despite the fact that the concentration of Zn in most the samples measured in this work, especially SRMs, is in the order of tens of $\mu\text{g}\cdot\text{g}^{-1}$, no more than 1 μg Zn of sample was used in an individual isotopic analysis to measure the isotopic fractionation using the double spike technique. It is important to mention that this size of sample (1 μg) is considered to be a small sample, and represents a significant achievement, and places the Zn TIMS isotopic composition analyses alongside other advanced analytical techniques such as ICPMS (see Tables 3.2, 3.3 in Sections 3.3 and 3.4 respectively). At the same time, the actual amount of Zn and hence the concentration of Zn in the sample was able to be determined using IDMS. If the aim of an analysis was only to measure the concentration of Zn, no more than 300 ng Zn was used for the measurement. The same technique was able to be used for small samples, comparable to the magnitude of the blank (8 ng), e.g. the amount of Zn used for IDMS measurement of the Warburton meteorite was only 19 ng (Table 4.15 in Section 4.5.2). At this level the uncertainty is limited by the variability of the blank, hence, it was important to develop a procedure to reduce the blank associated with each analysis, see Sections 3.2, and 3.3.

- **Chapter 7 Isotopic Composition of Zn: Discussion**

7.1 Analytical considerations

7.1.1 Introduction

Until recently, only relatively small isotopic mass fractionation variations in Zn have been measured in natural materials relative to arbitrary laboratory standards, and no systematic attempts have been made to measure these absolutely. This dissertation investigates the variation in the isotopic composition of Zn in natural materials, using for the first time TIMS and double spiking, an “SI traceable technique”, which systematically differentiates between the induced fractionation from sample processing and instrument bias, and that which occurs due to natural processes. Despite some speculations in the field, a lack of knowledge of the extent of Zn isotope fractionation has restricted what is known about the processes that controls Zn fractionation. The present study aims to develop Zn TIMS measurement techniques, and in particular to solve critical analytical issues such as, interferences, ionisation efficiency, sample contamination, and the completely ignored issue of the contribution of the sample processing to the fractionation. These measurements techniques were utilized to determine the “accurate” magnitude of Zn fractionation and as far as possible, the range of fractionation in natural materials. Accurate analytical results add and provide insights into the processes that affect fractionation. Where possible this has been done using terrestrial samples which are also SRMs, so that other laboratories investigating this phenomenon and its applications, can also use these materials as suitable reference. Measuring Zn fractionation in (SRMs) relative to the laboratory standard (δ zero) will provide an international metrological base line for the Zn isotopic composition to be exploited for future Zn investigations by the wider scientific community. For example, the isotopic composition of such standard materials is vital to assess fractionation in similar materials using different analytical techniques. As presented in Chapter five; except for BCR-1, this is the first time Zn fractionation has been measured in these SRMs.

In this Chapter the isotopic fractionation measurements of Zn in natural materials are discussed, comparisons are made with any previously published results, and the implications are further explored. The Zn fractionation values used in this Chapter for each sample are effectively the average of those obtained using ^{64}Zn , ^{67}Zn , ^{68}Zn and ^{70}Zn isotopes. The final fractionation result used for any given sample, is the average of all the analyses for that sample. In most cases this involved repeat dissolution of samples, except for some meteorites which had limited availability. Fractionation accuracy was closely monitored by regularly measuring the fractionation of a synthetically mixed solution of the laboratory standard, “the absolute Zn”, and the double spike. These measurements always yielded a zero fractionation within uncertainties as described in Section 5.4 (long term reproducibility of measured fractionation). The laboratory standard used in this work is an aliquot taken from the same metallic reservoir as the IRMM (Ponzevera et al., 2006) or proposed (δ zero) standard to IUPAC. As the fractionation value obtained for the IRMM 3702 standard was $0.09 \pm 0.18 \text{ ‰ amu}^{-1}$ relative to laboratory standard. As indicated in Section 1.4 (significance of this research), the use of a consistent standard by all isotope analysts is essential for the comparison Zn isotope fractionation. Measurement relative to this internationally recognised standard by the IUPAC will effectively result in internationally accepted Zn absolute isotopic compositions being determined. Measured fractionation relative to “ δ zero”, can then be used as a tool to underpin isotopic measurements on a global scale.

7.1.2 Comparisons considerations

Three significant problems regarding comparisons of this work with previous results are:

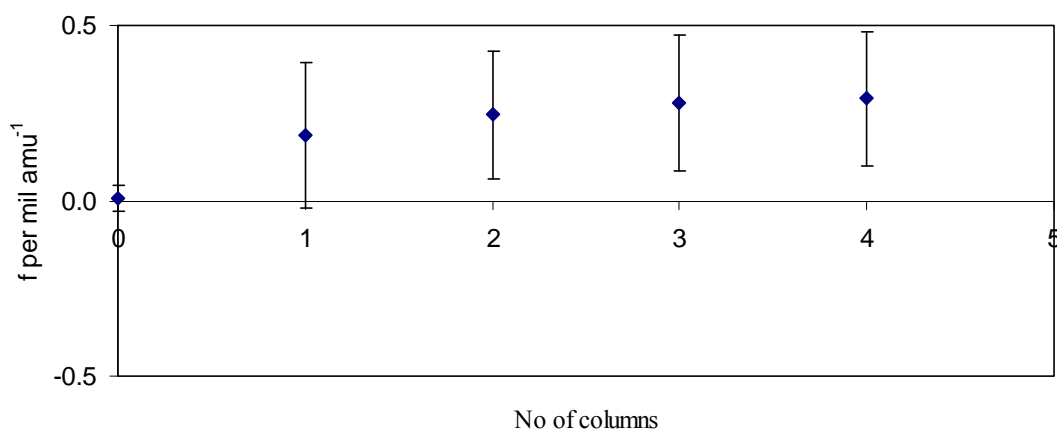
- Except for BCR- 1 and some meteorites; there are no samples in common with previously published research.
- Virtually all previous work has been measured by sample/standard comparison relative to an arbitrary laboratory standard, and/or elemental spiking e.g. using Cu, while this work uses the Zn double spike technique with all measurements performed relative to internationally proposed absolute Zn isotopic composition (δ zero).
- Ion exchange purification has long been suspected of introducing fractionation during sample processing (Stenberg et al., 2005). This affect is either ignored or

fractionation uncertainties are expanded to cover this possibility often without justification.

7.1.3 Effect of ion exchange chemistry on fractionation.

As shown in Section 5.5.5, and shown in Figure 7.1, the effect of anion exchange column (0.7 ml of AG1-X8 anion exchange resin 200-400 mesh size), similar to that described in Section 3.10 separation on Zn fractionation appears to be significant. Using a regression analysis, the contribution of the Anion column chemistry to the Zn fractionation was found to be $+0.07 \pm 0.02 \text{ ‰ amu}^{-1}$, which is generally greater than the external precision claimed by all recently published $\delta^{66}\text{Zn}$ data which should be noted is for two atomic mass units. This work represents an investigation of Zn fractionation in natural materials with full awareness of this effect. The clearly measurable effect of Anion exchange on fractionation will also provide a valuable bench top experimental system by which to study Zn fractionation in detail.

Figure 7. 1: Zn fractionation as a function of number of passes through an Anion exchange column.



As described above unless the effect of the anion exchange column separation on Zn fractionation is taken into account by analysts, reliable methods such as corrections for mass bias effects via other elements, with different ion exchange characteristics, are not possible. In the case of the latter problem, this highlights the power of the double spike technique in the measurement of isotopic fractionation, since the double

spike is combined with the sample before the chemical separation process; any bias imposed by the ion exchange process is done so equally on the Zn in the sample, as well as the double spike.

Marechal and her colleagues considered such affects as one of the main limitations of their measurements of isotopic fractionation of Cu using an Inductively-Coupled Plasma Double-focusing Magnetic sector multiple collector Mass spectrometer (Marechal et al., 1999). Marechal and Albarède (2002) reported “ Zn isotope fractionation between ion exchange resin and the HCl solution is undoubtedly present but is an order of magnitude less than for Cu”(Marechal and Albarede, 2002). It is important to emphasize that such effects appear to be significantly greater than the measurement precision reported using (MC-ICP-MS), and it is unclear whether these effects have been considered in their final reported values. Processing and eluting the sample from the ion exchange does not only fractionate Zn or Cu, but similar findings were reported for isotopic compositions of so many elements, Fe, Mo, Ca, thus the effect of such phenomena can't be ignored.

7.1.4 Elemental spiking

An elemental spike technique has been employed by other researchers in order to correct for instrumental imposed fractionation on the sample to measure natural Zn fractionation (Luck et al., 2005c, Marechal et al., 1999, Pichat et al., 2003a). Absolute Zn fractionation measurements are not possible using elemental spiking technique because, the fractionation behaviour of Zn will almost certainly differ from other elements during the ion exchange chemistry (Marechal et al., 1999, Anbar, 2004). In this work the double spike technique used is same element and serves as an internal standard to monitor mass fractionation introduced by any physical or chemical process following the spiking. In contrast to the elemental spiking, the isotopes of the double spike follow the same fractionation behaviour as the isotopes of Zn in the sample (Anbar, 2004).

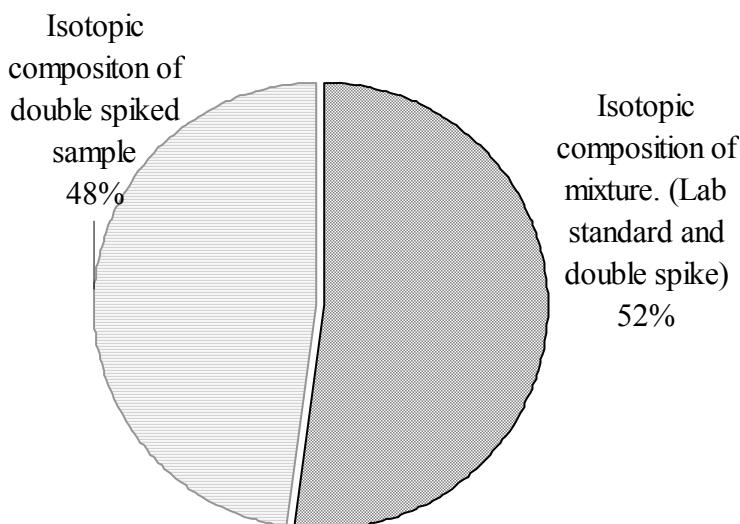
7.1.5 Fractionation uncertainty budget

In all the fractionation results presented, the accompanying uncertainty of each individual measurement (internal uncertainty) is the 95% confidence interval. The principal four uncertainty components contributing to the final fractionation are the uncertainties in the isotopic compositions of the:

- Laboratory standard,
- Double spike,
- Mixture (laboratory standard and double spike),
- Double spiked-sample.

To minimize the uncertainty arising from the sample fractionating during isotopic analysis, the measured isotopic ratios were internally normalized relative to the average $^{68}\text{Zn}/^{64}\text{Zn}$ ratio of each analysis. The uncertainties for the isotopic compositions of both the laboratory standard and the double spiked sample are also set to zero because they are constant for every analysis for added precision. Thus, the only contributors to the final internal uncertainty are the isotopic composition of the mixture (laboratory standard and double spike) and the isotopic composition of the double spiked sample. The typical contribution of each of these is shown in Figure 7.2, which is for an individual fractionation measurement of $\pm 0.2 \text{ ‰ amu}^{-1}$ for the Canyon Diablo meteorite.

Figure 7. 2: The contributions to the uncertainty of an individual measurement for the fractionation of Canyon Diablo.



As can be seen on Figure 7.2 the relative uncertainties for the isotopic composition of the double spiked sample and the laboratory standard double spike mixture are approximately the same.

The final uncertainty of an individual measured fractionation thus depends on the final uncertainty of these two key measurements. Also significant is the effect of sample to double spike ratio as discussed in the double spike technique (see Section 3.7.2). The final uncertainty on the average value for the fractionation of each sample was determined by averaging the individual measurements and using the ISO GUM approach using the normal-distribution to estimate the final uncertainty.

In following Sections the measured fractionation obtained for all the samples is discussed. The measurements are represented as relative to the internationally proposed absolute isotopic composition of Zn (proposed δ zero) with estimated uncertainties (95% confidence). Where possible, and within the limitation described in the previous Sections, comparisons are made with previously published results. As in the Chapter 5 the observed variations in the isotopic composition of Zn are confirmed to be mass dependent fractionation (f) reported as per mil per atomic mass unit (‰ amu^{-1}).

7.2 Geological Samples

Table 7.1 and Figure 7.3, show a compilation of the average isotopic fractionation of Zn in a range of geological materials measured in this work. The calculated average of the Zn fractionation for each rock type sample was calculated using ISO GUM assuming a normal distribution of the measurements. In general, the fractionation range⁹ obtained for all geological samples are between -0.09 ± 0.15 to $+0.43 \pm 0.18$ ‰ amu^{-1} (0.85‰ amu^{-1}), and the fractionation appears reasonably consistent for each type of material. This suggests the possibility of geological isotopic groups i.e. that rock types are different isotopically, possibly arising from different geological processes, but more measurements would be needed to support this possibility. The isotopic fractionation of Zn among each individual rock type will be discussed in detail in later Sections.

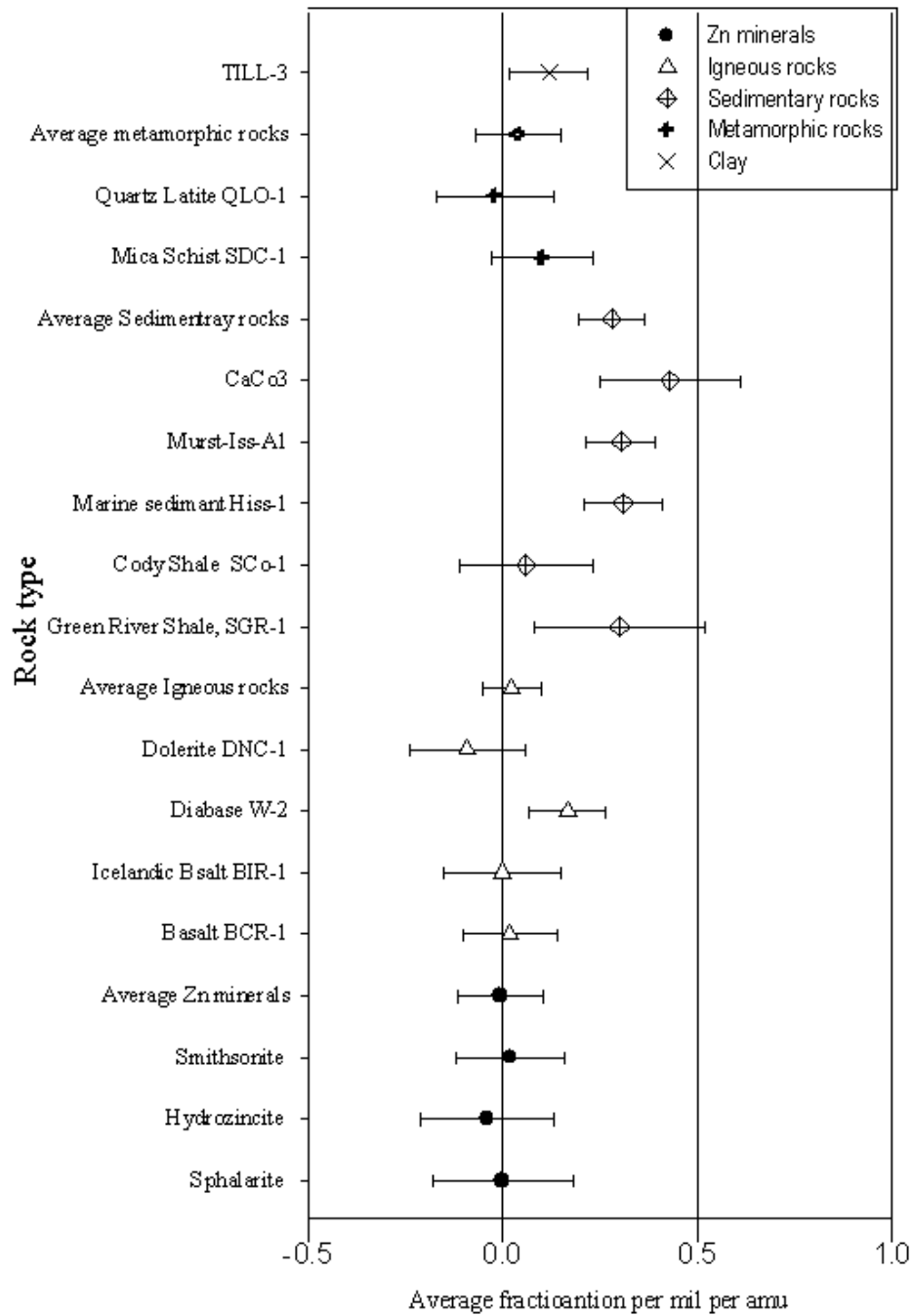
⁹ The range calculated as the difference between the maximum value and the minimum value considering the uncertainty in each value.

Table 7. 1: Compilation of the average isotopic fractionation of Zn in all geological materials measured in this work and compared to the previously measured values using different technique.

Category	Material	Average fractionation ‰ amu ⁻¹ (This work)	fractionation (Previous work)	Relative to
Minerals	Sphalerite	-0.01 ± 0.18	⁶⁶ δ = -0.17 to 1.33 ‰ ^â .	Relative to the Lyon JMC 3-0749L Zn standard
	Hydrozincite	-0.04 ± 0.17		
	Smithsonite	0.02 ± 0.14		
Igneous rocks	Basalt BCR-1	0.02 ± 0.12	⁶⁶ δ = 0.29 ± 0.12 ‰ ^ë	Relative to Zn standard JMC (3-0749L).
			+0.11 ± 1.8 ‰ amu ⁻¹	JMC
	Icelandic Basalt BIR-1	-0.01 ± 0.15		
	Diabase W-2	0.17 ± 0.10		
	Dolerite DNC-1	-0.09 ± 0.15		
Sedimentary rocks	Green River Shale, SGR-1	0.30 ± 0.22		
	Cody Shale SCo-1	0.06 ± 0.17		
	Marine sediment HISS-1	0.31 ± 0.10		
	Murst-Iss-A1	0.305 ± 0.089		
	CaCO ₃	0.43 ± 0.18		
Metamorphic rocks	Mica Schist SDC-1	0.10 ± 0.13		
	Quartz Latite QLO-1	-0.02 ± 0.15		
Clay	TILL-3	0.12 ± 0.10		

^â (Wilkinson et al. 2005). ^ë (Chapman et al. 2006). [®] Rosman (1972) measurement using the double spike technique.

Figure 7. 3: Graphical representation of the average measured Zn fractionation ‰ amu^{-1} in geological materials relative to the absolute isotopic composition of Zn.



7.2.1 Zinc minerals

As represented in Figure 7.3, of the three Zn mineral samples studied (Sphalerite, Hydrozincite and Smithsonite) none appears to be fractionated relative to the laboratory standard, or relative to each other. As described earlier in Section 7.1, direct comparisons with previous measurements are of limited value because none of the previous measurements were performed relative to any absolute isotopic standards. However, the range of fractionation measurements obtained can still be compared.

The only mineral for which previous measurements are available is Sphalerite, the Sphalerite measured in this research yielded an average fractionation of $-0.01 \pm 0.18 \text{ ‰ amu}^{-1}$. A previous measurement for Zn fractionation in Sphalerites from Irish ore fields by Wilkinson et al. (2005) obtained a fractionation between -0.085 and 0.66 ‰ amu^{-1} relative to Lyon JMC 3-0749L Zn standard. It is important to emphasize that Wilkinson et al. (2005) considered the $+0.66 \text{ ‰ amu}^{-1}$ value to be outlier, and consider a more realistic fractionation range to be between -0.085 to 0.32 ‰ amu^{-1} (Wilkinson et al., 2005). Because only one Sphalerite was measured in this work, a range comparison can't be made.

Sphalerite (ZnS) is a major ore of Zn, while Smithsonite is a supergene Zn mineral, formed from the oxidation of Sulphide bearing deposits. The non-sulphide Supergene Smithsonite occurs in carbonate rocks hosts owing to the reactivity of carbonate minerals with acidic, oxidized Zn rich fluids, derived from the breakdown of Sphalerite rich bodies (Hitzman et al., 2003). Since the fractionation for Sphalerite was found to be the same as for Smithsonite and Hydrozincite; one could conclude that geochemical processing of these Zn minerals does not fractionate Zn. However, since these two samples are unlikely to be from the same source, this can't be determined conclusively.

Chemically, Cd is very similar to Zn, and has some similarities with Mg; though Zn has a much greater tendency than Mg to form covalent compounds (Greenwood and

Earnshaw, 1998b). To compare measured fractionation of Cd and Mg of same samples to that of Zn may provide some insight into why and how the isotopic composition of Zn fractionates in natural systems. In an early study, Cd in Sphalerite samples collected from different localities also showed no significant fractionation within the experimental uncertainties $\sim 1.4 \text{ ‰ amu}^{-1}$ (Rosman and De Laeter, 1975). More conclusively, Wombacher et al. (2003) measured Cd fractionation in Sphalerite and described it to be insignificant $+0.6 \pm 0.5 \text{ ‰ amu}^{-1}$ (one part in ten thousand), suggesting that inorganic natural processes may be unable to generate substantial Cd isotopic fractionation (Wombacher et al., 2003).

7.2.2 Igneous rocks

Igneous rocks form the majority of the Earth's crust, and either directly or indirectly are the origin of all other rocks (Sharp, 2007), and hence are important rocks to study in any Zn fractionation survey. As represented in Figure 7.3, of the four igneous rocks examined, only Diabase (W-2) exhibits a consistently slightly heavier fractionated Zn, of $+0.17 \pm 0.10 \text{ ‰ amu}^{-1}$ relative to the laboratory standard. This agrees with a prediction made by Albarède (2004) that igneous rocks would not exhibit significant isotopic fractionation for Zn and Cu. Albarède's assumption was based on reviewing research done on Zn in igneous rocks by other researchers. Small Zn fractionation ($\leq 0.15 \text{ ‰ amu}^{-1}$) relative to their laboratory standard Zn (JMC-3); was considered to be insignificant by Albarède.

The average fractionation values obtained for igneous rocks ($0.02 \pm 0.08 \text{ ‰ amu}^{-1}$) agrees with internationally recommended absolute standard Zn Alfa Aesar 10759 reference material and 3702 both known as (δ zero) used in this research as the laboratory standard. Since igneous rocks are often considered as being representative of bulk Earth they are therefore suitable as an absolute standard. This suggests that the absolute laboratory standard as used in this research also represents the isotopic composition of Zn of "bulk Earth".

Chapman (2006) measured BCR-1 and reported a fractionation of $\delta^{66}\text{Zn} = 0.29 \pm 0.12 \text{ ‰}$ relative to their laboratory standard JMC (3-0749L). While this overlaps with the

fractionation result obtained for BCR-1 in this work, the fractionation of their isotopic standard relative to the one used in this work is unknown so a clear comparison can't be made. Chapman's study also used the elemental spike technique, which, described in Section 7.1.4, is also not as accurate as the double spike technique used in this research (Chapman et al., 2006). It is also worth mentioning that BCR-1 was measured in this work using 1 µg amounts of Zn compared to the 2.5 µg amount used by Chapman, (see Table 3.2 in Section 3.3).

It would be useful to compare the results for Zn fractionation obtained in igneous rocks to the fractionation of other elements in the same rock group using double spiking. This will open the way to reveal any fractionation systematic behaviours if existed. The only other double spike measurements for Basalt BCR-1 Zn are those by Rosman (1972) who obtained $+0.11 \pm 1.8 \text{ ‰ amu}^{-1}$; (95% confidence) (Rosman, 1972b). Despite his relatively large stated uncertainty, Rosman's result is still within the uncertainty of the result obtained in this research $+0.02 \pm 0.12$, suggesting an overestimation of uncertainties by Rosman. This highlights the significantly improvement in the uncertainties (approximately 15 times) obtained by this work, and the significantly smaller Zn amounts for analyses (1 µg of Zn) (see Section 3.3, 3.4 and 3.5). It is interesting to note that double spiked Mo, also a chalcophile element, shows relatively small to no fractionation in igneous rocks, relative to their Mo standard reference, material Johnson Matthey lot number 602332B (Siebert et al., 2003).

Diabase W2 differs from the three other basaltic samples studied, containing isotopically heavier Zn, i.e. "enhanced in the heavier isotopes", but still within the uncertainty of the isotopic composition of Zn of the rest of the group. At the same time, it appears to be the only igneous rock sample that is fractionated relative to the absolute standard. One explanation for this is that different samples come from a different mantle sources or reservoirs (Schilling, 1973, Allegre et al., 1995). If this is the case, then either the differences between the sources are very small, or the other samples come from the same source. Another possibility is that the mantle has a fixed isotopic composition but that samples such as the Diabase have gone through another unknown process that fractionated its Zn.

One possible explanation for the difference of Diabase W-2 relative to the laboratory standard (proposed absolute) is the theory of “segregation of subducted oceanic crust in the convecting mantle”, of Christensen and Hofmann (1994). The theory propose that subducted oceanic crust transformed into dense mineral assemblages at high pressure may gravitationally segregate at the bottom of the convecting mantle where it could be stored for a long time enough to develop an enhanced isotopic composition before it recycles in the plumes and control the geochemical character of the basalt. This segregation was first considered by Hofmann and White (1982) who first suggested that dense eclogitic rock is stored for one or two billion years in chemical boundary layer before it rises again in mantle plumes. This will allow enough time to vary the isotopic composition to more enhanced isotopic composition, and this is more evident in ocean island volcanic rocks (Christensen and Hofmann, 1994). These theories could explain the slightly enhancement of Zn heavier isotopes in Diabase W-2 relative to other basaltic rocks. As Hofmann and White (1982) explained; for the segregation of subducted oceanic crust in the convecting mantle theory to be true, the rising melts would be distinguished by high concentrations of incompatible trace elements and a relatively high degree of chemical and isotopic heterogeneity (Hofmann and White, 1982). This theory is controversial as the concentration of Zn in all our samples and Diabase W-2 $77.7 \pm 1.1 \mu\text{g g}^{-1}$ is marginally less than the average Zn abundance in Basaltic rock. which is $100 \mu\text{g g}^{-1}$ (Storey, 2007)

The relationship between the isotopic composition and the abundance of Zn in igneous rocks is not clear in our results. The concentration of Zn in Diabase $77.7 \pm 1.1 \mu\text{g g}^{-1}$ is lower than what is considered average Zn abundance in Basaltic rock $100 \mu\text{g g}^{-1}$ (Storey, 2007), which does not suggest additional contamination from the magma.

At magmatic temperatures, the isotopic composition of the melt can be considered identical to that of the source, which is what makes the isotopic composition of volcanic rocks ideal tracers of mantle composition (Hofmann, 2003). Accordingly, the isotopic composition of Zn in Basalt BCR-1, BIR, and DNC-1 is likely to be the isotopic composition of Zn of the Basalt source mantle, which forms the continents. On the other hand, Diabase carries a slightly heavier isotopic composition but still within the uncertainty of other basalts may represent a deeper mantle that is still

essentially undifferentiated. As the debate about this issue continues today, the results of this limited research show that igneous rocks appear to contain isotopically the same Zn isotopic composition despite their different localities. More igneous rocks should be studied to confirm this conclusion.

When comparing these results with those for Cd fractionation in igneous rocks, our conclusion agree with the interpretation of Wombacher et al. (2003) who concluded that isotopic fractionation of Cd is not expected during the formation of igneous rocks because of the high temperatures involved (Wombacher et al., 2003).

7.2.3 Sedimentary rocks

As described in Section 5.5.2.3, and summarised in Table 7.1 and Figure 7.3, the measured Zn fractionation of sedimentary rocks ranged from $+0.06 \pm 0.17 \text{ ‰ amu}^{-1}$ for SCO-1 to $+0.43 \pm 0.18 \text{ ‰ amu}^{-1}$ for CaCO₃.

Previous investigations of the isotopic composition of Zn in sedimentary materials found that they can be described as a group, consistent with each other, and attributed to biological activity in upper seawater. At the same time, other studies have concluded that Zn isotopic fractionation values of sediment trap samples collected near up welling off the coast of Mauritania (central Atlantic) show a seasonal isotopic fluctuations consistent with biological pumping during the high-productivity period (Maréchal et al. 2000). Values of Zn fractionation in sea nodules appear to be associated with the amplitude of seasonal variations rather than with the mean values of the biological productivity. As represented in Figure 7.3, apart from Cody shale, (SCO-1), which exhibits no fractionation relative to the laboratory standard, all of the other sedimentary rocks show a consistent fractionation relative to the laboratory standard. It is important to notice that all sediments samples measured in this research effectively exhibit the same isotopic composition within uncertainties, with an average fractionation $+0.28 \pm 0.08 \text{ ‰ amu}^{-1}$, relative to the laboratory standard “bulk Earth”. It should also be noted that all the measured samples are from different localities, Green river shales collected from the Green river of Wyoming in the United States, HISS-1 marine sediments collected from the coast of Canada, and Murst-Iss-

A1 Antarctic sediments respectively. This small survey suggests that the Zn in sedimentary rocks is fractionated, with either the Zn fractionated prior to, or some time during, the formation of the sediments. The range⁹ of Zn fractionation in all measured sediments found in this work is 0.72 ‰ amu⁻¹. This is six times larger than the range of 0.12 ‰ amu⁻¹ for three bulk sediments measured by Marechal et al. (1999) from three different localities “ $\delta^{66}\text{Zn} = 0.16 \pm 0.04$ ‰ to 0.33 ± 0.04 ‰”. (Marechal et al., 1999). This work demonstrates a wider range in the Zn fractionation for sediments, albeit with larger uncertainties.

Fractionation of Zn in deep sea sediments appears related to some form of biological activity and its preferential uptake in different biochemical reactions (Pichat et al., 2003c). As reviewed in Section 2.2.2, Pichat et al. (2003) measured Zn fractionation in carbonate fractions of oceanic sediments, and showed that sediments were enhanced with the heavier Zn isotopes, which they indicate is consistent with the lighter isotopes of Zn preferably being taken up by biological processes.

All the measurements of this research were performed on bulk sediment samples and hence, represent a cumulative Zn fractionation in the terrigenous sediments. There is every possibility that this represents a different isotopic composition from the carbonate component due to the biological activity in that component, making it difficult to compare our results with those of Pichat et al. (2003) study. Another Zn bulk sediment fractionation collected from the tropical Atlantic and another one from the tropical Pacific was analysed by Marechal et al (2000) producing isotopic fractionation $\delta^{66}\text{Zn} = 0.22 \pm 0.03$ and 0.26 ± 0.07 ‰ respectively, relative to their laboratory standard (Pichat et al., 2003c). Another interpretation is that this isotopic composition may represent the isotopic composition of Zn in upper or lower ocean waters where biological activity is always present (Maréchal et al., 2000). The results of Marechal et al. (2000) on bulk sediments are a good example of the importance of measuring fractionation relative to common standard; such that it could be compared to the results of this or any other work. It is important to mention the limitation of biological activity by the low concentration of Zn in the ocean; also known as the “Zn

⁹ The range calculated as the difference between the maximum value and the minimum value considering the uncertainty in each value.

hypothesis” of Morel et al. (1994) as discussed in Section 2.2.1, which can be evaluated using Zn isotopes.

Another important marine effect is that of the so called conveyor type oceanic circulations presented by Broecker in 1997. Oceanic conveyors deliver an enormous amount of heat to the northern Atlantic changing the water temperature and density. The dense water that sinks deep into deep ocean, reaches every where in the planet, including up to underneath the Arctic ice cap, which could suddenly change the oceans circulations (Broecker, 1997). The effects of these conveyers can be seen in the sedimentary rocks records as function of the change in the $^{14}\text{C}/^{12}\text{C}$ ratio (Broecker, 1997). Assuming that all our samples are taken from the same range of depths opens the way to connect our results to such effect. Conveyor circulations effects are not restricted to the North Atlantic but across the planet; which could be the reason why the fractionation of Zn is effectively the same magnitude even in different oceanic localities on the planet.

A study by Wombacher et al. (2003) provided the first evidence for small ($\leq -1.2 \text{ ‰}$ amu^{-1}) terrestrial Cd isotope variations in low temperature environments typical of sedimentary rocks. The same study by Wombacher et al. (2003) concluded that, inorganic natural, including low temperature processes are unlikely to fractionate Cd substantially. As shown in Table 7.1 and Figure 7.3, sedimentary Zn is fractionated by $\sim +0.3 \text{ ‰}$ amu^{-1} relative to the laboratory standard, and hence to igneous rocks which does not agree with the interpretation of Wombacher et al. for Cd. It should be noted that Cd is also a significantly heavier element than Zn and therefore less likely to fractionate in such situations. Another element for which double spike fractionation data in these types of samples is available, is Mo. Siebert et al. (2003) found that Mo isotopic fractionation for clastic sediments are very similar to that of igneous rocks and this was interpreted as a typical crustal Mo input (Siebert et al., 2003). This interpretation for Mo isotopic composition may explain why the measured Zn fractionation of SCO-1 ($+0.06 \pm 0.17 \text{ ‰}$ amu^{-1}) shows an isotopic similarity with the Zn igneous rocks measured in this research. For Fe, modern marine sediments, such as deep-sea clays, terrigenous sediments, turbidite clays, and volcano clastites, have a restricted range of Fe isotopic compositions clustered around the igneous $\delta^{56}\text{Fe}$ values (Dauphas and Rouxel, 2006). As reviewed by Dauphas and Rouxel (2006),

traditionally, the behaviour of Fe in modern seafloor hydrothermal systems was investigated by integrating results from laboratory studies, theoretical models, mineralogy, and fluid and mineral chemistry. Recent studies of the isotopic composition of Fe in seafloor hydrothermal fluids, and altered basalts revealed that Fe isotopes are fractionated during high and low temperature hydrothermal processes and might be useful geochemical tracers in these environments. Such interpretations for Fe, emphasize the importance of studying the conveyor type oceanic circulations as in the case of Zn isotopic fractionation (Dauphas and Rouxel, 2006).

7.2.4 Metamorphic rocks

Metamorphism is the transformation of pre existing rock into mineralogical distinct new rock as a result of high temperature, high pressure or both but without the rock melting in the process (Plummer and McGeary, 1985). The results of Zn fractionation in metamorphic rocks are represented in Figure 7.3 and Table 7.1 along with other geological rock materials. The limited results obtained from the two metamorphic samples indicate that the isotopic composition of Zn in these rocks carry the same Zn isotopic signature as terrestrial igneous rocks in the Earth crust, but are different from the Zn in sedimentary rocks. The results of Zn fractionation of metamorphic rocks supports the assumption by Wombacher et al.(2003) that high temperature and pressure processes that igneous rocks experience do not fractionate the isotopic composition of Cd, which has been found to be similar in this work for Zn. With only two metamorphic samples analysed, clearly more measurements needs to be done on these types of samples before any more definitive conclusions could be drawn.

7.2.5 Clay

Clay sample, TILL-3 appears to exhibit a consistently slightly positive Zn fractionation of $+0.12 \pm 0.10 \text{ ‰ amu}^{-1}$, although it is barely outside uncertainty, from the absolute. The fractionation obtained is similar to both igneous and that for sedimentary rocks. However, it is more likely that Clay sample, TILL-3 (exhibiting a consistently slightly positive Zn fractionation) will isotopically behave like sedimentary rocks, where both are slightly enhanced in heavier isotopes. This is not

surprising such that; TILL-3 is thought to be a formed from a range of mixed glacial sediments.

7.3 Biological materials

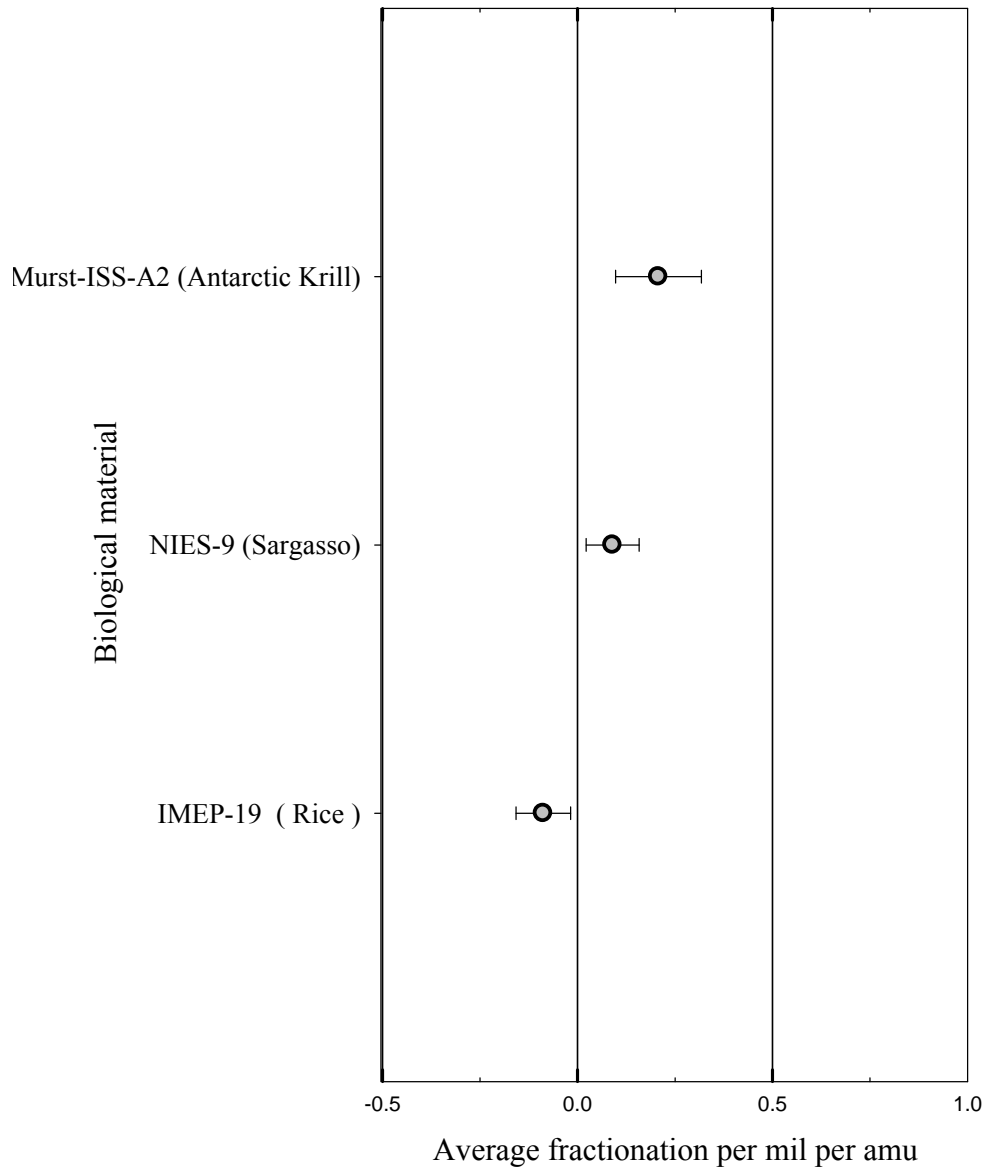
The isotopic composition of Zn in three biological materials was measured in two plants and one animal sample. The average values obtained are presented in Figure 7.4 and Table 7.2. The calculated average of the Zn fractionation for these samples was calculated using ISO GUM, using the normal distribution of the measurements. In general, the fractionation range obtained are between -0.088 ± 0.070 to $+0.21 \pm 0.11$ ‰ amu⁻¹, the range⁹ of fractionation between in the plant samples measured in this work is 0.316 ‰ amu⁻¹. The isotopic composition of Zn in these SRM materials have not been measured previously, hence, no comparisons can be made.

Table 7. 2: Compilation of the average isotopic fractionation of Zn in all biological materials measured in this work.

Biological material	Average fractionation ‰ amu ⁻¹	± ‰ amu ⁻¹
IMEP-19 (Rice)	-0.088	0.070
NIES-9 (Sargasso)	0.090	0.068
Murst-ISS-A2 (Antarctic Krill)	0.21	0.11

⁹ The range calculated as the difference between the maximum value and the minimum value considering the uncertainty in each value.

Figure 7. 4: Measured Zn fractionation in biological materials relative to the laboratory standard.



The two plant samples, IMEP-19 “Rice” and NIES-9 “Sargasso”, shows resolvable negative and positive fractionation, -0.088 ± 0.070 and $+0.090 \pm 0.068$ ‰ amu^{-1} respectively, relative to laboratory standard. This suggests different isotopic sources or modification process that fractionate Zn are in action. The seaweed “Sargasso” appears to be “enhanced with the heavier isotopes”, similar to that observed for sediments and could be reflecting the oceanic conditions under which it grows. Seawater is thought to be enhanced in the heavier isotopes from biological activities of phytoplankton and other organisms in waters (see Section 2.2.2) (Pichat et al., 2003a). On the other hand, IMEP-19 “Rice” is depleted or “enhanced in the lighter isotopes”, and assuming no significant external contamination, could be related either to the soil in which it is grown, or the organic processes associated with growth.

As represented in Figure 7.4, IMEP-19 Rice has a depleted Zn isotopic composition (negative fractionation) similar to that observed for C found by Chikaraishi and Naraoka in 2003 for C3 type plants. According to Chikaraishi & Naraoka (2003), the average of $\delta^{13}\text{C}$ in C3 plants is -36.1 ± 2.7 ‰ relative to the Pee Dee Belemnite “PDB” (Chikaraishi and Naraoka, 2003).

Because only two plant samples were analysed in this work, only a very limited amount of interpretation can be drawn from these results. The depletion of the isotopic composition of Zn in the Rice sample (a C3 type plant) may provide an insight to the similarity for the Zn and C isotopic fractionation systematics in plants.

Any clear relationship between $\delta^{13}\text{C}$ and Zn fractionation is difficult to conclude from this research if existed, such that C and Zn might have similar metabolic pathways. According to the same study of Chikaraishi and Naraoka in 2003, C3 plants have a small $\delta^{13}\text{C}$ relative to seaweed. Our results for IMEP-19 Rice and NIES -9 Sargasso are approximately the same Zn fractionation in magnitude but opposite in direction; i.e. -0.088 ± 0.070 ‰ amu^{-1} and $+0.09 \pm 0.068$ ‰ amu^{-1} respectively, or 0.178 ‰ amu^{-1} relative to each other. This can be compared to the measurement of Chikaraishi and Naraoka for $\delta^{13}\text{C}$, where Seaweed is fractionated by $\sim +13.3$ ‰ relative to the average $\delta^{13}\text{C}$ of C3 plants.

A strong correlation between $\delta^{13}\text{C}$ value of plant tissue cellulose and mean air temperature has been noted in the study by Skrzypek et al.(2007); where a 1°C increase in air temperature during the growing season resulting in a 1.6 ‰ decrease in $\delta^{13}\text{C}$ for Sphagnum mosses, and a 1.5‰ decrease in $\delta^{13}\text{C}$ for Polytrichum mosses. Changes in the humidity show no affect on the carbon isotope composition of mosses (Skrzypek et al., 2007b).

As Zn bonds covalently to C and to the Hydroxyl groups in the plants cell walls (Weiss et al., 2005), temperature effects on the isotopic composition of C in the plant kingdom could perhaps also fractionate the isotopic composition of Zn in plants.

Weiss et al. (2005) measured Zn fractionation in rice samples where they found that rice shoots were isotopically depleted relative to the rice roots samples grown in two different nutrient solutions, standard reference rice seeds material IR34 from the international rice research institute, yielded a $\delta^{66}\text{Zn} = 0.631 \pm 0.046$ ‰ relative to their laboratory standard (Johnson Matthey purontronic batch number NH 27040) (Weiss et al., 2005). However, the absolute Zn fractionation can't be compared to any other because of their measurements was performed relative to unknown laboratory standard. According to the systematics of Zn covalently bonding with cell walls of the plants, Weiss et al. (2005) suggested that Zn fractionation in plants could be due to the preferential binding of heavy Zn isotopes to the cell walls in non-exchangeable forms.

As shown in Figure 7.4, the only animal sample measured is MURST-Iss-A2 “Antarctic Krill”, taken from the southern ocean between 1993 and 1995. The results of this work is the first Zn analyses isotopic fractionation in a biological sample from the animal Kingdom excluding humans. The result obtained for MURST-Iss-A2 was $+0.21 \pm 0.11$ ‰ amu^{-1} relative to the laboratory standard, which is similar to the average Zn fractionation results of $+0.28 \pm 0.08$ ‰ amu^{-1} obtained for marine sediments. One explanation for this is that these animals simply reflect the fractionation of the same environment in which they live in. In terms of the isotopic composition of carbon, it is known that copepods from the Arctic reflect the isotopic composition of the food consumed during previous periods of feeding and growth.

However, faecal pellets of the copepods were also found to be depleted in ^{13}C by 6.3 to 11.2 ‰ relative to the food ingested, indicating that faecal pellet production is an important pathway for the trophic fractionation of $\delta^{13}\text{C}$, and more importantly, it adds to the variability of the isotopic composition of C in oceanic particulate organic matter (Tamelander et al., 2006). Such isotopic variations have been used to investigate the migration of animals including marine species (Kelly and Finch, 1998, Stowasser et al., 2006). The Zn fractionation result obtained for the Krill certainly appears to warrant further investigation, both in terms of looking for similar effects in other animals and in examining various biological pathways associated within individual organisms. Unfortunately such an investigation was outside the scope of this work.

7.4 Meteorites

It has been postulated and now highly probable that iron and stone meteorites are fragments of a planet or planets broken up since the early evolution of the Solar System, probably from the missing planet required by Bode's Law between Mars and Jupiter and/or parts of the original planetesimal from which the Earth and the moon accumulated (Urey, 1952). Among processes of planetary formation that fractionate isotopes, volatilization, mineral–silicate melt or mineral–liquid metal segregation, and metamorphism, are the most important and all lead to mass-dependent isotopic variability. (Luck et al., 2005b). As a moderately volatile element (650 to 700 K), Zn fractionation could be involved during partial kinetic evaporation or condensation (Wombacher et al., 2008). Mechanisms capable of generating isotopic fractionation have been associated with plasma effect in the solar nebula, (Russell et al., 1978) .

Amongst the important reasons for studying Zn isotopic compositions in meteorites are:

- Meteorites are a critical primitive component of the Solar System and provide a significant insight into the original isotopic composition of Zn in the solar nebular, its evolution, and the current Solar System

- Zn fractionation in meteorites may provide an insight into various environments and processes occurring during the formation of the Solar System.
- The isotopic composition of Zn assists with identification of meteorite types and Zn source in meteoritic breccias.

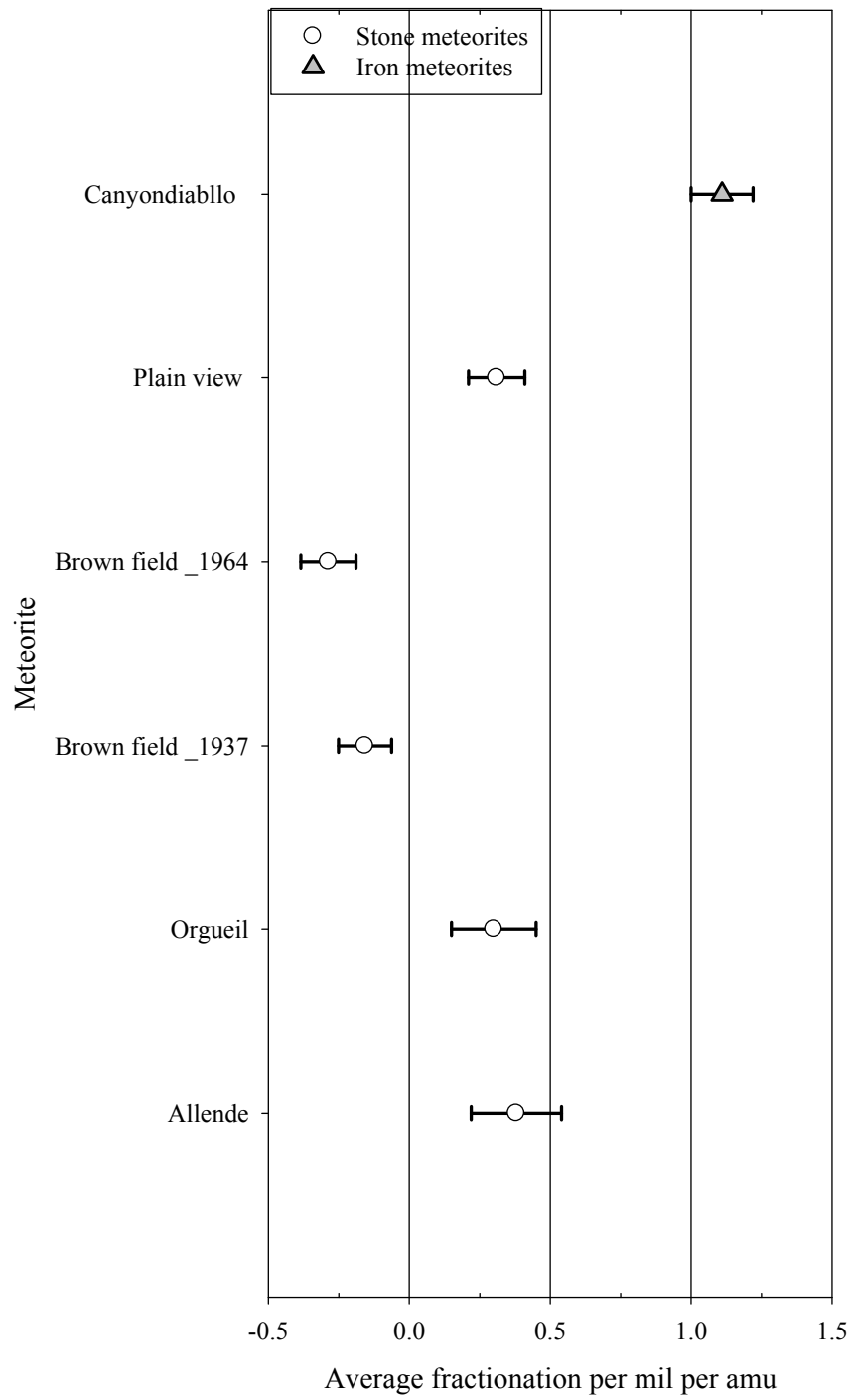
The isotopic fractionation of Zn was measured in five stony and two iron meteorites samples as shown in Figure 7.5. All the results for the measured fractionation relative to the laboratory standard are accompanied by 95% 2σ uncertainties. Where possible repeat analyses was performed on all samples apart from those that were either rare or for which limited samples were available, the procedure developed enabled small samples to be measured requiring a small blank (see Sections 3.3, 3.4 and 3.5). Table 7.3, shows a compilation of the average isotopic fractionation of Zn for the meteorites measured in this work, compared to previous measurements using different techniques. The calculated average of the Zn fractionation for each meteorite sample was calculated using ISO GUM using the normal distribution of the measurements

Table 7. 3 Compilation of the average isotopic fractionation of Zn in all meteorites measured in this work, compared to the previously measured values using different techniques.

Meteorite	Average fractionation ‰ amu ⁻¹ (This work)	Fractionation (Previous work)	Relative to
Allende	0.38 ± 0.16	$\delta^{66}\text{Zn} = (-0.57 \text{ to } +0.44)^{\text{a}}$ External uncertainty (0.04 to 0.05 ‰)	Relative to Zn JMC 400882B.
Orgueil	0.30 ± 0.15	$\delta^{66}\text{Zn} = (+0.46 \text{ to } +0.52)^{\text{a}}$ External uncertainty (0.04 to 0.05‰)	Relative to Zn JMC 400882B.
Brownfield _1937	-0.157 ± 0.094	$\delta^{66}\text{Zn} = -0.30 \text{ ‰}^{\text{a}}$ External uncertainty (0.04 to 0.05 ‰)	Relative to Zn JMC 400882B.
Brownfield _1964	-0.287 ± 0.098		
^o Plainview	0.31 ± 0.10	$+0.60 \pm 1.6^{\text{b}}$ ‰ amu ⁻¹	Relative to Zn JMC
Redfields	Abnormal Zn isotopic composition		
Canyon Diablo	1.11 ± 0.11	$\delta^{66}\text{Zn} = +2.10 \text{ ‰}^{\text{a}}$ External uncertainty (0.04 to 0.05 ‰)	Relative to Zn JMC 400882B.
		$+0.27 \pm 1.3^{\text{o}}$ ‰ amu ^{-1b}	Relative to Zn JMC

.^a (Luck et al., 2005b).^b (Rosman, 1972b). ^o The value was measured using the double spike technique.

Figure 7. 5: Average Zn fractionation in meteorites relative to the laboratory standard.



The results of this work regarding the measured fractionation of Zn in meteorite meteorites is approximately $0.5\% \text{ amu}^{-1}$ larger than the isotopic composition of Zn in natural terrestrial materials which is consistent with the findings of Luck et al. (2005). It is worth mentioning that, the range of Ni fractionation in meteorites was measured to be $0.41\% \text{ amu}^{-1}$ (Cook et al., 2007), which is less than what is found for Zn in this research ($1.4\% \text{ amu}^{-1}$) and consistent with Zn being more volatile than Ni. In contrast the range of variation of $\delta^{114/110}\text{Cd}$ observed is about 23‰, with ranging from $\delta^{114/110}\text{Cd}$ -7.8 to +15.0 ‰ in unequilibrated ordinary Chondrites (Wombacher et al., 2008). At the same time, the range of fractionation in Cu was reported to be $\delta^{65/63}\text{Cu}/2$ from -0.48 to +0.22 ‰ (Moynier et al., 2007).

7.4.1 Stony meteorites

The fractionation range obtained for all stony meteorites is between -0.29 ± 0.10 to $+0.38 \pm 0.16\% \text{ amu}^{-1}$. Although these meteorites are classified as stony, most are from significantly different chemical and metamorphic subgroups. Figure 7.5 shows that Allende, and Orgueil (Carbonaceous Chondrites), and Plainview (Ordinary Chondrite) meteorites are enhanced isotopically in the heavy isotopes of Zn by $+0.38 \pm 0.16$, $+0.30 \pm 0.15$, and $+0.31 \pm 0.10\% \text{ amu}^{-1}$ respectively, relative to the laboratory standard “proposed absolute Zn”, and are within uncertainty of each other. In contrast, both the Brownfield meteorites (Ordinary Chondrites) are negatively fractionated with approximately the same magnitude $-0.2\% \text{ amu}^{-1}$, relative to the standard, which is assumed (based on igneous rocks) to represent the isotopic composition of Zn of bulk Earth.

Absolute comparison with previous work of Luck et al. (2005) is limited due to a lack of knowledge of the absolute value of their laboratory standard. However, relative comparisons can still be made. Luck et al. suggested that $\delta^{66}\text{Zn}$ values slightly decrease, i.e. “Samples become isotopically lighter”, in the order CI, CM, CV-CO. This is not supported by limited studied in this work. Allende and Orgueil are the only carbonaceous Chondrites measured in this research and are regarded as being amongst the more primitive objects in the Solar System, (Luck et al., 2005b). Generally, a source for these isotopic fractionation in Chondrite meteorites are the Metamorphic

(thermal) and shock (impact) processes exerted on Chondrites, which can affect the isotopic compositions. oxygen isotopic evidence indicates that all Chondrites experienced some low-temperature alteration (Robert N. Clayton et al. 1991; Edward et al. 1999; Grossman et al. 2000). The effect of this on the Zn would require a more detailed study than time permitted for this work.

Luck et al. (2005) measured Zn fractionation in bulk Allende, Orgueil, and Brownfield-1937 meteorites; their results yielded a Zn fractionation of: range of -0.29 to +0.22 ‰ amu⁻¹, +0.23 and +0.26 ‰ amu⁻¹, and -0.15 ‰ amu⁻¹ respectively. In terms of relative comparisons of these results, normalising to the Zn isotopic composition of Brownfield 1937 produces; according to Luck et al. (2005), Zn in Allende being fractionated between - 0.13 to +0.37 ± 0.05^Y ‰ amu⁻¹, while for Orgueil between +0.38 to +0.41 ± 0.05. ‰ amu⁻¹, all relative to Brownfield-1937 (Luck et al., 2005b), compared to +0.54 ± 0.16, +0.46 ± 0.15 ‰ amu⁻¹ respectively for this work, Thus these normalized results agree within uncertainties, which are almost certainly underestimated by Luck et al. (2005), since they did not use any spike technique to correct for any introduced bias, as the researchers claimed that they have been able to extract Zn using anion exchange chemistry with an efficiency better than 99%, and performed extensive tests on standards as well as rock samples were carried out on complete duplicate, and triplicate analyses to confirm that the chemical procedure did not introduce isotopic fractionation (Luck et al., 2005b). The uncertainty quoted by Luck et al. (2005), is the overall precision or reproducibility on δ⁶⁶Zn of 0.04–0.05‰. It is important to note that, as discussed in Section 7.1, the contribution of the ion exchange chemistry to any measured fractionation is significantly greater than the claimed reproducibility of the measured fractionation by Luck et al. (2005). While high extraction efficiencies such as those obtained by Luke et al. (2005) are significant in terms of not losing precious and small samples, considerable care should be taken because of any unrecognised contamination which could be easily introduced to the Zn separation procedure. Using the double spike technique overcomes the necessity for high Zn extraction efficiency. As an example, the 100 ± 10% extraction efficiency of Zn achieved by Sivry et al. (2008) could be an example of unrecognised contamination.

^Y the accompanied uncertainty of the researcher was estimated for the δ⁶⁶Zn

These two points almost certainly explains the inconsistency of Luck et al. (2005) results for the Campo de Cielo meteorite; between + 3.40 ‰, and + 3.68 ‰ for $\delta^{66}\text{Zn}$ in two aliquots of one sample digestion, and + 0.95 ‰, and + 0.78 ‰ for $\delta^{66}\text{Zn}$ for two aliquots of other sample digestion of Campo de Cielo meteorite; which is obviously not within the uncertainty claimed by (Luck et al., 2005b).

The only previous double spike measurements for Zn in meteorites are those by Rosman (1972) for the Plainview meteorite of $+0.60 \pm 1.6 \text{ ‰ amu}^{-1}$ (95% confidence) relative to his laboratory standard. Despite the unknown relationship between standards, the measured fractionation for this meteorite in this work of $+0.31 \pm 0.10 \text{ ‰ amu}^{-1}$ (relative to the absolute); agrees with the previous results, but represents a sixteen fold improvement in the uncertainty and approximately 10 times smaller sample than those used previously by Rosman (1972) (see Section 3.4).

As Rosman (1972) measured Zn fractionation in both Plainview and Canyon Diablo meteorites using the double spike technique; a comparison of the fractionation relative to Canyon Diablo can be made. Accordingly, Plainview meteorite is fractionated by $+0.3 \pm 2\text{ ‰ amu}^{-1}$ relative to Canyon Diablo (Rosman, 1972b). On the other hand, Plainview is fractionated of $-0.80 \pm 0.15 \text{ ‰ amu}^{-1}$ relative to Canyon Diablo measured in this work.

In the study of Luck et al. (2005), a plot of $\delta^{66}\text{Zn}$ versus $\delta^{68}\text{Zn}$ values is represented in Section 2.2.2 (Figure 2.4), which should exhibit a mass-dependent slope of two. This type of representation is used to demonstrate that no interferences or other anomalies were affecting the measurements. While such a plot can be used to confirm the relationship between the ^{66}Zn and ^{68}Zn , it does not identify any possible anomalies in the other isotopes of Zn (^{67}Zn or ^{70}Zn or even both). This potential problem can be assessed in a more quantitative manner using the double spike technique by calculating the fractionation using different sets of isotopes. Using the $\delta^{66}\text{Zn}$ versus $\delta^{68}\text{Zn}$ plot, Luck et al. (2005) concluded that the primordial Zn reservoir (not reservoirs) was homogeneous, at least at some point during the evolution of the early

solar nebula (Luck et al., 2005b). This shall be more discussed in detail in Section 7.4.2.

The range⁹ of Zn fractionation in stone meteorites measured in this work is between -0.29 ± 0.1 to $+0.38 \pm 0.16$ ‰ amu⁻¹, appears to be consistent with previous research although more measurements would be needed to establish this for stone meteorites. The largest stony meteorite Zn fractionation measured thus far is for Allende, with a $+0.38 \pm 0.16$ ‰ amu⁻¹, which is consistent with the other bulk Carbonaceous Chondrite, Orgueil, $+0.30 \pm 0.15$ ‰ amu⁻¹, relative to the laboratory standard. Because the elemental abundances in CI Chondrite, Orgueil is considered to be representative of the Solar System; a significant question that needs to be asked is why the isotopic composition of Zn in Orgueil is different to that of bulk Earth. One possibility is that the portion of the solar nebula from which the inner Solar System bodies accreted e.g Orgueil and the Earth, was not completely homogeneous with respect to its Zn isotopic composition. Loss et al. (1994) discussed the anomalies they found in the Vigarano meteorite inclusions; such that; they indicated that, at the stage when condensates formed, the solar nebula was not well mixed or homogenized on a large scale, while more complete homogenisation may have occurred later during the latter stage of formation of the planets (Loss et al., 1994). In contrast Wombacher et al. (2008) showed that bulk Orgueil and the Allende meteorites contained indistinguishable Cd isotopic composition from terrestrial standard “JMC Cd”.

Xue et al. (1996) have shown that, Zn evaporation can lead to a residue which is enhanced in the heavy isotopes (Xue et al., 1996). Evaporation or condensation of Zn into or out of meteorites or their parent bodies could be a cause for Zn fractionation. As indicated in studies by Greenland and Goles (1965) and Larimer and Anders (1967), there is a suggestion that Chondrites are a mixture of materials from two different sources, one formed under low temperature and the other formed under high temperature”(Larimer and Anders, 1967, Greenland and Goles, 1965). If this is correct, the results for Chondrites in this work can be divided into two main groups,

⁹ The range calculated as the difference between the maximum value and the minimum value considering the uncertainty in each value.

“enhanced” and “depleted”. It is also possible that Zn fractionation in meteorites represents a primordial heterogeneity which has been preserved during the formation of the Solar System, an assumption made by Rosman et al. (1980) for Cd fractionation in Brownfield.

According to the results of this research, not all Chondrites are positively fractionated or enhanced in the heavy isotopes; Brownfield-1937, Brownfield-1964 are -0.157 ± 0.094 , and -0.287 ± 0.098 ‰ amu^{-1} respectively, relative to bulk Earth. Brownfield 1937 was measured by Luck et al.(2005) to be $\delta^{66}\text{Zn} -0.30 \pm 0.05$ ‰ relative to JMC 400882B (Luck et al., 2005b), while Brown field -1964 has not been measured previously. Although the magnitude and direction of the fractionation agree well within uncertainty, caution should be taken since the relationship between the laboratory standards are unknown. Luck et al.’s (2006) measurements of Brownfield and other Chondrites led them to infer that all chondrules contain “light”Zn (Luck et al., 2006). On the other hand, the Zn fractionation in the bulk samples of the Ordinary Chondrites measured in this research may indicate that Zn fractionation in ordinary Chondrites is related to the incomponents within Chondrites. Although in contrast to Ni, Zn is concentrated in non-metallic phases. It is also possible that Zn and Cu isotopes may be more fractionated in H than in L and LL Chondrites because of the larger size of chondrules in the latter (Moynier et al., 2007). While investigations of the isotopic composition of Zn in meteoritic components is outside the focus of this research, further isotopic studies of subcomponents may help unravel the extent of Zn variability in stony meteorites.

A similarity between the isotopic composition of Ni in Chondrites and iron meteorites for 36 bulk meteorites has been found by Cook et al. (2007), Cook’s data show isotopically similar to or heavier than their laboratory standard (SRM 986) with an average of $+0.14 \pm 0.11$, and $+0.12 \pm 0.17$ ‰ amu^{-1} for Chondrites, and iron meteorites respectively (Cook et al., 2007). This work shows that not all Chondrites are enhanced in the heavy isotopes of Zn, however determining a viable average for Zn fractionation for Chondrites is not possible based on the small number of samples analysed, and any comparison between average Zn and average Ni fractionation must consider the relative standard, which in the case of Ni we are unsure of. Any

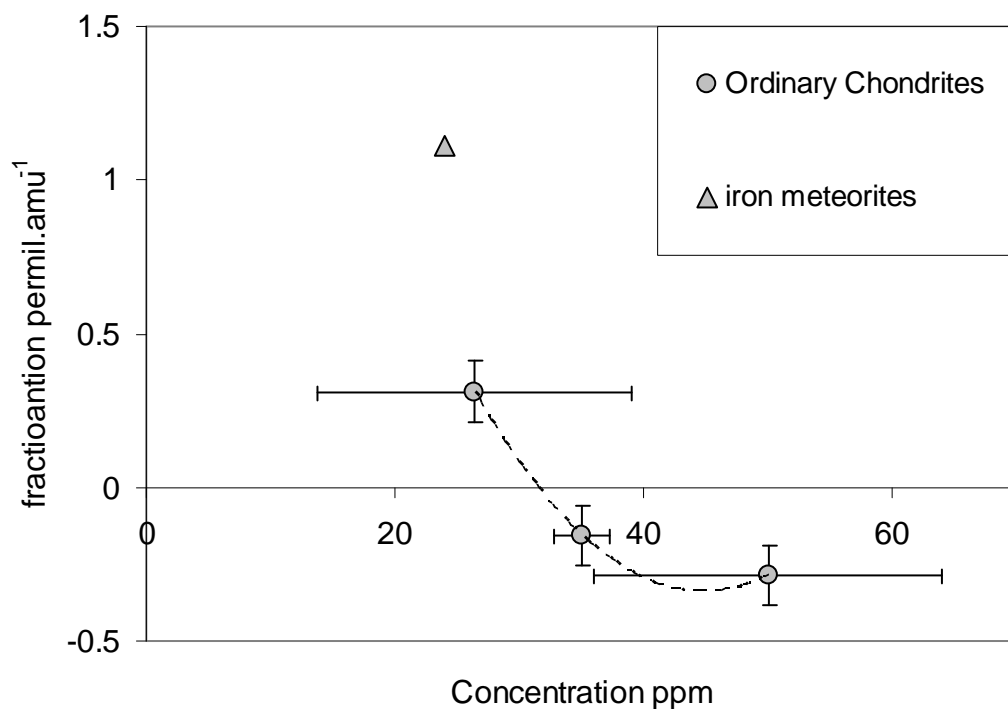
relationship between stone and iron meteorites in terms of Zn fractionation is impossible to assess because only two iron meteorites were analysed.

In 1976, Rosman and De Laeter used the double spike technique to discover a substantial fractionation for Cd ($+2.3 \pm 0.4 \text{ ‰ amu}^{-1}$) relative to their laboratory standard in the H3 Ordinary Chondrite Brownfield (Rosman et al., 1980, Rosman and De Laeter, 1976). In contrast, this work shows that, the two Brownfield meteorites are enhanced in the lighter isotopes of Zn (negative fractionation). One explanation for this is the significantly more volatile nature of Cd, and the existence of a number of highly thermally stable compounds of Zn (such as oxides) compared to Cd. To explain this let us consider a parent body containing Cd and Zn undergoing heating. Initially the lighter isotopes of Cd will preferentially evaporate because of its high volatility relative to Zn, while the Zn will be unaffected leaving the reservoir containing Cd enhanced in the heavier isotopes. Further heating will evaporate heavy Cd isotopes and light Zn isotopes producing a condensate which is consistent with the above findings. These significant differences could be used to explore the physical and chemical effects present in the early Solar System and Chondrite and other meteoritic component formation.

The relationship between the concentration and the isotopic fractionation of Zn in meteorites has been investigated by Luck, Othman and Albarede (2005). Their results showed that different samples of the same meteorite contained variable Zn concentrations and isotopic compositions, and suggested that this reflects the presence of minute Zn-rich phases and inclusions in the meteorites, which carry a different isotopic composition and concentration. More recently Wombacher et al. (2008) examined the relationship between Cd isotope fractionation and Cd concentration for lunar soils, where the data can be described by suppressed Rayleigh distillation from unfractionated starting materials, or by two-component mixing between end members with heavy Cd isotope composition. The correlation (mixing line) between the fractionation and concentration for Cd in lunar samples requires that the lunar starting material had a homogeneous Cd isotope composition and concentration (Wombacher et al., 2008). Although the data obtained in this work is limited for both the concentration and the fractionation, the results obtained may represent a similar relationship for Zn in Ordinary Chondrites for that of Cd in lunar soil. Figure 7.6 shows a possible relationship for the concentrations and the fractionation of the

meteorites concerned. Although the uncertainties are large, the relationship can't be excluded and needs further investigation. Relationships between the concentration and the Zn isotopic fractionation are not new for meteorite interpretations and have been used to explain the decrease of $\delta^{66}\text{Zn}$, from CI to unequilibrated ordinary Chondrites (UOC) meteorites (Luck et al., 2005b). In contrast, Ni fractionation in meteorites does not show any relationship with Ni content (Cook et al., 2007). If a relationship between the concentration and fractionation of Zn in Ordinary Chondrites introduced in this work exists (see Figure 7.6), it is most likely that the concentration and the fractionation of Zn in ordinary Chondrites represents a (mixing curve) which may require that the all ordinary Chondrites had a homogeneous isotope composition and concentration for Zn in solar starting material. This is an explanation introduced by Wombacher et al. (2008) interpreting the correlation between the fractionation and concentration for Cd in lunar samples.

Figure 7. 6: Concentration and the average fractionation of Zn in measured stony meteorites. The large uncertainties in the concentration are due to the range of values obtained.



7.4.2 Iron meteorites

As described in the overview and types of samples Section (3.8.1), Canyon Diablo is a coarse octahedrite, with a Zn fractionation, relative to the Zn absolute isotopic composition (AE 10759), of $+1.11 \pm 0.11 \text{ ‰ amu}^{-1}$. This makes it one of the largest fractionation values measured in this work. The deviation of the isotopic composition relative to the laboratory standard (proposed absolute) is represented in Figure 5.9 which clearly shows a fractionation of $+1.6 \pm 0.2 \text{ ‰ amu}^{-1}$. Correction for during analysis fractionation was performed on the laboratory standard the sample, this was done by applying an internal normalization to the measured ratios relative to their average $^{68}\text{Zn}/^{64}\text{Zn}$ ratio.

This result ($+1.11 \pm 0.11 \text{ ‰ amu}^{-1}$) agree with that measured by Luck et al's in 2005 $\delta^{66}\text{Zn} = 2.10 \pm 0.05 \text{ ‰}$ in bulk sample, or a fractionation of $+1.05 \pm 0.03 \text{ ‰ amu}^{-1}$ (not double spiked). Canyon Diablo was also measured by Rosman in 1972 using the double spike technique and found to be $+0.27 \pm 1.3 \text{ ‰ amu}^{-1}$ relative to his laboratory standard which also agrees within uncertainty. One way to compare the results of Rosman to that of this work is to compare the fractionation difference between Plainview relative to Canyon Diablo, for which Rosman obtained $+0.3 \pm 2.0 \text{ ‰ amu}^{-1}$, while this work obtained $-0.80 \pm 0.15 \text{ ‰ amu}^{-1}$. Unfortunately the large uncertainties do not allow for a precise enough comparison, but the values are well within uncertainty. A significant Zn reservoir in Canyon Diablo would surely be the Troilite (FeS), which together with other components require further exploration. According to Luck et al. (2005b), the IAB-IIICD group shows large (3‰) variations of $\delta^{66}\text{Zn}$ negatively correlated with $\delta^{65}\text{Cu}$ (1‰), where the isotopic and concentration data on the metal phase and troilite in Canyon Diablo show that this trend is unlikely to result from sulfide fractionation (Luck et al., 2005b). As emphasized by the recent study by Monynier et al. (2007), the available data on this meteorite remains fragmentary, and even a limited investigation may significantly change the current comparative stable isotopic geochemistry of Ni, Cu, Zn and Fe interpretations in iron meteorites.

Any similarity between the iron and stone meteorites in terms of concentration or isotopic composition would suggest a common parent body or solar nebula reservoir. These suggestions were first introduced for linking different meteorites relative to their O isotopic fractionation (Clayton and Mayeda, 1978), and are worthy of consideration for similar Zn studies. Unfortunately, any relationship between the concentrations of Zn and fractionation in iron meteorites can't be confirmed by this work due to a lack of results for Zn fractionation in most iron meteorites. This is due primarily to the relatively low Zn concentration in iron meteorites relative to other meteorites, and a reluctance to consume larger amounts of rare samples, since $\sim 1\mu\text{g}$ of Zn was needed for precise isotopic measurements, while some iron meteorites were of low Zn concentration as $\sim 19\text{ ngg}^{-1}$. One of the recommendations of this research to further reduce the amount of Zn required in order to perform a precise isotopic measurement.

Comparing these fractionation results with those previously reported for Ni could provide valuable information on this process. Canyon Diablo has been measured for Ni fractionation and showed $\delta^{61/58} = +0.39 \pm 0.06\text{ ‰}$ (not double spiked) (Cook et al., 2007). Since no isotope anomalies were observed for Ni, this led them to conclude that Ni isotopes were fractionated from an initially homogeneous reservoir. The Ni fractionation observed by Cook et al. (2007) is significantly less than that found in this research for Zn ($+1.11 \pm 0.11\text{ ‰ amu}^{-1}$), although both fractionation represent an enrichment in the heavier isotopes relative to their laboratory standards. The greater fractionation for Zn than Ni is consistent with the greater volatility of Zn relative to Ni, and that Ni is siderophilic (compatible with Fe), where as Zn is chalcophile (compatible with S). These results clearly point to a need for a detailed isotopic study of iron meteorites components.

7.4.3 The Redfields anomaly

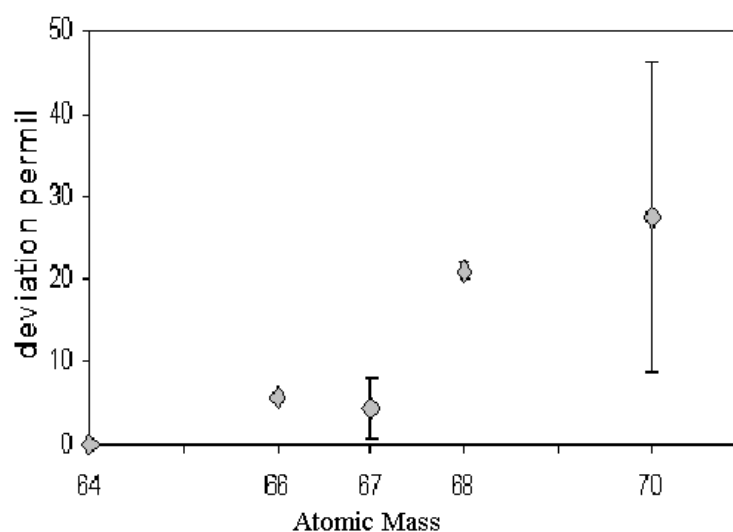
7.4.3.1 Interpreting the data

The other iron meteorite measured in this research is Redfields. As described in Section 3.8.1, Redfields is an unusual meteorite found in Wongan Hills district-Western Australia. The significance of this meteorite is that it does not fall readily

into any recognised class. According to its Ni abundance of 6.65 %, Redfields is close to group IIB, but lies outside the normal limits for this group (De Laeter et al., 1973). The isotopic composition and Zn concentration of this meteorite was measured in this work and the results are as represented in Section 5.5.4.2.1 (Table 5.21) and Section 4.5.2 Table 4.15 for the Zn concentration. This meteorite clearly showed an anomalous isotopic composition. This abnormality in the isotopic composition was discovered during the calculation for the fractionation by “double spiking” when the fractionation calculation using two sets of isotopes failed to agree within their uncertainty, despite the fact that any contribution from any interference was confirmed to be negligible. In order to fully explore the extent of the anomaly, measurements were repeated three times and from three different dissolutions without double spiking, using the same dissolution procedure of the iron meteorites (see Section 3.9.2). The possibility of isobaric ^{64}Ni interference on ^{64}Zn was very closely monitored confirming that any ^{64}Ni interference was always less than 0.06‰ relative to ^{64}Zn . The sample was placed in the TIMS bracketed the analysis of two laboratory standards, as described in Section 3.5 (isotopic analyses method). The only exception in measuring the isotopic composition of Zn in Redfields meteorites was the use of ion beam of $\leq 4 \times 10^{-13}$ A in experiment three (see Table 5.21), this was reflected on the larger uncertainty accompanied with experiment three.

As for all cases such as this, when major anomalies occur, possibly in conjunction with significant isotopic fractionation, determining exactly what is anomalous or otherwise becomes difficult. Using ^{64}Zn as a reference isotope, Figure 7.8 shows that data taken direct from the mass spectrometer contains significant differences of $+5.6 \pm 0.4\%$, $+4.4 \pm 3.6 \%$, and $+21.0 \pm 0.9 \%$ and $+27.4 \pm 18.8 \%$ on ^{66}Zn and ^{67}Zn , ^{68}Zn and ^{70}Zn respectively indicating that this meteorites possesses a significantly different Zn isotopic composition to all of the other natural materials measured. This could be related to the unusual chemistry of this meteorite, but even so to explain these differences are relatively difficult.

Figure 7. 7: Deviation in ‰ of the average of three independent measurements of the isotopic composition of Zn in Redfields iron meteorite, relative to the isotopic composition of Zn in laboratory standard. Ratios are not corrected for machine bias.



All accompanied uncertainties are 95% confidence and do not include any corrections for the machine fractionation.

The first Zn anomaly in natural materials was reported by Loss and Lugmair in 1990, with a ^{66}Zn isotopic anomaly of $\leq +1\epsilon$ in Allende inclusions. They suggested that any large ^{66}Zn anomaly might be diluted before and to a lesser extent during the early stages of CAI formations (Loss and Lugmair, 1990). The second $+16.7\epsilon$ ^{66}Zn anomaly was reported by Volkening and Papanastassiou (1990) for Allende FUN inclusion EK 1-4-1. Another Zn anomaly was found in a CAI inclusion of Vigarano in 1994 by Loss et al. of $-6.5 \pm 1.5 \epsilon$ on the ^{66}Zn , indicating a large scale inhomogeneity of the condensates which formed the solar nebula (Loss et al., 1994).

The magnitude and type of these anomalies found in this research in Redfields are clearly unusual and represents abnormal isotopic composition with large difference relative to bulk Earth, and it is the first of its kind for the isotopic composition of Zn in natural materials. It is also a significant that it is in the bulk meteoritic sample and not in the inclusions. Ubiquitous isotope anomalies have been reported in bulk meteorites for elements such as Ti (Niederer et al., 1985), primarily in primitive meteorites. A complication in interpreting these anomalies is that no other isotopic composition has ever been measured in this meteorite, and few concentration data are

available, and what is available remains inconclusive, The Redfields anomaly raises a number of interesting questions including,

- How could large non-linear isotope anomaly which are usually attributed to remnant of nucleosynthetic processes, occur?
- How could such a large isotope anomaly survive the formation of the Solar System and formation of its planetary body?

7.4.3.2 Nucleosynthetic consideration

To interpret the isotopic composition of Zn in the bulk Redfields requires a consideration of the nucleosynthetic production processes of each of the Zn isotopes. The majority of Zn in Solar System is considered to have been produced by a late stage stellar evolution process known as Nuclear Statistical Equilibrium (NSE), (Hartmann et al., 1985). The main difficulty in interpreting the Redfields anomaly is determining the base line for which the systematic variation in the Zn isotopic abundances can be clearly identified, and in particular what to use as a reference isotope, especially if all isotopes are affected. This is further discussed below. The Redfields type isotope anomalies are normally interpreted as a combination of average Solar System Zn and reservoirs containing excesses and or depletions resulting from nucleosynthetic processes (Lee, 1988).

As shown in Table 7.4, Zn isotopic variation for the Redfields meteorite, reference to different isotopes relative to the laboratory standard. Figure 7.7 shows the deviation of the average isotopic composition of Redfields relative to the isotopic composition of Zn of the laboratory standard is as follows: $+5.6 \pm 0.4\%$, $+4.4 \pm 3.6 \%$, and $+21.0 \pm 0.9 \%$ and $+27.4 \pm 18.8 \%$ for $^{66}\text{Zn}/^{64}\text{Zn}$, $^{67}\text{Zn}/^{64}\text{Zn}$, $^{68}\text{Zn}/^{64}\text{Zn}$ and $^{70}\text{Zn}/^{64}\text{Zn}$ respectively. The results are shown relative to ^{64}Zn because this how it was measured, and because ^{64}Zn isotope is one of the least affected according to the Multi Zone mixing model (MZM) (Hartmann et al., 1985, Loss and Lugmair, 1990).

Table 7. 4: Zn isotope variation (Zn*) for the Redfields meteorite, reference relative to different isotopes relative to the laboratory standard %.

Reference	⁶⁴ Zn*	⁶⁶ Zn*	⁶⁷ Zn*	⁶⁸ Zn*	⁷⁰ Zn*
⁶⁴ Zn	0.0	5.6 ± 0.4	4.4 ± 3.6	21.0 ± 0.9	27.4 ± 18.8
⁶⁶ Zn	-5.5 ± 0.4	0.0	-1.2 ± 3.6	15.4 ± 0.9	21.7 ± 18.7
⁶⁷ Zn	-4.4 ± 3.6	1.2 ± 3.6	0.0	16.6 ± 3.8	22.9 ± 19
⁶⁸ Zn	-20.6 ± 0.8	-15.1 ± 0.9	-16.3 ± 3.6	0.0	6.2 ± 18.3
⁷⁰ Zn	-26.6 ± 17.7	-21.2 ± 17.9	-22.4 ± 18.0	-6.2 ± 18.2	0.0

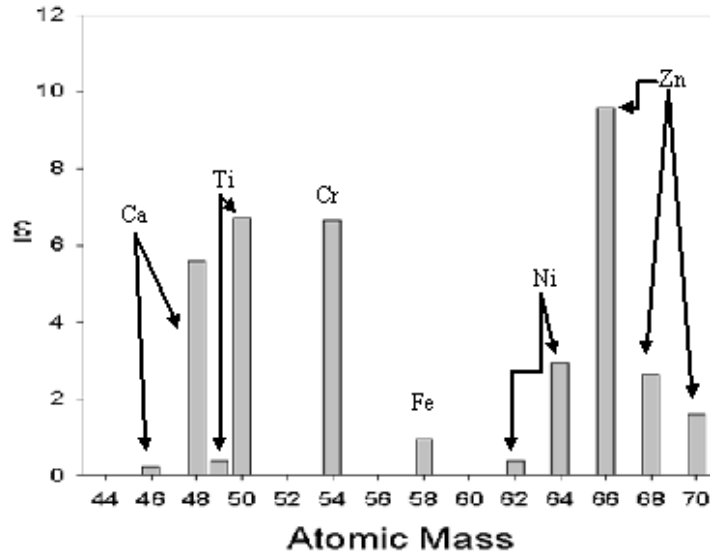
Assuming that Redfields is not fractionated relative to the “laboratory standard”; the clearest anomalies are on the ⁶⁶Zn (⁶⁶Zn*) and ⁶⁸Zn (⁶⁸Zn*), and to a lesser extent on the ⁶⁷Zn (⁶⁷Zn*) and ⁷⁰Zn (⁷⁰Zn*) isotopes. A simple explanation for an anomaly on the ⁶⁸Zn and ⁷⁰Zn could be in terms of the rapid neutron capture “r” process, which is also known to synthesize these isotopes in what is known as the neutrino driven neutron star wind. Such a mechanism has been considered for the r-process and the Zn synthesis was found to be very sensitive to the wind condition factors such as neutron excess (Hoffman et al., 1996, Umeda and Nomoto, 2002).

There is little more that can be obtained from these results to confirm these explanations without detailed analysis of the isotopic composition of other elements. One interpretation for Zn isotope anomalies in meteorites is the “MZM” for isotopic anomalies found in CAIs, particularly for the neutron rich isotopes of Ca, Ti, Cr, and Ni, and predicted for ⁶⁶Zn and ⁶⁸Zn. According to the MZM, zones evolving deep within a star characterized by different neutron enrichments and thus give rise to products with different mass yields for various nuclear species. During the ejection process of matter from the exploding star, products from multiple zones are mixed. It is remarkable even following the 4.5 Ga life of the Solar System that mixing processes within the Solar System allowed the isotopic signature of exotic components to survive. An illustration of the prediction of the “MZM” anomalies for elements is represented in Figure 7.8. According to the “MZM” model, a (⁶⁶Zn*) / (⁶⁸Zn*) of 4, is predicted (see Figure 7.9). In Redfields we observe a (⁶⁶Zn*) / (⁶⁸Zn*)

* represents anomaly

of $\sim 1/5$. While this does not agree with MZM, it could represent the complement of predicted MZM component for CAI inclusions.

Figure 7. 8: The prediction of MZM anomalies for elements by (Hartmann et al., 1985) presented in (Loss and Lugmair, 1990).



Returning to Table 7.4, let us consider ^{66}Zn and ^{68}Zn in turn to be the least affected in the Redfield anomaly. In the case of $^{66}\text{Zn}^* = 0$, this reduces the positive anomalies in the 68 and 70, and produces a deficiency in the 64. In the case of $^{68}\text{Zn}^* = 0$, this makes both 64 and 66 even more deficient while the 68 and 70 are essentially zero. Both of these possibilities are difficult to explain in terms of known nuclear synthetic processes.

Let us now consider the possibility of a combination of fractionation and isotopic anomalies such as are found in the “FUN CAIs” (fractionation and unknown nuclear isotopic effects) in the Allende meteorite (Wasserburg, Lee & papanastassiou 1977)

As observed in Figure 7.8, depending on which pair of isotopes is used, a linear fractionation can be fitted to the data of between 1.5 and 5 ‰ amu^{-1} if the Zn is fractionated anywhere in this range this represents the largest fractionation observed in meteorites. At the lower end of the fractionation range, this is close to the fractionation measured in Canyon Diablo ($+1.11 \pm 0.11$ ‰ amu^{-1}) and similar to the magnitude of the fractionation for Cd in bulk meteorites by Rosman and De Laeter

(1976). At the upper end of the fractionation range 5‰ amu^{-1} is similar to that found for some high purity Zn materials (see Section 5.5.1) that could be an indication of what causes large fractionation. If any, fractionation is present, small anomalies still clearly appear to reside on top of this fractionation. To illustrate this let us consider a fractionation line as represented by the ^{64}Zn and ^{67}Zn isotopes; this makes both ^{66}Zn and ^{68}Zn positively anomalous, and the MZM discussions as represented previously can be used to explain these residual anomalies. The main difficulty in interpreting the abnormality in the isotopic composition of Zn in Redfields meteorite is determining which reference isotope to use and the extent of any superimposed fractionation. It is possible to interpret the results as a combination of an anomalous $^{66}\text{Zn}^*$ and $^{68}\text{Zn}^*$, and fractionated Zn similar to that found in FUN inclusion in the Allende meteorite. Other combinations of fractionation and anomalies can be determined from these results, for example, a negative anomaly on the ^{67}Zn and ^{70}Zn superimposed on a $+5\text{‰ amu}^{-1}$ fractionation. However, this example or other combinations can't be easily explained. Anomalous isotopic composition observed in Allende in macroscopic samples and in bulk iron meteorite samples was discovered for Mo by Dauphas et al. (2002) and interpreted as either excess in p- and r-process material, or a corresponding deficit in s-process nuclides. In either case, the researchers suggested that the observed anomalies provide evidence for large-scale inherited isotope heterogeneity of the protosolar nebula (Dauphas et al., 2002). Unfortunately, Dauphas et al. (2002) did not measure any isotopic composition of other elements such as, Zn, Ti, Cr, or Ni.

7.4.3.3 Planetary science considerations

Whether Redfields is a primitive type of iron meteorite or not, the Redfields anomaly strongly suggests isotopic heterogeneity and does not support the conclusion by Luck et al. (2005) that “Zn was derived from an initially single homogeneous reservoir” (Luck et al., 2005b). One explanation is that Redfields is a type of primitive iron meteorite originating from a parent body that has formed within its own isotopically anomalous reservoir. If so, then, this represents the possibility for a very large isotopically unique reservoir from which to form a parent body, given that an iron type core is required to be generated, similar reservoirs, large enough to be cosmochemically differentiated than has been previously reported (Loss and Lugmair, 1990, Loss et al., 1994). Comparisons between these results are complicated because

the Loss et al. (1990, 1994) anomalies were found in meteoritic inclusions whereas this work is for a bulk meteorite. However, both anomalies are strong evidence for large scale inhomogeneity at the time condensates, and major parent bodies, formed in the solar nebula.

Clearly one of the recommendations of this work is to further investigate the isotopic composition and the concentration of Zn and other iron peak elements and transition elements in the Redfields meteorite and its components.

7.5 Water

The significance of water in the hydro-geo-bio cycles of the Earth means that in any study of Zn isotope variations it is essential that Zn in various waters be examined. Zinc in water is well known, and has potential special significance in global scale environmental effects, such as in the Zn hypothesis (Morel et al., 1994a).

Measurements of the isotopic compositions of Zn in various waters were attempted as a pilot with mixed success. While the concentration of Zn in river and tap water samples were being measured, the fractionation measurements were able to be performed, using the less precise (albeit more sensitive) Daly detector on the mass spectrometer. This detector was used because of very low concentration of Zn in the river water (ngg^{-1}) and unrestrained (fresh) tap water. However, the fractionation uncertainties obtained are relatively large. To obtain sufficient quantities of Zn to be measured using the Faraday, at least ten times more sample (~ 150 g) than what was collected would need to be used. The average Zn fractionation measured in this research is shown in Table 7.5 as a summary taken from Section 5.5.6 in Table 5.23.

Table 7. 5: Summary of Zn fractionation of water samples measured in this research

Source	f ‰ amu ⁻¹ Using ⁶⁴ Zn, ⁶⁷ Zn, ⁶⁸ Zn, ⁷⁰ Zn
Swan river -Victoria Park	-1.4 ± 0.9
Swan river- Bayswater	-0.81 ± 1.09
(Swan River)	-1.09 ± 0.70
Restrained tap water	-6.4 ± 0.7
Unrestrained (fresh) tap water	0.6 ± 2.7

These relatively large fractionation values obtained offer considerable promise for future fractionation measurements of low level, ngg⁻¹, Zn concentration samples such as river and potable water. Unfortunately, there was insufficient time to further investigate these samples.

7.5.1 Swan River water

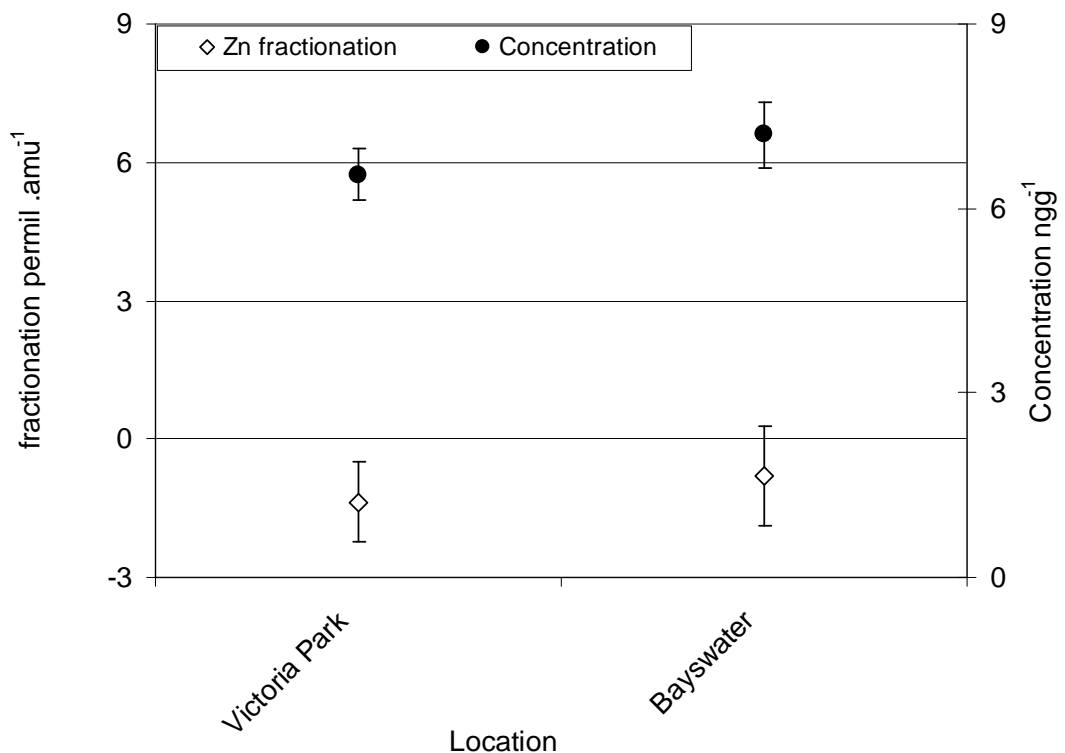
The concentration and the isotopic composition of Zn in Swan River water are represented as in Figure 7.10 which shows that, the concentration of Zn in Swan River did not change from the “Victoria Park” location to “Bayswater”, located some 6.4 km upstream, with a combined average of 6.9 ± 0.8 ngg⁻¹. In terms of location, the Victoria Park Location is within the oceanic or saline encroachment zone of the river whereas Bayswater location is nominally in the freshwater zone for at least part of the year.

Similar to the concentration of Zn, the isotopic fractionation also did not change between locations, this was expected because the Swan River is not restrained, and flows towards the ocean with a relatively strong current during the major rainfall seasons. The average Zn fractionation is -1.09 ± 0.70 ‰ amu⁻¹, which is much larger than all other natural samples, although the uncertainty is also significantly greater due to the use of the Daly detector. It is possible that this measured fractionation is due to Zn leached into the river from fertilizers used on nearby agricultural land and other anthropogenic sources. This interpretation is also supported by the following two factors, firstly, the high concentration of Zn in these waters as explained in

Section 6.5. Secondly, the similarity between the concentration of Zn in the samples and the measured isotopic fractionation in the two locations (see Figure 7.9).

A recent study by Balistrieri et al. (2008) in river waters showed that isotopic fractionation values for Zn are generally invariant at low pH (4.0); with $\delta^{66}\text{Zn}$ averaging $0.09 \pm 0.03\text{‰}$ (relative to their laboratory standard) (Balistrieri et al., 2008).

Figure 7. 9: Average isotopic fractionation and concentration of Zn in Swan River in two different locations



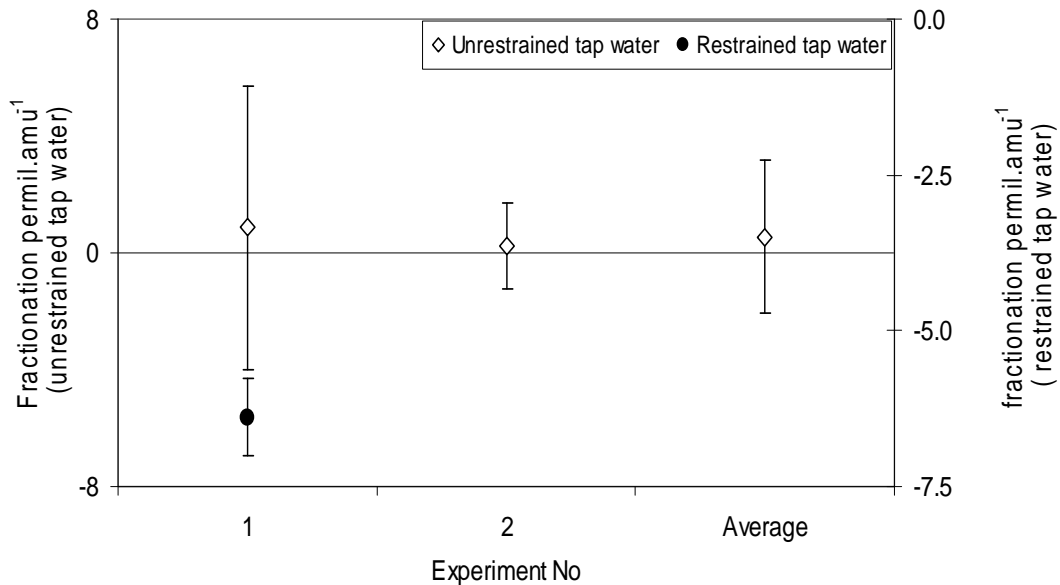
As fractionation of Zn due to anthropogenic processes was not the aim of this research, this was not followed up, and no further samples were examined. Nevertheless, the results obtained indicate that this aqueous system should be further explored. Soil and fertilizers, and for example, water samples could be analyzed as a function of weather, season, and following fertilizer application, to assess the systematics of Zn into, and within the river. Although water samples were collected from two locations only of Swan River, the results might be considered as an indication to the possibility of using this approach to investigate the mixed natural and anthropogenic environments such as agriculture, where fertilizers, soils, waters and plants can be examined. It is also possible that other anthropogenic sources, such

vehicle and factory emission, and mining wastes could be traced in this way in the environment.

7.5.2 Tap water

The concentration and isotopic composition of Zn was also investigated in restrained and unrestrained (fresh) tap water. The results for the isotopic composition are as presented in Section 5.5.6 and as illustrated in Figure 7.10. The large uncertainty accompanying these results is due to the use of the less precise Daly detector, since the experiment did not aim to measure Zn isotopic fractionation, but the concentration of Zn in the samples.

Figure 7. 10: Isotopic fractionation of Zn ‰ amu⁻¹ in tap water (unrestrained (fresh) tap water and restrained tap water)



Although the uncertainties are large, Figure 7.10 shows, the Zn isotopic composition in unrestrained (fresh) tap water is not fractionated relative to the laboratory standard. In contrast, the restrained tap water shows an isotopic composition of -6.39 ± 0.62 ‰ amu⁻¹ relative to the laboratory standard. The simplest explanation is that the unrestrained (fresh) water represents the isotopic composition of the water source, while the Zn in restrained water contains an additional source of Zn, which is most likely to be the pipes or solders used to join the pipes themselves. While there is sufficient Zn in the restrained water and the pipes to examine this effect, a lack of time did not allow this to be further explored and is a major recommendation of this work.

7.6 High purity Zn metals

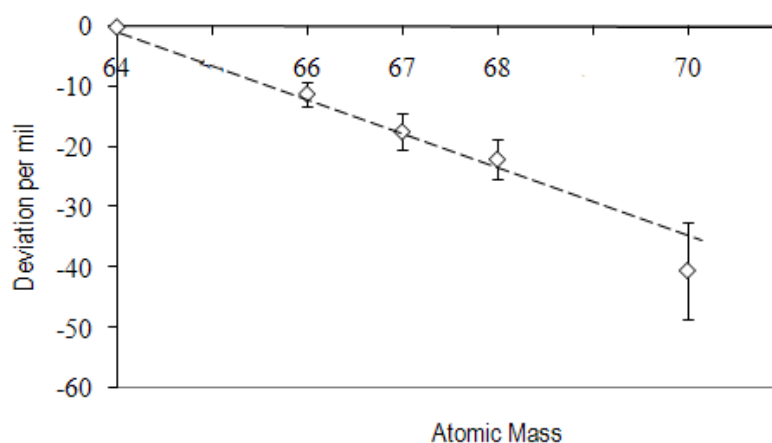
A variety of high purity Zn metals provided by IRMM were measured for their Zn fractionation relative to the laboratory standard “ δ zero”. Accordingly, the absolute Zn isotopic composition for these pure metals (commonly used as laboratory standards) was calculated as presented in Section 5.5.1. The aims of measuring these materials was that Zn absolute isotopic composition of these laboratory standards will serve as a valuable resource for analysts in order to accurately measure Zn fractionation. More over, these will provide a metrological base line for Zn isotopic compositions to be exploited by the international scientific community for future Zn investigations. This will enable analysts to measure Zn isotopic fractionation and compare their results with others, hence contribute to greater understanding of the Zn fractionation.

Another rationale for measuring pure standard metals is to determine the extent of Zn isotope variation among anthropogenic products (John et al. 2007). The results of such studies add to the knowledge of whether the range of Zn fractionation found in laboratory standards are a common feature of refined Zn metals, or if they result from extra purification steps unique to laboratory standards. The study of John et al. (2007) addressed the important of Zn fractionation to better understand how Zn isotopes may be used as tracers of anthropogenic contamination, where raw Zn metal is the precursor used to make many Zn-containing products, such as paints, rubber, hardware, and brassware. Their results obtained using a Cu elemental spiking technique, showed $\delta^{66}\text{Zn}$ (seven samples) range from -9.15 ‰ to $+0.17\text{ ‰}$, relative to Lyon-JMC Zn laboratory standard. None of the seven measured Zn pure standard materials was compared to the internationally (δ zero) or measured in this work. This severely limits the use of these results by other researchers.

As represented in Section 5.5.1, the isotopic fractionation of Zn in high purity metals was measured relative to the laboratory standard Alfa Aesar 10759 (δ zero). Figure 7.11 shows a plot of the difference of the isotopic composition of Zn in Alfa Aesar 10760 compared to the laboratory standard (Alfa Aesar 10759). Such a plot of the Zn

fractionation is used as an indication for the Zn fractionation in some highly fractionated materials but is inadequate for the Zn fractionation to be measured accurately. This is further explained in the coming paragraph where the slope of the line is calculated.

Figure 7. 11: Deviation of the isotopic composition of Zn in Alfa Aesar 10760 relative to the laboratory standard (Daly detector, not double spiked) showing a clear fractionation line of -6.34 ± 0.21 ‰ amu^{-1} uncertainty obtained using the weighted slope)



The accompanying uncertainties in Figure 7.11 are the 95% confidence. The measured ratios were normalized relative to their average $^{68}\text{Zn}/^{64}\text{Zn}$ ratio in both the laboratory standard and the sample, in order to minimize the effect of during-analysis fractionation. While the accompanying uncertainties are less precise relative to double spike determined fractionation measured in this research, this is primarily the result of using the less precise Daly detector. However, the fractionation line of -6.34 ± 0.21 ‰ amu^{-1} , clearly does not agree with the calculated Zn fractionation of Alfa Aesar 10760 using the double spike technique -5.1 ± 0.4 ‰ amu^{-1} (see Table 5.5) in Section 5.5.1.

It is important to comment on the uncertainties obtained for both approaches. The 0.21 ‰ uncertainty is determined using the weighted slope while the 0.4 ‰ represent a full external uncertainty budget using the double spike technique. The difference between the measured fractionation using the classical approach (-6.34, obtained by measuring the isotopic composition of the sample, and -5.4, represents the biases in the measurement, corrected by the double spike technique which is more accurate

result. A summary of the measured Zn fractionation for the pure Zn metal measured in this research is shown in Table 7.6. (Summary of Table 5.5 in Section 5.5.1).

Table 7. 6: Summary of the average fractionation of pure Zn metal relative to the laboratory standard (proposed absolute)

Standard Zn metal	Average fractionation ‰ amu ⁻¹	± ‰ amu ⁻¹
IRMM 10440	0.12	0.16
GF 6120	-0.09	0.14
Alfa Aesar 10759 (Laboratory standard)	0.01	0.04
ZnO6	-4.52	0.13
IRMM 3702	0.09	0.18
GF 6110	-0.21	0.18
IRMM 10760	-5.11	0.4
JMC-2	0.04	0.14

As shown on Table 7.6, the isotopic fractionation of Zn in the pure Zn metal standards ranged from $+0.04 \pm 0.14$ for JMC-2 to -5.1 ± 0.4 for ac AE 10760 ‰ amu⁻¹, relative to the absolute Alfa Aesar 10759. This is significantly higher than the measured fractionation range of Tanimizu and Hirata (2002) for pure Zn standard materials of -2.4 ± 1.2 ‰ amu⁻¹ for SRM 682 relative to their laboratory standard Zn JMC (an absolute comparison can't be made because of unknown absolute fractionation of their standard).

The effect of chemical processing on Zn isotopic composition was investigated as early as 1948 by Hess and his colleagues who claimed that Zn purification processes by evaporation, and Zn production by electrolytic or chemical reduction of the ore does not change its isotopic abundance. The work of Gramlich and Machlan (1985) detected Ga isotopic fractionation approaching 1 %, suggesting that isotopic fractionation was possible during the recrystallization, and thus variations among lots and manufacturers depending upon the exact treatment of the material (Gramlich and Machlan, 1985).

As all these standard materials were produced in industrial scale processes, these may contribute to fractionating the Zn in these materials, e.g. distillation can produce a depletion in the Zn heavy isotopes (Tanimizu et al., 2002). This suggestion does not explain why the high purity proposed absolute standard (Alfa Aesar 10759) has the same isotopic composition of Zn as igneous rocks and other types of rocks. It is also important to mention the study by John et al. (2007) where they measured the isotopic composition of Zn in seven pure Zn metal samples and found that differences in the purification method used, or use of multiple additional purification steps, may also contribute to a significant variability in isotopic composition of Zn.

To further investigate if any relationship exists between chemical purity and isotopic composition, the isotopic fractionation of these metals is plotted as a function of their % impurity, as represented in Figure 7.12. The fractionation is plotted as a function of impurity to more clearly show any clustering of the samples. Clearly shown in this Figure is the agreement between the laboratory standard (Alfa Aesar 10759) and (δ zero) which is to be expected given they are from the same stock or reservoir. Although the types of purification processes specifically used for these metals is unknown; there appears to be some clustering of the data. Apart from laboratory standards (Alfa Aesar 10759 and 3702) and GF 6110, the other metals appear to follow a relationship between Zn fractionation and the purity with higher purity samples being more negatively fractionated. The reason that Alfa Aesar 10759, 3702 and GF 6110 do not fit this relationship could be a result of different processing. Such relationship is consistent with the finding of Gramlich and Machlan in (1985) for Ga.

Figure 7. 12: Zinc isotopic fractionation of pure Zn standard metals relative to Alfa Aesar 10759 “proposed absolute” versus their impurity

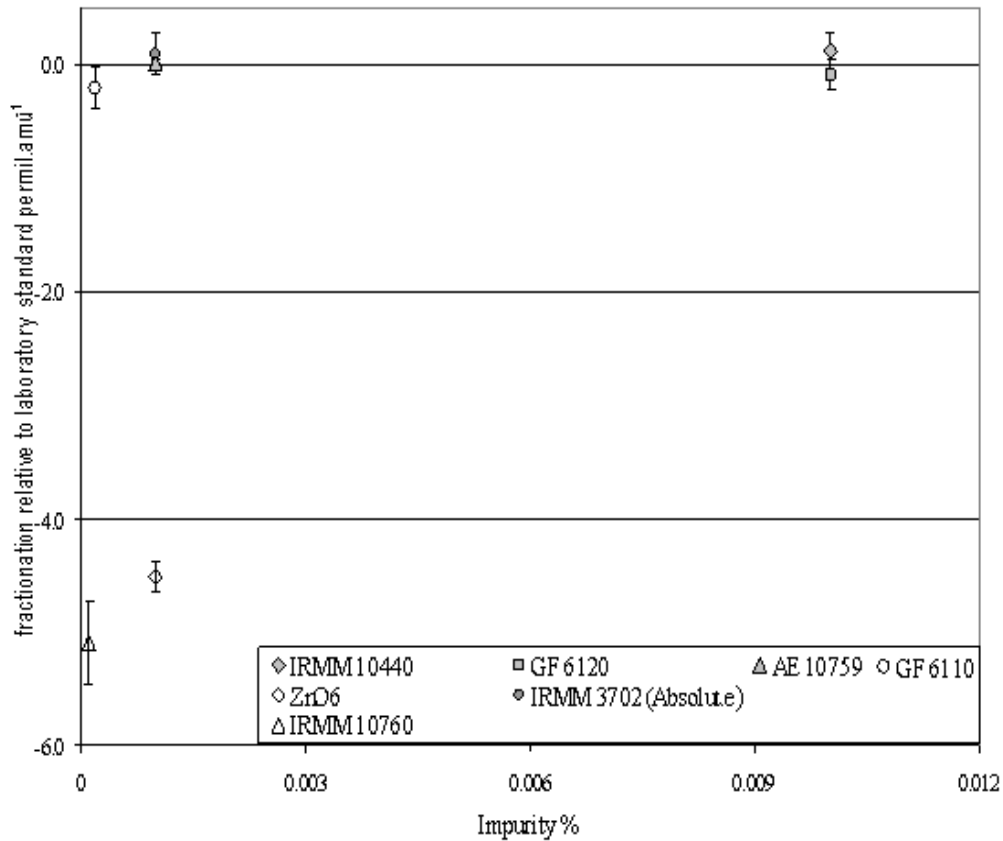
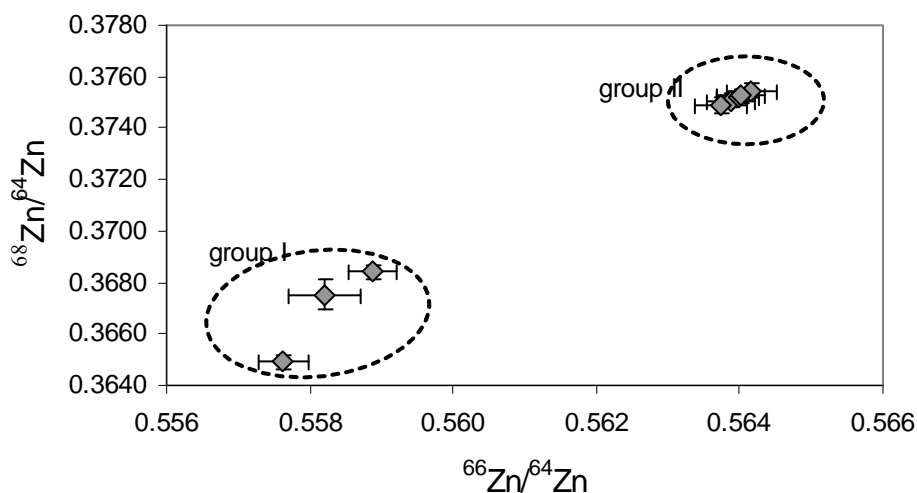


Figure 7.13 shows a “three isotope plot” of $^{68}\text{Zn}/^{64}\text{Zn}$ versus $^{66}\text{Zn}/^{64}\text{Zn}$ for these high purity metals. All samples fit into two groups. In group I (IRMM 10440 with purity 99.99, ac AE 10760 purity 99.9999 and ZnO6 purity 99.999), group II (IRMM 3702, Alfa Aesar 10759, GF 6110, GF 6120, with purity 99.999, 99.999, 99.9998, 99.99 respectively, also JMC-2 with unknown purity). It is important to mention that, this group includes “natural Zn” or “ δ zero” which is the same as the isotopic composition of Zn in bulk Earth. The groups are not characterized by common metal purities but may be grouped according to their metal source, or and more likely according to common artificial processes that the metals went through before production. As the sources and processes are unknown this can’t be further investigated. The study by John et al. (2007) discussed whether these large fractionation are caused by either the type of refining process, or if they result from extra purification steps unique to laboratory standards. If there is no fractionation produced during the production process, or if the raw Zn starting materials are completely consumed during production, the Zn isotope ratio of these products should match the Zn isotope ratio

the Zn raw material, with an expected $\delta^{66}\text{Zn}$ from +0.1‰ to +0.3‰ (John et al., 2007).

Figure 7. 13: Three isotope plot for number of pure Zn standard metals. Uncertainties in graph are 95% confidence level.



As represented in Figure 7.13 (3 isotope plot), the differences in the isotopic composition of Zn can potentially be used as an environmental tracer, to trace the movement and source of natural and anthropogenic Zn in the environment this requires the isotopic composition of anthropogenic Zn be known as that the processes that mix anthropogenic and other sources that lead to deviations from this composition can be explored as an environmental tracer (John et al., 2007). The three isotopic plot as represented in Figure 7.13 could be the evidence of the conclusion by Weiss et al. (2007) such that; the isotopic composition of Zn be used to identify different atmospheric Zn sources, including Zn derived from anthropogenic activities such as mining and smelting (Weiss et al., 2007). A study by Sivry et al. (2008) assessed the potential of Zn isotopes to be used as an anthropogenic tracer in environmental systems. Where Zn isotopic compositions of surface soils, smelting/mining wastes, river and reservoir sediments from a river system were determined (Sivry et al., In press).

7.7 Other materials

The concentration and isotopic composition of Zn in a Zn vitamin Tablet and Zn plated steel roof fragments were also measured as pilot experiments. The aim of these experiments was primarily to measure the concentration of Zn and demonstrate

measurement of Zn isotopic fractionation using the Daly detector. The significance of investigating the isotopic composition of this nutritional sample is that these Vitamin Tablets are made from processed chemical compounds like Zn Gluconate and Zn oxides also are presumably undergo some form of purification (John et al., 2007).

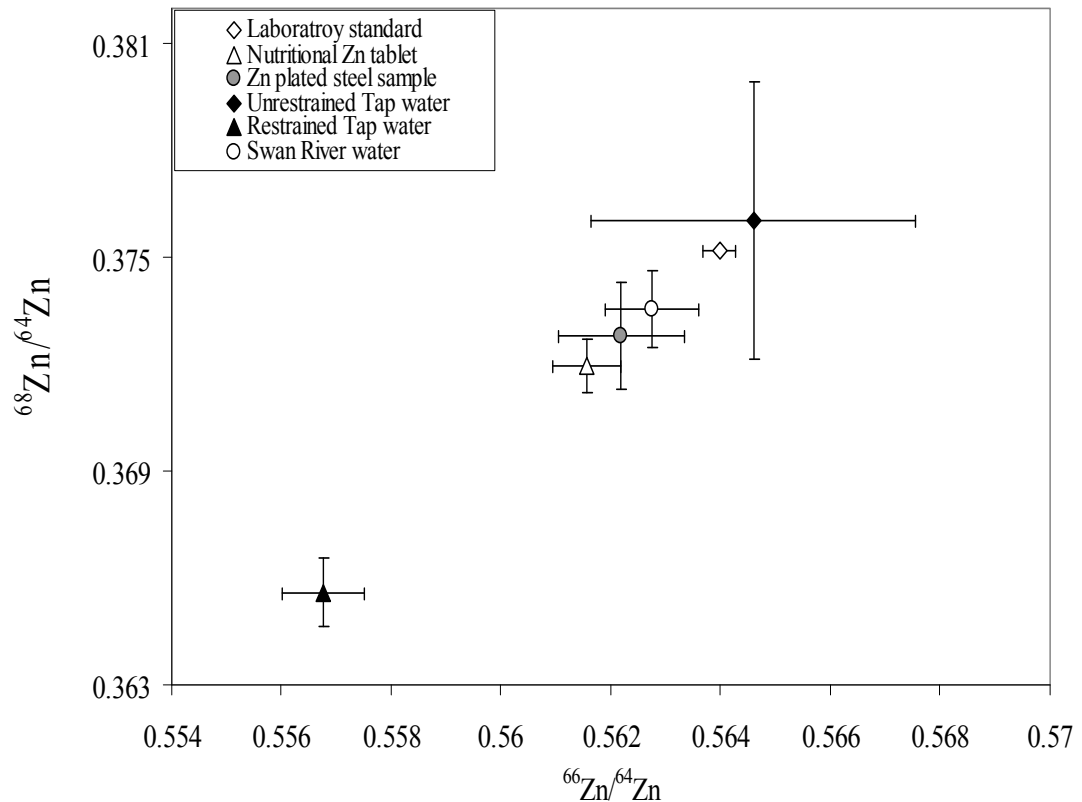
In the same manner as was found for the water samples, the final uncertainties achieved in the measured fractionation were not of the same quality as those for the natural samples. The Zn isotopic deviation of a Zn nutritional sample relative to the laboratory standard “fractionation” is represented in Figure 5.10. According to Figure 5.10, the deviation of the isotopic composition of Zn in the Zn nutritional Tablet relative to the laboratory standard measured without double spiking is $-4.2 \pm 4.3 \text{ ‰ amu}^{-1}$ which is far more imprecise than that measured using the double spike technique. This is because the measurement was done using the Daly detector. Using the double spike technique, the Zn nutritional Tablet was found to have a significant Zn fractionation of $-2.14 \pm 1.0 \text{ ‰ amu}^{-1}$. This is another example that direct sample/standard comparison is an inadequate tool for the Zn fractionation to be measured accurately. Using the double spike method, the average Zn fractionation in the Zn plated steel sample (using the double spike) was found to be $-1.6 \pm 1.0 \text{ ‰ amu}^{-1}$. These fractionation values are similar in magnitude to those found for the high purity metal samples and most likely reflect the different industrial processes applied during sample manufacture. However unlikely, it is also possible that these Zn fractionation results reflect the isotopic composition in the original or source material. In the same manner as for environmental samples these results offer some potentially useful indicators to investigate these industrial processes.

Although a number of Zn fractionation measurements have been made for anthropogenic materials, e.g. John et al.(2007), none have being measured relative to the international recognized isotopic composition of Zn by IUPAC (δ zero). Hence the results of John et al. (2007) for a Zn Vitamin can't be compared with the results of this work. This highlights the need for all anthropogenic Zn fractionation measurements to be performed relative to (δ zero).

It is interesting that all artificial materials and Swan River water samples exhibited a negative fractionation, the only exception for this for the Zn in the unrestrained (fresh)

tap water. It is possible that these samples are dominated by a specific or common industrial process, for example, the effect of fertilizers. Figure 7.14, shows a three isotope plot for the absolute isotopic ratios of all samples suspected of Zn fractionation due to anthropogenic origin. Despite the limited precision for the isotopic ratios, it appears that the samples can be differentiated into two or possibly even three groups as identified on the graph.

Figure 7. 14: The three isotope plot for the Zn fractionation of materials for samples suspected to be affected by, or from an anthropogenic source.



The restrained tap water is most likely dominated from Zn leaching from the copper piping and plumbing joints and solders. It is perhaps surprising to see the Zn plated steel sample does not group with this sample. Nevertheless, as described above, it would be useful to further investigate the isotope systematics of all these samples and especially points to the strong potential of Zn isotopic composition as an environmental tracer.

7.8 Contribution of Zn isotopic fractionation to the atomic weight of Zn.

The atomic weight of an element E is the sum of the multiplication of the atomic masses and the mole fractions of the isotopes of that element. The atomic mass can be represented as $A_r(E)$ (Coplen et al., 2002), represented for Zn as, $A_r(\text{Zn})$ hereafter. The internationally recognized atomic weight of Zn by the IUPAC is 65.38 ± 0.02 (IUPAC, 2007). To investigate the effect of the variations in isotopic “fractionation” of Zn in natural material measured in this research; the atomic weight of Zn was calculated for the largest isotope fractionation measured, which is for the restrained tap water of $-6.39 \pm 0.62 \text{ ‰ amu}^{-1}$ (see Section 5.5.6, Table 5.23) (also discussed in Section 7.5, Table 7.5), and this yields an atomic weight of 65.3614 ± 0.0025 (all uncertainties in the calculated atomic weight were determined using GUM) which is within the uncertainty of IUPAC value. Also the maximum Zn fractionation found in this research for pure Zn standard metals is for AE 10760 ($-5.11 \pm 0.36 \text{ ‰ amu}^{-1}$) yields an atomic weight of 65.3647 ± 0.0015 (95% confidence) which is inside the IUPAC stated uncertainty without even taking into account the large uncertainty of the calculated atomic weight of AE 10760. IUPAC recommended atomic weights do not consider extraterrestrial materials as those that would not normally be found in an analysts laboratory but even the largest ($\leq +1.11 \pm 0.11 \text{ ‰ amu}^{-1}$) measured natural fractionation for Canyon Diablo iron meteorite, which yields an atomic weight of 65.38058 ± 0.00062 ; will not effect the current atomic weight of Zn. All other measured isotopic compositions of Zn in natural materials yields an atomic weight within the internationally recognized absolute atomic weight by IUPAC.

The range of Zn fractionation due to natural and artificial processes for all the materials measured in this research can be summarized on Figure 7.15 and 7.16 respectively. Representing both natural fractionation and anthropogenic fractionation in one Figure is not ideal; because of the spread of the fractionation for both categories. As represented in Figure 7.15, the range⁹ of natural Zn isotopic fractionation in terrestrial materials is 0.85 ‰ amu^{-1} , and in meteorites is 1.605 ‰

⁹ The range calculated as the difference between the average of the maximum value and the average of the minimum value considering the uncertainty in each value.

amu^{-1} (except for the Redfields meteorite, which contains an abnormal Zn isotopic composition). None of these fractionation change the IUPAC recommended atomic weight of Zn within uncertainty. This is illustrated in Figure 7.15, where the Zn fractionation is the lower horizontal axis and the atomic weight of Zn is calculated shown on the upper horizontal axis. Likewise in Figure 7.16, Zn isotopic fractionation in processed materials and in some natural materials thought to be caused by anthropogenic processes like that found in river water, tap water, and other samples, are presented.

Figure 7. 15: Atomic weight and Zn fractionation ranges in natural materials. The ranges in atomic weights and fractionation in these samples are dominated by the meteorites.

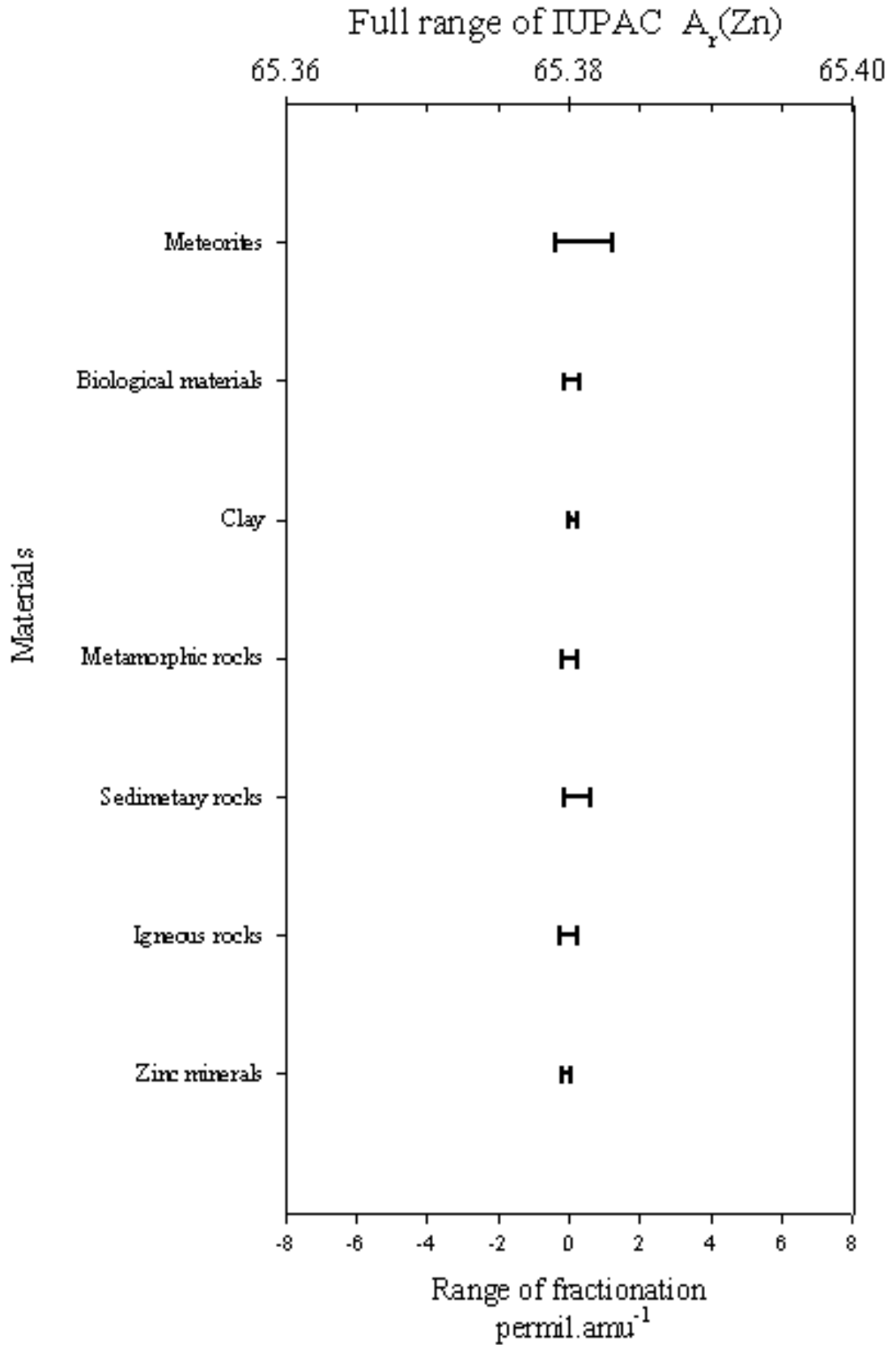
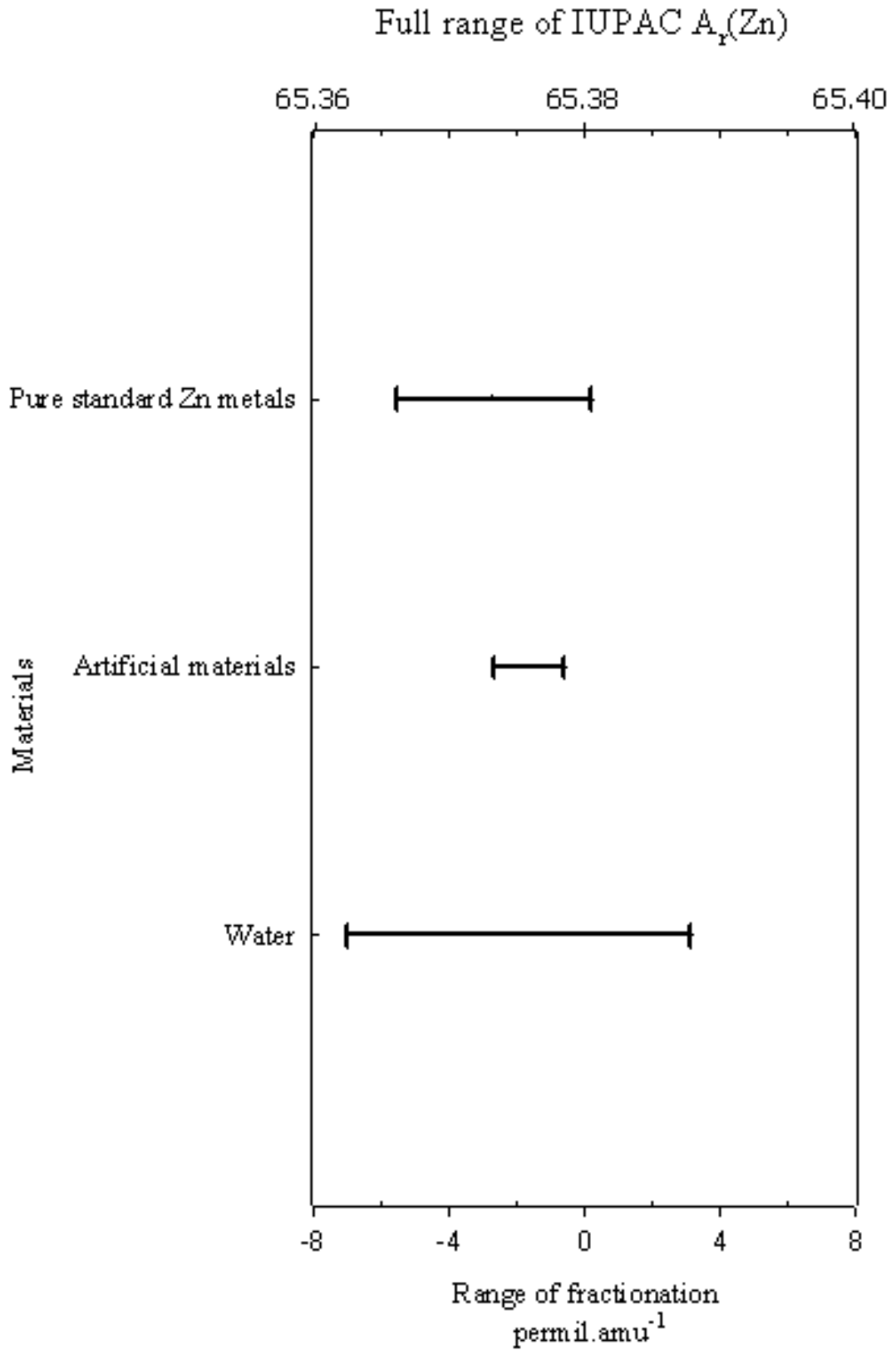


Figure 7. 16: Range of Zn fractionation in processed and natural materials affected by anthropogenic processes. In the case of water samples approximately 50% of the range is due to the associated uncertainties.



As represented in 7.16; the range of natural Zn isotopic anthropogenic fractionation in natural materials “water” dominates the range of fractionation and hence their effect on the atomic weight. These ranges of fractionation in either natural or artificial materials do not alter the IUPAC recommended atomic weight of Zn.

- **Chapter 8: Conclusions and recommendations**

8.1 Summary of results

This work represents the first and the most comprehensive development for the measurement of Zn isotopic fractionation in natural materials using TIMS.

The procedures developed in this research evaluate and solve several critical analytical issues involved in TIMS Zn isotopic measurements such as, reducing the size of sample needed to perform an accurate and precise measurement, minimizing the effect of interferences on the Zn fractionation, reducing the blank associated with the analyses, dissolution and purification of different natural samples, and addressing the completely ignored issue of the contribution of the ion exchange chemistry (Zn separation) to the fractionation of Zn. This will assist isotope analysts wishing to use Zn in their investigations. Also, these techniques may be applicable for the isotopic analyses of other transition elements.

A survey of the isotopic fractionation of Zn in natural materials measured using the “rigorous” double spike technique, relative to the absolute Zn isotopic composition Alfa Aesar 10759 laboratory standard (IRMM 3702) has been carried out. Repeated analyses of the laboratory standard relative to itself yielded a fractionation reproducibility “detection limit” of $\pm 0.039 \text{ ‰ amu}^{-1}$. A significant fractionation ($+0.066 \pm 0.018 \text{ ‰ amu}^{-1}$ per column) resulting from ion exchange chemical purification of Zn was observed. The fractionation has been measured for a range of standard reference materials “SRMs” relative to laboratory standard proposed (δ zero) allowing the absolute Zn isotopic composition for all these SRMs to be calculated.

The techniques developed in this work enable the existence of Zn fractionation in nature and its extent to be determined, with no more than $1 \mu\text{g}$ of Zn being used for any of the isotopic analyses. Zinc fractionation was observed in number of materials usually at the sub part per thousand levels. In geological materials, Zn fractionation ranged from, -0.04 ± 0.17 to $+0.02 \pm 0.14 \text{ ‰ amu}^{-1}$ in Zn minerals, -0.09 ± 0.15 to

$+0.17 \pm 0.10$ ‰ amu^{-1} in igneous rocks, from $+0.06 \pm 0.17$ to $+0.43 \pm 0.18$ ‰ amu^{-1} in sedimentary rocks, from -0.02 ± 0.15 to $+0.12 \pm 0.10$ ‰ amu^{-1} in metamorphic rocks, and $+0.12 \pm 0.10$ ‰ amu^{-1} in a clay sample. In biological materials, Zn fractionation ranged from -0.088 ± 0.070 ‰ amu^{-1} in plants, to $+0.21 \pm 0.11$ ‰ amu^{-1} in Antarctic Krill. In river water, Zn fractionation was found to be -1.09 ± 0.70 ‰ amu^{-1} , while a Zn fractionation difference of 6.95 ± 2.67 ‰ amu^{-1} was found between stale and fresh tap water. In meteorites, Zn fractionation range from -0.29 ± 0.10 to $+0.38 \pm 0.16$ ‰ amu^{-1} in stone meteorites, up to $+1.11 \pm 0.11$ ‰ amu^{-1} in the Canyon Diablo iron meteorite. In high purity Zn metal, Zn isotopic fractionation ranged from -5.1 ± 0.4 to $+0.04 \pm 0.14$ ‰ amu^{-1} . Systematic linear fractionation of Zn was observed in all measured samples, except for Redfields meteorite, where an abnormal isotopic composition of Zn was clearly identified. In terms of Nucleosynthesis a simple explanation could be in terms of the rapid neutron capture “r” process. On the other hand; the Redfields anomaly is strong evidence for large scale inhomogeneity of the solar nebula at the time of condensation, and also within major parent bodies formed in the solar nebula. None of these fractionation change the IUPAC recommended atomic weight of Zn within uncertainty.

Although this work demonstrates the existence of Zn fractionation in many materials at the sub-permil level, smaller fractionation than the uncertainties obtained in this work may exist. A recommendation for future research is to develop more precise techniques to able to measure smaller fractionation.

The absolute isotopic composition for a variety of pure standard Zn materials provided by IRMM was determined, and will serve as a valuable resource for analysts in order to measure Zn fractionation relative to the “ δ zero”. These will provide a metrological base line for Zn isotopic compositions that the international scientific community can exploit for future Zn investigations. The measured fractionation of these pure laboratory standards materials relative to (δ zero) will enable analysts to measure Zn isotopic fractionation and compare their results with others, hence contribute to greater understanding of the Zn fractionation.

In addition, the isotopic fractionation of Zn were also measured in several processed materials thought to be affected by anthropogenic processes. Where possible, a

comparison of the results of this research with previous measurements using other techniques, relative to any common samples was performed. However, because the significant contribution of the column chemistry to Zn fractionation ($+0.07 \pm 0.02 \text{ ‰ amu}^{-1}$) is significantly greater than the values and external uncertainties of the claimed fractionation published by all previous researchers, e.g. for $\delta^{66}\text{Zn}$ as (± 0.04 to 0.05 ‰) for two amu, and because all previously published data has been measured relative to unknown laboratory standards, this makes definitive interlaboratory comparison impossible. These two factors seriously call into question some aspect of the reported claims of highly precise and accurate published data on Zn fractionation.

An additional significant contribution has also been in the determinations of the elemental abundances of Zn in these materials using the “Gold standard” IDMS technique. The procedure developed in this work enabled ng amounts of Zn samples to be measured by IDMS with relatively high external reproducibility, ultimately determined by the variability in the blank ($8 \pm 5 \text{ ng}$). Zn concentrations in geological materials ranges from 67.3 ± 1.1 to $130.7 \pm 1.8 \text{ } \mu\text{gg}^{-1}$ in igneous rocks, 3.867 ± 0.058 to $101.4 \pm 2.0 \text{ } \mu\text{gg}^{-1}$ in sedimentary rocks, 61 ± 3 to $101.5 \pm 1.7 \text{ } \mu\text{gg}^{-1}$ in metamorphic rocks, and $48.38 \pm 0.99 \text{ } \mu\text{gg}^{-1}$ in TILL-3 clay sample. For biological materials, the concentration of Zn ranges from 14.62 ± 0.27 to $63.5 \pm 1.8 \text{ } \mu\text{gg}^{-1}$ in plants and Antarctic Krill. The concentration of Zn in meteorites ranges from (20.1 to 32.7) to $302 \pm 14 \text{ } \mu\text{gg}^{-1}$ in stone meteorites, and from $19.2 \pm 7.5 \text{ ngg}^{-1}$ to $23.88 \pm 0.54 \text{ } \mu\text{gg}^{-1}$ in iron meteorites. The concentration of Zn in Swan River ranged from 6.5 ± 0.4 to $7.2 \pm 0.5 \text{ ngg}^{-1}$. The concentration of Zn in fresh (unrestrained (fresh)) tap water, and is ~ 400 times less than the concentration of Zn in the restrained tap water with average concentrations of $13.1 \pm 0.7 \text{ ngg}^{-1}$ and $5.2 \pm 0.4 \text{ } \mu\text{gg}^{-1}$ respectively. In particular, the results obtained for the SRMs will assist the analytical community in developing techniques and for analytical comparative purposes.

8.2 Significant Interpretations

Except for meteorites, almost all the samples analysed in this work are commonly available standard reference materials; hence the results obtained should serve as valuable reference data for analysts establishing Zn elemental abundance and isotopic analytical procedures. The results obtained represent significantly improved overall precision and accuracy over existing concentration and isotopic composition data for Zn in geochemical and biological reference materials. Accordingly, it is recommended that analysts exploit the use of the SRMs measured in this research to develop and test analytical techniques.

The effect of a significant ($+0.066 \pm 0.018 \text{ ‰ amu}^{-1}$ per column) fractionation resulting from ion exchange chemical purification of Zn was observed, and strongly supports the use of the double spike technique to correct for any external bias. Even though the double spiking is more expensive and time consuming, it is recommended that analysts using MC-ICP-MS use the double spike technique to check their procedures and instrumentation. This will assist in substantiating the claimed accuracy of the previous measurements of Zn fractionation using other techniques, and the systematic application of Zn fractionation in natural samples. High column efficiency should not be used as a guarantee for no fractionation introduced by the column chemistry particularly for low level samples, since Zn contamination can be easily introduced from unrecognised sources.

All the fractionation determinations were performed relative to the international recommended Zn proposed absolute standard “Alfa Aesar 10759”, proposed as “ δ zero”, enabling the measured fractionation to be used as a tool to underpin isotopic measurements on a global scale. Accurate results of this type will contribute to development of a systematic explanation for why, and how, Zn fractionation occurs, and more importantly its application in other sciences.

Ideally “bulk Earth”, as represented by igneous type rocks should be used as a terrestrial standard. Fortunately none of the igneous rocks investigated in this work

appears significantly fractionated relative to the laboratory standard except for Diabase W-2 ($+0.17 \pm 0.1 \text{ ‰ amu}^{-1}$). These results support the interpretation of Wombacher et al. (2003) for Cd, where they concluded that isotopic fractionation of Cd is not expected to occur during the formation of igneous rocks because of high temperature involved in the formation of mantle-derived igneous rocks. Within the limitation of the number of samples analysed, the same interpretation appears possible for Zn. The isotopic composition of the Basalt BCR-1, BIR, and DNC-1 is the isotopic composition of Zn of the Basalt source mantle, which forms the continents. On the other hand, Diabase W-2 appears to represent a deeper mantle that is still essentially undifferentiated. It is recommended that more absolute measurements should be performed on igneous rocks to confirm this interpretation. Since there was no fractionation relative to the laboratory standard (proposed absolute isotopic composition or δ zero material) obtained for igneous, metamorphic rocks and Zn minerals, this supports the use of the absolute isotopic composition as a suitable absolute international isotope standard, against which all Zn isotope measurements should be performed

In the case of sedimentary rocks, apart from Cody shale, (SCO-1) which exhibits no fractionation relative to the laboratory standard, all of the other sedimentary rocks show a consistent fractionation of $\sim +0.3 \text{ ‰ amu}^{-1}$. Though all the sedimentary rocks measured in this research agree with each other, and exhibit no isotopic fractionation relative to each other, this suggests that the sedimentary rocks measured in this research form an isotopic group, despite their different localities. Assuming no dependence on depth, this could open the way to connect Zn fractionation in sedimentary rocks to oceanic conveyor circulations, and could explain why the fractionation of Zn is the same magnitude, even though the samples are taken from significantly different locations on the planet.

The Zn fractionation observed in metamorphic rocks supports the early assumption that high temperature and pressure processes such as that experienced by igneous rocks does not fractionate the isotopic composition of Zn. For example, it is more likely that the result of sedimentary rocks represents the cumulative Zn fractionation in the terrigenous fraction of the sediments.

Clay sample, TILL-3 appears to exhibit a consistently slightly positive Zn fractionation of $+0.12 \pm 0.10 \text{ ‰ amu}^{-1}$, although it is barely outside uncertainty, from the absolute. The fractionation obtained is similar to that for sedimentary rocks, with both being slightly enhanced in heavier isotopes, which is not surprising such that; TILL-3 is thought to be formed from a range of mixed glacial sediments.

Isotopic fractionation of Zn in plants has been clearly identified for the first time using the double spike technique in samples, IMEP-19 “Rice” and NIES-9 “Sargasso” sea weed. The reason why Sargasso is isotopically enhanced relative to the Rice sample; it is most likely due to it being a marine sample which is consistent with previous work (Pichat et al., 2003c) which showed that sea water is enhanced in the Zn heavier isotopes, possibly due to the biological activity of phytoplankton and other organisms. Meanwhile, and as discussed in 7.3, Scientists suggested that Zn isotopic fractionation in all plants could be due to many factors; including the formation of “Phytate” Protein complexes. It is well known that Zn plays a structural role in the enzymes of the plants, although the exact process is not clear, Zn could be fractionated during the remobilization process of this element in plants (Cavagnaro and Jackson, 2007). In a similar manner, the relation between dietary intake and the isotopic composition Zn in animals appears to be worthy of further investigation using the double spike technique. A strong indicator for this effect is the isotopic fractionation of Zn in Antarctic Krill, since it is known that Krill feed primarily on phytoplankton or sea ice algae. It is recommended that the Zn fractionation be measured in plant and animal species using the double spike technique with the view to the development of tools to investigate specific biological and ecological systems.

Although the absolute values of fractionation cannot be compared, the range of Zn isotopic fractionation found in meteorites appears to generally agree with that found by previous researchers. An additional impediment to direct comparisons are that the claimed uncertainty of previous work does not include the contribution of the column chemistry to the fractionation which in most cases appears to be far more than their quoted uncertainties.

In stone meteorites, the variation found in the Zn fractionation in the bulk samples of ordinary Chondrites is consistent with the heterogeneous structure of Chondrites. More measurements are needed to determine if groups or classes of meteorites can be identified which exhibit clearly defined “enhanced and depleted Zn”. The results may also reflect the history of the different parent bodies and or difference processes that occurred in their formation in the early Solar System. Another recommendation of this research is to utilise the double spike technique to measure Zn fractionation in a range of meteorite components to determine if the fractionation can be identified within specific phases or minerals within the meteorites. This information would further aid in the data and interpretations needed in other recommendations. It is also possible that Zn fractionation in meteorites represents a primordial heterogeneity, which has been preserved during the formation of the Solar System, an assumption made by Rosman et al. (1980) for Cd fractionation in Brownfield. For iron meteorites, Canyon Diablo represented the maximum Zn fractionation in meteorites found this work. It is recommended that an in-depth study of Zn fractionation should be performed on this meteorite’s components using the double spike technique.

Whether Redfields is a primitive type of meteorite or not, such an isotopic composition in a bulk meteorite strongly suggests isotopic heterogeneity and does not support the proposal by Luck et al.(2005b) that “Zn was derived from an initially single homogeneous reservoir”. Unfortunately, the isotopic anomalies for Zn found earlier by Loss and Lugmair (1990) and Loss et al. (1994) can’t be easily compared with these results because those anomalies were found in meteoritic inclusions. The main difficulty in interpreting the abnormality in the isotopic composition of Zn in Redfields meteorite is determining which reference isotope to use and the extent of any superimposed fractionation. It is possible to interpret the results as a combination of as anomalous $^{66}\text{Zn}^*$ and $^{68}\text{Zn}^*$, and fractionated Zn similar to that found in FUN inclusion in the Allende meteorite. The $^{66}\text{Zn}^*$ and $^{68}\text{Zn}^*$, can also be interpreted as a type of previously reported MZM anomalies found in the isotopic composition of Ni and other Fe peak elements. It is recommended that further investigations of the isotopic composition along with the elemental abundance of other elements, specially the iron peak elements along with Ti, Ca, and Cr be undertaken in the Redfields meteorites and its components

The isotopic composition of Zn in tap indicates that it is more likely that the unrestrained (fresh) water represents the isotopic composition of the water source, while the fractionated isotopic composition of Zn in restrained water represents an anthropogenic source, which is most likely to be the pipes or fittings. This is strongly supported by the significant difference between the concentrations of Zn in these materials.

For processed Zn samples, this work revealed a wide range in the isotopic composition, which for high purity Zn materials, which has been previously observed but never before put on an absolute scale. Of the eight high purity materials analysed, five of these show a relationship between Zn fractionation and the purity, with an enhancement in the lighter isotopes of Zn. The three samples that do not follow this relationship could have been purified by a different process. This interpretation is consistent for what was found for Ga by Gramlich and Machlan in (1985).

Accordingly, it is recommended that, all analysts who wish to perform measurements for which the atomic weight or isotopic composition is required to be known accurately, measure the isotopic composition of their materials.

Also investigated was the effect of the variations in isotopic “fractionation” of Zn on the atomic weight of Zn in all materials. The results obtained indicated that none of the measured fractionation will effect the current atomic weight of Zn (65.38 ± 0.02) (IUPAC, 2007), the atomic weight of Zn for the largest fractionation measured in this research is that for restrained tap water ($-6.39 \pm 0.62 \text{ ‰ amu}^{-1}$) relative to the absolute laboratory standard, and this yields an atomic weight of 65.361 ± 0.002 (95% confidence) which is still within the uncertainty of IUPAC value.

For the Zn elemental abundances measurements, the geological materials, BCR-1, NIES No 9 and IMEP-19, previously measured by TIMS IDMS, and HISS-1, for which an IDMS analyses was performed using ICP-MS, are the only samples for which a direct technique comparison is possible. All concentration measurements in this work agree with the previously available IDMS measurements but with smaller relative uncertainties. For the remaining samples, this work appears to be the first reported Zn concentration using this technique. Except for meteorites, the final

uncertainties consistently cover the ranges of individual concentration measurements and support the homogeneity of the SRMs including several cases for samples taken from different bottles. The results obtained all agree with each other within individual measurement uncertainties, with final uncertainties generally being less than 2.5%, demonstrating the high level of precision possible using IDMS. Since the recommended values for SRMs are generally statistically compiled from a wide range of analysts and techniques over many years, they represent a limited physical meaning and it is not unexpected that these will have a wider range of uncertainty, which can limit the value of SRMs to verify high accuracy analytical results. For the remaining SRMs, this work appears to be the first reported Zn concentration measurements for these samples using the isotope dilution technique. Only an approximate value for the concentration of Zn in TILL-3 was provided by the National Resources Canada hence a certified value for the element is not available (National Resources Canada, 2007)

The range of Zn concentration found in igneous rocks in this work (67.3 ± 1.1 to 130.7 ± 1.8) $\mu\text{g g}^{-1}$, is most likely explained by different mantles sources (Allegre et al., 1995). In contrast to the concentration of Zn in igneous rocks, the concentration of Zn in sedimentary rocks varies widely, from 3.867 ± 0.058 $\mu\text{g g}^{-1}$ to 101.4 ± 2.0 $\mu\text{g g}^{-1}$, for HISS-1 and SCo-1 respectively.

In biological materials, the concentration of Zn in Rice and Sargasso Sea weed is found to be 22.15 ± 0.42 and 14.62 ± 0.27 $\mu\text{g g}^{-1}$ respectively. Such Zn availability is classified by the World Health Organisation “WHO” as moderate Zn nutrient category (WHO, 2004). The concentration of Zn in Rice “IMEP-19” was found to be 22.15 ± 0.42 $\mu\text{g g}^{-1}$, which agrees with the recommended value by the IRMM for the IMEP-19 is 22.99 ± 0.44 $\mu\text{g g}^{-1}$ measured using the IDMS-TIMS technique as a Primary method measurement (IRMM, 2007).

The concentration of Zn in SRM MURST-Iss-A2 “Krill” standard material is 63.5 ± 1.8 $\mu\text{g g}^{-1}$. This material was previously measured using inductively coupled plasma atomic emission spectrometry (ICP-AES), and graphite furnace atomic absorption spectrometry (GF-AAS) methods by (Gasparics et al., 2000) yielding a concentration

of $69.5 \pm 2.3 \mu\text{gg}^{-1}$, which does not agree with the results obtained in this research samples. It is recommended that the IDMS value supersede the previous result.

For the concentration of Zn in stone meteorites, this research confirms the inhomogeneity of Zn in stony meteorites, and that they show a wider range of Zn abundance than iron meteorites. These results supports the observation of Luck et al's (2005b) that different chunks of meteorites show variable concentration and isotopic composition for Zn, and reflects the presence of minute Zn-rich phases and inclusions. A possible relationship between the concentration and isotopic fractionation of Zn for meteorites and their components offers some interesting possibilities for future research.

The concentration and the isotopic fractionation of Zn in water from Swan River was not found to be significantly different between two locations 6.4 km apart in the lower reaches of the river. This was expected because Swan river water is generally moving towards the ocean with a relatively strong current. The average Zn fractionation measured in Swan River water is $-1.09 \pm 0.70 \text{‰ amu}^{-1}$. As the concentration of dissolved Zn in the rivers derived from natural resources is expected to be $\sim 0.2 \text{ ngg}^{-1}$ (Shiller and Boyle, 1985), which is thirty five times less than what was found in Swan River water ($6.9 \pm 0.8 \text{ ngg}^{-1}$), suggesting an anthropogenic source for Zn in the river. However, the Zn concentration in the river is significantly less than the normal maximum permissible for drinking water. It is also possible that the high concentration and isotopic fractionation of Zn in Swan River water samples is due to Zn from fertilizers used on nearby farming lands, and other anthropogenic sources.

The measured concentration of Zn in unrestrained (fresh) tap water is about 400 times less than the concentration of Zn in the restrained tap water and is well above the recommended Zn abundance in drinking water, which is a strong indicator of a corroded water pipe system. These findings emphasize the strong potential of Zn isotopic composition as an environmental tracer and recommends that the variability of the isotopic composition of Zn be exploited for this purpose.

There are also many areas in nature and in human activity involving Zn for which there has not been sufficient time to investigate. Some natural samples that warrant further investigations are; lunar, atmospheric dust, oceanic and polar ice, and a wide variety of biological samples, including those from humans. As far as human activity is concerned, samples, processes and systems that could be investigated include air pollution, archaeological and anthropological studies, and trade, and human health. As discussed in previous Sections, Zn is an important element in human biology and there appears to be a strong likelihood that small variations in Zn fractionation can be used to study aspects of human health. Of particular interest is the role of Zn at the molecular level such as the Zn finger protein. It is therefore recommended that new techniques be developed to isotopically analyse very small amounts of Zn, so that these areas can be investigated.

8.3 Summary of the recommendations

From this work it is recommended that;

- That the laboratory standard used in this work which is an aliquot of IRMM Zn 3702), the absolute isotopic composition of Zn (δ_{zero}), be adopted as the International absolute isotopic composition of Zn, to be used by all analysts.

- All analysts performing high precision analytical work using high purity Zn materials should measure the isotopic composition of their materials relative to the internationally recognized proposed absolute Zn.
 - Analysts working with Zn exploit the SRMs measured in this research rather than use internal laboratory standards to develop and test analytical techniques.

- Analysts working with Zn using MC-ICP-MS use the double spike technique to calibrate their entire fractionation measuring system.

- More absolute isotopic measurement measurements should be performed on a wide range of igneous rocks to confirm that the Zn isotopic composition in these rocks adequately represents “bulk Earth Zn”.

- Zn fractionation be measured in wide range of biological and geological systems using the double spike technique, with the view to the development of tools to investigate these systems. Special techniques may need to be developed including those required to handle small amounts of Zn.
- More concentration and isotopic fractionation measurements are needed on meteorites and meteoritic components. For example, to determine if groups or classes of meteorites can be identified which exhibit clearly defined “enhanced and depleted Zn”, and to determine if the fractionation can be identified within specific phases or minerals within the meteorites.
- An in-depth Zn isotopic study be performed on Canyon Diablo to identify the source and magnitude of the $1.11 \pm 0.11 \text{ ‰ amu}^{-1}$.
- An in depth Zn isotopic study be performed on the Redfields meteorite and in particular in the Redfield anomaly, and isotopic measurements be performed on other elements in this meteorite.
- Zn fractionation can be used to study aspects of human health. Of particular interest will be the role of Zn at the molecular level such as the Zn finger protein. It is therefore recommended that new techniques be developed to isotopically analyse very small amounts of Zn so that these areas can be investigated.
- The uncertainty of the isotopic composition measurements of Zn be further reduced to investigate whether smaller fractionation exist in nature.

These recommendations have the potential to open up a whole new field of new Zn isotope research. The general results obtained in this work serve as a valuable base for other researchers investigating the isotopic composition of Zn in natural materials. There are also many areas in nature and in human activity involving Zn for which there has not been sufficient time to investigate during this research. A number of significant analytical break throughs will be needed to fully investigate these systems. This includes, a reduction of the blank, the ability to analyse correspondingly smaller

samples, and special sample handling techniques. The use of TIMS would benefit from significantly improving the ionisation efficiency of Zn, although completely new traceable analytical techniques may be required to solve many of these problems.

- **References**

- ALBARÈDE, F. (2004) The Stable Isotope Geochemistry of Copper and Zinc. *Reviews in Mineralogy & Geochemistry*, 55, 409-427.
- ALBARÈDE, F. & BEARD, B. (2004) Analytical Methods for Non- Traditional Isotopes. *Reviews in Mineralogy & Geochemistry*, 55, 113-152.
- ALLEGRE, C. J., SCHIANO, P. & LEWIN, E. (1995) Differences between oceanic basalts by multitrace element ratio topology. *Earth and Planetary Science Letters*, 129, 1-12.
- ANBAR, A. D. (2004) Molybdenum Stable isotopes: Observations, interpretations and directions. *Reviews in Mineralogy & Geochemistry*, 55, 429-454.
- ARIZONA STATE UNIVERSITY (2006) Catalog of meteorites. USA.
- BAINBRIDGE, K. T. (1932) The Isotopic Constitution of Zinc. *Physical Review*, 39, 847.
- BALISTRIERI, L. S., BORROK, D. M., WANTY, R. B. & RIDLEY, W. I. (2008) Fractionation of Cu and Zn isotopes during adsorption onto amorphous Fe(III) oxyhydroxide: Experimental mixing of acid rock drainage and ambient river water. *Geochimica et Cosmochimica Acta*, 72, 311-328.
- BERMIN, J., VANCE, D., ARCHER, C. & STATHAM, P. J. (2006) The determination of the isotopic composition of Cu and Zn in seawater. *Chemical Geology*, 226, 280-297.
- BEVAN, A. (2007) Specimen identification. IN GHIDAN, O. (Ed.). Perth.
- BRISCOE, H. V. A. & ROBINSON, P. L. (1925) A Redetermination of the Atomic Weight of Boron. *Journal of the chemical society transaction*, 127, 696-720.
- BROECKER, W. S. (1997) Thermohaline circulation, the achilles heel of our climate system: Will man-made Co2 upset the balance? *Science*, 278, 1582.
- CAMERON, A. E. & WICHERS, E. (1962) Report of the International Commission on Atomic Weights*(1961). *J. Am. Chem. Soc.*, 84, 4175-4197.
- CAMMAROTA, V. A. J. (1980) Production and uses of Zinc. IN NRIAGU, J. O. (Ed.) *Zinc in the Environment*. Ontario, John Wiley & Sons.
- CAMPANA, S. E., GAGNE, J. A. & MCLAREN, J. W. (1995) Elemental fingerprinting of fish otoliths using ID-ICPMS. *Marine Ecology Progress Series*, 122, 115-120.
- CANDELONE, J.-P., JAFFREZO, J.-L., HONG, S., DAVIDSON, C. I. & BOUTRON, C. F. (1996) Seasonal variations in heavy metals concentrations in present day Greenland snow. *Science of The Total Environment*, 193, 101-110.
- CAROLI, S., SENOFONTE, O., CAIMI, S., PAUWELS, J., KRAMER, G. N. & ROBOUCH, P. (2001) Production of a new certified material for trace elements in Antarctic krill. *J. Anal. At. Spectrom.*, 1142-1146.
- CAVAGNARO, T. R. & JACKSON, L. E. (2007) Isotopic fractionation of zinc in field grown tomato. *Canadian Journal of Botany*, 85, 230.
- CHAN, E. Y., QIAN, W.-J., DIAMOND, D. L., TAO LIU, GRITSEN, K. A., MONROE, M. E., CAMP II, D. G., SMITH, R. D. & KATZE, M. G. (2007) Quantitative Analysis of Human Immunodeficiency Virus Type 1-Infected CD4⁺ Cell Proteome: Dysregulated Cell Cycle Progression and Nuclear

- Transport Coincide with Robust Virus Production. *JOURNAL OF VIROLOGY*, Vol. 81.
- CHANG, T.-L., ZHAO, M.-T., JUN LI, W., WANG, J. & QIAN, Q.-Y. (2001) Absolute Isotopic Composition And Atomic Weight Of Zinc. *International Journal Of mass Spectrometry*, 208, pp.113-118.
- CHAPMAN, J. B., MASON, T. F. D., WEISS, D. J., COLES, B. J. & WILKINSON, J. J. (2006) Chemical Separation and Isotopic Variation of Cu and Zn from five Geological Reference Materials. *Geostandards and geoanalytical research*, 30, 5-16.
- CHIKARAISHI, Y. & NARAOKA, H. (2003) Compound-specific δD – $\delta^{13}C$ analyses of n-alkanes extracted from terrestrial and aquatic plants. *Phytochemistry*, 63, 361–371.
- CHRISTENSEN, U. R. & HOFMANN, A. W. (1994) Segregation of subducted oceanic crust in the convecting mantle. *Journal of Geophysical research*, 99, 19876-19884.
- CLAYTON, R. N. & MAYEDA, T. K. (1978) Genetic relations between iron and stony meteorites. *Earth and Planetary Science Letters*, 40, 168-174.
- COOK, D. L., WADHWA, M., CLAYTON, R. N., DAUPHAS, N., JANNEY, P. E. & DAVIS, A. M. (2007) Mass-dependent fractionation of nickel isotopes in meteoritic metal. *Meteoritics and planetary science*, 42, 2067-2077.
- COPLEN, T. B., HOPPLE, J. A., BOHLKE, J. K., PEISER, H. S., RIEDER, S. E., KROUSE, H. R., ROSMAN, K. J. R., DING, T., VOCKE, R. D., JR., REVESZ, K. M., LAMBERTY, A., TAYLOR, P. & BIEVRE, P. D. (2002) Compilation of minimum and maximum isotope ratios of selected elements in naturally occurring terrestrial materials and reagents. IN SURVEY, U. S. G. (Ed.). Virginia, U.S. Geological survey.
- CRISS, R. E. (1999) *Principles of stable isotope distribution*, Oxford University Press.
- DAUPHAS, N., MARTY, B. & REISBERG, L. (2002) Molybdenum evidence for inherited planetary scale isotope heterogeneity of the protosolar nebula. *The Astrophysical Journal*, 565, 640-644.
- DAUPHAS, N. & ROUXEL, O. (2006) Mass spectrometry and natural variations of Iron isotopes. *Mass Spectrometry Reviews*, 25, 515-550.
- DE BIEVRE, P. (1993) Isotope dilution Mass spectrometry as a primary method of analysis. *Analytical Proceedings*, 30, 328-332.
- DE LAETER, J. R. (2001) *Application of Inorganic Mass Spectrometry*, John Wiley & Sons.
- DE LAETER, J. R. (2004) The role of isotopic reference materials for the analysis of "Non Traditional" stable isotopes. *Geostandards and Geoanalytical Research*, 29, 53-61.
- DE LAETER, J. R., MCCALL, G. J. H. & REED, S. J. B. (1973) The Redfields meteorite- a unique iron from Western Australia. *Mineralogical Magazine*, 39, 30-35.
- DICKIN, A. P. (2000) *Radiogenic Isotope Geology*, Cambridge university press.
- ELLIS, A. S., JOHNSON, T. M. & BULLEN, T. D. (2004) Using Chromium Stable Isotope Ratios To Quantify Cr(VI) Reduction: Lack of Sorption Effects. *Environ. Sci. Technol.*, 38, 3604-3607.
- FANTLE, M. S. & BULLEN, T. D. (2008) Essentials of iron, chromium, and calcium isotope analysis of natural materials by thermal ionisation mass spectrometry. *Chemical Geology*, In Press, Accepted Manuscript.

- FIRESTONE, R. B. & SHIRLEY, V. S. (1998) *Table of Isotopes*, John Wiley & Sons.
- GASPARICS, T., MARTINEZ, R. M. G., CAROLI, S. & ZARAY, G. (2000) Determination of trace elements in Antarctic krill samples by inductively coupled atomic emission and graphite furnace atomic absorption spectrometry. *Microchemical Journal*, 67, 279-284.
- GHIDAN, O. Y. & LOSS, ROBERT D. (In preparation) Accurate Zn isotope fractionations in terrestrial materials as determined by double spike thermal ionisation mass spectrometry
- GHIDAN, O. Y. A. & LOSS, R. D. (Submitted) The Concentration of Zn in Standard Reference Materials as determined by Isotope Dilution Mass Spectrometry TIMS Technique. *Geostandards geoanalytical research*.
- GLADNEY, E. S. & ROELANDTS, I. (1988) 1987 Compilation of elemental concentration data for USGS BIR-1, DNC-1, and W-2. *Geostandards Newsletter*, 12, 63-118.
- GRAMLICH, J. W. & MACHLAN, L. A. (1985) Isotopic variations in commercial high-purity gallium. *Anal. Chem.*, 57, 1788-1790.
- GREENLAND, L. & GOLES, G. G. (1965) Copper and zinc abundances in chondritic meteorites. *Geochimica et Cosmochimica Acta*, 29, 1285-1292.
- GREENWOOD, N. N. & EARNSHAW, A. (1998a) *Chemistry of the Elements*, Oxford, Reed Educational and Professional Publishing Ltd.
- GREENWOOD, N. N. & EARNSHAW, A. (1998b) Zinc, Cadmium and Mercury. *Chemistry of the Elements*. Oxford., Reed Educational and Professional Publishing Ltd.
- HART, S. R. & ZINDLER, A. (1989) Isotope fractionation laws: a test using calcium. *International Journal of Mass Spectrometry and Ion Processes*, 89, 287-301.
- HARTMANN, D., WOOSLEY, S. E. & EL EID, M. F. (1985) Nucleosynthesis in neutron rich supernova ejecta. *The Astrophysical Journal*, 297, 837-845.
- HEINRICH, H., SCHULZ-DOBRICK, B. & WEDEPOHL, K. H. (1980) Terrestrial geochemistry of Cd, Bi, Tl, Pb, Zn and Rb. *Geochimica et Cosmochimica Acta*, 44, 1519-1533.
- HESS, D. C., INGRAM, M. G. & HAYDEN, R. J. (1948) The Relative Abundance of the Zinc Isotopes. *Physical Review*, 74, 1531.
- HEUSER, A., EISENHAUER, A., GUSSONE, N., BOCK, B., HANSEN, B. T. & NÄGLER, T. F. (2002) Measurement of calcium isotopes ($\delta^{44}\text{Ca}$) using a multicollector TIMS technique. *International Journal of Mass Spectrometry*, 220, 385-397.
- HITZMAN, M. W., REYNOLDS, N. A., SANGSTER, D. F., ALLEN, C. R. & CARMAN, C. E. (2003) Classification, Genesis, and exploration Guides for nonsulfide Zinc deposits. *Economic Geology* 98, 685-714.
- HOFFMAN, R. D., WOOSLEY, S. E., FULLER, G. M. & MEYER, B. S. (1996) Production of the light P-process nuclei in neutron-driven winds. *The Astrophysical Journal*, 460, 478-488.
- HOFMANN, A. W. (2003) Sampling Mantle Heterogeneity through Oceanic Basalts: Isotopes and Trace Elements. IN CARLSON, R. W., HOLLAND, H. D. & TUREKIAN, K. K. (Eds.) *Treatise on Geochemistry* Elsevier.

- HOFMANN, A. W. & WHITE, W. M. (1982) Mantle plumes from ancient oceanic crust. *Earth and Planetary Science Letters*, 57, 421-436.
- HOLMES, J. R. (2002) Development of operational and teaching software for a complex analytical instrument using "Virtual instrument" technology. *Departement of applied Physics*. Perth, Curtin University of Technology.
- HONG, S., CANDELONE, J.-P., TURETTA, C. & BOUTRON, C. F. (1996) Changes in natural lead, copper, zinc and cadmium concentrations in central Greenland ice from 8250 to 149,100 years ago: their association with climatic changes and resultant variations of dominant source contributions. *Earth and Planetary Science Letters*, 143, 233-244.
- IRMM (2003) IMEP-19 - Trace Elements in Rice.
- IRMM (2007) IMEP-19. IN UNIT, I. M. (Ed.) *IMEP-19 Trace Elements in Rice EUR 20551 EN Report to Participants*. GEEL (Belgium).
- ITALIAN NATIONAL PROGRAMME FOR RESEARCH IN ANTARCTICA (1996) MURST-ISS-A1 Antarctic Marine Sediment Certified Reference Material for Trace Elements *Journal of Analytical Atomic Spectrometry*, 11.
- IUPAC (1997) History of the recommended atomic weight values from 1882 to 1997: A comparison of differences from current values to the estimated uncertainties of earlier values.
- IUPAC (2003) Atomic weights of the elements 2001(IUPAC Technical Report). *Pure and Applied chemistry*, 75, PP1107-1122.
- IUPAC (2007) Standard Atomic Weights Revised. *Chemistry International*, 29.
- JACKSON, M. J. (1988) Physiology of Zinc: General Aspects. IN MACDONALD, I. (Ed.) *Zinc in Human Biology*. London, Springer-Verlag.
- JOHN, S. G., GENEVIEVE PARK, J., ZHANG, Z. & BOYLE, E. A. (2007) The isotopic composition of some common forms of anthropogenic zinc. *Chemical Geology*, 245, 61-69.
- JOHN, S. G., ROUXEL, O. J., CRADDOCK, P. R., ENGWALL, A. M. & BOYLE, E. A. (2008) Zinc stable isotopes in seafloor hydrothermal vent fluids and chimneys. *Earth and Planetary Science Letters*, 269, 17-28.
- JOSEPH A. LOO, T. P. H. S. K. F. P. M. C. A. B. N. M. H. W. T. M. T. I. S. D. P. M. (1998) Application of electrospray ionisation mass spectrometry for studying human immunodeficiency virus protein complexes. *Proteins: Structure, Function, and Genetics*, 33, 28-37.
- KELLY, J. F. & FINCH, D. M. (1998) Tracking migrant songbirds with stable isotopes. *Trends in Ecology & Evolution*, 13, 48-49.
- LACATUSU, R., DUMITRU, M., RISNOVEANU, I., CIOBANU, C., LUNGU, M., CARSTEA, S., KOVACSOVICS, B. & BACIU, C. (1999) Soil pollution by acid rains and heavy metals in Zlatna region, Romania. *10th international soil conservation organization meeting*. Purdue University and the USDA-ARS National soil Erosion Research Laboratory., D.E.Stott,R.H.Mohtar and G.C.Steinhardt(eds).
- LARIMER, J. W. (1967) Chemical fractionations in meteorites--I. Condensation of the elements. *Geochimica et Cosmochimica Acta*, 31, 1215-1238.
- LARIMER, J. W. (1973) Chemical fractionations in meteorites--VII. Cosmothemometry and cosmobarometry. *Geochimica et Cosmochimica Acta*, 37, 1603-1623.

- LARIMER, J. W. & ANDERS, E. (1967) Chemical fractionations in meteorites--II. Abundance patterns and their interpretation. *Geochimica et Cosmochimica Acta*, 31, 1239-1270.
- LARIMER, J. W. & ANDERS, E. (1970) Chemical fractionations in meteorites--III. Major element fractionations in chondrites. *Geochimica et Cosmochimica Acta*, 34, 367-387.
- LEE, T. (1988) Implications of isotopic anomalies for nucleosynthesis. IN KERRIDGE, J. F. & MATTHEWS, M. S. (Eds.) *Meteorites and the early solar system*. The university of Arizona press.
- LI, Y.-C. & JIANG, S.-J. (1998) Determination of Cu,Zn,Cd and Pb in Fish Samples by Slurry Sampling Electrothermal Vaporization Inductively Coupled Plasma Mass Spectrometry. *Analytica Chimica Acta*, 359, PP205-212.
- LODDERS, K. (2003) Solar system abundances and condensation temperatures of the elements. *The Astrophysical Journal*, , 591, 1220–1247.
- LOSS, R. D. & LUGMAIR, G. W. (1990) Zinc isotope anomalies in Allende meteorite inclusions. *The Astrophysical Journal*, 360, L59-L62.
- LOSS, R. D., LUGMAIR, G. W., DAVIS, A. M. & MACPHERSON, G. J. (1994) Isotopically distinct reservoirs in the solar nebula: Isotope anomalies in Vigarano meteorite inclusions. *The Astrophysical Journal*, 435, L193-L195.
- LOSS, R. D., ROSMAN, K. J. R. & DE LAETER, J. R. (1990) The isotopic composition of zinc, palladium, silver, cadmium, tin, and tellurium in acid-etched residues of the Allende meteorite. *Geochimica et Cosmochimica Acta*, 54, 3525-3536.
- LUCK, J.-M., BEN OTHMAN, D. & ALBAREDE, F. (2005a) Zn and Cu isotopic variation in chondrites and iron meteorites: Early solar nebula reservoirs and parent-body processes. *Geochimica et Cosmochimica Acta*, 69, 5351-5363.
- LUCK, J.-M., OTHMAN, D. B. & ALBAREDE, F. (2005b) Zn and Cu isotopic variations in chondrites and iron meteorites: Early solar nebula reservoirs and parent-body processes. *Geochimica et Cosmochimica Acta*, 69, 5351-5363.
- LUCK, J. M., BEN OTHMAN, D. & ALBAREDE, F. (2005c) Zinc isotopes in meteorites: early solar nebula reservoirs and parent-body processes. *Geophysical Research Abstracts*, 7.
- LUCK, J. M., BEN OTHMAN, D., ZANDA, B. & ALBAREDE, F. (2006) Zn-Cu isotopes in chondritic components. *Geochimica et Cosmochimica Acta*, 70, A373.
- MACNAMARA, J. & THODE, H. G. (1950) Comparison of the Isotopic Constitution of Terrestrial and Meteoritic Sulfur. *Physical Review*, 78, 307.
- MARECHAL, C. & ALBAREDE, F. (2002) Ion-exchange fractionation of copper and zinc isotopes. *Geochimica et Cosmochimica Acta*, 66, 1499-1509.
- MARÉCHAL, C. N., NICOLAS, E., DOUCHET, C. & ALBAREDE, F. (2000) Abundance of zinc isotopes as a marine biogeochemical tracer *Geochemistry Geophysics Geosystems*, 1.
- MARECHAL, C. N., TELOUK, P. & ALBAREDE, F. (1999) Precise analysis of copper and zinc isotopic compositions by plasma-source mass spectrometry. *Chemical Geology*, 156, 251-273.
- MARTIN, J. H., KNAUER, G. A. & FLEGAL, A. R. (1980) Distribution of Zn in natural waters. IN NRIAGU, J. O. (Ed.) *Zinc in the Environment*. Ontario, John Wiley&Sons.
- MASON, T. F. D., WEISS, D. J., CHAPMAN, J. B., WILKINSON, J. J., TESSALINA, S. G., SPIRO, B., HORSTWOOD, M. S. A., SPRATT, J. &

- COLES, B. J. (2005) Zn and Cu isotopic variability in the Alexandrinka volcanic-hosted massive sulphide (VHMS) ore deposit, Urals, Russia. *Chemical Geology*, 221, 170-187.
- MESTEK, O., KOMINKOVA, J., KOPLIK, R. & SUCHANEK, M. (2001) Determination of zinc in plant samples by isotope dilution inductively coupled plasma mass spectrometry. *Talanta*, 54, 927-934.
- METRODATA GMBH (1996) Gum Workbench trainMet. IRMM.
- MONNA, F., BEN OTHMAN, D. & LUCK, J. M. (1995) Pb isotopes and Pb, Zn and Cd concentrations in the rivers feeding a coastal pond (Thau, southern France): constraints on the origin(s) and flux(es) of metals. *Science of The Total Environment*, 166, 19-34.
- MOREL, F. M. M., REINFELDER, J. R. & ROBERTS, S. B. (1994a) Zinc and carbon co-limitation of marine phytoplankton. *Nature*, 369, 740.
- MOREL, F. M. M., REINFELDER, J. R. & ROBERTS, S. B. (1994b) Zinc and Carbon co-limitation of marine phytoplankton. *Nature*, 369, 740-742.
- MOYNIER, F., ALBAREDE, F. & HERZOG, G. F. (2006) Isotopic composition of zinc, copper, and iron in lunar samples. *Geochimica et Cosmochimica Acta*, 70, 6103-6117.
- MOYNIER, F., BLICHERT-TOFT, J., TELOUK, P., LUCK, J.-M. & ALBARÈDE, F. (2007) Comparative stable isotope geochemistry of Ni, Cu, Zn, and Fe in chondrites and iron meteorites. *Geochimica et Cosmochimica Acta*, 71, 4365-4379.
- MUNIZ, C. S., GAYON, M. J. M., ALONOSO, G. I. & SANZ-MEDEL, A. (1999) Accurate determination of Iron, Copper and Zinc in human serum by isotope dilution analysis using double focusing ICP-MS. *Journal of Analytical Atomic Spectrometry*, 14, 1505-1510.
- NATIONAL HEALTH AND MEDICAL RESEARCH COUNCIL (2004) The Australian Drinking water guidelines
- NATIONAL INSTITUTE FOR ENVIRONMENTAL STUDIES (2007) Certified reference material No.9 "Sargasso". IN NATIONAL INSTITUTE FOR ENVIRONMENTAL STUDIES (Ed.). Ibaraki-Japan.
- NATIONAL RESEARCH COUNCIL CANADA (2007) Certified reference material HISS-1, MESS-3, PACS-2.
- NATIONAL RESOURCES CANADA (2007) TILL-1, TILL-2, TILL-3, and TILL-4 Geochemical Soil and Till Reference Materials. IN CANMET-MMSL (Ed.) *Certified Reference Materials at CANMET-MMSL*. Ontario.
- NIEDERER, F. R., PAPANASTASSIOU, D. A. & WASSERBURG, G. J. (1985) Absolute isotopic abundances of Ti in meteorites. *Geochimica et Cosmochimica Acta*, 49, 835-851.
- NIER, A. O. (1936) A Mass-Spectrographic Study of the Isotopes of Argon, Potassium, Rubidium, Zinc and Cadmium. *Physical Review*, 50, 1041.
- NRIAGU, J. O. & DAVIDSON, C. I. (1980) Zinc in the Atmosphere. IN NRIAGU, J. O. (Ed.) *Zinc in the Environment*. Ontario, John Wiley & Sons.
- NRIAGU, J. O. & PACYNA, J. M. (1988) Quantitative assessment of worldwide contamination of air, water and soils by trace metals. *Nature*, 333.
- OUYANG, Y., HIGMAN, J., THOMPSON, J., O'TOOLE, T. & CAMPBELL, D. (2002) Characterization and spatial distribution of heavy metals in sediment from Cader and Ortega rivers subbasin. *Journal of Contaminant Hydrology*, 54, PP 19-35.

- PATTERSON, K. Y., VEILLON, C., MOSER-VEILLON, P. B. & WALLACE, G. F. (1992) Determination of zinc stable isotopes in biological materials using isotope dilution inductively coupled plasma mass spectrometry. *Analytica Chimica Acta*, 258, 317-324.
- PETIT, J. C. J., DE JONG, J., CHOU, L. & MATTIELLI, N. (2008) Development of Cu and Zn Isotope MC-ICP-MS Measurements: Application to Suspended Particulate Matter and Sediments from the Scheldt Estuary. *Geostandards and Geoanalytical Research*, 32, 149-166.
- PICHAT, S., ALBARÈDE, F. & DOUCHET, C. (2003a) Zinc Isotope Variations In Deep -sea Carbonates From The Eastern Equatorial Pacific Over The Last 175 Ka. *Earth And Planetary Science Letters*, 6598, 1-12.
- PICHAT, S., DOUCHET, C. & ALBAREDE, F. (2003b) Zinc isotope variations in deep -sea carbonates from the eastern equatorial Pacific over the last 175 ka. *Earth and Planetary Science Letters*, 210, 167-178.
- PICHAT, S., DOUCHET, C. & ALBAREDE, F. (2003c) Zinc isotope variations in deep-sea carbonates from the eastern equatorial Pacific over the last 175 ka. *Earth and Planetary Science Letters*, 210, 167-178.
- PLATZNER, I. T., HABFAST, K., WALDER, A. J. & GOETZ, A. (1997) *Modern Isotope Ratio Mass Spectrometry*, West Sussex, John Wiley and Sons Ltd.
- PLUMMER, C. C. & MCGEARY, D. (1985) *Physical Geology*.
- PONZEVERA, E., QUETEL, C. R., BERGLUND, M., TAYLOR, P. D. P., EVANS, P., LOSS, R. D. & FORTUNATO, G. (2006) Mass Discrimination During MC-ICPMS Isotopic Ratio Measurements: Investigation by Means of Synthetic Isotopic Mixtures (IRMM-007 Series) and Application to the Calibration of Natural-Like Zinc Materials (Including IRMM-3702 and IRMM-651). *Journal of the American Society for Mass Spectrometry*, 17, 1413-1428.
- ROGERS, H. H., RUNION, G. B. & KRUPA, S. V. (1994) Plant responses to atmospheric CO₂ enrichment with emphasis on roots and the rhizosphere. *Environmental Pollution*, 83, 155-189.
- ROSMAN, K. J. R. (1972a) The Isotopic and Elemental Abundance of Zinc in Terrestrial and Meteoritic Matter. Perth, University of Western Australia.
- ROSMAN, K. J. R. (1972b) A survey of the isotopic and elemental abundance of zinc. *Geochimica et Cosmochimica Acta*, 36, 801-819.
- ROSMAN, K. J. R. (2008) Calibration of the double spike solution. IN GHIDAN, O. Y. (Ed.). Perth.
- ROSMAN, K. J. R. & DE LAETER, J. R. (1974) The abundance of cadmium and zinc in meteorites. *Geochimica et Cosmochimica Acta*, 38, 1665-1677.
- ROSMAN, K. J. R. & DE LAETER, J. R. (1975) The isotopic composition of cadmium in terrestrial minerals. *International Journal of Mass Spectrometry and Ion Physics*, 16, 385-394.
- ROSMAN, K. J. R. & DE LAETER, J. R. (1976) Isotopic fractionation in meteoritic cadmium. *Nature*, 261, 216-218.
- ROSMAN, K. J. R., DE LAETER, J. R. & GORTON, M. P. (1980) Cadmium isotope fractionation in fractions of two H3 chondrites. *Earth and Planetary Science Letters*, 48, 166-170.
- ROSMAN, K. J. R. & JEFFERY, P. M. (1971) The Determination of Zinc in Standard Reference Materials by Isotope Dilution and Atomic Absorption Analysis. *Chemical Geology*, 8, 25-32.

- RUSSELL, R. D. (1971) The systematics of double spiking. *Journal of Geophysical Research*, 76, 4949-4955.
- RUSSELL, W. A., PAPANASTASSIOU, D. A. & TOMBRELLO, T. A. (1978) Ca isotope fractionation on the Earth and other solar system materials. *Geochimica et Cosmochimica Acta*, 42, 1075-1090.
- SATOKO, A. (2006) Investigation of molecular interaction within biological macromolecular complexes by mass spectrometry. *Medicinal Research Reviews*, 26, 339-368.
- SCHEDIWIY, S., ROSMAN, K. J. R. & DE LAETER, J. R. (2006) Isotope fractionation of cadmium in lunar material. *Earth and Planetary Science Letters*, 243, 326-335.
- SCHILLING, J. G. (1973) Iceland mantle plume: Geochemical study of Reykjanes ridge. *Nature*, 242, 565-571.
- SERFASS, R. E., THOMPSON, J. J. & HOUK, R. S. (1986) Isotope ratio determinations by inductively coupled plasma/mass spectrometry for zinc bioavailability studies. *Analytica Chimica Acta*, 188, 73-84.
- SHARP, Z. (2007) *Principles of Stable Isotope Geochemistry*, Pearson education.
- SHILLER, A. M. & BOYLE, E. (1985) Dissolved Zinc in rivers. *Nature*, 317, PP 49-52.
- SHUBINA, N. A. & KOLESOV, G. M. (2002) Determination of heavy metals as environmental pollutants: Use of Instrumental Neutron Activation Analysis. *Journal of Analytical Chemistry*, 57, 912-919.
- SIEBERT, C., NAGLER, T. F., VON BLANCKENBURG, F. & KRAMERS, J. D. (2003) Molybdenum isotope records as a potential new proxy for paleoceanography. *Earth and Planetary Science Letters*, 211, 159-171.
- SIVRY, Y., RIOTTE, J., SONKE, J. E., AUDRY, S., SCHÄFER, J., VIERS, J., BLANC, G., FREYDIER, R. & DUPRÉ, B. (In press) Zn isotopes as tracers of anthropogenic pollution from Zn-ore smelters. The Riou Mort-Lot River system. *Chemical Geology*, In Press, Accepted Manuscript.
- SKRZYPEK, G., KALUZNY, A. & JEDRYSEK, M. O. (2007a) Carbon Stable Isotope Analyses of Mosses--Comparisons of Bulk Organic Matter and Extracted Nitrocellulose. *Journal of the American Society for Mass Spectrometry*, 18, 1453-1458.
- SKRZYPEK, G., KALUZNY, A., WOJTUN, B. & JEDRYSEK, M.-O. (2007b) The carbon stable isotopic composition of mosses: A record of temperature variation. *Organic Geochemistry*, 38, 1770-1781.
- SLOWEY, J. F. & HOOD, D. W. (1971) Copper, Manganese and Zinc concentrations in the gulf of Mexico waters. *Geochimica et Cosmochimica Acta*, 35, PP121-138.
- STENBERG, A., ANDREN, H., MALINOVSKY, D., ENGSTROM, E., RODUSHKIN, I. & BAXTER, D. C. (2004) Isotopic Variations of Zn in Biological Materials. *Anal. Chem.*, 76, 3971-3978.
- STENBERG, A., MALINOVSKY, D., OHLANDER, B., ANDREN, H., FORSLING, W., ENGSTROM, L.-M., WAHLIN, A., ENGSTROM, E., RODUSHKIN, I. & BAXTER, D. C. (2005) Measurement of iron and zinc isotopes in human whole blood: Preliminary application to the study of HFE genotypes. *Journal of Trace Elements in Medicine and Biology*, 19, 55-60.
- STOREY, B. (2007) Zinc. IN BARKER, A., PILBEAM, D., FRANCIS & TAYLOR (Eds.) *Handbook of plant nutrition*.

- STOWASSER, G., PIERCE, G. J., MOFFAT, C. F., COLLINS, M. A. & FORSYTHE, J. W. (2006) Experimental study on the effect of diet on fatty acid and stable isotope profiles of the squid *Lolliguncula brevis*. *Journal of Experimental Marine Biology and Ecology*, 333, 97-114.
- STURUP, S. (2000) Application of HR-ICP-MS for the simultaneous measurement of Zinc isotope ratios and total Zinc content in human samples. *Journal of Analytical Atomic Spectrometry*, 15, 315-321.
- TAMELANDER, T., SOREIDE, J. E., HOP, H. & CARROLL, M. L. (2006) Fractionation of stable isotopes in the Arctic marine copepod *Calanus glacialis*: Effects on the isotopic composition of marine particulate organic matter. *Journal of Experimental Marine Biology and Ecology*, 333, 231-240.
- TANIMIZU, M., ASADA, Y. & HIRATA, T. (2002) Absolute isotopic composition and atomic weight of commercial zinc using Inductively Coupled Plasma Mass Spectrometry. *Anal. Chem.*, 74, 5814-5819.
- THORPE, S. E., MURPHY, E. J. & WATKINS, J. L. (2007) Circumpolar connections between Antarctic krill (*Euphausia superba* Dana) populations: Investigating the roles of ocean and sea ice transport. *Deep Sea Research Part I: Oceanographic Research Papers*, 54, 792-810.
- TURNLUND, J. R. & KEYES, W. R. (1990) Automated analysis of stable isotopes of Zinc, Copper, Iron, Calcium and Magnesium by Thermal Ionisation Mass Spectrometry using double isotope dilution for tracer studies in humans. *Journal of Micronutrient Analysis*, 7, 117-145.
- UMEDA, H. & NOMOTO, K. I. (2002) Nucleosynthesis of zinc and iron-peak elements in Pop III type II supernovae: comparison with abundances of very metal-poor halo stars. *Astrophysical Journal* 565.
- UREY, H. C. (1952) The origin and development of the earth and other terrestrial planets: A correction. *Geochimica et Cosmochimica Acta*, 2, 263-268.
- USGS (1995a) Certificate of Analysis, Cody Shale, SCo-1.
- USGS (1995b) Certificate of Analysis, Diabase, W-2
- USGS (1995c) Certificate of Analysis, Dolerite, DNC-1.
- USGS (1998a) Certificate of Analysis, Icelandic Basalt, BIR-1. United States Geological Survey.
- USGS (1998b) Certificate of Analysis, Mica Schist, SDC-1. Colorado.
- USGS (1998c) Certificate of Analysis, Quartz Latite, QLO-1.
- USGS (2001) Certificate of Analysis, Green River Shale, SGR-1.
- USGS (2006a) BCR-1. IN GHIDAN, O. (Ed.). Perth.
- USGS (2006b) Certificate of analysis, Basalt, Columbia River, BCR-2.
- USGS (2008) Currently Available Reference Materials. IN USGS (Ed.). U.S. Department of the Interior.
- WEBSTER, R. K. (1960) Mass spectrometric isotope dilution analysis. IN SMALES, A. A. & WAGER, L. R. (Eds.) *Methods in Geochemistry*. Interscience Publishers Inc.
- WEISS, D. J., MASON, T. F. D., ZHAO, F. J., KIRK, G. J. D., COLES, B. J. & HORSTWOOD, M. S. A. (2005) Isotopic discrimination of zinc in higher plants. *New Phytologist*, 165, 703-710.
- WEISS, D. J., RAUSCH, N., MASON, T. F. D., COLES, B. J., WILKINSON, J. J., UKONMAANAHO, L., ARNOLD, T. & NIEMINEN, T. M. (2007)

- Atmospheric deposition and isotope biogeochemistry of zinc in ombrotrophic peat. *Geochimica et Cosmochimica Acta*, 71, 3498-3517.
- WHO (2001) Environmental health criteria:221 Zinc. *International Programme of chemical safety(IPCS)*.
- WHO (2003) Zinc in Drinking- water. *Guidlines for drinking-water quality*, 2.
- WHO (2004) Environmental health criteria:221 Zinc. *International Programme of chemical safety(IPCS)*.
- WIESER, M. E. & DE LAETER, J. R. (2003) Preliminary study of isotope fractionation in molybdenites. *International Journal of Mass Spectrometry*, 225, 177-183.
- WIESER, M. E. & DE LAETER, J. R. (2008) Dissolving procedure for iron meteorites. IN O., G. (Ed.). Perth.
- WIESER, M. E., DE LAETER, J. R. & VARNER, M. D. (2007) Isotope fractionation studies of molybdenum. *International Journal of Mass Spectrometry*, 265, 40-48.
- WILBER, W. G., V., H. J. & BALMAT, J. (1980) Zinc in urban storm and wastewaters. IN NRIAGU, J. O. (Ed.) *Zinc in the environment*. Ontario, John Wiley&Sons.
- WILKINSON, J. J., WEISS, D. J., MASON, T. F. D. & COLES, B. J. (2005) ZINC ISOTOPE VARIATION IN HYDROTHERMAL SYSTEMS: PRELIMINARY EVIDENCE FROM THE IRISH MIDLANDS ORE FIELD. *Economic Geology*, 100, 583-590.
- WOMBACHER, F., REHKAMPER, M., MEZGER, K., BISCHOFF, A. & MUNKER, C. (2008) Cadmium stable isotope cosmochemistry. *Geochimica et Cosmochimica Acta*, 72, 646-667.
- WOMBACHER, F., REHKAMPER, M., MEZGER, K. & MUNKER, C. (2003) Stable isotope compositions of cadmium in geological materials and meteorites determined by multiple-collector ICPMS. *Geochimica et Cosmochimica Acta*, 67, 4639-4654.
- XUE, S., YU, Y., ROGER, H., HEWINS, G. S. & HERZOG, G. F. (1996) Zinc losses from and Zinc isotopic abundances in residues formed by heating of Zn, ZnO and Zn-DOPED Silicate glass. *Lunar and planetary institute-NASA Astrophysics data system*.
- YIN, Q.-Z. (2004) From dust to planets: the tale told by moderately volatile element depletion(moved). *Workshop on chondrites and protoplanetary Disk(2004)*, 9066.
- YOSHINAGA, J., MORITA, M. & EDMONDS, J. S. (1999) Determination of copper, zinc, cadmium and lead in a fish otolith certified reference material by isotope dilution inductively coupled plasma mass spectrometry using off-line solvent extraction. *Journal of Analytical Atomic Spectrometry*, 14, PP1589-1592.
- ZHU, X. K., GUO, Y., WILLIAMS, R. J. P., O'NIONS, R. K., MATTHEWS, A., BELSHAW, N. S., CANTERS, G. W., DE WAAL, E. C., WESER, U., BURGESS, B. K. & SALVATO, B. (2002) Mass fractionation processes of transition metal isotopes. *Earth and Planetary Science Letters*, 200, 47-62.
- ZOLLER, W. H., GLADNEY, E. S. & DUCE, R. A. (1974) Atmospheric concentrations and sources of trace metals at the south pole. *Science*, 183, PP198-200.

- **Appendix A: Abstract of the Australian Institute of Physics Post Graduate Research Conference. Institute of Human Development Jarrahdale- August 23-25, 2006**

ISOTOPIC MEASUREMENTS OF Zn IN NATURAL MATERIALS

O.Y. Ghidan, R. Loss and K. Rosman

Department of Applied Physics
Curtin University of Technology
Perth, 6845 Western Australia
O.Ghidan@curtin.edu.au

A thermal ionisation mass spectrometer was used to accurately measure the concentration of zinc by isotope dilution mass Spectrometry (IDMS) in a range of materials. IDMS is considered the most accurate of analytical concentration determination techniques. The materials analysed were: a zinc dietary supplement tablet, galvanised roofing material, tap water, Swan River water and USGS geochemical rock standards: diabase W-2, basalt BIR-1, Quartz Latite QLO-1, and Mica Schist SDC-1. The concentrations of Zn ranged from $(2.6 \text{ to } 7.9) \pm 0.4 \text{ ng.g}^{-1}$ for Swan River water samples to $20.7 \pm 0.6 \text{ mg /tablet}$ in the Zn tablet, and from $(59 \pm 1) \mu\text{g.g}^{-1}$ for the QLO-1 to $(100 \pm 1) \mu\text{g.g}^{-1}$ for the SDC-1 in the geochemical standards. Measurements of the geochemical standards agreed with the recommended values of $(61 \pm 3) \mu\text{g.g}^{-1}$ for the QLO-1 and $(103 \pm 8) \mu\text{g.g}^{-1}$ for the SDC-1. Find references in [1].

Preliminary measurements of the isotopic composition of Zn have also been performed on some geochemical standards and Swan River water samples. The isotopic composition of Zn was found to be the same as that of a laboratory standard (Zn10759) within the uncertainty of each individual measurement. Further experiments are currently in progress to accurately determine Zn isotopic fractionation systematics.

This work is part of a major investigation into the consistency of the isotopic composition of Zn in nature. Small variations in the isotopic composition are believed to provide useful insight into aspects of biogeochemistry as well as potentially affecting the atomic weight of this element. Find references in [2].

References

- [1]. USGS, *Currently Available Reference Materials*, USGS. 2006, U.S.Department of the Interior.
- [2]. Pichat, S., C. Douchet, and F. Albarede, *Zinc isotope variations in deep -sea carbonates from the eastern equatorial Pacific over the last 175 ka*. Earth and Planetary Science Letters, 2003. **210**: p. 167-178.

- **Appendix B: Abstract of the Isotope Science Symposium- International Commission on Isotopic Abundances and Atomic Weights.
23rd July 2007
CNR Pisa Italia**

**The Isotopic Composition of Zn
O. Ghidan and R. Loss, Curtin University of Technology
Perth, Western Australia.**

Zinc is an important element in biological and geological cycles and plays a significant role in human health. Recently, mass dependent, sub-permil per amu, variations (isotopic fractionation) in the isotopic composition of Zn have been reported as potential indicators of various cycle processes but no widespread assessment of this isotopic fractionation of this element has ever been undertaken. In this presentation we will describe the measurement of the fractionation of Zn in a range of natural materials and potential high purity laboratory standards, using TIMS and the double spiking technique with an external accuracy of around 0.15 per mil per amu. Thus far the Zn fractionation in a range of geochemical reference materials (GRMs) and high purity Zn laboratory reagents have been measure with all of the GRMs falling within uncertainty of each other and the accepted zero fractionation Zn standard (IRMM - 3702). Several of the high reagents show substantial fraction of which reinforces the need for great care to be taken in the use of high purity Zn reagents in isotope laboratories. Ongoing work is investigating fractionation in Zn minerals and other natural materials. The results are also being used to determine the variation in the atomic weight of Zinc to help assess a final uncertainty for the atomic weight of this element.

- **Appendix C: Abbreviations and units**

AA	General Flame Atomic Absorption
a	Annum
AFC	Assimilation with Fractional Crystallization
amu	Atomic mass unit
CAI	Calcium Aluminium rich inclusions
DCPES	Direct Coupled Plasma Atomic Emission Spectrometry
EEN	Empirical External Normalization
eV	Electron Volt
EXRF	Energy Dispersive X-ray Fluorescence
FUN	Fractionation and unknown nuclear isotopic effects
GFAAS	Graphite Furnace Atomic Absorption Spectrometry
HEPA	High Efficiency Particulate Air
ICP-AES	Inductively coupled plasma atomic emission spectrometry
ICPES	Inductively coupled plasma atomic emission spectrometry
ID-ICP-MS	Isotope Dilution Inductively Coupled Plasma -Mass spectrometry
IDMS	Isotope Dilution Mass Spectrometry
IFF	Isotopic fractionation factor
IRMM	Institute for Reference Materials and Measurements
ITNA	Instrumental Thermal Neutron Activation
IUPAC	International Union for Pure and Applied Chemistry
MC-ICP-MS	Multiple Collector -Inductively Coupled Plasma -Mass spectrometry/ spectrometers
MC-ICP-SFMS	Inductively Coupled Plasma Sector Field Mass Spectrometer
MZM	Multi Zone Mixing Model
NBS	National Bureau of Standards
NSE	Nuclear Statistical Equilibrium
OES	General, DC Arc Optical Emission Spectrometry

PDB	Peede Belemnite
pgg^{-1}	pico gram per gram
RUBISCO	ribulose biphosphate carboxylase oxidase ,
SCBM	Sample-calibrator bracketing on measured isotopic ratios
SRM	Standard Reference Materials
SSMS	Spark-source Mass Spectrometry
TIMS	Thermal Ionisation Mass Spectrometry/ Spectrometer
XRF	X-ray fluorescence
ϵ	One part in ten thousand
μgg^{-1}	micro gram per gram

- **Appendix D: Detailed isotopic Data**

Data for measured isotopic fractionation in the samples using the double spike technique and the data of isotopic ratio of unspiked samples.

Table A. 1: Data for the precision of the calculated precision of the measured fractionation.

Sample Type	Sample	n	Carousel Number	$^{66}\text{Zn}/^{64}\text{Zn}$	$^{67}\text{Zn}/^{64}\text{Zn}$	$^{68}\text{Zn}/^{64}\text{Zn}$	$^{70}\text{Zn}/^{64}\text{Zn}$	f ‰ amu ⁻¹	±
Mixtures of Laboratory standard and the double spike " fractionation precision"	M1	1	4540,4	0.563727	0.231797	0.374630	0.090964	0.03	0.18
	± 95%			0.000035	0.000024	0.000000	0.000020		
	M1	2	4540,5	0.563650	0.231682	0.374497	0.090894	0.00	0.19
	± 95%			0.000036	0.000025	0.000000	0.000023		
	M1	3	4540,6	0.563583	0.231684	0.374420	0.090872	0.06	0.16
	± 95%			0.000024	0.000015	0.000000	0.000012		
	M1	4	4540,7	0.56413	0.23192	0.375105	0.09110	-0.04	0.20
	± 95%			0.00005	0.00002	0.000000	0.00003		
	M1	5	4545,3	0.564176	0.232066	0.375234	0.091199	-0.07	0.29
	± 95%			0.000057	0.000050	0.000000	0.000051		
	M1	6	4545,5	0.5636997	0.231886	0.374609	0.091010	0.01	0.25
	± 95%			0.000062	0.000048	0.000000	0.000042		
	M1	7	4548,4	0.563841	0.231787	0.374706	0.090974	0.00	0.23
	± 95%			0.000065	0.000035	0.000000	0.000037		
	M1	8	4558_2	0.56375	0.231694	0.37471	0.090916	0.05	0.30
	± 95%			0.00010	0.000064	0.000000	0.000060		
	Average						0.006		
	σ						0.042		
	Counts						8		
	± 95%						0.039		

Table A. 2: Data used to calculate the contribution of the Anion exchange column chemistry to the fractionation

Sample Type	Sample	Carousel Number	N Columns	$^{66}\text{Zn}/^{64}\text{Zn}$	$^{67}\text{Zn}/^{64}\text{Zn}$	$^{68}\text{Zn}/^{64}\text{Zn}$	$^{70}\text{Zn}/^{64}\text{Zn}$
Standard and double spike (double spike mixed after the column chemistry)	Standard Alfa Aesar 10759	4591,13	1	0.571907	0.38625	0.387194	0.172048
	± 95%			0.000082	0.00006	0.000000	0.000058
	Standard Alfa Aesar 10759	5605,11	2	0.575792	0.491948	0.393692	0.226901
	± 95%			0.000094	0.000070	0.000000	0.000059
	Standard Alfa Aesar 10759	4629,14	3	0.576124	0.486246	0.393800	0.224091
	± 95%			0.000072	0.000084	0.000000	0.000061
	Standard Alfa Aesar 10759	4605,12	4	0.571300	0.388999	0.386597	0.173211
	± 95%			0.00007	0.000043	0.000067	0.000049

Table A. 3: Data for the measured double spiked ratios for the measured Zinc minerals.

Sample Type	Sample	Experiment Number	Carousel Number	$^{66}\text{Zn}/^{64}\text{Zn}$	$^{67}\text{Zn}/^{64}\text{Zn}$	$^{68}\text{Zn}/^{64}\text{Zn}$	$^{70}\text{Zn}/^{64}\text{Zn}$	
Zinc minerals	Sphalarite	1	4558,4	0.571232	0.32088	0.385642	0.138600	
	± 95%			0.000095	0.00015	0.000000	0.000096	
	Sphalarite	2	4558,6	0.568695	0.319185	0.382198	0.136919	
	± 95%			0.000069	0.000066	0.000000	0.000046	
	Hydrozincite	1	4558,10	0.567804	0.434793	0.382198	0.194679	
	± 95%			0.000059	0.000062	0.000000	0.000048	
	Hydrozincite	2	4558,11	0.57729	0.44485	0.394865	0.20413	
	± 95%			0.00010	0.00016	0.000000	0.00011	
	Smithsonite a	1	4561,11	0.5662820	0.267314	0.378451	0.109704	
	± 95%			0.0000088	0.000034	0.000000	0.000025	
	Smithsonite a	2	4561,13	0.566776	0.267687	0.379118	0.110088	
	± 95%			0.000049	0.000042	0.000000	0.000036	

Table A. 4: Data for the measured double spiked ratios for the measured Zn pure standard metals.

Sample Type	Sample	Experiment Number	Carousel Number	Detector	$^{66}\text{Zn}/^{64}\text{Zn}$	$^{67}\text{Zn}/^{64}\text{Zn}$	$^{68}\text{Zn}/^{64}\text{Zn}$	$^{70}\text{Zn}/^{64}\text{Zn}$
Pure standard Zn metals	AE 10760	1		Daly	0.55762	0.33406	0.36760	0.14289
	± 95%				0.00033	0.00019	0.00028	0.00014
	AE 10760	2		Daly	0.55962	0.38731	0.37069	0.17016
	± 95%				0.00020	0.00019	0.00017	0.00026
	AE 10760	3		Daly	0.55697	0.32409	0.36732	0.13798
	± 95%				0.00024	0.00016	0.00022	0.00014

AE 10760	4			Daly	0.55703	0.30964	0.36661	0.13036
± 95%					0.00031	0.00023	0.00033	0.00017
AE 10760	5			Daly	0.55466	0.26573	0.36303	0.10790
± 95%					0.00019	0.00024	0.00022	0.00011
AE 10760	6			Daly	0.55314	0.27142	0.36111	0.10979
± 95%					0.00079	0.00083	0.00093	0.00097
AE 10760	7			Daly	0.55508	0.29031	0.36462	0.12036
± 95%					0.00051	0.00039	0.00050	0.00034
AE 10760	8			Daly	0.55723	0.31897	0.36826	0.13575
± 95%					0.00025	0.00020	0.00034	0.00023
AE 10760	9			Daly	0.55543	0.29583	0.36505	0.12332
± 95%					0.00013	0.00012	0.00017	0.00006
AE 10760	10			Daly	0.55466	0.27949	0.36343	0.11487
± 95%					0.00020	0.00021	0.00026	0.000090
AE 10760	11			Daly	0.55368	0.25826	0.36277	0.10407
± 95%					0.00027	0.00018	0.00022	0.00011
AE 10760	12	4538,9		Faraday Multi collector	0.558246	0.222957	0.367184	0.086714
± 95%					0.000075	0.000051	0.000000	0.000039
AE 10760	13	4538,8		Faraday Multi collector	0.557920	0.222716	0.367076	0.086629
± 95%					0.000085	0.000072	0.000000	0.000067

Table A. 5: Data for the measured double spiked ratios for the measured Zn pure standard metals.

Sample Type	Sample	Experiment Number	Carousel Number	Detector	$^{66}\text{Zn}/^{64}\text{Zn}$	$^{67}\text{Zn}/^{64}\text{Zn}$	$^{68}\text{Zn}/^{64}\text{Zn}$	$^{70}\text{Zn}/^{64}\text{Zn}$
Pure Zn standard metals	IRMM 10440	1	4551,13	Faraday Multi collector	0.564641	0.244290	0.375983	0.097535
	± 95%			0.000035	0.000029	0.000000	0.000023	
	IRMM 10440	2	4551,14	Faraday Multi collector	0.564799	0.244298	0.376152	0.097564
	± 95%			0.000071	0.000059	0.000000	0.000044	

Table A. 6: Data for the measured double spiked ratios for the measured Zn pure standard metals.

Sample Type	Sample	Experiment Number	Carousel Number	Detector	$^{66}\text{Zn}/^{64}\text{Zn}$	$^{67}\text{Zn}/^{64}\text{Zn}$	$^{68}\text{Zn}/^{64}\text{Zn}$	$^{70}\text{Zn}/^{64}\text{Zn}$
Pure Zn standard metals	IRMM 3702	1	4554,5	Faraday Multi collector	0.561497	0.176138	0.371054	0.061852
	± 95%			0.000027	0.000016	0.000000	0.000014	
	IRMM 3702	2	4554,7	Faraday Multi collector	0.560995	0.175946	0.370573	0.061740
	± 95%			0.000059	0.000042	0.000000	0.000025	

Table A. 7: Data for the measured double spiked ratios for the measured Zn pure standard metals.

Sample Type	Sample	Experiment Number	Carousel Number	Detector	$^{66}\text{Zn}/^{64}\text{Zn}$	$^{67}\text{Zn}/^{64}\text{Zn}$	$^{68}\text{Zn}/^{64}\text{Zn}$	$^{70}\text{Zn}/^{64}\text{Zn}$
Pure Zn standard metals	ZnO6	1	4554,14	Faraday Multi collector	0.557968	0.215274	0.367075	0.082542
	± 95%			0.000036	0.000022	0.000000	0.000023	
	ZnO6	2	4554,15	Faraday Multi collector	0.557984	0.215296	0.367075	0.082590
	± 95%			0.000040	0.000038	0.000000	0.000030	
	ZnO6	3		Faraday Multi collector	0.557996	0.215226	0.367020	0.082564
	± 95%			0.000048	0.000040	0.000000	0.000036	

Table A. 8: Data for the measured double spiked ratios for the measured Zn pure standard metals.

Sample Type	Sample	Experiment Number	Carousel Number	Detector	$^{66}\text{Zn}/^{64}\text{Zn}$	$^{67}\text{Zn}/^{64}\text{Zn}$	$^{68}\text{Zn}/^{64}\text{Zn}$	$^{70}\text{Zn}/^{64}\text{Zn}$
Pure Zn standard metals	GF 6110	1	4564,14	Faraday	0.563498	0.231123	0.374330	0.090630
	$\pm 95\%$			Multi collector	0.000057	0.000051	0.000000	0.000042
	GF 6110	2	4564,16	Faraday	0.563736	0.231188	0.374695	0.090716
	$\pm 95\%$			Multi collector	0.000052	0.000047	0.000000	0.000035

Table A. 9: Data for the measured double spiked ratios for the measured Zn pure standard metals.

Sample Type	Sample	Experiment Number	Carousel Number	Detector	$^{66}\text{Zn}/^{64}\text{Zn}$	$^{67}\text{Zn}/^{64}\text{Zn}$	$^{68}\text{Zn}/^{64}\text{Zn}$	$^{70}\text{Zn}/^{64}\text{Zn}$
Pure Zn standard metals	JMC-2	1	4608,2	Faraday	0.569918	0.353171	0.384082	0.154615
	$\pm 95\%$			Multi collector	0.000058	0.000057	0.000000	0.000044
	JMC-2	2	4608,4	Faraday	0.569284	0.352825	0.383373	0.154228
	$\pm 95\%$			Multi collector	0.000048	0.000059	0.000000	0.000037

Table A. 10: Data for the measured double spiked ratios for the measured Zn pure standard metals.

Sample Type	Sample	Experiment Number	Carousel Number	Detector	$^{66}\text{Zn}/^{64}\text{Zn}$	$^{67}\text{Zn}/^{64}\text{Zn}$	$^{68}\text{Zn}/^{64}\text{Zn}$	$^{70}\text{Zn}/^{64}\text{Zn}$
Pure Zn standard metals	GF 6120	1	4568,14	Faraday Multi collector	0.562600	0.208286	0.372796	0.078699
	± 95%			0.000053	0.000048	0.000000	0.000039	
	GF 6120	2	4568,15	Faraday Multi collector	0.563125	0.208670	0.373677	0.078959
	± 95%			0.000053	0.000042	0.000000	0.000033	
	GF 6120	3	4586,13	Faraday Multi collector	0.575670	0.466510	0.393098	0.214182
	± 95%			0.000089	0.000075	0.000000	0.000078	

Table A. 11: Data for the measured double spiked ratios for igneous rocks.

Sample Type	Sample	Experiment Number	Carousel Number	$^{66}\text{Zn}/^{64}\text{Zn}$	$^{67}\text{Zn}/^{64}\text{Zn}$	$^{68}\text{Zn}/^{64}\text{Zn}$	$^{70}\text{Zn}/^{64}\text{Zn}$
Igneous rocks	BCR-1	1	4548,9	0.573581	0.40926	0.389598	0.184290
	± 95%			0.000069	0.00006	0.000000	0.000053
	BCR-1	2	4548,10	0.57357	0.409046	0.389449	0.18417
	± 95%			0.00015	0.000098	0.000000	0.00013
	BCR-1	3	4551,4	0.57300	0.40807	0.388936	0.18349
	± 95%			0.00013	0.00011	0.000000	0.00011
	BCR-1	4	4561,5	0.565563	0.247540	0.377350	0.099410
	± 95%			0.000067	0.000033	0.000000	0.000034
	BCR-1	5	4561,7	0.565581	0.247540	0.377369	0.099412
	± 95%			0.000055	0.000045	0.000000	0.000024
	BCR-1	6	4564,6	0.565924	0.263390	0.378015	0.107638
	± 95%			0.000056	0.000047	0.000000	0.000043

Table A. 12: Data for the measured double spiked ratios for igneous rocks

Sample Type	Sample	Experiment Number	Carousel Number	$^{66}\text{Zn}/^{64}\text{Zn}$	$^{67}\text{Zn}/^{64}\text{Zn}$	$^{68}\text{Zn}/^{64}\text{Zn}$	$^{70}\text{Zn}/^{64}\text{Zn}$
Igneous rocks	BIR-1	1	4548,7	0.567880	0.288520	0.380697	0.120991
	± 95%			0.000054	0.000052	0.000000	0.000039
	BIR-1	2	4548,8	0.567690	0.288359	0.380458	0.120891
	± 95%			0.000067	0.000045	0.000000	0.000045

Table A. 13: Data for the measured double spiked ratios for igneous rocks

Sample Type	Sample	Experiment Number	Carousel Number	$^{66}\text{Zn}/^{64}\text{Zn}$	$^{67}\text{Zn}/^{64}\text{Zn}$	$^{68}\text{Zn}/^{64}\text{Zn}$	$^{70}\text{Zn}/^{64}\text{Zn}$
Igneous rocks	W-2	1	4548,9	0.573581	0.409257	0.389598	0.184290
	± 95%			0.000069	0.000063	0.000000	0.000053
	W-2	2	4548,10	0.57357	0.409046	0.389449	0.18417
	± 95%			0.00015	0.000098	0.000000	0.00013
	W-2	3	4551,4	0.57300	0.40807	0.388936	0.18349
	± 95%			0.00013	0.00011	0.000000	0.00011
	W-2	4	4561,5	0.565563	0.247540	0.377350	0.099410
	± 95%			0.000067	0.000033	0.000000	0.000034
	W-2	5	4561,7	0.565581	0.247540	0.377369	0.099412
	± 95%			0.000055	0.000045	0.000000	0.000024
	W-2	6	4564,6	0.565924	0.263390	0.378015	0.107638
	± 95%			0.000056	0.000047	0.000000	0.000043

Table A. 14: Data for the measured double spiked ratios for igneous rocks.

Sample Type	Sample	Experiment Number	Carousel Number	$^{66}\text{Zn}/^{64}\text{Zn}$	$^{67}\text{Zn}/^{64}\text{Zn}$	$^{68}\text{Zn}/^{64}\text{Zn}$	$^{70}\text{Zn}/^{64}\text{Zn}$
Igneous rocks	DNC-1	1	4551,10	0.566427	0.262524	0.378723	0.107377
	± 95%			0.000043	0.000021	0.000000	0.000009
	DNC-1	2	4551,11	0.56715	0.262880	0.379585	0.10770
	± 95%			0.00011	0.000075	0.000000	0.00006
	DNC-1	3	4561,8	0.56657	0.24813	0.378621	0.09987
	± 95%			0.00008	0.00009	0.000000	0.00006
	DNC-1	4	4561,9	0.565493	0.247535	0.377092	0.099438
	± 95%			0.000111	0.000079	0.000000	0.000078

Table A. 15: Data for the measured double spiked ratios for igneous rocks.

Sample Type	Sample	Experiment Number	Carousel Number	$^{66}\text{Zn}/^{64}\text{Zn}$	$^{67}\text{Zn}/^{64}\text{Zn}$	$^{68}\text{Zn}/^{64}\text{Zn}$	$^{70}\text{Zn}/^{64}\text{Zn}$
Sedimentary rocks	SGR-1	1	4548,12	0.57167	0.36322	0.386571	0.16023
	± 95%			0.00016	0.00017	0.000000	0.00012
	SGR-1	2	4548,13	0.572197	0.363644	0.387194	0.160572
	± 95%			0.000075	0.000088	0.000000	0.000064

Table A. 16: Data for the measured double spiked ratios for sedimentary rocks.

Sample Type	Sample	Experiment Number	Carousel Number	$^{66}\text{Zn}/^{64}\text{Zn}$	$^{67}\text{Zn}/^{64}\text{Zn}$	$^{68}\text{Zn}/^{64}\text{Zn}$	$^{70}\text{Zn}/^{64}\text{Zn}$
Sedimentary rocks	SCO-1	1	4551,7	0.562180	0.214720	0.372574	0.081939
	± 95%			0.000079	0.000050	0.000000	0.000036
	SCO-1	2	4551,8	0.562379	0.214789	0.372801	0.081998
	± 95%			0.000082	0.000066	0.000000	0.000049
	SCO-1	3	4551,9	0.562405	0.214878	0.372927	0.082049
	± 95%			0.000059	0.000057	0.000000	0.000042

Table A. 17: Data for the measured double spiked ratios for sedimentary rocks

Sample Type	Sample	Experiment Number	Carousel Number	$^{66}\text{Zn}/^{64}\text{Zn}$	$^{67}\text{Zn}/^{64}\text{Zn}$	$^{68}\text{Zn}/^{64}\text{Zn}$	$^{70}\text{Zn}/^{64}\text{Zn}$
Sedimentary rocks	HISS-1	1	4583,4	0.57864	0.53073	0.397717	0.247598
	± 95%			0.00013	0.00013	0.000000	0.000095
	HISS-1	2	4586,2	0.57853	0.529374	0.397567	0.246951
	± 95%			0.00011	0.000090	0.000000	0.000082
	HISS-1	3	4596,10	0.573319	0.421671	0.389475	0.190433
	± 95%			0.000057	0.000065	0.000000	0.000045
	HISS-1	4	4596,11	0.573349	0.421725	0.389532	0.190499
	± 95%			0.000057	0.000069	0.000000	0.000050

Table A. 18: Data for the measured double spiked ratios for sedimentary rocks.

Sample Type	Sample	Experiment Number	Carousel Number	$^{66}\text{Zn}/^{64}\text{Zn}$	$^{67}\text{Zn}/^{64}\text{Zn}$	$^{68}\text{Zn}/^{64}\text{Zn}$	$^{70}\text{Zn}/^{64}\text{Zn}$
Sedimentary rocks	MURST-Iss-A1	1	4592,14	0.572029	0.387229	0.387328	0.172533
	± 95%			0.000039	0.000040	0.000000	0.000030
	MURST-Iss-A1	2	4592,15	0.570978	0.386280	0.386072	0.171669
	± 95%			0.000056	0.000059	0.000000	0.000047
	MURST-Iss-A1	3	4592,16	0.572344	0.387475	0.387697	0.172764
	± 95%			0.000042	0.000041	0.000000	0.000032
	MURST-Iss-A1	4	4596,6	0.571746	0.383387	0.386870	0.170470
	± 95%			0.000066	0.000054	0.000000	0.000052

Table A. 19: Data for the measured double spiked ratios for metamorphic rocks

Sample Type	Sample	Experiment Number	Carousel Number	$^{66}\text{Zn}/^{64}\text{Zn}$	$^{67}\text{Zn}/^{64}\text{Zn}$	$^{68}\text{Zn}/^{64}\text{Zn}$	$^{70}\text{Zn}/^{64}\text{Zn}$
Metamorphic rocks	CaCo3	1	4579,14	0.565383	0.234616	0.377047	0.092607
	± 95%			0.000067	0.000049	0.000000	0.000047
	CaCo3	2	4579,15	0.564952	0.234496	0.376406	0.092502
	± 95%			0.000051	0.000046	0.000000	0.000036

Table A. 20: Data for the measured double spiked ratios for metamorphic rocks

Sample Type	Sample	Experiment Number	Carousel Number	$^{66}\text{Zn}/^{64}\text{Zn}$	$^{67}\text{Zn}/^{64}\text{Zn}$	$^{68}\text{Zn}/^{64}\text{Zn}$	$^{70}\text{Zn}/^{64}\text{Zn}$
Metamorphic rocks	SDC-1	1	4554,11	0.56582	0.238275	0.377451	0.094624
	± 95%			0.00010	0.000089	0.000000	0.000072
	SDC-1	2	4554,12	0.565341	0.237873	0.376699	0.094335
	± 95%			0.000053	0.000051	0.000000	0.000041
	SDC-1	3	4554,13	0.564591	0.237529	0.375861	0.094028
	± 95%			0.000071	0.000043	0.000000	0.000041
	SDC-1	4	4561,2	0.565235	0.237142	0.376761	0.093983
	± 95%			0.000054	0.000060	0.000000	0.000043
	SDC-1	5	4561,3	0.56518	0.237208	0.376761	0.094019
	± 95%			0.00007	0.000050	0.000000	0.000049

Table A. 21: Data for the measured double spiked ratios for metamorphic rocks

Sample Type	Sample	Experiment Number	Carousel Number	$^{66}\text{Zn}/^{64}\text{Zn}$	$^{67}\text{Zn}/^{64}\text{Zn}$	$^{68}\text{Zn}/^{64}\text{Zn}$	$^{70}\text{Zn}/^{64}\text{Zn}$
Metamorphic rocks	QLO-1	1	4554,8	0.565960	0.258733	0.377859	0.105242
	± 95%			0.000062	0.000042	0.000000	0.000031
	QLO-1	2		0.565915	0.258613	0.377859	0.105218
	± 95%			0.000066	0.000052	0.000000	0.000037

Table A. 22: Data for the measured double spiked ratios for clay.

Sample Type	Sample	Experiment Number	Carousel Number	$^{66}\text{Zn}/^{64}\text{Zn}$	$^{67}\text{Zn}/^{64}\text{Zn}$	$^{68}\text{Zn}/^{64}\text{Zn}$	$^{70}\text{Zn}/^{64}\text{Zn}$
Clay	TILL-3	1	4592,11	0.572947	0.415482	0.388843	0.187234
	± 95%			0.000046	0.000041	0.000000	0.000027
	TILL-3	2	4592,12	0.572966	0.415638	0.389016	0.187388
	± 95%			0.000065	0.000059	0.000000	0.000042
	TILL-3	3	4596,4	0.573642	0.399317	0.389650	0.179383
	± 95%			0.000067	0.000062	0.000000	0.000056

Table A. 23: Data for the measured double spiked ratios for biological materials

Sample Type	Sample	Experiment Number	Carousel Number	$^{66}\text{Zn}/^{64}\text{Zn}$	$^{67}\text{Zn}/^{64}\text{Zn}$	$^{68}\text{Zn}/^{64}\text{Zn}$	$^{70}\text{Zn}/^{64}\text{Zn}$
Biological materials	IMEP-19 Rice	1	4578,6	0.570744	0.369735	0.385391	0.163351
	± 95%			0.000044	0.000050	0.000000	0.000032
	IMEP-19 Rice	2	4578,7	0.570982	0.369947	0.385861	0.163612
	± 95%			0.000063	0.000057	0.000000	0.000058
	IMEP-19 Rice	3	4586,6	0.570317	0.369411	0.384896	0.163053
	± 95%			0.000029	0.000027	0.000000	0.000025
	IMEP-19 Rice	4	4586,7	0.570512	0.369540	0.385050	0.163167
	± 95%			0.000049	0.000042	0.000043	0.000041
	IMEP-19 Rice	5	4586,8	0.570320	0.369408	0.384887	0.163044
	± 95%			0.000028	0.000032	0.000000	0.000023
	IMEP-19 Rice	6	4596,8	0.570554	0.372919	0.385238	0.164883
	± 95%			0.000029	0.000022	0.000000	0.000015

Table A. 24: Data for the measured double spiked ratios for biological materials

Sample Type	Sample	Experiment No	Carousel Number	$^{66}\text{Zn}/^{64}\text{Zn}$	$^{67}\text{Zn}/^{64}\text{Zn}$	$^{68}\text{Zn}/^{64}\text{Zn}$	$^{70}\text{Zn}/^{64}\text{Zn}$
Biological materials	NIES-9 (Sargasso)	1	4578,9	0.572721	0.389260	0.388221	0.173943
	± 95%			0.000074	0.000053	0.000000	0.000073
	NIES-9 (Sargasso)	2	4578,10	0.571747	0.388391	0.386962	0.173071
	± 95%			0.000050	0.000048	0.000000	0.000044
	NIES-9 (Sargasso)	3	4586,3	0.572304	0.388932	0.387525	0.173534
	± 95%			0.000069	0.000064	0.000075	0.000052
	NIES-9 (Sargasso)	4	4586,4	0.571300	0.387981	0.386398	0.172736
	± 95%			0.000035	0.000032	0.000000	0.000029
	NIES-9 (Sargasso)	5	4586,5	0.571038	0.387834	0.386279	0.172617
	± 95%			0.000064	0.000058	0.000000	0.000052
	NIES-9 (Sargasso)	6	4596,2	0.571056	0.413904	0.386398	0.185691
	± 95%			0.000049	0.000045	0.000000	0.000040
	NIES-9 (Sargasso)	7	4596,3	0.573109	0.416225	0.389158	0.187692
	± 95%			0.000052	0.000055	0.000000	0.000047
	NIES-9 (Sargasso)	8	4605,7	0.574318	0.428177	0.390874	0.194313
	± 95%			0.000077	0.000086	0.000000	0.000066

Table A. 25: Data for the measured double spiked ratios for biological materials.

Sample Type	Sample	Experiment Number	Carousel Number	$^{66}\text{Zn}/^{64}\text{Zn}$	$^{67}\text{Zn}/^{64}\text{Zn}$	$^{68}\text{Zn}/^{64}\text{Zn}$	$^{70}\text{Zn}/^{64}\text{Zn}$
Biological materials	Murst-ISS-A2 (Antarctic Krill)	1	4596,14	0.576246	0.474816	0.394042	0.218554
	± 95%			0.000078	0.000076	0.000000	0.000069
	Murst-ISS-A2 (Antarctic Krill)	2	4605,9	0.574583	0.438989	0.391269	0.199775
	± 95%			0.000069	0.000054	0.000000	0.000053
	Murst-ISS-A2 (Antarctic Krill)	3	4605,10	0.573600	0.437944	0.390190	0.198851
	± 95%			0.000088	0.000082	0.000000	0.000072

Table A. 26: Data for the measured double spiked ratios for meteorites.

Sample Type	Sample	Experiment Number	Carousel Number	$^{66}\text{Zn}/^{64}\text{Zn}$	$^{67}\text{Zn}/^{64}\text{Zn}$	$^{68}\text{Zn}/^{64}\text{Zn}$	$^{70}\text{Zn}/^{64}\text{Zn}$
Meteorites	Allende	1	4579,5	0.57189	0.383440	0.387405	0.170609
	± 95%			0.00011	0.000091	0.000000	0.000069
	Allende	2	4579,6	0.571691	0.383127	0.387184	0.170340
	± 95%			0.000079	0.000096	0.000000	0.000058

Table A. 27: Data for the measured double spiked ratios for meteorites

Sample Type	Sample	Experiment Number	Carousel Number	$^{66}\text{Zn}/^{64}\text{Zn}$	$^{67}\text{Zn}/^{64}\text{Zn}$	$^{68}\text{Zn}/^{64}\text{Zn}$	$^{70}\text{Zn}/^{64}\text{Zn}$
Meteorites	Orgueil	1	4579,7	0.570024	0.337737	0.384301	0.146741
	± 95%			0.000076	0.000061	0.000000	0.000063
	Orgueil	2	4579,8	0.569838	0.337615	0.383970	0.146560
	± 95%			0.000067	0.000057	0.000000	0.000041

Table A. 28: Data for the measured double spiked ratios for meteorites.

Type	Sample	Experiment Nu	Carousel Number	$^{66}\text{Zn}/^{64}\text{Zn}$	$^{67}\text{Zn}/^{64}\text{Zn}$	$^{68}\text{Zn}/^{64}\text{Zn}$	$^{70}\text{Zn}/^{64}\text{Zn}$
Meteorites	Brown field _1937	1	4592,2	0.581593	0.603401	0.402384	0.285638
	± 95%			0.000041	0.000057	0.000000	0.000047
	Brown field _1937	2	4592,3	0.581760	0.603728	0.402707	0.285980
	± 95%			0.000063	0.000072	0.000000	0.000066
	Brown field _1937	3	4592,4	0.581375	0.603120	0.402088	0.285440
	± 95%			0.000063	0.000075	0.000000	0.000052

Table A. 29: Data for the measured double spiked ratios for meteorites.

Sample Type	Sample	Experiment Number	Carousel Number	$^{66}\text{Zn}/^{64}\text{Zn}$	$^{67}\text{Zn}/^{64}\text{Zn}$	$^{68}\text{Zn}/^{64}\text{Zn}$	$^{70}\text{Zn}/^{64}\text{Zn}$
Meteorites	Brown field 1964	1	4592,5	0.573808	0.445048	0.390318	0.202660
	± 95%			0.000053	0.000042	0.000000	0.000040
	Brown field 1964	2	4592,6	0.573778	0.444976	0.390419	0.202711
	± 95%			0.000046	0.000053	0.000000	0.000042
	Brown field 1964	3	4592,7	0.573832	0.444810	0.390328	0.202598
	± 95%			0.000064	0.000060	0.000000	0.000043

Table A. 30: Data for the measured double spiked ratios for meteorites.

Sample Type	Sample	Experiment Number	Carousel Number	$^{66}\text{Zn}/^{64}\text{Zn}$	$^{67}\text{Zn}/^{64}\text{Zn}$	$^{68}\text{Zn}/^{64}\text{Zn}$	$^{70}\text{Zn}/^{64}\text{Zn}$
Meteorites	Plainview	1	4592,8	0.571573	0.382495	0.386735	0.169940
	± 95%			0.000042	0.000039	0.000000	0.000040
	Plainview	2	4592,9	0.571566	0.382357	0.386564	0.169895
	± 95%			0.000050	0.000048	0.000000	0.000044
	Plainview	3	4592,10	0.571237	0.382155	0.386263	0.169648
	± 95%			0.000049	0.000044	0.000000	0.000039

Table A. 31: Data for the measured double spiked ratios for meteorites.

Sample Type	Sample	Experiment Number	Carousel Number	$^{66}\text{Zn}/^{64}\text{Zn}$	$^{67}\text{Zn}/^{64}\text{Zn}$	$^{68}\text{Zn}/^{64}\text{Zn}$	$^{70}\text{Zn}/^{64}\text{Zn}$
Meteorites	Canyon Diablo	1	4565,13	0.584813	0.637126	0.406919	0.303516
	± 95%			0.000078	0.000095	0.000000	0.000088
	Canyon Diablo	2	4566,13	0.584369	0.635947	0.406399	0.302620
	± 95%			0.000080	0.000084	0.000000	0.000082
	Canyon Diablo	3	4566,14	0.584634	0.636689	0.406758	0.303173
	± 95%			0.000035	0.000060	0.000000	0.000048

Table A. 32: Data for the measured double spiked ratios for water.

Sample Type	Sample	Location	Carousel Number	Detector	$^{66}\text{Zn}/^{64}\text{Zn}$	$^{67}\text{Zn}/^{64}\text{Zn}$	$^{68}\text{Zn}/^{64}\text{Zn}$	$^{70}\text{Zn}/^{64}\text{Zn}$
Water	Swan River	Victoria Park	4434,2	Daly	0.59576	0.93562	0.42564	0.46002
	± 95%				0.00043	0.00092	0.00061	0.00041
	Swan River	Bayswater	4433,2	Daly	0.59147	0.8740	0.41840	0.42494
	± 95%				0.00040	0.0016	0.00000	0.00069
	Swan River	Bayswater	4433,3	Daly	0.58459	0.8005	0.41179	0.38847
	± 95%				0.00031	0.0016	0.00000	0.00069

Table A. 33: Data for the measured double spiked ratios for water.

Sample Type	Sample	Type	Carousel Number	Detector	$^{66}\text{Zn}/^{64}\text{Zn}$	$^{67}\text{Zn}/^{64}\text{Zn}$	$^{68}\text{Zn}/^{64}\text{Zn}$	$^{70}\text{Zn}/^{64}\text{Zn}$
Tap water	Tap water	Restrained Tap water	4430,2	Daly	0.55811	0.20179	0.36854	0.076146
	± 95%				0.00029	0.00016	0.00000	0.000087
	Tap water	Unrestrained (fresh) Tap water	4428,3	Daly	0.5640	0.4949	0.3808	0.2228
	± 95%				0.0031	0.0028	0.0000	0.0023
	Tap water	Unrestrained (fresh) Tap water	4430,5	Daly	0.5775	0.6056	0.39769	0.28401
	± 95%				0.0012	0.0011	0.00000	0.00091

Table A. 34: Data for the measured double spiked ratios for nutritional Zn Tablet.

Sample Type	Sample	Carousel Number	Detector	$^{66}\text{Zn}/^{64}\text{Zn}$	$^{67}\text{Zn}/^{64}\text{Zn}$	$^{68}\text{Zn}/^{64}\text{Zn}$	$^{70}\text{Zn}/^{64}\text{Zn}$
Nutritional Tablet	Zn Tablet	4409,6	Daly	0.55627	0.24604	0.36649	0.097649
	± 95%			0.00025	0.00014	0.00000	0.000097

Table A. 35: Data for the measured double spiked ratios for nutritional Zn Tablet.

Sample Type	Sample	Carousel Number	Detector	$^{66}\text{Zn}/^{64}\text{Zn}$	$^{67}\text{Zn}/^{64}\text{Zn}$	$^{68}\text{Zn}/^{64}\text{Zn}$	$^{70}\text{Zn}/^{64}\text{Zn}$
Roof Sample	Zinc plated Roof Sample	4416,2	Daly	0.55086	0.11361	0.35771	0.029191
	± 95%			0.00034	0.00013	0.00000	0.000055
	Zinc plated Roof Sample	4416,5	Daly	0.55324	0.118676	0.35907	0.031850
	± 95%			0.00033	0.000080	0.00000	0.000060

Table A. 36: Data for the measured un double spiked ratios for different materials.

	Carousel Number	$^{66}\text{Zn}/^{64}\text{Zn}$	$^{67}\text{Zn}/^{64}\text{Zn}$	$^{68}\text{Zn}/^{64}\text{Zn}$	$^{70}\text{Zn}/^{64}\text{Zn}$
CaCo3	4571,5	0.55945	0.080939	0.367404	0.011849
	4571,6	0.558631	0.080775	0.36638	0.011861
	4571,7	0.558478	0.080799	0.366143	0.01192
	Average	0.558853	0.080837	0.366642	0.011876
Canyon Diablo	4579,3	0.55912	0.08100	0.36694	0.01192
		0.00015	0.00011	0.00000	0.00012
Alfa-Aesar 10760	4447	0.545881	0.078083	0.349868	0.011073
		0.00030	0.000091	0.00048	0.000037
	4448	0.546309	0.078333	0.350192	0.011116
		0.00018	0.000059	0.00022	0.000018
	4449	0.547055	0.078315	0.350966	0.011189
		0.00014	0.000055	0.00010	0.000017
	4449	0.545764	0.078157	0.349572	0.011129
		0.00036	0.000071	0.00041	0.000020
	Average	0.546252	0.078222	0.350149	0.011127

- **Appendix E: Detailed data for the concentration determinations**

Data acquired for the calculations of the concentration of Zn in the samples using the IDMS technique. As the aim of measuring some samples was for the measurements of the n fractionation those were measured using the Faraday multi collector and their results were normalized relative to their average $^{68}\text{Zn}/^{67}\text{Zn}$ ratio.

Table B. 1: Data acquired for the calculation of Zn concentration of Zn in BCR-1 using IDMS technique.

Experiment identification	No	Mass Sample(g)	\pm (g)	Double Spike (μg)	\pm (μg)	$^{68}\text{Zn}/^{67}\text{Zn}$	\pm 95%
BCR1-A	1	0.0965	0.0004	2.451	0.007	1.376	0.0010
BCR1-B	2	0.0870	0.0003	2.260	0.007	1.374	0.0012
BCR1-C	3	0.0841	0.0003	1.760	0.005	1.574	0.0013
BCR1-D	4	0.0623	0.0004	1.487	0.005	1.453	0.0006
4545,6	5	0.1738	0.0005	8.161	0.025	0.931	0.0000
4546,7	6	0.1738	0.0005	8.161	0.025	0.927	0.0000
4545,8	7	0.1738	0.0002	8.161	0.025	0.928	0.0000

Table B. 2: Data acquired for the calculation of Zn concentration of Zn in BIR-1 using IDMS technique.

Experiment Identification)	No	Double Spike (μg)	\pm (μg)	$^{68}\text{Zn}/^{67}\text{Zn}$	\pm 95%	Mass Sample(g)	\pm (g)
BIR-1A	1	2.202	0.006	0.98406	0.00081	0.0949	0.0003
BIR1-B	2	2.006	0.005	0.96103	0.00061	0.0835	0.0003
BIR1-C	3	2.097	0.006	0.89559	0.00043	0.079	0.0018
BIR-1D	4	1.375	0.004	1.31948	0.00000	0.0890	0.0003
BIR1-F	5	1.375	0.004	1.31939	0.00000	0.0890	0.0003

Table B. 3: Data acquired for the calculation of Zn concentration of Zn in W-2 using IDMS technique.

Experiment identification	sample No	Double Spike (μg)	\pm (μg)	$^{68}\text{Zn}/^{67}\text{Zn}$	\pm 95%	Mass Sample(g)	\pm (g)
W2-a	1	2.517	0.007	0.70210	0.00045	0.0620	0.0003
W2-b	2	2.586	0.007	0.77594	0.00036	0.0737	0.0003
W2-c F	3	3.677	0.011	0.95196	0.00000	0.13805	0.0003
W2-e F	4	3.677	0.011	0.95206	0.00000	0.13805	0.0003
W2-f F	5	3.677	0.011	0.95183	0.00000	0.13805	0.0003
W2-g F	6	3.677	0.011	0.95312	0.00000	0.13805	0.0003
W2-h F 4551_3	7	3.677	0.011	0.95217	0.00000	0.13805	0.0003
W2-i F 4561,5	8	0.578	0.002	1.52440	0.00000	0.0429	0.0003
W2-j 4561,6F	9	0.578	0.002	1.53033	0.00000	0.0429	0.0003
W2-K F 4561,7	10	0.578	0.002	1.52448	0.00000	0.0429	0.0003
W2-l F 4564,5	11	0.883	0.003	1.439044	0.00000	0.06055	0.0003
W2-m F 4564,6	12	0.883	0.003	1.435192	0.00000	0.06055	0.0003
W2-n F 4564,7	13	0.883	0.003	1.43581	0.00000	0.06055	0.0003

Table B. 4: Data acquired for the calculation of Zn concentration of Zn in SGR-1 and SCO-1 using IDMS.

Experiment identification	sample No	Mass Sample(g)	± (g)	Double Spike (µg)	± (µg)	⁶⁸ Zn/ ⁶⁷ Zn	± 95%
SGR1-A	1	0.0528	0.0003	1.690	0.005	0.808	0.001
SGR1-B	2	0.0442	0.0003	1.826	0.006	0.678	0.001
SGR1-C	3	0.0367	0.0003	1.912	0.006	0.573	0.001
SGR1-d	4	0.1173	0.0003	2.504	0.008	1.064	0.000
SGR1-e	5	0.1173	0.0003	2.504	0.008	1.065	0.000
SGR1-f	4551_5	0.1173	0.0003	2.504	0.008	1.071	0.000
SGR1-g	4551_6	0.1173	0.0003	2.504	0.008	1.069	0.000
Experiment identification	sample No	Mass Sample(g)	± (g)	Double Spike (µg)	± (µg)	⁶⁸ Zn/ ⁶⁷ Zn	± 95%
SCO-1A	1	0.1213	0.0003	2.258	0.007	1.442	0.00094
SCO-1B	2	0.0904	0.0003	1.842	0.006	1.381	0.00080
SCO-1C	3	0.0810	0.0003	2.438	0.007	1.055	0.00085
SCO-1d F	4	0.1051	0.0003	1.459	0.004	1.735	0.00000
SCO-1e F	5	0.1051	0.0003	1.459	0.004	1.736	0.00000
SCO-1f F	6	0.1051	0.0003	1.459	0.004	1.736	0.00000

Table B. 5: Data acquired for the calculation of Zn concentration of Zn in DNC-1 using IDMS technique.

Experiment identification	sample No	Mass Sample(g)	± (g)	Double Spike (µg)	± (µg)	⁶⁸ Zn/ ⁶⁷ Zn	± 95%
DNC-1A	1	0.0556	0.0003	1.917	0.006	0.7140	0.0005
DNC-1B	2	0.0587	0.0003	1.945	0.006	0.7310	0.0008
DNC-1C	3	0.0628	0.0003	1.906	0.006	0.7810	0.0006
DNC-1 d F	4	0.0905	0.0003	1.132	0.003	1.443	0.0000
DNC-1 e F	5	0.0905	0.0003	1.132	0.003	1.444	0.0000
DNC-1 f F	4551_12	0.0905	0.0003	1.132	0.003	1.446	0.0000
DNC-1 g F	4561,8	0.0456	0.0003	0.527	0.002	1.52590	0.0000
DNC-1 h F	5461,9	0.0456	0.0003	0.527	0.002	1.52339	0.0000
DNC-1 i F	4561,10	0.0456	0.0003	0.527	0.002	1.5253	0.0000
Average							

Table B. 6: Data acquired for the calculation of Zn concentration of Zn in HISS-1 using IDMS technique.

Experiment identification	sample No	Mass Sample(g)	± (g)	Double Spike (µg)	± (µg)	⁶⁸ Zn/ ⁶⁷ Zn	± 95%
4578,2	1	2.2131	0.0005	2.833	0.008	0.9781	0.0000
4578,3	2	2.2131	0.0005	2.833	0.008	0.9779	0.0000
4578,4	3	2.2131	0.0005	2.833	0.008	0.9781	0.0000
4579,7	4	2.2131	0.0005	2.833	0.008	0.9784	0.0000
4579,8	5	2.2131	0.0005	2.833	0.008	0.9790	0.0000
4579,9	6	2.2131	0.0005	2.833	0.008	0.9880	0.0000
4583,2	7	0.4496	0.0001	0.696	0.002	0.8490	0.0000
4583,3	8	0.2787	0.0000	0.331	0.001	1.0228	0.0000
4583,4	9	0.8557	0.0001	1.534	0.005	0.7494	0.0000
4586,2	10	0.8557	0.0001	1.534	0.005	0.7510	0.0000
4596,10	11	2.5908	0.0003	3.761	0.011	0.9236	0.0000
4596,11	12	2.5908	0.0003	3.761	0.011	0.9237	0.0000

Table B. 7: Data acquired for the calculation of Zn concentration of Zn in MURST-Iss-1 using IDMS technique.

Experiment identification	sample No	Mass Sample(g)	± (g)	Double Spike (µg)	± (µg)	⁶⁸ Zn/ ⁶⁷ Zn	± 95%
4592,14	1	0.3732	0.0002	6.482	0.019	1.0003	0.0000
4592,15	2	0.3732	0.0002	6.482	0.019	0.9995	0.0000
4592,16	3	0.3732	0.0002	6.482	0.019	1.0006	0.0000
4596,6	4	0.3883	0.0003	6.593	0.019	1.0091	0.0000

Table B. 8: Data acquired for the calculation of Zn concentration of Zn in CaCO₃ using IDMS technique.

Experiment identification	No	Mass Sample(g)	± (g)	Double Spike (µg)	± (µg)	⁶⁸ Zn/ ⁶⁷ Zn	± 95%
4579,14	1	0.9060	0.0003	0.629	0.002	1.6071	0.0000
4579,15	2	0.9060	0.0003	0.629	0.002	1.6052	0.0000

Table B. 9: Data acquired for the calculation of Zn concentration of Zn in SDC-1 using IDMS technique.

Experiment identification	No	Mass Sample(g)	± (g)	Double Spike (µg)	± (µg)	⁶⁸ Zn/ ⁶⁷ Zn	± 95%
SDC1-A	1	0.0709	0.0003	2.015	0.005	1.0960	0.0008
SDC1-B	2	0.0767	0.0003	1.869	0.005	1.201	0.001
SDC1-C	3	0.0585	0.0003	1.796	0.005	1.034	0.001
SDC1-d F	4	0.0701	0.0003	1.145	0.003	1.5841	0.0000
SDC1-e F	5	0.0701	0.0003	1.145	0.003	1.5836	0.0000
SDC1-f F	6	0.0701	0.0003	1.145	0.003	1.5824	0.0000
SDC1-g F	7	0.0701	0.0003	1.145	0.003	1.5888	0.0000
SDC1-i F	8	0.0701	0.0003	1.145	0.003	1.5883	0.0000

Table B. 10: Data acquired for the calculation of Zn concentration of Zn in QLO-1 using IDMS technique.

Experiment identification	No	Mass Sample(g)	± (g)	Double Spike (µg)	± (µg)	⁶⁸ Zn/ ⁶⁷ Zn	± 95%
QLO1-A	1	0.0461	0.0003	1.770	0.005	0.6070	0.0006
QLO1-B	2	0.0426	0.0003	1.816	0.005	0.5680	0.0004
QLO1-C	3	0.0384	0.0003	1.628	0.004	0.5626	0.0004
QLO1-d F 4554,8	4	0.0946	0.0002	1.058	0.003	1.4604	0.0000
QLO1-e F 4554,9	5	0.0946	0.0002	1.058	0.003	1.4648	0.0000
QLO1-f F 4554,10	6	0.0946	0.0002	1.058	0.003	1.4611	0.0000

Table B. 11: Data acquired for the calculation of Zn concentration of Zn in TILL-3 using IDMS technique.

Experiment identification	No	Mass Sample(g)	± (g)	Double Spike (µg)	± (µg)	⁶⁸ Zn/ ⁶⁷ Zn	± 95%
4586,11	1	0.2325	0.0003	3.428	0.010	1.0389	0.0000
4586,12	2	0.2325	0.0003	3.428	0.010	1.0374	0.0000
4592,11	3	0.4113	0.0001	7.026	0.021	0.9359	0.0000
4592,12	4	0.4113	0.0001	7.026	0.021	0.9359	0.0000
4592,13	5	0.4113	0.0001	7.026	0.021	0.9363	0.0000
4596,4	6	0.3269	0.0001	5.247	0.015	0.9758	0.0000

Table B. 12: Data acquired for the calculation of Zn concentration of Zn in IMEP-19 using IDMS technique.

Experiment identification	No	Mass Sample(g)	± (g)	Double Spike (µg)	± (µg)	⁶⁸ Zn/ ⁶⁷ Zn	± 95%
4578,5	1	0.4581	0.0003	2.936	0.009	1.0432	0.0000
4578,6	2	0.4581	0.0003	2.936	0.009	1.0423	0.0000
4578,7	3	0.4581	0.0003	2.936	0.009	1.0430	0.0000
	4	0.4581	0.0003	2.936	0.009	1.0419	0.0000
	5	0.4581	0.0003	2.936	0.009	1.0420	0.0000
	6	0.4581	0.0003	2.936	0.009	1.0419	0.0000
4596,8	7	0.4831	0.0003	3.129	0.009	1.0330	0.0000
4596,9	8	0.4831	0.0003	3.129	0.009	1.034	0.0000

Table B. 13: Data acquired for the calculation of Zn concentration of Zn in MURST-Iss-A2 using IDMS technique.

Experiment identification	No	Mass Sample(g)	± (g)	Double Spike (µg)	± (µg)	⁶⁸ Zn/ ⁶⁷ Zn	± 95%
4596,13	1	0.1052	0.0002	2.621	0.008	0.8763	0.0000
4596,14	2	0.1073	0.0002	2.830	0.008	0.8299	0.0000
4596,15	3	0.1073	0.0002	2.830	0.008	0.8305	0.0000
4605,8	4	0.1207	0.0003	2.891	0.009	0.8928	0.0000
4605,9	5	0.1207	0.0003	2.891	0.009	0.8913	0.0000
4605,10	6	0.1207	0.0003	2.891	0.009	0.8910	0.0000

Table B. 14: Data acquired for the calculation of Zn concentration of Zn in NIES-19 using IDMS technique.

Experiment identification	No	Mass Sample(g)	± (g)	Double Spike (µg)	± (µg)	⁶⁸ Zn/ ⁶⁷ Zn	± 95%
4578,8	1	0.5213	0.0004	2.473	0.007	0.9971	0.0000
4578,9	2	0.5213	0.0004	2.473	0.007	0.9973	0.0000
4578,10	3	0.5213	0.0004	2.473	0.007	0.9963	0.0000
4586,3	4	0.5213	0.0004	2.473	0.007	0.9964	0.0000
4586,4	5	0.5213	0.0004	2.473	0.007	0.9959	0.0000
4586,5	6	0.5213	0.0004	2.473	0.007	0.9960	0.0000
	7	0.3777	0.0003	1.930	0.006	0.9335	0.0000
	8	0.3777	0.0003	1.930	0.006	0.9350	0.0000
4605,6	9	0.5788	0.0004	3.128	0.009	0.9118	0.0000
4605,7	10	0.5788	0.0004	3.128	0.009	0.9129	0.0000

Table B. 15: Data acquired for the calculation of Zn concentration of Zn in Allende meteorites using IDMS technique.

Experiment identification	No	Mass Sample(g)	± (g)	Double Spike (µg)	± (µg)	⁶⁸ Zn/ ⁶⁷ Zn	± 95%
4579,4		0.3830	0.0003	9.172	0.027	1.0120	0.0000
4579,5		0.3830	0.0003	9.172	0.027	1.0103	0.0000
4579,6		0.3830	0.0003	9.172	0.027	1.0106	0.0000

Table B. 16: Data acquired for the calculation of Zn concentration of Zn in Brownfield-1964 meteorites using IDMS technique.

Experiment identification	No	Mass Sample(g)	± (g)	Double Spike (µg)	± (µg)	⁶⁸ Zn/ ⁶⁷ Zn	± 95%
4583,5	1	0.1142	0.0003	1.263	0.004	1.0303	0.0000
4583,6	2	0.1142	0.0003	1.263	0.004	1.0308	0.0000
4583,7	3	0.1142	0.0003	1.263	0.004	1.0280	0.0000
4592,5	4	0.4222	0.0003	5.484	0.016	0.8770	0.0000
4592,6	5	0.4222	0.0003	5.484	0.016	0.8774	0.0000
4592,7	6	0.4222	0.0003	5.484	0.016	0.8775	0.0000

Table B. 17: Data acquired for the calculation of Zn concentration of Zn in Brownfield-1937 meteorites using IDMS technique.

Experiment identification	No	Mass Sample(g)	± (g)	Double Spike (µg)	± (µg)	⁶⁸ Zn/ ⁶⁷ Zn	± 95%
4583,8	1	0.1589	0.0003	2.109	0.006	1.5542	0.0000
4583,9	2	0.1589	0.0003	2.109	0.006	1.5549	0.0000
4583,10	3	0.1589	0.0003	2.109	0.006	1.5543	0.0000
4592,2	4	0.3638	0.0003	9.481	0.028	0.6669	0.0000
4592,3	5	0.3638	0.0003	9.481	0.028	0.6670	0.0000
4592,4	6	0.3638	0.0003	9.481	0.028	0.6667	0.0000

Table B. 18: Data acquired for the calculation of Zn concentration of Zn in Orgueil meteorite using IDMS technique.

Experiment identification	No	Mass Sample(g)	± (g)	Double Spike (µg)	± (µg)	⁶⁸ Zn/ ⁶⁷ Zn	± 95%
4579,7	1	0.0142	0.0003	1.143	0.003	1.137872	0.0000
4579,8	2	0.0142	0.0003	1.143	0.003	1.137302	0.0000

Table B. 19: Data acquired for the calculation of Zn concentration of Zn in Plainview meteorite using IDMS technique.

Experiment identification	No	Mass Sample (g)	± (g)	Double Spike (µg)	± (µg)	⁶⁸ Zn/ ⁶⁷ Zn	± 95%
4579,9	1	0.2035	0.0003	0.975	0.003	1.2836	0.0000
4579,10	2	0.2035	0.0003	0.975	0.003	1.2289	0.0000
4578,14	3	0.2176	0.0003	1.865	0.006	1.0390	0.0000
4578,15	4	0.2176	0.0003	1.865	0.006	1.0212	0.0000
4578,16	5	0.2176	0.0003	1.865	0.006	1.0079	0.0000
4583,11	6	0.2851	0.0002	3.187	0.009	0.958	0.0000
4583,12	7	0.2851	0.0002	3.187	0.009	0.958	0.0000
4583,13	8	0.2851	0.0002	3.187	0.009	0.955	0.0000
4586,10	9	0.2851	0.0002	3.187	0.009	0.958	0.0000
4592,8	10	0.8058	0.0002	6.549	0.047	1.011	0.0000
4592,9	11	0.8058	0.0002	6.549	0.047	1.011	0.0000
4592,10	12	0.8058	0.0002	6.549	0.047	1.011	0.0000

Table B. 20: Data acquired for the calculation of Zn concentration of Zn in Canyon Diablo iron meteorite using IDMS technique.

Experiment identification	No	Mass Sample (g)	± (g)	Double Spike (µg)	± (µg)	⁶⁸ Zn/ ⁶⁷ Zn	± 95%
4565,11	1	0.0933	0.0004	1.344	0.004	0.643	0.0000
4565,12	2	0.0933	0.0004	1.344	0.004	0.642	0.0000
4565,13	3	0.0933	0.0004	1.344	0.004	0.639	0.0000
4566,13	4	0.0933	0.0004	1.344	0.004	0.639	0.0000
4566,14	5	0.0933	0.0004	1.344	0.004	0.639	0.0000

Table B. 21: Data acquired for the calculation of Zn concentration of Zn in Kumerina iron meteorite using IDMS technique

Experiment identification	No	Mass Sample (g)	± (g)	Double Spike (µg)	± (µg)	$^{68}\text{Zn}/^{67}\text{Zn}$	± 95%
4568,12	1	2.09	0.01	0.437	0.002	0.696473	0.0000
4568,13	2	2.09	0.01	0.437	0.002	0.676525	0.0000

Table B. 22: Data acquired for the calculation of Zn concentration of Zn in Mundrabilla iron meteorite using IDMS technique.

Experiment identification	No	Mass Sample (g)	± (g)	Double Spike (µg)	± (µg)	$^{68}\text{Zn}/^{67}\text{Zn}$	± 95%
4564,8	1	0.3665	0.0012	1.264	0.004	0.136	0.0000
4564,9	2	0.3665	0.0012	1.264	0.004	0.137	0.0000
4564,10		0.3665	0.0012	1.264	0.004	0.136	0.0000

Table B. 23: Data acquired for the calculation of Zn concentration of Zn in Odessa iron meteorite using IDMS technique.

Experiment identification	No	Mass Sample (g)	± (g)	Double Spike (µg)	± (µg)	$^{68}\text{Zn}/^{67}\text{Zn}$	± 95%
4579,11	1	0.4100	0.0003	2.815	0.008	1.1468	0.0000
4579,12	2	0.4100	0.0003	2.815	0.008	1.1478	0.0000
4579,13	3	0.4100	0.0003	2.815	0.008	1.1485	0.0000
4578,11	4	1.5214	0.0003	7.787	0.023	0.8818	0.0000
4578,12	5	1.5214	0.0003	7.787	0.023	0.8920	0.0000
4578,13	6	1.5214	0.0003	7.787	0.023	0.8882	0.0000

Table B. 24: Data acquired for the calculation of Zn concentration of Zn in Redfields iron meteorite using IDMS technique.

Experiment identification	No	Mass Sample (g)	± (g)	Double Spike (µg)	± (µg)	$^{68}\text{Zn}/^{67}\text{Zn}$	± 95%
4568,5	1	0.46	0.01	1.214	0.003	0.908473	0.0000
4568,6	2	0.46	0.01	1.214	0.003	0.91237	0.0000
Red fields-c	3	0.46	0.01	1.214	0.003	0.91005	0.0000

Table B. 25: Data acquired for the calculation of Zn concentration of Zn in Warburton iron meteorite using IDMS technique.

Experiment identification	No	Mass Sample (g)	± (g)	Double Spike (µg)	± (µg)	$^{68}\text{Zn}/^{67}\text{Zn}$	± 95%
4568,5	1	1.1	0.1	0.482	0.001	0.147428	0.000000
4568,6	2	1.1	0.1	0.482	0.001	0.147652	0.000000

Table B. 26: Data acquired for the calculation of Zn concentration of Zn in Younami iron meteorite using IDMS technique.

Experiment identification	No	Mass Sample (g)	± (g)	Double Spike (µg)	± (µg)	$^{68}\text{Zn}/^{67}\text{Zn}$	± 95%
4568,10	1	1.61	0.01	0.598	0.002	0.875118	0.0000
4568,11	2	1.61	0.01	0.598	0.002	0.871380	0.0000

Table B. 27: Data acquired for the calculation of Zn concentration of Zn in unrestrained (fresh) tapwater using IDMS technique.

Experiment identification	No	Mass Sample (g)	± (g)	Double Spike (ng)	± (ng)	$^{68}\text{Zn}/^{67}\text{Zn}$	± 95%
4428,3	1	14.972	0.002	99	1	0.7695	0.0000
4430,5	2	15.010	0.002	125	1	0.6567	0.0000

Table B. 288: Data acquired for the calculation of Zn concentration of Zn in roof Zinc plated steel sample using IDMS technique.

Experiment identification	No	Mass Sample (g)	± (g)	Double Spike (ng)	± (ng)	$^{68}\text{Zn}/^{67}\text{Zn}$	± 95%
4416,2	1	0.0153	0.0002	0.1937	0.0006	3.1487	0.0000
4416,3	2	0.0153	0.0002	0.1937	0.0006	3.1114	0.0000
4416,4	3	0.0153	0.0003	0.1796	0.0008	3.0179	0.0000
4416,5	4	0.0153	0.0003	0.1796	0.0008	3.0257	0.0000

Table B.29: Data acquired for the calculation of Zn concentration of Zn in Zinc nutritional Tablet using IDMS technique.

Experiment identification	No	Double Spike (g)	± (ng)	$^{68}\text{Zn}/^{67}\text{Zn}$	± 95%
4409,6	1	1.1055	0.0067	1.48955	0.00000